UNIVERSITY OF CALIFORNIA

Los Angeles

Gene Regulation by Epigenetic Modifiers in Stem Cells, Cancer, and Immunology

A dissertation submitted in partial satisfaction of the requirements for the degree Doctor of Philosophy in Biological Chemistry

by

Kathleen Miuyi Yee

2016

ABSTRACT OF THE DISSERTATION

Gene Regulation by Epigenetic Modifiers in Stem Cells,

Cancer, and Immunology

by

Kathleen Miuyi Yee

Doctor of Philosophy in Biological Chemistry

University of California, Los Angeles, 2016

Professor Ke Shuai, Chair

DNA methylation is an essential epigenetic mechanism to control gene expression, with important implications for development, cellular homeostasis, and cancer progression. A lack of DNA methylation is not compatible with embryonic development. Likewise, dysregulation in DNA methylation is hallmark associated with cancer development. This dissertation focuses on the role of two epigenetic modifying proteins: protein inhibitor of activated STAT1 (PIAS1) and ten-eleven translocation 2 (TET2). Here I describe a newly discovered role for PIAS1 as an epigenetic gene silencer, with important implications in immunosuppression, stem cell maintenance and differentiation, and breast tumorigenesis. First, PIAS1 recruits DNMT3 and HP1 to the *Foxp3* promoter for epigenetic silencing in regulatory T cells (Tregs). In the absence of PIAS1, the *Foxp3* promoter is hypomethylated with a corresponding increase in expression. This allows for an increase in the number of Treg cells in *Pias1-/-* mice that provides resistance to the development of experimental autoimmune encephalomyelitis (EAE). Second, PIAS1 plays an important role in the maintenance and differentiation of hematopoietic stem cells (HSCs) by mediating proper DNA methylation at key differentiation genes such as *Gata1*. Without PIAS1

mediated gene silencing, dormant stem cells enter the cell cycle and exhaust their self-renewal properties. Additionally, stem cells aberrantly produce more myeloid cells than lymphoid cells in *Pias1-/-* mice. Third, elevated PIAS1 expression is observed in human breast cancer samples and is associated with increased tumorigenicity. In the breast cancer cell line MDA-MD231, PIAS1 mediates the silencing of important tumor suppressor genes such as *WNT5A* and *CCND2* by epigenetic mechanisms. Knockdown of PIAS1 expression decreases the tumorigenicity of this cell line. Lastly, I explore the role of TET proteins in macrophage gene activation. Little is known about the role of TET proteins in the innate immune response. Surprisingly, TET2 is a repressor of several M1 macrophage genes whereas is required for the expression of a subset of M2 macrophage genes. Correspondingly, *Tet2-/-* macrophages exhibit an overexpression of several inflammatory genes important for microbial resistance, which may account for the increased protection to *Listeria monocytogenes* infection in seen in *Tet2-/-* mice.

The dissertation of Kathleen Miuyi Yee is approved.

John J. Colicelli

Siavash K. Kurdistani

Jing Huang

Ke Shuai, Committee Chair

University of California, Los Angeles

2016

TABLE OF CONTENTS

LIST OF FIGURES

LIST OF FIGURES (continued…)

LIST OF TABLES

ACKNOWLEDGEMENTS

First and foremost I would like to thank my committee chair, Dr. Ke Shuai, for offering me the opportunity and resources necessary to complete my Ph.D. He has been generous in guiding and training me throughout this dissertation process. Thank you again. I would like to thank my committee members; Dr. John Colicelli, Dr. Jing Huang, Dr. Siavash Kurdistani, and Dr. Michael Grunstein, for critical feedback and support that was instrumental for my growth as a researcher. To Dr. Bin Liu, my greatest thanks for all your help and advice throughout my graduate career as my unofficial second mentor. You have always made yourself available, and I appreciate all the help you have give me through these years. I give thanks to the other Shuai lab members present during my graduate career: Sam, Yonghui, Cary F., Cary H., Christian, Ryan, Irving and Jason. Thank you to my undergrads Heather Chow, Hubert Wang, Zhang (Steven) Zhe and Minsub Lee – sorry to all that I couldn't use any of your hard work in my dissertation. Thank you to my fellow floor mates from the Heaney lab and the Gomperts lab for the comradery and moral support. Thank you Tammy for critique of my dissertation. Thank you Miguel, Eriko, Ronik, Gustavo and Susie for being great friends and cheering me on. Thank you to my parents and siblings Kent and Kimmy, for constantly wishing me the best. Finally, with love, I thank my husband, Ronald.

Chapter 2 is the "Accepted Version," plus all Supplemental Material, of Liu, B., S. Tahk, K.M. Yee, G. Fan, and K. Shuai. (2010). **The Ligase PIAS1 restricts natural regulatory T cell differentiation by epigenetic repression.** *Science*. 330:521–525 Note: This is the author's version of the work. It is posted here by permission of the AAAS for personal use, not for redistribution. The definitive version was published in Science (220, (2010)) doi:10.1126/science.1193787.

B.L. performed the ELISAs, flow cytometry, sorting, and bone marrow reconstitutions involving the PIAS1 mice. B.L. and V.C. performed the EAE experiment. S.T. performed the iTreg studies, ChIP and bisulfite sequencing assays. K.Y. performed the DNMT3A/DNMT3B reconstitution assays including sorting and flow cytometry, and assisted in the bisulfite sequencing of these mice. G.F. provided the DNMT3A$^{2lox/2lox}$/DNMT3B$^{2lox/2lox}$ mice and retroviral-GFP constructs. B.L. and K.S. wrote the manuscript.

Chapter 3 is a reprint, plus Supplemental Material, of Liu, B., K.M. Yee, S. Tahk, R. Mackie, C. Hsu, and K. Shuai. (2013). **PIAS1 SUMO ligase regulates the self-renewal and**

differentiation of hematopoietic stem cells. *The EMBO Journal*. 33:101–113. doi:10.1002/embj.201283326. K.M. Yee is listed as a co-first author.

B.L performed qPCRs, flow cytometry, sorting, cell cycle and apoptosis assays, homing and niche retention assays, several long-term bone marrow (BM) reconstitution assays and all BM injections. K.Y. performed the limiting dilution assays, most of the long-term BM reconstitution assays, flow analysis and responsible for the irradiation and health follow-up and analysis of BM reconstituted mice. K.Y. performed the DNMT3A co-IP and ChIP studies, and assisted with bisulfite sequencing. S.T. performed the PIAS1 ChIPs and bisulfite sequencing. R.M. and C.H. perfomed the qPCRs. B.L. and K.S. wrote the manuscript. Table 2 presented here is unpublished work that was ongoing when the manuscript was accepted for publication. Note: while both Table 1 and Table 2 have the same conclusion, Table 2 is more representative as this set of experiments involved over twice the amount of recipient mice.

Chapter 4 is a reprint, plus Supplemental Material, of Liu, B., S. Tahk, K.M. Yee, R. Yang, Y. Yang, R. Mackie, C. Hsu, V. Chernishof, N. O'Brien, Y. Jin, G. Fan, T.F. Lane, J. Rao, D. Slamon, and K. Shuai. (2014). **PIAS1 regulates breast Tumorigenesis through selective epigenetic gene silencing**. *PLoS ONE*. 9:e89464. doi:10.1371/journal.pone.0089464.

B.L. performed the growth curve, mammospheres, ALDEFLUOR, and xenograph studies with the PIAS1 shRNA cell lines, in addition to analysis of MB231 microarray and qPCR. S.T. and K.Y. performed the ChIP assays and S.T performed the bisulfite sequencing. K.Y re-created shRNA cell lines to independently validate microarray and mammosphere results. R.Y. created the shRNA constructs and knockdown cell lines. Y.Y assisted with immunoblots. R.M. assisted with qPCRs and the box and whiskers plot. C.H. assisted with qPCRs. V.C. assisted with xenograph studies and qPCR. N.O-B. and D.S. provided the cancer cell lines. Y.J. and J.R. performed histology and tumor scores. T.F.L. analyzed histology and mammary glands. G.F. analyzed bisulfite sequencing. B.L. and K.S. wrote the manuscript.

.

VITA

Education and Experience

1999-2003	B.S. Microbiology, Immunology and Molecular Genetics B.S. Ecology, Behavior, and Evolution University of California, Los Angeles
2001-2003	Undergraduate Researcher Department of MIMG University of California, Los Angeles Advisors: Dr. Genhong Cheng, Ryan O'Connell
2004-2007	Staff Research Associate I/II Department of OBGYN University of California, Los Angeles Advisors: Dr. Timothy Lane, Dr. Gustavo Miranda
2007-2008	Staff Research Associate II Department of MCDB University of California, Los Angeles Advisor: Dr. Luisa Iruela-Arispe
2008-2009	UCLA ACCESS Ph.D program
2009-present	Graduate Student Researcher Department of Biological Chemistry University of California, Los Angeles Advisor: Dr. Ke Shuai
2010	Teaching Assistant MCDB Department. Cell Biology 140
2011	Teaching Assistant MCDB Department. Cell Biology 140

PUBLICATIONS

Liu, B., S. Tahk, **K.M. Yee**, R. Yang, Y. Yang, R. Mackie, C. Hsu, V. Chernishof, N. O'Brien, Y. Jin, G. Fan, T.F. Lane, J. Rao, D. Slamon, and K. Shuai. 2014. PIAS1 regulates breast Tumorigenesis through selective epigenetic gene silencing. *PLoS ONE*. 9:e89464. doi:10.1371/journal.pone.0089464.

Liu, B., **K.M. Yee**, S. Tahk, R. Mackie, C. Hsu, and K. Shuai. 2013. PIAS1 SUMO ligase regulates the self-renewal and differentiation of hematopoietic stem cells. *The EMBO Journal*. 33:101–113. doi:10.1002/embj.201283326.
***co-first author**

Liu, B., S. Tahk, **K.M. Yee**, G. Fan, and K. Shuai. 2010. The Ligase PIAS1 restricts natural regulatory T cell differentiation by epigenetic repression. *Science*. 330:521–525. doi:10.1126/science.1193787.

Miranda-Carboni, G.A., S.A. Krum, **K. Yee**, M. Nava, Q.E. Deng, S. Pervin, A. Collado-Hidalgo, Z. Galic, J.A. Zack, K. Nakayama, and T.F. Lane. 2008. A functional link between Wnt signaling and SKP2-independent p27 turnover in mammary tumors. *Genes & Development*. 22:3121–3134. doi:10.1101/gad.1692808.

Zovein, A.C., A. Luque, K.A. Turlo, J.J. Hofmann, **K.M. Yee**, M.S. Becker, R. Fassler, I. Mellman, T.F. Lane, and M.L. Iruela-Arispe. 2010. B1 Integrin establishes endothelial cell polarity and arteriolar lumen formation via a par3-Dependent mechanism. *Developmental Cell*. 18:39–51. doi:10.1016/j.devcel.2009.12.006.

Doyle, S.E., R. O'Connell, S.A. Vaidya, E.K. Chow, **K. Yee**, and G. Cheng. 2003. Toll-like receptor 3 Mediates a more potent antiviral response than toll-like receptor 4. *The Journal of Immunology*. 170:3565–3571. doi:10.4049/jimmunol.170.7.3565.

SELECT PRESENTATIONS

"PIAS Proteins in Epigenetic Regulation and Regulatory T-cell Differentiation" Kathleen M. Yee, Bin Liu, Samuel Tahk, Irving Garcia, Jason Romero, and Ke Shuai. UCLA Department of Biological Chemistry Retreat, Lake Arrowhead, 2011, poster presentation.

"The Role of PIASy in the Regulation of Cell Differentiation." Kathleen M. Yee, Bin Liu, Cary Hsu, Ryan Mackie, and Ke Shuai. UCLA Department of Medicine Research Day, 2012, poster presentation.

"PIAS1 SUMO Ligase Regulates the Self-Renewal and Differentiation of Hematopoietic Stem Cells." Kathleen M. Yee, Bin Liu, Samuel Tahk, Ryan Mackie, and Ke Shuai. UCLA Department of Medicine Research Day, 2014, poster presentation.

Chapter 1: Modifiers of Gene Expression and Hematopoietic Stem Cells and the Immune Response

Introduction

The proper control of gene expression is essential for normal development, from stem cell development, to cell homeostasis and function, and finally to apoptosis. Dysregulation in gene control can have wide-ranging effects, from embryonic lethality to cancer cell transformations. Epigenetic refers to the regulation of genes that does not involve changes to the underlying DNA sequence. Many mechanisms can be attributed as epigenetic, but the three most common are histone modifications, DNA methylation, and non-coding RNA. My primary focus will be gene regulation by DNA methylation mechanisms with a small emphasis on histone modifications. I will analyze the role of epigenetic modifications in T cell development, stem cell maintenance and differentiation, cancer cell progression, and immune responses to microbial stimuli.

Section 1: Modifiers of Gene Expression

Histones modifications

Chromatin refers to the orderly packaging of DNA into units called nucleosomes. A nucleosome is composed of an octamer of four core histones (H3, H4, H2A, H2B) of which 147 bases of DNA wrap around. An important feature of histones is that they have exposed protein "tails" that stick out from the nucleosome and can undergo post-translational modifications (PTM) that affect the availability of the DNA for gene expression. There are over 11 types of PTM that can occur on over 60 different amino acid residues on the histones (Kouzarides, 2007; Tan et al., 2011). As enzymes that can add and remove PTMs have been discovered, histone modifications are generally thought of as transient and reversible. The more common modifications are histone acetylation and histone methylation, both on lysine residues. Acetylation of H3 lysine tails (AcH3) by histone acetyltransferases (HATs) are associated with transcriptional activation, as the positive charge of the acetyl group neutralizes the negative

charge on the lysine, allowing the chromatin to open up and allow DNA to be more accessible for transcription. Conversely, histone deacetylases (HDACs) are associated with gene repression as they compact the chromatin. Tri-methylation of H3 histones on lysine K9 (H3K9me3) and lysine K27 (H3K27me3) are both associated with transcriptional repression (Kouzarides, 2007).

DNA methylation and gene silencing

DNA methylation by DNA methyltransferases (DMNTs) is an epigenetic modification primarily found symmetrically distributed on CpG dinucleotides. Specifically, a methyl group is added to the carbon-5 position of cytosine to create 5-methylcytosine (5mC) (Doerfler 1983). There are three family members in mammalian cells: DNMT1, DNMT3A and DNMT3B. DNMT3A and DNMT3B are the *de novo* methyltransferases that establish DNA methylation patterns at unmodified CpG sites. These two proteins can partially compensate for each other, as a double deletion of DNMT3A and DNMT3B has a more severe phenotype on mouse embryos than deletion of an individual protein (Okano et al., 1999). DNMT1, known as the maintenance methyltransferase, interacts with UHRF1 at the DNA replication foci during S-phase and restores the symmetrical CpG methylation patterns on the nascent DNA stand. DNMT1 targeting to CpG sites relies on UHRF1 recognition of hemi-methylated CpG during DNA replication (Rottach et al., 2009; Williams, et al., 2011b; Bostick et al., 2007; Sharif et al., 2007).

DNA methylation has a long established role in gene regulation. By controlling gene expression, this highly conserved modification has a profound impact on embryonic development, imprinting, X-inactivation, genome stability, and normal development (Smith and Meissner, 2013). There are at least two mechanisms by which DNA methylation can repress transcription. The first is that the methyl modification can directly prevent transcription factors from binding their target DNA sites (Bird 2002). Second, the methylated CpGs can attract

methyl CpG binding proteins (MBPs) who recruit repressive chromatin modifiers associated with transcriptional silencing, such as the MeCP1 HDAC complex (Hendrich and Tweedie, 2003). Coincidentally, human cancer cells generally display altered DNA methylation. Cancer cells can simultaneously develop aberrant hypomethylation at key genes known as oncogenes, and hypermethylation at key genes known as tumor suppressors. This hypermethylation is associated with gene silencing and is a hallmark of cancer pathogenesis (Herman and Baylin, 2003; Esteller, 2007).

TET proteins on active DNA demethylation and gene expression

While the concept of DNA methylation has long been established, controversy existed over whether DNA CpG methylation can be actively removed in mammalian cells and if so, the mechanism(s) by which this may occur. The discovery of the enzymatic activity of ten-eleven translocation (TET) proteins in 2009 allowed unambiguous evidence of active DNA demethylation (Tahiliani et al., 2009). The TET family members were first discovered by two independent groups analyzing human leukemia samples and found that an unknown protein, located on chromosome 10 (now known as TET1), was translocated with mixed lineage leukemia (MLL), creating t(10;11)(q22;q23), hence the nomenclature “ten-eleven translocation” (Ono et al., 2002; Lorsbach et al., 2003).

TET proteins are 2-oxoglutarate and Fe(II)-dependent oxygenases that can catalyze the conversion of 5mC to 5-hydroxylmethylcytosine (5hmC) and further modify 5hmC to 5-formylcytosine (5fC) and to 5-carboxylcytosine (5caC) (Kriaucionis and Heintz, 2009; Tahiliani et al., 2009; Ito et al., 2011) (Figure 1.1b). DNA repair enzymes, such as thymine-DNA glycosylase (TDG), can remove 5caC and base excision repair enzymes can replaced the resulting abasic site with an unmodified cytosine, culminating in active DNA demethylation (He et al., 2011; Maite and Drohat, 2011). All three TET members in mammalian cells (TET1, TET2, and TET3) have 5hmC catalytic activity. Additionally, TET1 and TET3 (but not TET2) possess a CXXC

DNA binding domain that may allow targeting to chromatin (Rasmussen and Helin, 2016) (Figure 1.1a). As TET2 does not contain a CXXC domain, evidence suggests that TET2 may find its DNA targets by interaction with transcription factors (Ichiyama et al., 2015; Zhang et al., 2015)

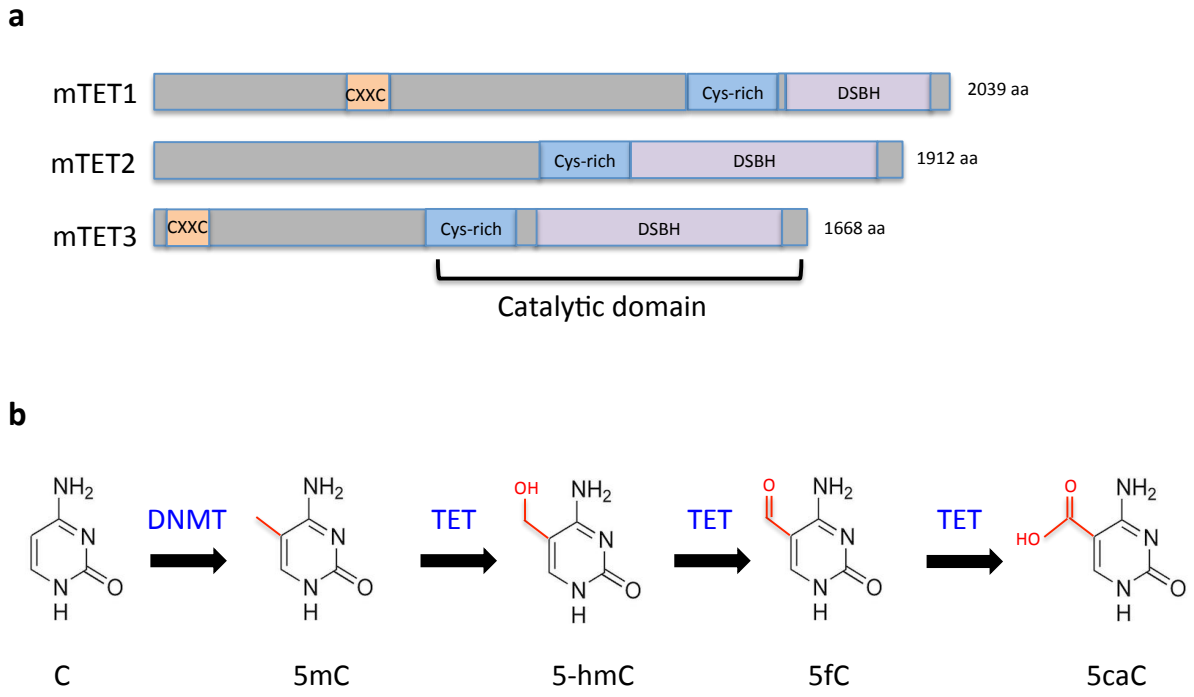

Figure 1.1. The structure and enzymatic activity of TET proteins
(a) Schematic drawing of TET proteins indicating the approximate locations of the CXXC binding domain and the catalytic domain. The catalytic domain consists of a cysteine-rich region and the DSBH, where the actual catalytic activity occurs (Ko et al., 2010). **(b)** Stepwise modification of 5-position cytosine by DNMT and TET enzymes. Abbreviations: DNMT (DNA methyltransferase), TET (ten-eleven translocation), Cys-rich (cysteine rich), DSBH (double stranded beta-helix). Figure is adapted from (Wu and Zhang, 2014).

In addition to actively removing DNA methylation, TET mediated 5hmC generation may allow gene expression by several mechanisms. The first is the finding that UHRF1 is less efficient at binding 5hmC than 5mC *in vitro*, thus 5hmC can potentially interfere with the DNA maintenance function of DNMT1 (Hashimoto et al., 2012). Also, 5hmC strongly inhibits the

binding of MBP proteins MBD1, MBD2, and MeCP2 to DNA (Hashimoto et al., 2012; Jin, Kadam and Pfeifer, 2010; Valinluck et al., 2004) and therefore 5hmC may contribute to gene activation. To directly show the positive effect of TET catalytic activity in gene activation, *in vitro* studies utilizing artificially methylated GFP reporter constructs showed that overexpression of human TET1 can allow the re-expression of GFP, whereas a catalytic mutant of TET1 cannot (Zhang et al., 2010). Additionally, studies on mouse embryonic stem cells (ESCs) show that expression of the transcription factor *Nanog* is dependent on TET1 binding to and removing the DNA methylation that would otherwise silence the gene (Ito et al., 2010).

Surprisingly, TET proteins can also have repressive effects on gene transcription. Gene-expression profiling of TET1-depleted embryonic stem cells (ESC) show that while most genes were unaffected by TET1 knockdown, more genes were up-regulated than down-regulated when TET1 is removed (Williams et al., 2011a; Wu et al., 2011). To account for the repressive activity of TET1, these two groups showed TET1 is highly enriched at promoters that are repressed by Polycomb repression complex 2 (PRC2) indicating a link between these two. However these two groups were unable to show a physical interaction between TET1 and PRC2. To further account for TET1 induced gene repression, TET1 was shown to bind to the co-repressor complex SIN3A (Williams et al., 2011a), which can contribute to transcriptional repression by facilitating histone deacetylation (Grzenda et al., 2009). Moreover, as evidence that TET proteins can have a repressive role, TET2 can recruit HDAC2 for gene repression, and this interaction is independent of TET2 catalytic activity (Zhang et al., 2015).

Gene regulation by PIAS proteins

The protein inhibitor of activated STAT (PIAS) proteins were first discovered in our lab while searching for novel proteins that can interact with signal transducer and activator of transcription (STAT) transcription factors. There are four members of the mammalian PIAS family: PIAS1, PIAS2 (also known as PIASx), PIAS3, and PIAS4 (also known as PIASy). Each

member has been shown to be involved in STAT signaling, and there is both specificity and redundancy among the various PIAS-STAT interactions (Chung et al., 1997; Liu et al., 1998; Liu et al., 2001; Arora et al., 2000).

PIAS family members have a high degree of sequence homology and share several highly conserved domains (Shuai and Liu, 2005; Rytinki et al., 2009). One of the most conserved domains is the N-terminal **SAP** domain (**s**caffold attachment factor-A/B, **a**poptotic chromatin-condensation inducer in the nucleus (ACINUS) and **P**IAS domain. The SAP domain is found in many chromatin-binding proteins and it contains a signature LxxLL motif found in proteins that interact with nuclear receptors (Plevin et al., 2005). Another highly conserved and striking domain in PIAS proteins is the RING-finger-like zinc-binding domain (RLD), which is required for the SUMO-E3 ligase activity of PIAS proteins (Hochstrasser, 2011). Small ubiquitin-like modifier (SUMO) is a molecule similar to ubiquitin and is conjugated in a similar fashion, utilizing an E1, E2, and E3 ligase in a step-wise fashion. Unlike ubiquitinylation, which typically leads to protein degradation, SUMOylation of target proteins can regulate an assortment of cellular processes, including interactions between proteins, stability of proteins, regulation of transcription factors, targeting proteins to the nucleus, and higher order chromatin structure (Johnson, 2004; Shuai and Liu, 2005).

The negative regulation of gene expression by PIAS proteins is well characterized. PIAS proteins can inhibit the transcriptional activities of activated STATs and NF-κB by preventing their binding to DNA, although the precise mechanism of this inhibition is still unknown (Chung et al., 1997; Liu et al., 1998; Liu et al., 2005). PIAS proteins can interact with HDACs and repress gene activity by the transcription factors androgen receptor (AR) and Smad3, a repression that was abolished in the presence of the HDAC inhibitor trichostatin A (TSA) (Arora et al., 2003; Long et al., 2003; Gross et al., 2004). PIAS proteins can also SUMOylate target transcription factors, potentially affecting the target protein in a negative or positive fashion as seen with Sp3 and p53, respectively (Sapetschnig et al., 2002; Bischof et al.,

2006).

Section 2: Hematopoietic Stem Cells and the Immune Response

Hematopoietic Stem Cells

The mouse hematopoietic stem cell (HSC) is one of the best characterized adult stem cell systems in mammalian cells (Figure 1.2). HSCs are an ideal system to study stem cells and differentiation because well defined cell surface markers exist to track stem cells at various stages of differentiation by flow cytometry. The cell that contains the vast majority of self-renewing activity is the long-term HSC (LT-HSC). However, there is a limit to the self-renewal capacity, as computational assays estimate that the LT-HSC only divides about five times during the lifespan of a mouse before the self-renewal capacity is exhausted (Wilson et al., 2009). DNA methylation plays a significant role in self-renewal, as *Dnmt1-/-*, and double knockout *Dnmt3a/3b* mice have defective HSC self-renewal capacities (Trowbridge et al., 2009; Tadokoro et al., 2007). Additionally, *Dnmt1-/-* mice exhibit an increase in myeloerythroid cells, indicating that DNA methylation is important for proper lineage differentiation (Trowbridge et al., 2009; Broske et al., 2009).

Regulatory T cells and *Foxp3*

Regulatory T cells (Treg) are key players in the suppression of over-active immune responses. During Treg development, the “master switch” transcription factor *Foxp3* must be expressed and permanent expression is required throughout the lifespan of a Treg cell (Floess et al., 2007). Expression of *Foxp3* is controlled by its promoter and three evolutionarily conserved noncoding DNA sequence (CNS) elements. While CNS3 is important for increasing the frequency of Treg cells, evidence suggests that CNS2 is most important for gene expression, as it contains permissive histone marks and is demethylated in Treg cells but fully methylated in the other T cell lineages (Kim and Leonard, 2007; Zheng et al., 2010; Toker and

Huehn, 2011).

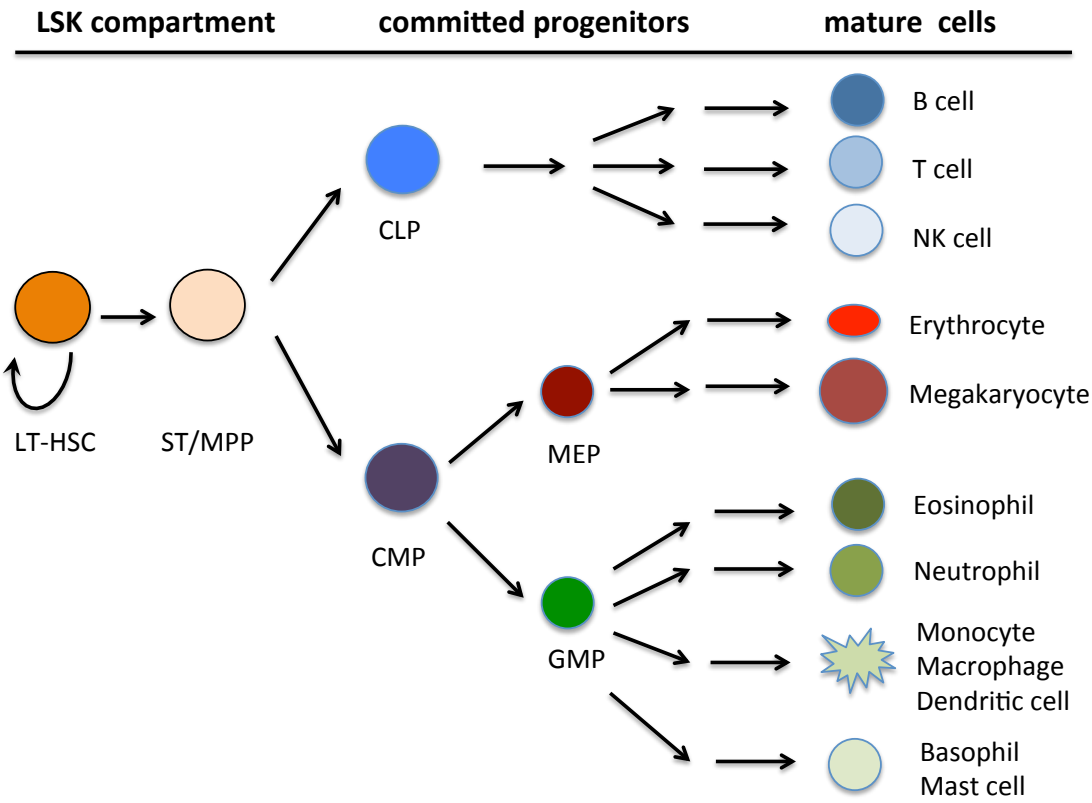

Figure 1.2. Hematopoietic stem cell differentiation and maturation.
Differentiation from the dormant LT-HSC to the committed progenitor to mature cells occurs in a step-wise, hierarchical manner. Curved arrow indicates self-renewal. Note: not all progenitor stages and not all potential mature cells are depicted here. Abbreviations: LSK (Lin-Sca+c-Kit+), LT-HSC (long-term hematopoietic stem cell (HSC)), ST/MPP (short-term multi-potent progenitor), CLP (common lymphoid progenitor), CMP (common myeloid progenitor), MEP (megakaryocyte-erythroid progenitor), GMP (granulocyte-macrophage progenitor). Figure is adapted from Metcalf, 2007 and Blank, Karlsson, and Karlsson, 2008.

T cell development first begins in the bone marrow, where lymphoid progenitors travel to the thymus and the thymus becomes populated with immature thymocytes. Immature thymocytes are characterized by the lack of both T cell receptors CD4 and CD8 (labeled as CD4-CD8-). Upon further maturation, still immature thymocytes now express both CD4 and CD8 (labeled as CD4+CD8+). When thymocytes express only either CD4 or CD8, but not both, they are now mature T cells and can exit the thymus (Germain, 2002). For reference, Treg cells are

CD4+Foxp3+.

Macrophage polarization and controversy

Macrophages are a heterogeneous population of professional phagocytes that play a key role in the innate immune response. Macrophages can be activated by a multitude of stimuli, including growth factors, cytokines, nucleotide derivatives, and viral and bacterial components. Depending on the activation stimuli, macrophages can play key roles in the initiation and/or resolution of inflammation, wound repair, tissue homeostasis, fibrosis, allergic responses, and tumorigenesis, among others (Murray et al., 2011, 2014).

The classification of activated macrophages is quite complicated. In the 1960s George Mackaness introduced the term macrophage activation ("classical activation") to describe the effect of microbial stimuli on macrophages (Martinez and Gordon, 2014). Currently, classical activation is ascribed to the inflammatory gene activation induced by IFN-γ and/or LPS (Murray et al., 2014). In 1992 the concept of "alternative" macrophage polarization was introduced to describe the effect of interleukin-4 (IL-4), that is distinct from the effect of IFN-γ, on the augmentation of the mannose receptor (Stein et al., 1992). Then in 2000, the concept of the M1 and M2 macrophage polarization was introduced. The naming of "M1" and "M2" was inspired by the T helper 1 (Th1) vs. T helper 2 (Th2) concept, in which Th1 strains of mice produce large quantities of nitric oxide (a classical marker of macrophage activation against microbes), whereas Th2 strains are stimulated to metabolize arginine, which antagonizes with nitric oxide production (Mills et al., 2000). Over time, the classical vs. alternative and the M1 vs. M2 polarization ideas fused together. Now, the classical / M1 phenotype is associated with the proinflammatory gene activation induced by IFN-γ and/or LPS and relying on STAT1 to produce nitric oxide, TNF-α, and IL-1, and other inflammatory proteins, whereas the alternative / M2 phenotype is associated with IL-4 and relying on STAT6 and the production of mannose

receptor, arginase, chitinase-like 3 (CHIL3, YM1), resistin like beta (RETNLB), IL-10, and others. (Biswas and Mantovani, 2010; Nahrendorf and Swirski, 2016).

However, based on the plasticity of macrophage activation *in vivo,* one must recognize that the "M1" or "M2" (or "classical" or "alternative") activation states derived *in vitro* are on the extreme end of a spectrum and most likely the *in vivo* macrophage activation state will lie somewhere in between these polar opposites (Murray et al., 2014). Additionally, *in vivo* there are no clear polarization states, as macrophages can switch between M1 and M2, depending on the environmental cues, and macrophages of different organs can respond differently to the same cues (Martinez and Gordon, 2014; Davies and Taylor, 2015; Nahrendorf and Swirski, 2016). Therefore for simplicity the M1 / M2 concept is still useful for studying macrophage activation and function *in vitro*, but can be tricky for *in vivo* studies due to the wide heterogeneity of tissue macrophages.

Section 3: Aims of the Dissertation

Fully understanding the role and application of PIAS proteins has been a great research interest ever since our discovery of these proteins. The creation of the *Pias1-/-* animal model allowed us to explore the role of PIAS1 in various physiological and developmental settings previously unavailable (Liu et al., 2004). Additionally, our knowledge on how PIAS1 regulates gene expression greatly expanded upon the recent exciting discovery of a novel mechanism of PIAS-mediated gene regulation: PIAS1 interaction with DNMTs for epigenetic gene silencing (Chapter 2). The primary focus of this dissertation is to solidify the novel mechanism of PIAS1-mediated epigenetic gene silencing in various cell types and settings (Chapters 2, 3, and 4). As PIAS1 promotes DNA methylation, we became interested in TET proteins as they promote the opposite function: DNA demethylation. Currently the role of TET proteins in innate immunity is poorly understood. As previous work from our lab indicate a role for PIAS1 in inflammatory

responses, we first addressed if TET proteins also have a role in the immune response (Chapter 5).

Chapter 2 will discuss the exciting role of PIAS1 in the epigenetic silencing of the *Foxp3* promoter. Characterization of lymphocyte subpopulations in *Pias1-/-* mice revealed an increase in CD4+Foxp3+ Treg cells. As mentioned earlier, previous groups have uncovered epigenetic mechanisms controlling *Foxp*3 expression. We too asked if a similar epigenetic mechanism is involved in our *Pias1* mice. It was from this study that we discovered a new role for PIAS1 in the negative regulation of genes, specifically, that PIAS1 interacts with the *de novo* DNMT3 methyltransferases in T cells to mediate epigenetic silencing of the *Foxp3* promoter. Furthermore, the repressive H3K9me3 and H3K27me3 modifications are found at PIAS1 target sites.

Chapter 3 explores the role of PIAS1 in the epigenetic regulation of HSC self-renewal and differentiation. Several groups have implicated DNA methylation as an important mechanism for both self-renewal and the proper differentiation of progenitors in hematopoiesis. With the newly discovered mechanism of PIAS1-mediated DNA methylation described in chapter 2, we asked if PIAS1 has a role in HSC maintenance and function through the recruitment of DNMTs. Here we show that PIAS1-mediated epigenetic regulation is required to maintain quiescence of HSCs, and also for the proper expression of lineage-associated genes.

Chapter 4 investigates the role of PIAS1 in epigenetic gene silencing but in the context of human breast cancer cells, specifically in the MDA-MB231 cancer cell line. Numerous studies have correlated DNA hypermethylation of a subset of genes with tumor initiation and progression in human cancers. We asked if PIAS1-mediated DNA methylation has an impact in human cancer. Here, we show that PIAS1 silences a subset of tumor suppressor genes by epigenetic mechanisms, including DNA methylation and histone modifications, resulting in increased tumorigenesis in cells with elevated PIAS1 expression.

Chapter 5 investigates a new direction in our exploration of the immune response, as we explore the relatively unknown role of TET proteins in the innate immune response. We find that *Tet1* and *Tet2* are induced by inflammatory stimuli, suggesting a role for TET in the immune response. Importantly, TET2 is both a repressor and activator of genes in the activation of macrophage responses. Additionally, TET2 silences a subset of inflammatory genes in macrophages, and this has a negative impact in combating bacterial infections.

References

Arora, T., B. Liu, H. He, J. Kim, T.L. Murphy, K.M. Murphy, R.L. Modlin, and K. Shuai. 2003. PIASx is a Transcriptional Co-repressor of signal transducer and Activator of transcription 4. *Journal of Biological Chemistry*. 278:21327–21330. doi:10.1074/jbc.c300119200.

Bischof, O., K. Schwamborn, N. Martin, A. Werner, C. Sustmann, R. Grosschedl, and A. Dejean. 2006. The E3 SUMO Ligase PIASy is a regulator of cellular Senescence and Apoptosis. *Molecular Cell*. 22:783–794. doi:10.1016/j.molcel.2006.05.016.

Biswas, S.K., and A. Mantovani. 2010. Macrophage plasticity and interaction with lymphocyte subsets: Cancer as a paradigm. *Nature Immunology*. 11:889–896. doi:10.1038/ni.1937.

Blank, U., G. Karlsson, and S. Karlsson. 2008. Signaling pathways governing stem-cell fate. *Blood*. 111:492–503. doi:10.1182/blood-2007-07-075168.

Bostick, M., J.K. Kim, P.-O. Esteve, A. Clark, S. Pradhan, and S.E. Jacobsen. 2007. UHRF1 plays a role in maintaining DNA Methylation in mammalian cells. *Science*. 317:1760–1764. doi:10.1126/science.1147939.

Bröske, A.-M., L. Vockentanz, S. Kharazi, M.R. Huska, E. Mancini, M. Scheller, C. Kuhl, A. Enns, M. Prinz, R. Jaenisch, C. Nerlov, A. Leutz, M.A. Andrade-Navarro, S.E.W. Jacobsen, and F. Rosenbauer. 2009. DNA methylation protects hematopoietic stem cell multipotency from myeloerythroid restriction. *Nature Genetics*. 41:1207–1215. doi:10.1038/ng.463.

Chung, C.D., J. Liao, B. Liu, X. Rao, P. Jay, P. Berta, and K. Shuai. 1997. Specific inhibition of stat3 signal transduction by PIAS3. *Science*. 278:1803–1805. doi:10.1126/science.278.5344.1803.

Davies, L.C., and P.R. Taylor. 2015. Tissue-resident macrophages: Then and now. *Immunology*. 144:541–548. doi:10.1111/imm.12451.

Doerfler, W. 1983. DNA methylation and gene activity. *Annual Reviews Biochemistry*. 52:93–124. doi:10.1146/annurev.bi.52.070183.000521.

Esteller, M. 2007. Cancer epigenomics: DNA methylomes and histone-modification maps. *Nature Reviews Genetics*. 8:286–298. doi:10.1038/nrg2005.

Floess, S., J. Freyer, C. Siewert, U. Baron, S. Olek, J. Polansky, K. Schlawe, H.-D. Chang, T. Bopp, E. Schmitt, S. Klein-Hessling, E. Serfling, A. Hamann, and J. Huehn. 2007. Epigenetic control of the foxp3 locus in regulatory T cells. *PLoS Biology*. 5:e38. doi:10.1371/journal.pbio.0050038.

Germain, R.N. 2002. T-cell development and the CD4–CD8 lineage decision. *Nature Reviews Immunology*. 2:309–322. doi:10.1038/nri798.

Gross, M., R. Yang, I. Top, C. Gasper, and K. Shuai. 2004. PIASy-mediated repression of the androgen receptor is independent of sumoylation. *Oncogene*. 23:3059–3066. doi:10.1038/sj.onc.1207443.

Grzenda, A., G. Lomberk, J.-S. Zhang, and R. Urrutia. 2009. Sin3: Master scaffold and transcriptional corepressor. *Biochimica et Biophysica Acta (BBA) - Gene Regulatory Mechanisms*. 1789:443–450. doi:10.1016/j.bbagrm.2009.05.007.

Hashimoto, H., Y. Liu, A.K. Upadhyay, Y. Chang, S.B. Howerton, P.M. Vertino, X. Zhang, and X. Cheng. 2012. Recognition and potential mechanisms for replication and erasure of cytosine hydroxymethylation. *Nucleic Acids Research*. 40:4841–4849. doi:10.1093/nar/gks155.

Hendrich, B., and S. Tweedie. 2003. The methyl-cpG binding domain and the evolving role of DNA methylation in animals. *Trends in Genetics*. 19:269–277. doi:10.1016/s0168-9525(03)00080-5.

Herman, J.G., and S.B. Baylin. 2003. Gene silencing in cancer in association with promoter Hypermethylation. *New England Journal of Medicine*. 349:2042–2054. doi:10.1056/nejmra023075.

He, Y.-F., B.-Z. Li, Z. Li, P. Liu, Y. Wang, Q. Tang, J. Ding, Y. Jia, Z. Chen, L. Li, Y. Sun, X. Li, Q. Dai, C.-X. Song, K. Zhang, C. He, and G.-L. Xu. 2011. Tet-Mediated formation of 5-Carboxylcytosine and its excision by TDG in mammalian DNA. *Science*. 333:1303–1307. doi:10.1126/science.1210944.

Hochstrasser, M. 2001. SP-RING for SUMO. *Cell*. 107:5–8. doi:10.1016/s0092-8674(01)00519-0.

Ichiyama, K., T. Chen, X. Wang, X. Yan, B.-S. Kim, S. Tanaka, D. Ndiaye-Lobry, Y. Deng, Y. Zou, P. Zheng, Q. Tian, I. Aifantis, L. Wei, and C. Dong. 2015. The Methylcytosine Dioxygenase Tet2 promotes DNA Demethylation and activation of cytokine gene expression in T cells. *Immunity*. 42:613–626. doi:10.1016/j.immuni.2015.03.005.

Ito, S., A.C. D'Alessio, O.V. Taranova, K. Hong, L.C. Sowers, and Y. Zhang. 2010. Role of Tet proteins in 5mC to 5hmC conversion, ES-cell self-renewal and inner cell mass specification. *Nature*. 466:1129–1133. doi:10.1038/nature09303.

Ito, S., L. Shen, Q. Dai, S.C. Wu, L.B. Collins, J.A. Swenberg, C. He, and Y. Zhang. 2011. Tet proteins can convert 5-Methylcytosine to 5-Formylcytosine and 5-Carboxylcytosine. *Science*. 333:1300–1303. doi:10.1126/science.1210597.

Jin, S.-G., S. Kadam, and G.P. Pfeifer. 2010. Examination of the specificity of DNA methylation profiling techniques towards 5-methylcytosine and 5-hydroxymethylcytosine. *Nucleic Acids Research*. 38:e125–e125. doi:10.1093/nar/gkq223.

Johnson, E. s. 2004. Protein modification by SUMO. *Annual Reviews Biochem*. 73:355–82. doi:10.1146/annurev.biochem.73.011303.074118.

Kim, H.-P., and W.J. Leonard. 2007. CREB/ATF-dependent T cell receptor–induced FoxP3 gene expression: A role for DNA methylation. *The Journal of Experimental Medicine*. 204:1543–1551. doi:10.1084/jem.20070109.

Kouzarides, T. 2007. Chromatin modifications and their function. *Cell*. 128:693–705. doi:10.1016/j.cell.2007.02.005.

Kriaucionis, S., and N. Heintz. 2009. The nuclear DNA base 5-Hydroxymethylcytosine is present in Purkinje Neurons and the brain. *Science*. 324:929–930. doi:10.1126/science.1169786.

Liu, B., M. Gross, J. ten Hoeve, and K. Shuai. 2001. A transcriptional corepressor of stat1 with an essential LXXLL signature motif. *Proceedings of the National Academy of Sciences*. 98:3203–3207. doi:10.1073/pnas.051489598.

Liu, B., J. Liao, X. Rao, S.A. Kushner, C.D. Chung, D.D. Chang, and K. Shuai. 1998. Inhibition of stat1-mediated gene activation by PIAS1. *Proceedings of the National Academy of Sciences*. 95:10626–10631. doi:10.1073/pnas.95.18.10626.

Liu, B., R. Yang, K.A. Wong, C. Getman, N. Stein, M.A. Teitell, G. Cheng, H. Wu, and K. Shuai. 2005. Negative regulation of NF- B signaling by PIAS1. *Molecular and Cellular Biology*. 25:1113–1123. doi:10.1128/mcb.25.3.1113-1123.2005.

Liu, B., S. Mink, K.A. Wong, N. Stein, C. Getman, P.W. Dempsey, H. Wu, and K. Shuai. 2004. PIAS1 selectively inhibits interferon-inducible genes and is important in innate immunity. *Nature Immunology*. 5:891–898. doi:10.1038/ni1104.

Long, J., I. Matsuura, D. He, G. Wang, K. Shuai, and F. Liu. 2003. Repression of Smad transcriptional activity by PIASy, an inhibitor of activated STAT. *Proceedings of the National Academy of Sciences*. 100:9791–9796. doi:10.1073/pnas.1733973100.

Lorsbach, R.B., J. Moore, S. Mathew, S.C. Raimondi, S.T. Mukatira, and J.R. Downing. 2003. TET1, a member of a novel protein family, is fused to MLL in acute myeloid leukemia containing the t(10;11)(q22;q23). *Leukemia*. 17:637–641. doi:10.1038/sj.leu.2402834.

Maiti, A., and A.C. Drohat. 2011. Thymine DNA Glycosylase can rapidly excise 5-Formylcytosine and 5-Carboxylcytosine: POTENTIAL IMPLICATIONS FOR ACTIVE DEMETHYLATION OF CpG SITES. *Journal of Biological Chemistry*. 286:35334–35338. doi:10.1074/jbc.c111.284620.

Martinez, F.O., and S. Gordon. 2014. The M1 and M2 paradigm of macrophage activation: Time for reassessment. *F1000Prime Reports*. 6. doi:10.12703/p6-13.

Mills, C.D., K. Kincaid, J.M. Alt, M.J. Heilman, and A.M. Hill. 2000. M-1/M-2 Macrophages and the th1/th2 paradigm. *The Journal of Immunology*. 164:6166–6173. doi:10.4049/jimmunol.164.12.6166.

Murray, P.J., J.E. Allen, S.K. Biswas, E.A. Fisher, D.W. Gilroy, S. Goerdt, S. Gordon, J.A. Hamilton, L.B. Ivashkiv, T. Lawrence, M. Locati, A. Mantovani, F.O. Martinez, J.-L. Mege, D.M. Mosser, G. Natoli, J.P. Saeij, J.L. Schultze, K.A. Shirey, A. Sica, J. Suttles, I. Udalova, J.A. van Ginderachter, S.N. Vogel, and T.A. Wynn. 2014. Macrophage activation and polarization: Nomenclature and experimental guidelines. *Immunity*. 41:339–340. doi:10.1016/j.immuni.2014.07.009.

Murray, P.J., and T.A. Wynn. 2011. Protective and pathogenic functions of macrophage subsets. *Nature Reviews Immunology*. 11:723–737. doi:10.1038/nri3073.

Nahrendorf, M., and F.K. Swirski. 2016. Abandoning M1/M2 for a network model of Macrophage function. *Circulation Research*. 119:414–417. doi:10.1161/circresaha.116.309194.

Okano, M., D.W. Bell, D.A. Haber, and E. Li. 1999. DNA Methyltransferases Dnmt3a and Dnmt3b are essential for de novo Methylation and mammalian development. *Cell*. 99:247–257. doi:10.1016/s0092-8674(00)81656-6.

Ono, R., T. Taki, T. Taketani, M. Taniwaki, H. Kobayashi, and Y. Hayashi. 2002. LCX, Leukemia-associated Protein with a CXXC Domain, Is Fused to MLL in Acute Myeloid Leukemia with Trilineage Dysplasia Having t(10;11)(q22;q23). *Cancer Research*. 62:4075–4080.

Plevin, M.J., M.M. Mills, and M. Ikura. 2005. The LxxLL motif: A multifunctional binding sequence in transcriptional regulation. *Trends in Biochemical Sciences*. 30:66–69. doi:10.1016/j.tibs.2004.12.001.

Rasmussen, K.D., and K. Helin. 2016. Role of TET enzymes in DNA methylation, development, and cancer. *Genes & Development*. 30:733–750. doi:10.1101/gad.276568.115.

Rottach, A., H. Leonhardt, and F. Spada. 2009. DNA methylation-mediated epigenetic control. *Journal of Cellular Biochemistry*. 108:43–51. doi:10.1002/jcb.22253.

Rytinki, M.M., S. Kaikkonen, P. Pehkonen, T. Jääskeläinen, and J.J. Palvimo. 2009. PIAS proteins: Pleiotropic interactors associated with SUMO. *Cellular and Molecular Life Sciences*. 66:3029–3041. doi:10.1007/s00018-009-0061-z.

Sapetschnig, A., G. Rischitor, H. Braun, A. Doll, M. Schergaut, F. Melchior, and G. Suske. 2002. Transcription factor sp3 is silenced through SUMO modification by PIAS1. *The EMBO Journal*. 21:5206–5215. doi:10.1093/emboj/cdf510.

Sharif, J., M. Muto, S. Takebayashi, I. Suetake, A. Iwamatsu, T.A. Endo, J. Shinga, Y. Mizutani-Koseki, T. Toyoda, K. Okamura, S. Tajima, K. Mitsuya, M. Okano, and H. Koseki. 2007. The SRA protein Np95 mediates epigenetic inheritance by recruiting Dnmt1 to methylated DNA. *Nature*. 450:908–912. doi:10.1038/nature06397.

Shuai, K., and B. Liu. 2005. Regulation of gene-activation pathways by PIAS proteins in the immune system. *Nature Reviews Immunology*. 5:593–605. doi:10.1038/nri1667.

Smith, Z.D., and A. Meissner. 2013. DNA methylation: Roles in mammalian development. *Nature Reviews Genetics*. 14:204–220. doi:10.1038/nrg3354.

Stein, M., S. Keshav, N. Harris, and S. Gordon. 1992. Interleukin 4 potently enhances murine macrophage mannose receptor activity: A marker of alternative immunologic macrophage activation. *Journal of Experimental Medicine*. 176:287–292. doi:10.1084/jem.176.1.287.

Tadokoro, Y., H. Ema, M. Okano, E. Li, and H. Nakauchi. 2007. De novo DNA methyltransferase is essential for self-renewal, but not for differentiation, in hematopoietic stem cells. *The Journal of Experimental Medicine*. 204:715–722. doi:10.1084/jem.20060750.

Tahiliani, M., K.P. Koh, Y. Shen, W.A. Pastor, H. Bandukwala, Y. Brudno, S. Agarwal, L.M. Iyer, D.R. Liu, L. Aravind, and A. Rao. 2009. Conversion of 5-Methylcytosine to 5-Hydroxymethylcytosine in mammalian DNA by MLL partner TET1. *Science*. 324:930–935. doi:10.1126/science.1170116.

Tan, M., H. Luo, S. Lee, F. Jin, J.S. Yang, E. Montellier, T. Buchou, Z. Cheng, S. Rousseaux, N. Rajagopal, Z. Lu, Z. Ye, Q. Zhu, J. Wysocka, Y. Ye, S. Khochbin, B. Ren, and Y. Zhao. 2011. Identification of 67 Histone marks and Histone Lysine Crotonylation as a new type of Histone modification. *Cell*. 146:1016–1028. doi:10.1016/j.cell.2011.08.008.

Toker, A., and J. Huehn. 2011. To be or not to be a Treg cell: Lineage decisions controlled by epigenetic mechanisms. *Science Signaling*. 4:pe4–pe4. doi:10.1126/scisignal.2001783.

Trowbridge, J.J., J.W. Snow, J. Kim, and S.H. Orkin. 2009. DNA Methyltransferase 1 is essential for and uniquely regulates Hematopoietic stem and Progenitor cells. *Cell Stem Cell*. 5:442–449. doi:10.1016/j.stem.2009.08.016.

Valinluck, V., H.-H. Tsai, D.K. Rogstad, A. Burdzy, A. Bird, and L.C. Sowers. 2004. Oxidative damage to methyl-cpG sequences inhibits the binding of the methyl-cpG binding domain (MBD) of methyl-cpG binding protein 2 (MeCP2). *Nucleic Acids Research*. 32:4100–4108. doi:10.1093/nar/gkh739.

Williams, K., J. Christensen, and K. Helin. 2011a. DNA methylation: TET proteins—guardians of CpG islands? *EMBO reports*. 13:28–35. doi:10.1038/embor.2011.233.

Williams, K., J. Christensen, M.T. Pedersen, J.V. Johansen, P.A.C. Cloos, J. Rappsilber, and K. Helin. 2011b. TET1 and hydroxymethylcytosine in transcription and DNA methylation fidelity. *Nature*. 473:343–348. doi:10.1038/nature10066.

Wilson, A., E. Laurenti, G. Oser, R.C. van der Wath, W. Blanco-Bose, M. Jaworski, S. Offner, C. Dunant, L. Eshkind, E. Bockamp, P. Lio, H.R. MacDonald, and A. Trumpp. 2009. Hematopoietic stem cells Reversibly switch from Dormancy to self-renewal during Homeostasis and repair. *Cell*. 138:209. doi:10.1016/j.cell.2009.06.020.

Wu, H., A.C. D'Alessio, S. Ito, K. Xia, Z. Wang, K. Cui, K. Zhao, Y. Eve Sun, and Y. Zhang. 2011. Dual functions of Tet1 in transcriptional regulation in mouse embryonic stem cells. *Nature*. 473:389–393. doi:10.1038/nature09934.

Wu, H., and Y. Zhang. 2014. Reversing DNA Methylation: Mechanisms, Genomics, and biological functions. *Cell*. 156:45–68. doi:10.1016/j.cell.2013.12.019.

Zhang, H., X. Zhang, E. Clark, M. Mulcahey, S. Huang, and Y.G. Shi. 2010. TET1 is a DNA-binding protein that modulates DNA methylation and gene transcription via hydroxylation of 5-methylcytosine. *Cell Research*. 20:1390–1393. doi:10.1038/cr.2010.156.

Zhang, Q., K. Zhao, Q. Shen, Y. Han, Y. Gu, X. Li, D. Zhao, Y. Liu, C. Wang, X. Zhang, X. Su, J. Liu, W. Ge, R.L. Levine, N. Li, and X. Cao. 2015. Tet2 is required to resolve inflammation by recruiting Hdac2 to specifically repress IL-6. *Nature*. 525:389–393. doi:10.1038/nature15252.

Zheng, Y., S. Josefowicz, A. Chaudhry, X.P. Peng, K. Forbush, and A.Y. Rudensky. 2010. Role of conserved non-coding DNA elements in the Foxp3 gene in regulatory t-cell fate. *Nature*. 463:808–812. doi:10.1038/nature08750.

Chapter 2: The Ligase PIAS1 Restricts Natural Regulatory T Cell Differentiation By Epigenetic Repression

Abstract

$CD4^+Foxp3^+$ regulatory T (Treg) cells are important for maintaining immune tolerance. Understanding the molecular mechanism that regulates Treg differentiation will facilitate the development of effective therapeutic strategies against autoimmune diseases. We report here that the PIAS1 SUMO E3 ligase restricts the differentiation of natural Treg cells by maintaining a repressive chromatin state of the *Foxp3* promoter. PIAS1 acts by binding to the *Foxp3* promoter to recruit DNA methyltransferases and HP1 (heterochromatin protein 1) for epigenetic modifications. *Pias1* deletion caused promoter demethylation, reduced H3K9 methylation, and enhanced promoter accessibility. Consistently, *Pias1*$^{-/-}$ mice displayed an increased natural Treg cell population and were resistant to the development of experimental autoimmune encephalomyelitis. Our studies have identified a novel epigenetic mechanism that negatively regulates the differentiation of natural Treg cells.

Introduction and Results

Naturally occurring thymus-derived regulatory T (nTreg) cells plays a critical role in the maintenance of self-tolerance and homeostasis within the immune system (*1*-*4*). The transcription factor Foxp3 controls the development and function of Treg cells (*5*-*7*). Several regulatory DNA elements within the *Foxp3* locus have been suggested to play important roles in mediating Foxp3 expression, including the promoter region and conserved noncoding sequences (*6*-*9*). Although significant progress has been made toward the identification of transcription factors that positively regulate Foxp3 expression (*10*-*13*), little is known about the negative regulatory mechanism involved in the process.

PIAS1 (protein inhibitor of activated STAT1) is a SUMO E3 ligase that binds to the chromatin to repress gene activation (*14, 15*). The recruitment of PIAS1 to the chromatin requires the SUMO ligase-dependent Ser90 phospohrylation of PIAS1 induced by a variety of immune regulatory stimuli including TCR (T-cell receptors) activation (*16*). To explore the potential regulatory role of PIAS1 in T cells, the activation status of PIAS1 was examined in thymus and spleen. PIAS1 was activated in freshly isolated thymocytes and splenocytes, as evident by the presence of PIAS1 Ser90 phosphorylation (Fig. 2.1A). FACS analyses indicated that there was a small increase of the percentage of thymic single positive $CD4^+$ or $CD8^+$ T cells in *Pias1*$^{-/-}$ mice, although the total T cell number was not significantly altered (Supplementary Fig. 2.1). Interestingly, the population of thymic $CD4^+Foxp3^+$ Treg cells (natural Treg or nTreg) was significantly increased (about 80%) in *Pias1*$^{-/-}$ male and female mice (Fig. 2.1B). An increase of the periphery $CD4^+Foxp3^+$ Treg cells was also observed in *Pias1*$^{-/-}$ mice (Fig. 2.1B). However, the mean intensity of Foxp3 expression in $Foxp3^+$ cells was not significantly altered by *Pias1* deletion (Fig. 2.1C). In addition, *Pias1* disruption did not affect the *in vivo* proliferation or survival of Treg cells (Supplementary Fig. 2.2).

To test whether PIAS1 directly regulates the intrinsic differentiation potential of nTreg cells, bone marrow from wild type and *Pias1*$^{-/-}$ mice depleted of $CD4^+$ and $CD8^+$ T cells was transplanted into sublethally irradiated *Rag1*$^{-/-}$ recipient mice. 4 weeks post transplantation, the $CD4^+Foxp3^+$ population of T cells in the thymus was examined by FACS analysis. *Pias1* disruption caused a 4-fold increase of the thymic $CD4^+Foxp3^+$ cell population (Fig. 2.1D). To further validate these findings, transplantation experiments were performed by injecting *Rag1*$^{-/-}$ mice with a mixture of bone marrow from wild type $CD45.1^+$C57SJL mice and either wild type or *Pias1*$^{-/-}$ mice (CD45.2). Consistently, the percentage of thymic $CD4^+Foxp3^+$ from *Rag1*$^{-/-}$ mice reconstituted with *Pias1*$^{-/-}$ bone marrow (CD45.2) was significantly higher than that of the wild type controls, while no difference was observed in thymic $CD4^+Foxp3^+$ differentiation of the

CD45.1$^+$ control T cells (Fig. 2.1E). These studies support a role of PIAS1 in the negative regulation of nTreg cell differentiation.

Peripheral naive CD4$^+$ T cells can be differentiated into so-called induced Treg cells (iTreg) (*17-19*). *In vitro* differentiation studies indicate that transient TCR activation positively regulates iTreg differentiation, while persistent TCR stimulation antagonizes Foxp3 induction (*20*). *Pias1* disruption enhanced iTreg differentiation when naive CD4$^+$ T cells were transiently stimulated by TCR for 15 hrs followed by culturing for additional 60 hrs with or without TGF-β treatment in the absence of TCR stimulation (Fig. 2.1F). In contrast, iTreg differentation was inhibited under persistent TCR stimulating conditions (Supplementary Fig. 2.3C). Thus, *Pias1* disruption amplified the effect of TCR on iTreg differentiation, which is consistent with a negative regulatory role of PIAS1 in TCR signaling.

nTreg cells play an important role in suppressing autoimmune diseases. To test the biological significance of PIAS1-mediated regulation of nTreg *in vivo*, the response of *Pias1*$^{-/-}$ mice together with the wild type littermate controls to Myelin Oligodendrocyte Glycoprtein (MOG)-induced experimental autoimmune encephalomyelitis (EAE) was examined. 10 days post MOG immunization, an increased population of CD4$^+$Foxp3$^+$ Treg cells in the lymph nodes of *Pias1*$^{-/-}$ mice was detected as compared to the wild type controls (Fig. 2.2A). The antigen-specific induction of IFN-γ and IL-17 was significantly suppressed, while a higher level of TGF-β was detected in *Pias1*$^{-/-}$ lymphocytes (Fig. 2.2B). Consistently, intracellular staining assays showed a reduced percentage of antigen-specific IFN-γ or IL-17-producing T cells (Fig. 2.2C). In addition, a defect in lymphocyte proliferation in response to MOG, but not polyclonal anti-CD3 stimulation was observed in *Pias1*$^{-/-}$ mice (Fig. 2.2D). To exclude the possibility that PIAS1 may have an intrinsic ability to regulate the differentiation of Th1 or Th17 cells, purified naive CD4$^+$ cells were cultured under several differentiation conditions. The results showed that the differentiation of

Th1 or Th17 cells was not defective *in vitro* in the absence of PIAS1 (Supplementary Fig. 2.3A-C). These results suggest that the increased Treg cells in *Pias1*$^{-/-}$ mice suppressed the induction of Th1 and Th17 cells in response to MOG challenge. Indeed, *Pias1*$^{-/-}$ mice displayed resistance toward the development of EAE (Fig. 2.2E). In accordance with the observed phenotypes, significantly reduced levels of IFN-γ and IL-17, but increased levels of TGF-β, was detected in the lymph nodes of *Pias1*$^{-/-}$ mice (Fig. 2.2F). These findings support an important regulatory role of PIAS1 in nTreg cell differentiation and the onset of autoimmune diseases.

Next, we performed experiments to examine the molecular mechanism of PIAS1-mediated regulation of nTreg cell differentiation. PIAS1 contains a chromatin-binding domain that targets PIAS1 to gene promoters to regulate transcription (*14-16*). We tested the hypothesis that *Foxp3* may be a direct PIAS1-target gene by ChIP assays. PIAS1 binds to the *Foxp3* promoter, but not the two intronic elements in thymic $CD4^+CD8^+$ or naive $CD4^+CD25^-$ T cells (Fig. 2.3A and Supplementary Fig. 2.4B). In contrast, the binding of PIAS1 to the *Foxp3* promoter was weak in thymic and peripheral $CD4^+CD25^+$ cells, which is consistent with the reduced expression of PIAS1 detected in these cells (Supplementary Fig. 2.4A).

We hypothesized that the binding of PIAS1 to the *Foxp3* gene promoter may influence the chromatin status of the *Foxp3* locus. We performed three independent assays to test this hypothesis, including the examination of the chromatin modifications, transcription factor recruitment, and restriction enzyme accessibility analysis of the *Foxp3* locus in *Pias1*$^{-/-}$ T cells.

DNA methylation of the *Foxp3* promoter and the intronic elements play an important role in the regulation of *Foxp3* expression (*6, 7*). The *Foxp3* promoter is hypermethylated in $CD4^+CD25^-$, but hypomethylated in $CD4^+CD25^+$ cells (*21-26*), which inversely correlates with the levels of PIAS1 expression (Supplementary Fig. 2.4A). To test if PIAS1 indeed affects the promoter

methylation of *Foxp3* gene, bisulfite-sequencing analysis was performed to examine the methylation of the *Foxp3* locus in various subpopulations of wild type and *Pias1*$^{-/-}$ cells. Several CpG sites in the *Foxp3* promoter were hypermethylated in wild type thymic CD4^{+}CD8^{+} DP, CD4^{+}CD25^{-} and peripheral naive CD4^{+}CD25^{-} T cells, but were hypomethylated in thymic and peripheral CD4^{+}CD25^{+} Treg cells (Fig. 2.3B). Importantly, *Pias1* disruption caused a significant reduction of DNA methylation of the *Foxp3* promoter in thymic CD4^{+}CD8^{+} DP, CD4^{+}CD25^{-} and peripheral naive CD4^{+}CD25^{-} T cells (Fig. 2.3B). In contrast, the removal of PIAS1 showed no effect on the DNA methylation of the heavily methylated CNS2 element (Supplementary Fig. 2.5A), which is consistent with the lack of significant PIAS1 binding to the CNS2 region (Fig. 2.3A). In wild type Lineage marker^{-}, Scal1^{+}, c-Kit^{+} (LSK) cells, a population highly enriched in hematopoietic stem cells (HSC), the *Foxp3* promoter was only modestly methylated, but upon differentiation to the common lymphoid progenitors (CLP) and thymic CD4^{-}CD8^{-} DN cells, the extent of the *Foxp3* promoter methylation was significantly increased. Interestingly, the *Foxp3* promoter methylation was significantly reduced in *Pias1*$^{-/-}$ CLP (Supplementary Fig. 2.5B).

To examine if PIAS1 also plays a role in the methylation of other gene promoters, we performed similar studies on CD25, a key regulator of Treg cell differentiation (*4, 6*). ChIP studies showed that PIAS1 binds to the *Cd25* gene promoter, suggesting that *Cd25* is also a PIAS1-target gene (Supplementary Fig. 2.6A). Bisulphite-sequencing analysis indicates that the *Cd25* gene promoter was clearly hypermethylated in HSCs, but was hypomethylated in naive CD4^{+} CD25^{-} cells (Supplementary Fig. 2.6B). Interestingly, *Pias1* disruption resulted in the hypomethylation of the *Cd25* gene promoter in HSC cells. The finding that PIAS1-mediated epigenetic regulation of the *Cd25* gene occurs at as early as the HSC stage supports the proposed two-step model of Treg cell differentiation (*27*). Consistent with a negative regulatory role of PIAS1 in the epigenetic control of the *Cd25* gene, an increased CD4^{+}CD25^{+} population of T cells was observed in *Pias1*$^{-/-}$ thymocytes and spleen (Supplementary Fig. 2.6D), and also in bone

marrow transplantation studies (Supplementary Fig. 2.6E & 2.6F), similar to the results observed with the *Foxp3* gene (Fig. 2.1B, 2.1D, 2.1E).

We also examined the chromatin status of the *Foxp3* promoter by analyzing histone modifications. ChIP analysis showed a reduction of the repressive histone H3K9 methylation code in *Pias1*$^{-/-}$ CD4^{+}CD8^{+} thymocytes, while *Pias1* disruption showed no significant effect on H3K27 or H3 histone acetylation marks (Fig. 2.3C). These findings further support a role of PIAS1 in maintaining a repressive chromatin state of the *Foxp3* promoter.

To further validate the role of PIAS1 in regulating the chromatin structure of the *Foxp3* promoter, restriction enzyme accessibility analysis (REA) on the *Foxp3* locus was performed as previously described (*21*). Enhanced accessibility of the *Foxp3* promoter, but not the PIAS1 non-binding CNS2 region, was observed in *Pias1*$^{-/-}$ thymic CD4^{+}CD8^{+} DP and naive CD4^{+}CD25^{-} T cells (Fig. 2.3D), supporting a more open chromatin structure of the *Foxp3* promoter in *Pias1*$^{-/-}$ T cells.

To further test the hypothesis that PIAS1 regulates the chromatin status of the *Foxp3* promoter, we examined the binding of STAT5, a key transcription factor involved in *Foxp3* induction (*10-12*), to the *Foxp3* locus in wild type and *Pias1*$^{-/-}$ CD4^{+}CD8^{+} DP thymocytes. No significant STAT5 binding to the *Foxp3* promoter or the CNS regions was detected in wild type DP thymocytes. However, *Pias1* disruption resulted in the binding of a significant amount of STAT5 to the *Foxp3* gene promoter, but not the CNS elements, in DP thymocytes (Fig. 2.3E), although the level of STAT5 protein or STAT5 phosphorylation was not significantly affected by *Pias1* disruption (Supplementary Fig. 2.7A & 2.7B). A significant increase of NFAT binding to the *Foxp3* promoter in *Pias1*$^{-/-}$ DP thymocytes was also observed (*13*) (Fig. 2.3E). The enhanced accessibility of the *Foxp3* promoter toward transcription factors in the absence of PIAS1 should increase the probability of Foxp3 expression. Indeed, *Pias1* disruption resulted in the increased

frequency of Foxp3$^+$ DP thymocytes (Supplementary Fig. 2.8). Enhanced STAT5 activity in DP thymocytes promotes nTreg differentiation (*10-12*), which is consistent with the increased population of Foxp3$^+$ nTreg cells in the thymus of *Pias1*$^{-/-}$ mice. Taken together, our results support the hypothesis that PIAS1 maintains a repressive chromatin status of the *Foxp3* promoter. The removal of PIAS1 enhances the accessibility of *Foxp3* gene promoter toward transcription factors, and thus the increased probability for the differentiation of Foxp3$^+$ Treg cells.

We wished to understand how PIAS1 regulates the chromatin status of the *Foxp3* promoter. We tested the hypothesis that PIAS1, a chromatin-associated protein, may maintain a repressive chromatin structure through the recruitment of chromatin-modifying enzymes. DNA methyltransferases (DNMTs) promote DNA methylation of the chromatin (*28*). Indeed, DNMT1 has been suggested to regulate the DNA methylation of the CNS2 region (*21, 26, 29*). We performed experiments to test the hypothesis that PIAS1 may participate in the recruitment of DNMTs to the *Foxp3* locus. PIAS1 has been shown to interact with DNMT3B in a yeast two-hybrid screen and in 293T cells under overexpression conditions (*30, 31*). Co-IP assays were performed to examine if the endogenous PIAS1 is associated with DNMTs in thymocytes or peripheral naive CD4$^+$CD25$^-$ cells. DNMT3A and DNMT3B, but not DNMT1, were present in the PIAS1 immunoprecipitates (Fig. 2.4A). No such interactions were detected in the IgG negative controls (Fig. 2.4A). These studies indicate that the endogenous PIAS1 protein is associated with DNMT3A and DNMT3B in T cells.

Next, sequential ChIP assays were performed to test if PIAS1 is associated with DNMT3A and DNMT3B on the *Foxp3* promoter. Extracts prepared from wild type thymocytes were subjected to ChIP assays with anti-PIAS1 antibody, followed by re-ChIP assays with anti-DNMT3A or anti-DNMT3B. Sequential ChIP studies indicate that PIAS1 forms a complex with DNMT3A and DNMT3B on the *Foxp3* gene promoter (Fig. 2.4B).

We tested if PIAS1 plays a role in the recruitment of DNMT3A and DNMT3B to the *Foxp3* gene promoter by ChIP assays. DNMT3B showed a significant binding to both the *Foxp3* promoter and the CNS2 region, but not the CNS1 element, in the wild type DP thymocytes (Fig. 2.4C). A modest amount of DNMT3A was also found to be associated with both the *Foxp3* promoter and the CNS2 element. However, no significant binding of DNMT3A or DNMT3B to the *Foxp3* promoter was detected in $CD4^+CD25^+$ Treg cells that have low levels of PIAS1 expression and promoter hypomethylation (Supplementary Fig. 2.9). Most importantly, *Pias1* deletion completely abolished the binding of both DNMT3A and DNMT3B to the *Foxp3* gene promoter in thymic DP cells (Fig. 2.4C), although the levels of DNMT expression were not affected by *Pias1* disruption (Supplementary Fig. 2.7C). In contrast, the binding of DNMT3A and DNMT3B to the CNS2 region was not affected by *Pias1* disruption (Fig. 2.4C), consistent with the finding that PIAS1 does not bind to the CNS2 element (Fig. 2.3A). The PIAS1-dependent recruitment of DNMTs to the *Foxp3* promoter was also observed in peripheral naive $CD4^+CD25^-$ cells (Supplementary Fig. 2.10). These results indicate that PIAS1 is required for the recruitment of DNMT3A and DNMT3B to the *Foxp3* gene promoter.

To test if DNMT3A and DNMT3B play a role in the *Foxp3* promoter methylation, transplantation experiments were performed using mice in which the functional domains of both *Dnmt3a* and *Dnmt3b* genes are flanked by two loxP sites ($Dnmt3a^{2lox/2lox}$/$Dnmt3b^{2lox/2lox}$) (*32, 33*). Bone marrow cells from $Dnmt3a^{2lox/2lox}$/$Dnmt3b^{2lox/2lox}$ mice were infected with GFP or Cre-GFP retrovirus. Genotyping analysis confirmed the deletion of *Dnmt3a* and *Dnmt3b* by the retroviral *Cre* gene transduction (Supplementary Fig. 2.11A). GFP^+ bone marrow was sorted by flow cytometry and transplanted into sublethally irradiated $Rag1^{-/-}$ mice. 4 weeks post transplantation, thymocytes from the recipient mice were harvested for bisulphite-sequencing analysis. Decreased *Foxp3* promoter methylation (Fig. 2.4D) was observed in thymocytes from the $Rag1^-$

$^{/-}$ mice reconstituted with the Cre retroviral-transduced bone marrow. Consistently, enhanced thymic Foxp3^{+} cell population was observed in the Cre retroviral-transduced recipient mice (Supplementary Fig. 2.11B). Interestingly, decreased DNMT3A and DNMT3B expression by the Cre transduction had no significant effect on the binding of PIAS1 to the *Foxp3* promoter (Supplementary Fig.2.11C). These results support the hypothesis that PIAS1 recruits DNMTs to the *Foxp3* gene promoter to negatively regulation Treg differentiation.

PIAS1 is required for maintaining the repressive H3K9 methylation mark on the *Foxp3* promoter (Fig. 2.3C). Since HP1 (heterochromatin protein 1) plays an important role in promoting H3K9 methylation and is known to interact with DNMTs (*34*), we tested the hypothesis that PIAS1 may also be required for the recruitment of HP1 to the *Foxp3* promoter. ChIP analysis showed that HP1γ was strongly associated with the *Foxp3* promoter in wild type thymocytes. *Pias1* deletion disrupted the promoter recruitment of HP1γ (Fig. 2.4E). These results are consistent with a role of PIAS1 in the maintenance of H3K9 methylation on the *Foxp3* promoter. A similar effect was also detected on the *Cd25* gene promoter (Supplementary Fig. 2.6C). The PIAS1-mediated epigenetic gene regulation is selective since the chromatin status of genes such as *Ctla4*, which is not a PIAS1 downstream target, was not significantly affected by *Pias1* disruption (Supplementary Fig. 2.12).

Discussion

Studies described in this manuscript have identified a novel epigenetic control mechanism in the negative regulation of Foxp3^{+} nTreg differentiation. Our findings suggest that PIAS1 is a newly identified epigenetic regulator that controls the chromatin status of the *Foxp3* locus. PIAS1 acts by maintaining a repressive chromatin state of the *Foxp3* promoter, at least partly through the recruitment of DNMTs and HP1 to promote epigenetic modifications (Fig. 2.4F). *Pias1* disruption

results in the formation of a permissive chromatin structure of the *Foxp3* promoter and the enhanced promoter accessibility toward transcription factors such as STAT5 and NFAT, leading to the increased probability for precursor cells to differentiate into $Foxp3^+$ Treg cells (Fig. 2.4G). The physiological role of PIAS1 in the regulation of *Foxp3* gene is supported by the observed increase of the $Foxp3^+$ nTreg population in *Pias1*$^{-/-}$ mice, and the resistance of *Pias1*$^{-/-}$ mice toward the development of EAE. Thus, the PIAS1 pathway may represent a novel therapeutic target for the treatment of autoimmune diseases. DNMTs have no intrinsic sequence specificity (*28*). Our finding that PIAS1 regulates the binding of DNMTs to the *Foxp3* promoter, but not the CNS2 element, suggests that PIAS1 may be an important cofactor that confers specificity in the DNMT-mediated chromatin methylation. The PIAS1-mediated DNA methylation and histone modifications may serve as a fine-tuning mechanism in the control of epigenetic modifications during T-cell differentiation.

References

1. S. Hori, T. Nomura, S. Sakaguchi, *Science* **299**, 1057-61 (2003).

2. J. D. Fontenot, M. A. Gavin, A. Y. Rudensky, *Nat Immunol* **4**, 330-6 (2003).

3. J. L. Riley, C. H. June, B. R. Blazar, *Immunity* **30**, 656-65 (2009).

4. S. Sakaguchi, T. Yamaguchi, T. Nomura, M. Ono, *Cell* **133**, 775-87 (2008).

5. L. F. Lu, A. Rudensky, *Genes Dev* **23**, 1270-82 (2009).

6. S. Z. Josefowicz, A. Rudensky, *Immunity* **30**, 616-25 (2009).

7. J. Huehn, J. K. Polansky, A. Hamann, *Nat Rev Immunol* **9**, 83-9 (2009).

8. G. Lal *et al.*, *J Immunol* **182**, 259-73 (2009).

9. Y. Zheng *et al.*, *Nature* **463**, 808-12 (2010).

10. M. A. Burchill *et al.*, *J Immunol* **171**, 5853-64 (2003).

11. M. A. Burchill, J. Yang, C. Vogtenhuber, B. R. Blazar, M. A. Farrar, *J Immunol* **178**, 280-90 (2007).

12. Z. Yao *et al.*, *Blood* **109**, 4368-75 (2007).

13. Y. Wu *et al.*, *Cell* **126**, 375-87 (2006).

14. K. Shuai, B. Liu, *Nat Rev Immunol* **5**, 593-605 (2005).

15. B. Liu, K. Shuai, *Trends Pharmacol Sci* **29**, 505-9 (2008).

16. B. Liu *et al.*, *Cell* **129**, 903-14 (2007).

17. W. Chen *et al.*, *J Exp Med* **198**, 1875-86 (2003).

18. K. Kretschmer *et al.*, *Nat Immunol* **6**, 1219-27 (2005).

19. M. A. Curotto de Lafaille, J. J. Lafaille, *Immunity* **30**, 626-35 (2009).

20. S. Sauer *et al.*, *Proc Natl Acad Sci U S A* **105**, 7797-802 (2008).

21. H. P. Kim, W. J. Leonard, *J Exp Med* **204**, 1543-51 (2007).

22. U. Baron *et al.*, *Eur J Immunol* **37**, 2378-89 (2007).

23. S. Floess *et al.*, *PLoS Biol* **5**, e38 (2007).

24. P. C. Janson *et al.*, *PLoS One* **3**, e1612 (2008).

25. J. K. Polansky *et al.*, *Eur J Immunol* **38**, 1654-63 (2008).

26. M. Nagar *et al.*, *Int Immunol* **20**, 1041-55 (2008).

27. C. W. Lio, C. S. Hsieh, *Immunity* **28**, 100-11 (2008).

28. M. G. Goll, T. H. Bestor, *Annu Rev Biochem* **74**, 481-514 (2005).

29. S. Z. Josefowicz, C. B. Wilson, A. Y. Rudensky, *J Immunol* **182**, 6648-52 (2009).

30. Y. Ling *et al.*, *Nucleic Acids Res* **32**, 598-610 (2004).

31. J. Park *et al.*, *J Mol Med* **86**, 1269-77 (2008).

32. M. Kaneda *et al.*, *Nature* **429**, 900-3 (2004).

33. J. E. Dodge *et al.*, *J Biol Chem* **280**, 17986-91 (2005).

34. C. Maison, G. Almouzni, *Nat Rev Mol Cell Biol* **5**, 296-304 (2004).

35. We thank V. Chernishof for technical assistance. Supported by grants from the NIH (K.S.). B.L. is supported by a Research Scientist Development Award from the National Institutes of Health (K01 AR52717-01). S. T. is supported by UCLA Tumor Immunology Training Fellowship.

Figures

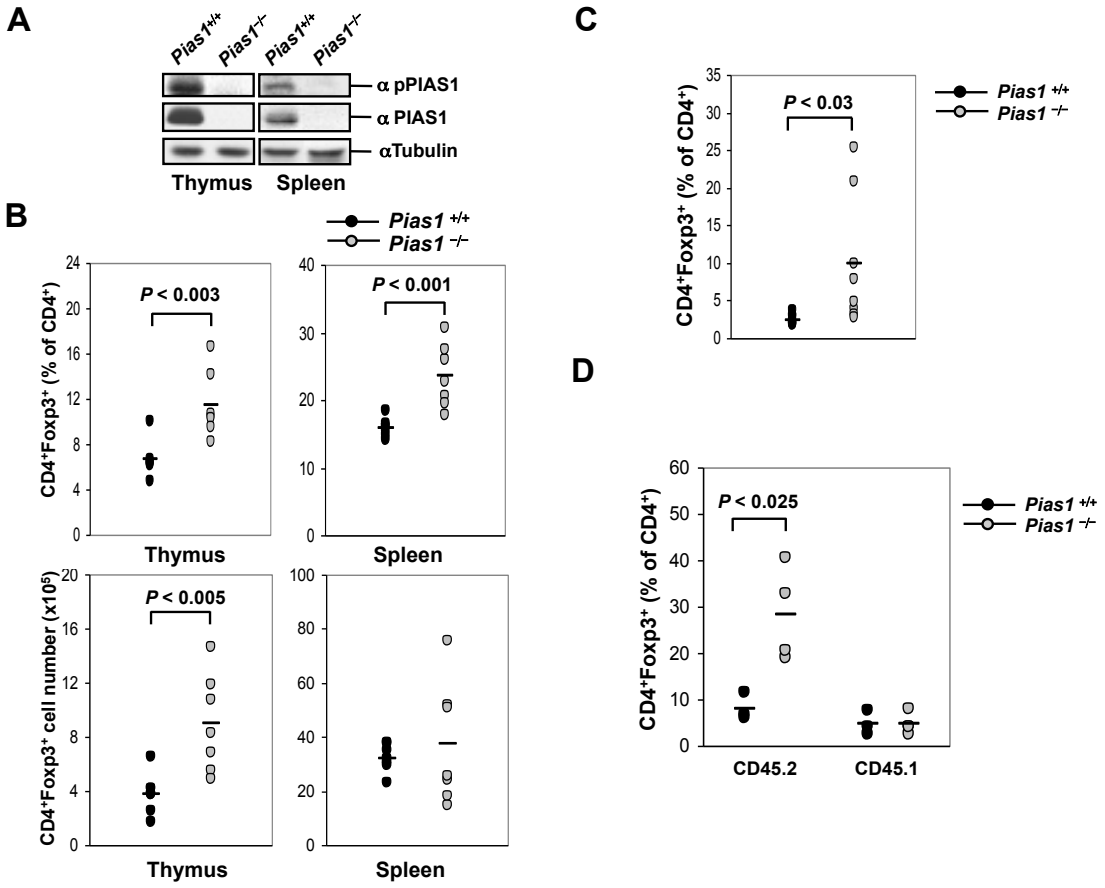

Figure 2.1. Enhanced CD4$^+$Foxp3$^+$ Treg differentiation in *Pias1*$^{-/-}$ mice. **(A)** Western blot analysis of whole cell extracts from freshly isolated thymocytes and splenocytes using an antibody specific for Ser90-phosphorylated PIAS1 (αpPIAS1), total PIAS1 (αPIAS1), or Tubulin. (**B**) Cells from thymus or spleen of male (n=7) or female (n=5) WT and *Pias1*$^{-/-}$ littermates were analyzed by flow cytometry to determine the percentage of Foxp3$^+$ cells out of CD4$^+$ cells (gated on CD4$^+$CD8$^-$ population). *P* value was determined by non-paired *t*-test. (**C**) The same as in **B** except that the mean fluorescence intensity (MFI) of Foxp3 of the CD4$^+$Foxp3$^+$ population was shown (n=12). **(D)** Bone marrow was isolated from WT and *Pias1*$^{-/-}$ littermates, and injected into the sublethally irradiated *Rag1*$^{-/-}$ recipient mice (n=8). The thymic CD4$^+$Foxp3$^+$ population was analyzed 4 weeks post reconstitution by flow cytometry. *P* value was determined by non-paired *t*-test. **(E)** Same as in **D** except that *Pias1*$^{-/-}$ or WT bone marrow (CD45.2) was mixed with WT C57SJL bone marrow (CD45.1), and injected into the *Rag1*$^{-/-}$ mice (n=3 for WT and n=4 for *Pias1*$^{-/-}$). **(F)** *In vitro* inducible Treg (iTreg) differentiation assays were performed with FACS-sorted CD4$^+$CD25$^-$ splenic T cells under transient TCR treatment, and the percentage of Foxp3$^+$ cells out of CD4$^+$ cells were determined by flow cytometry (indicated by the numbers in the upper right quadrants). Shown is a representative of 3 independent experiments with 4-6 pairs of mice for each experiment.

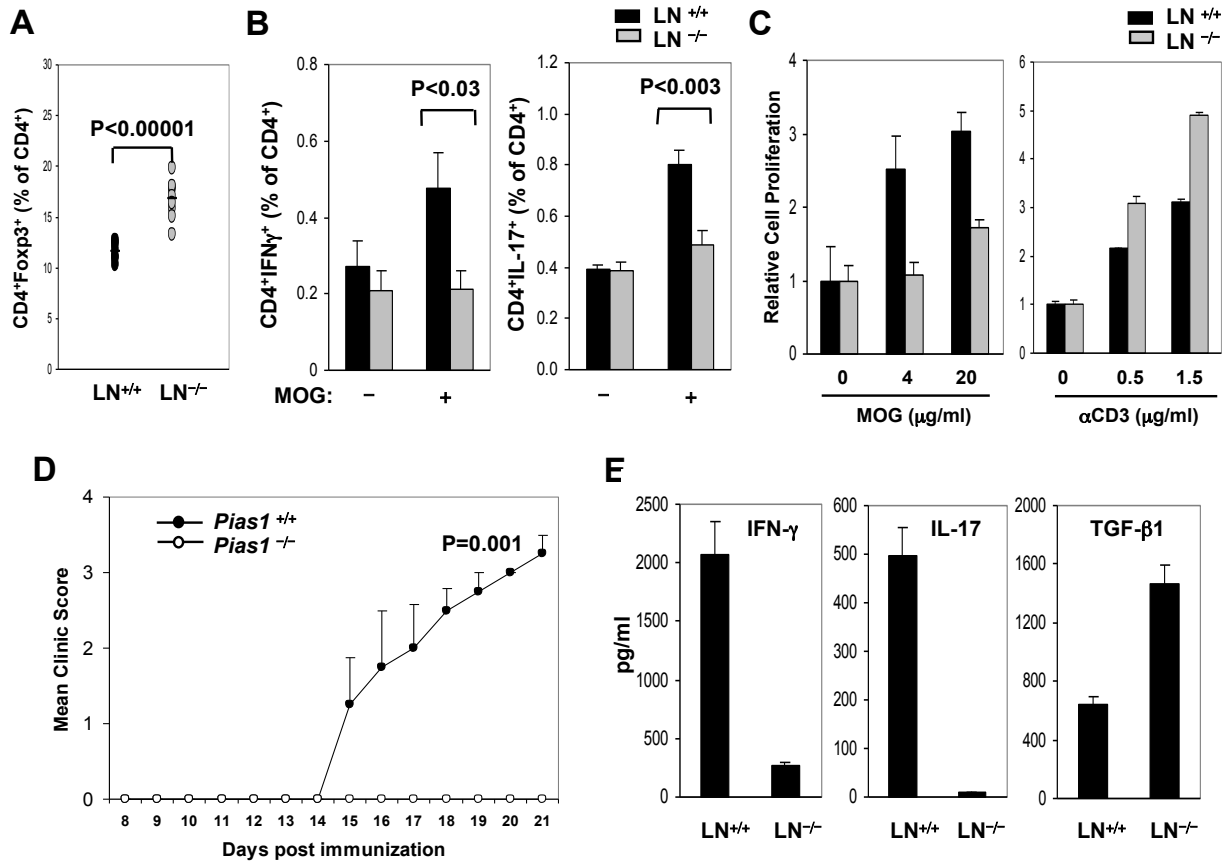

Figure 2.2. *Pias1*$^{-/-}$ mice are resistant to MOG-induced EAE. (A) The percentage of CD4^{+}Foxp3^{+} cells in WT (LN$^{+/+}$) and *Pias1*$^{-/-}$ (LN$^{-/-}$) lymph node cells 10 days post MOG_{35-55} immunization (n=7). *P* value was determined by non-paired *t*-test. (**B**) Lymphocytes from *Pias1*$^{-/-}$ mice and WT littermates 10 days post MOG_{35-55} immunization were either untreated or treated with MOG peptide for 3 days, and IFN-γ, IL-17 and TGF-β1 production was measured by ELISA. Shown is a representative of 3 independent experiments with 3-4 pairs of mice for each experiment. Error bars represent SEM. **(C)** Same as in B except that cells were either untreated or treated with 4 μg/ml of MOG_{35-55} for 3 days in the presence of brefeldin A during the last 5 h of culture. IFN-γ or IL-17 producing CD4· cells were assayed by intracellular staining followed by flow cytometry. *P* value was determined by non-paired *t*-test. **(D)** Same as in B except that cells were either untreated or treated with MOG_{35-55} (left panel) or anti-CD3 (right panel) for 3 days. Cell proliferation was measured by one-color cell proliferation kit. **(E)** *Pias1*$^{-/-}$ female mice and their WT littermates were immunized with MOG_{35-55} and pertussis toxin. The development of EAE was scored (n=4). Error bars represent SEM. *P* value was determined by non-paired *t*-test. **(F)** Lymphocytes were isolated from WT and *Pias1*$^{-/-}$ littermates 21 days post MOG_{35-55} immunization, and cultured for 3 days *in vitro* (n=4). Cytokine production was measured by ELISA. Error bars represent SEM.

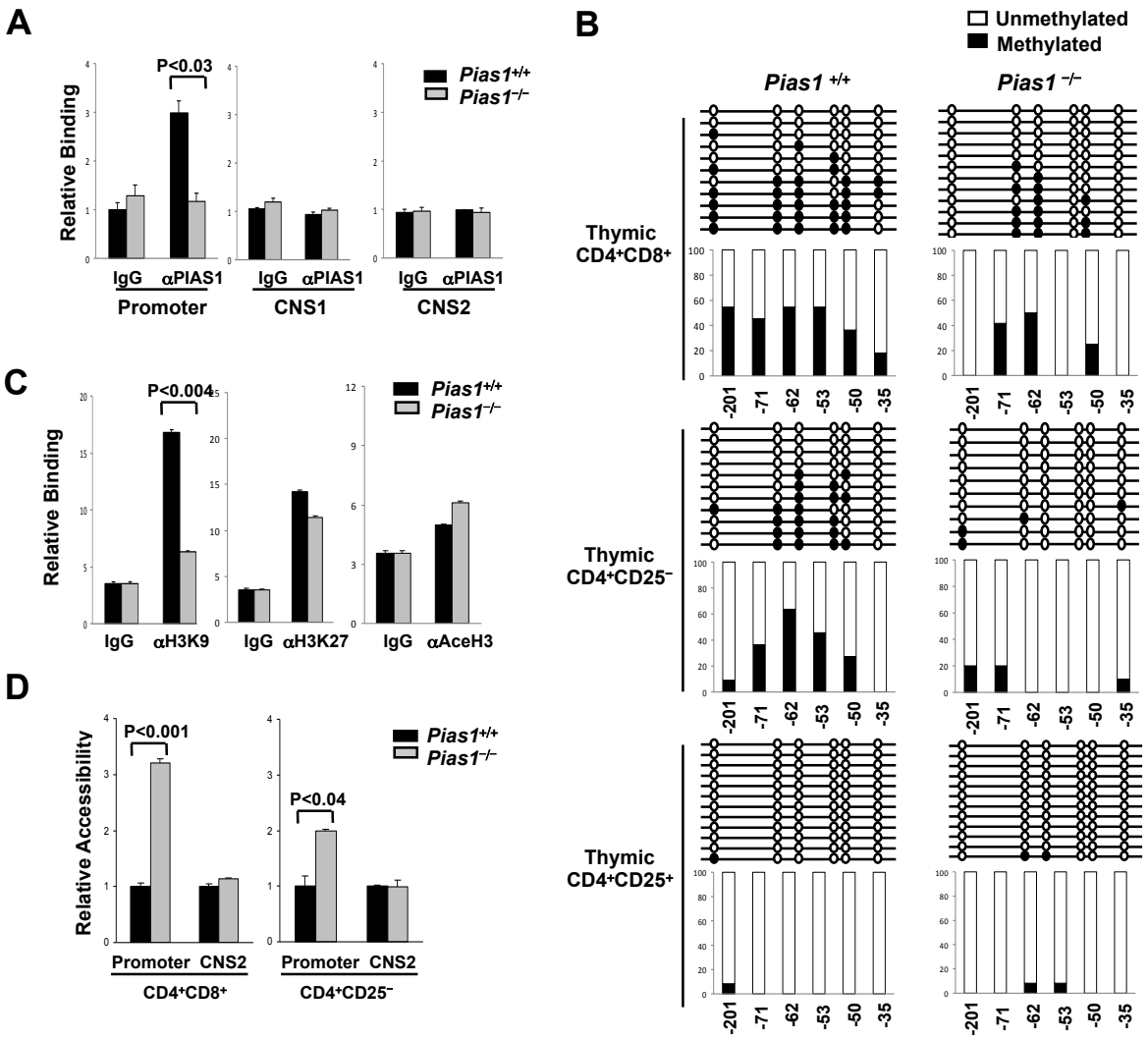

Figure 2.3. PIAS1 maintains a repressive chromatin state of the *Foxp3* promoter. (A) ChIP assays were performed with freshly FACS-sorted $CD4^+CD8^+$ thymocytes from male *Pias1*$^{+/+}$ or *Pias1*$^{-/-}$ mice (n=4), using anti-PIAS1 or IgG. Bound DNA was quantified by Q-PCR with the indicated primers and normalized with the input DNA. **(B)** Methylation analysis was performed by bisulfite conversion of genomic DNA from various FACS-sorted T cell populations of WT and *Pias1* $^{-/-}$ male mice (n=4-6). The X-axis represents the positions of the CpG sites relative to the transcription start site (+1) in the *Foxp3* gene. (**C**) ChIP assays were performed the same as in **A** except that α-Trimethyl-Histone H3 Lys9 (H3K9), α-Trimethyl-Histone H3 Lys27 (H3K27), or α-acetylated-Histone H3 (AceH3) was used. **(D)** Restriction Enzyme Accessibility (REA) assays were performed with thymic $CD4^+CD8^+$ or splenic $CD4^+CD25^-$ T cells. The data were quantified by Q-PCR and expressed as a ratio of digestion at the *Foxp3* promoter or CNS2 region to digestion at a non-digested CNS1 region of the *Foxp3* locus. (**E**) ChIP assays were performed the same as in **A** except that α-STAT5, α-NFAT or IgG were used.

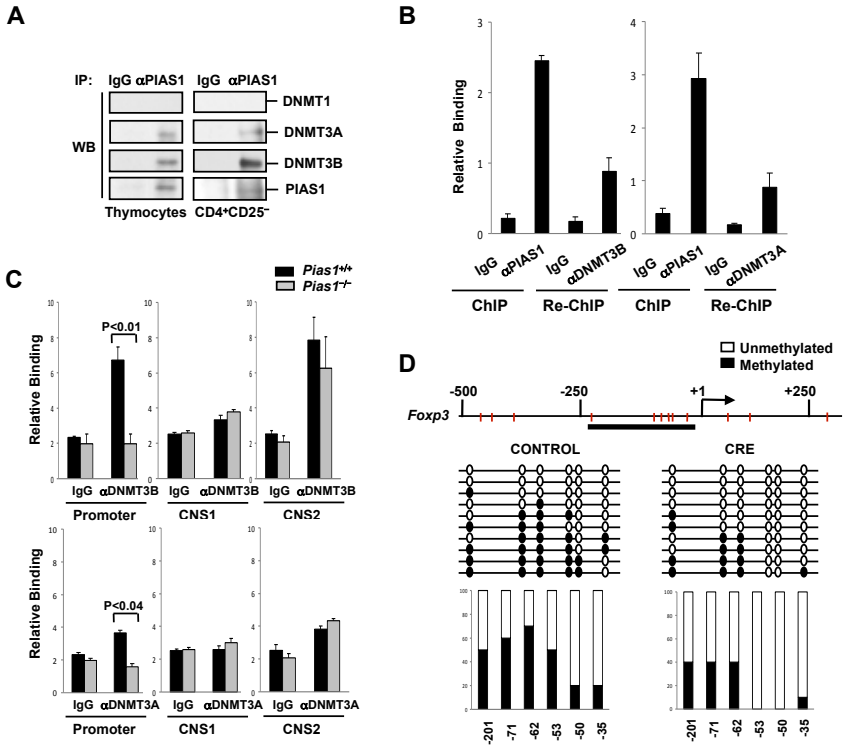

Figure 2.4. PIAS1 is required for the promoter recruitment of DNMT3A, DNMT3B and HP1γ. (A) Co-IP assays. Protein extracts from thymocytes or splenic naïve $CD4^+CD25^-$ T cells were subjected to immunoprecipitation with anti-PIAS1 or IgG, followed by immunoblotting with the indicated antibodies. **(B)** Sequential ChIP assays. ChIP assays were performed with WT thymocytes using anti-PIAS1 or IgG. The presence of the *Foxp3* promoter region in the precipitates were quantified by Q-PCR. In the re-ChIP experiments, anti-PIAS1 precipitates were released, re-immunoprecipitated with anti-DNMT3A or anti-DNMT3B, and analyzed for the presence of the *Foxp3* promoter sequence. **(C)** ChIP assays were performed with freshly FACS-sorted $CD4^+CD8^+$ thymocytes from male $Pias1^{+/+}$ or $Pias1^{-/-}$ mice (n=4), using anti-DNMT3A or anti-DNMT3B. Bound DNA was quantified by Q-PCR with the specific primers against *Foxp3* promoter, CNS1 or CNS2 region. **(D)** Methylation analysis was performed by bisulfite conversion of genomic DNA from thymocytes of $Rag1^{-/-}$ mice reconstituted with either control GFP (Con) or Cre-GFP (Cre) retrovirus-infected $Dnmt3a^{2lox/2lox}$/ $Dnmt3b^{2lox/2lox}$ bone marrow. Shown is a representative of 3 independent experiments with 4 pairs of mice for each experiment. **(E)** ChIP assays were performed with wild type and *Pias1* null thymocytes using anti-HP1γ. **(F)** A proposed model of PIAS1-mediated epigenetic regulation of Treg differentiation. PIAS1 binds to the *Foxp3* promoter to maintain a repressive chromatin state through the recruitment of DNMT3A, DNMT3B, and HP1γ. *Pias1* disruption leads to the formation of a permissive chromatin structure of the *Foxp3* promoter and the enhanced promoter accessibility toward transcription factors such as STAT5 and NFAT, resulting in the increased probability for precursor cells to differentiate into $Foxp3^+$ Treg cells. S90p, phosphorylated Ser90; H3K9, Trimethyl-Histone H3 Lys9; Met, DNA methylation. Filled rectangle represents a repressive chromatin state, while open loop represents a permissive chromatin state.

Supporting Online Material

Materials and Methods

Mice. The generation of *Pias1*$^{-/-}$ mice has been described (*1*)**.** *Rag1*$^{-/-}$ mice (C57BL/6) and C57SJL (CD45.1) mice were purchased from the Jackson Labs. *Dnmt3a*$^{2lox/2lox}$*/Dnmt3b*$^{2lox/2lox}$ mice have been described (*2, 3*). For genotyping *Dnmt3a*$^{2lox/2lox}$*/Dnmt3b*$^{2lox/2lox}$ mice, PCR was performed using a Touchdown PCR program beginning with an annealing temperature of 65ºC down to 54ºC in 1ºC increments per cycle, and additional 22 cycles were performed at 54ºC. To detect both the *Dmnt3a-2lox* and *–1lox* alleles, the primers used are 5'-CTGTGGCATCTCAGGGTGATGAGCA-3' and 5'-TGAGTGGTGAGGCCCAGCTTATCGA-3'. To detect the *Dnmt3b-2lox* allele, the primers used are 5'-AGAGCACTGCACCACTACTGCTGGA-3' and 5'-CAGGTCAGACCTCTCTGGTGACAAG-3.' To detect the *Dnmt3b-1lox* allele, the primers used are 5'-GAACTTGGTCTGCAGGACGATCGCT-3' and 5'-CAGGTCAGACCTCTCTGGTGACAAG-3.' The primers for *Cre* recombinase are 5'-GCGGTCTGGCAGTAAAAACTATC-3' and 5'-GTGAAACAGCATTGCTGTCACTT-3'.

Reagents. The antibody specific for Ser90-phosphorylated PIAS1 has been described (*4*). The following antibodies were obtained from commercial sources: anti-Tubulin (Sigma), anti-STAT5 (sc-835; Santa Cruz Biotechnology), anti-NF-ATc2 (sc-7296; Santa Cruz Biotechnology), anti-Trimethyl-Histone H3 Lys9 (17-625; Upstate Biotechnology), anti-HP1γ (05-690, Upstate Biotechnology), anti-DNMT1 (ab16632 and ab13537; Abcam); anti-DNMT3A (ab13888; Abcam) or anti-DNMT3B (ab2851 and ab13604; Abcam); anti-CD4 and anti-CD8 conjugated to fluorescein isothiocyanate (FITC), phycoerythrin (PE), PE-Cy5 or allophycocyanin (APC) and isotype controls (BD Biosciences), FITC-conjugated anti-CD45.2 and APC/Cy7-conjugated CD62L (BioLegend), PE-conjugated anti-Foxp3 and APC-conjugated anti-CD25 (eBiosciences);

anti-CD3, anti-CD28, anti-IFN-γ, anti-IL-4, anti-IL-17, and anti-IL-12 were from BD Biosciences. Recombinant murine IL-12, murine IL-4, murine IL-6, human TGF-β1 and human IL-2 were from PeproTech.

***Rag1*$^{-/-}$ mice reconstitution.** *Rag1*$^{-/-}$ reconstitution experiments were performed as described (*5*). Bone marrow was isolated from 4-8 week-old *Pias1*$^{-/-}$ mice and their WT littermates (CD45.2^{+}), or 5- to 6-week-old CD45.1^{+} C57SJL wild-type mice. Bone marrow was then depleted of T cells with anti-CD4 and anti-CD8α magnetic beads (Miltenyi). Donor bone marrow from *Pias1*$^{-/-}$ or WT mice (1x10^{6} cells) was mixed with bone marrow from CD45.1^{+} C57SJL mice (2x10^{6} cells), and injected intravenously into 6-7-week-old sublethally irradiated (450 rads) *Rag1*$^{-/-}$ C57BL/6 mice. In some experiments, sublethally irradiated *Rag1*$^{-/-}$ C57BL/6 mice were injected with 3x10^{6} T cell–depleted bone marrow from *Pias1*$^{-/-}$ or WT mice. At 4 weeks after reconstitution, thymi were collected and analyzed by flow cytometry.

For *Rag1*$^{-/-}$ reconstitution with *Dnmt3a*$^{2lox/2lox}$/*Dnmt3b*$^{2lox/2lox}$ bone marrow, bone marrow was isolated from 4-8 week-old *Dnmt3a* $^{2lox/2lox}$/*Dnmt3b*$^{2lox/2lox}$ mice, and spin infected twice with retrovirus encoding GFP or GFP-Cre. FACS-sorted GFP^{+} cells (0.4-1x10^{5}) were injected intravenously into 6-7-week-old sublethally irradiated (450 rads) *Rag1*$^{-/-}$ C57BL/6 mice. At 4 weeks after reconstitution, thymi were collected and analyzed by flow cytometry.

Chromatin immunoprecipitation (ChIP) and sequential-ChIP. Various T cell populations were purified using a FACS Sorter to a purity >99%. ChIP assays were performed as described (*4*). For sequential-ChIP experiments, complexes from initial anti-PIAS1 ChIP were eluted with 10mM DTT at 37°C for 30min and diluted in a buffer containing 50 mM Tris pH 8.0, 5 mM EDTA, 200 mM NaCl, 0.5% NP40 and re-immunoprecipitated with anti-DNMT3A or anti-DNMT3B. The sequences of the primers are: *Foxp3* promoter: forward-5'-

CTCACTCAGAGACTCGCAGCA; reverse- 5'-GCAAGCATGCATATGATCACC (*6*). *Foxp3* CNS1: forward-5'-TGTTGGCTTCCAGTCTCCTT; reverse-5'- TGCTGAGCACCTACCATCAT (*7*). *Foxp3* CNS2: forward-5'-CAGAAAAATCTGGCCAAGTT; reverse-5'-AGGACCTGAATTGG ATATGGT (*6*). *Cd25* promoter: forward-5'-AAGACAGCTTGGTGACACTATGAG; reverse-5'-TCAAAGGAAAATGATAAGCAAACA. *Ctla4* promoter: forward-5'-TGGGGGATTAAAGATGACCA; reverse-5'-AGCCGTGGGTTTAGCTGTTA.

Co-immunoprecipitation (Co-IP). Total thymocytes or FACS-sorted CD4+CD25- T cells were lyzed in IP buffer (1% Brij, 50mM Tris pH 8.0, 150mM NaCl, 1mM EDTA), and cell nuclei were disrupted by sonication. Co-IP was performed by incubating the whole cell lysates with IgG or anti-PIAS1 at 4^{o}C overnight. After extensive washes, the immunoprecipitates were resolved by SDS-PAGE, followed by sequential blotting with the following mouse monoclonal antibodies: anti-DNMT1, anti-DNMT3A, and anti-DNMT3B. The same filter was reprobed with anti-PIAS1.

Methylation Analysis. Genomic DNA was purified with the ZR genomic DNA II kit (Zymo Research). Methylation analysis was performed by bisulfite conversion of genomic DNA using the EZ DNA methylation-Gold kit (Zymo Research). The following primers are used: *Foxp3* promoter: forward-5'-TATATTTTTAGA TGATTTGTAAAGGGTAAA; reverse-5'-TCACCTTAATAAAATAAACTACTA. *Foxp3* CNS2: forward 5'-TATTTTTTTGGGTTTT GGGATATTA; reverse-5'- AACCAACCAACTTCCTACACTATCTAT (*9*). *Cd25* promoter: forward-5'-TGTGAATTTTATATTTATGGAATTATGAAT; reverse-5'-AATCTACTCAACAAAAACTTATACCTACTCTA. The PCR product was cloned using the TOPO TA cloning kit (Invitrogen).

Cell sorting. The naïve $CD4^{+}CD25^{-}CD62L^{+}$ cells were purified from spleen and lymph nodes as the following. B cells were first depleted from total cells using CD45R-microbeads and MACS

columns (Miltenyi Biotech). Cells were then labeled with CD4-FITC, CD8-PE, CD25-APC and CD62L-APC/Cy7, followed by FACS sorting to collect $CD4^+CD25^-CD62L^+$ cells (Fig. S2-21A). Thymic $CD4^+CD8^+$, $CD4^+CD25^+$ and $CD4^+CD25^-$ cells were sorted following the scheme in Fig. S2-21B. Splenic $CD4^+CD25^+$ and $CD4^+CD25^-$ cells were sorted in the same fashion as in Fig. S2-21B. Hematopoietic stem cell (HSC; $Lin^-IL7Ra^-Sca1^+c\text{-}Kit^+$) and common lympoid progenitor (CLP; $Lin^-IL7R\alpha^+Sca1^{low}c\text{-}Kit^{low}$) cells were purified by FACS sorting as described (*8*) following the scheme in Fig. S2-21C. The following antibodies were used: PE-conjugated Lineage markers (CD3, CD4, CD5, CD8a, B220, Gr1, Ter119), APC-IL7Ra (CD127), FITC-c-Kit and PE/Cy5-Sca1 (BioLegend).

***In vitro* T cell differentiation.** *In vitro* T cell differentiation experiments were carried out as described (*10-12*). The naïve $CD4^+CD25^-CD62L^+$ cells were purified from spleen and lymph nodes using a combination of $CD4^+CD62L^+$ and $CD4^+CD25^-$ T cell purification kits (Miltenyi Biotech) or by FACS sorting. For primary response, cells were stimulated with plate-bound anti-CD3 (2 μg/ml) and soluble anti-CD28 (2 μg/ml) (N; neutral condition), or Th1 conditions [N + IL-12 (5 ng/ml) + anti-IL-4 (5 μg/ml)] for 3 days, and cytokines in the supernatant were measured by ELISA (BioLegend). For secondary response, cells were stimulated under N, Th1, Th2 [N + IL-4 (10 ng/ml) + anti-IFN-γ (10 μg/ml) +anti-IL-12 (5 μg/ml)], or Th17 [N + TGF-β1 (2.5 ng/ml) + IL-6 (20 ng/ml) + anti-IL-4 (5 μg/ml) + anti-IFN-γ (5 μg/ml)] conditions in the presence of human IL-2 (100U/ml) for 3-5 days. Cells were then restimulated with anti-CD3 and anti-CD28 for 16 h, and cytokines in the supernatant were measured by ELISA. Cells were also restimulated with PMA (50 ng/ml) (Sigma) and ionomycin (0.5 μg/ml) (Sigma) for 4 h in the presence of the protein transporter inhibitor brefeldin A (2 μg/ml) (BD Biosciences) in the last 2 h. Cytokine-producing T cells were analyzed by intracellular staining followed by flow cytometry.

For conventional *in vitro* inducible Treg differentiation (iTreg) assay, FACS-sorted $CD4^+CD25^-$ $CD62L^+$ T cell were cultured under neutral [N] or Treg [N + TGF-β1 (2 ng/ml)] condition in the presence of human IL-2 (100U/ml) for 3 days. $CD4^+Foxp3^+$ cells were analyzed by intracellular staining using a mouse Regulatory T cell staining kit as instructed (eBioscience), followed by flow cytometry. For modified iTreg assays, FACS-sorted $CD4^+CD25^-$ $CD62L^+$ T cell were treated with plate-bound anti-CD3 (2 μg/ml) and soluble anti-CD28 (2 μg/ml) (TCR) for 15 hrs, and then transferred to new wells and cultured in the presence of human IL-2 (100U/ml) and various doses of TGF-β1 with or without TCR (persistant vs. transient TCR, respectively) for additional 48 hrs. $Foxp3^+CD4^+$ cells were analyzed by intracellular staining followed by flow cytometry.

Intracellular staining. Intracellular staining was performed as described (*11, 12*). Cells were stained with surface markers first, and then fixed and permeabilized with the cytofix/cytoperm kit (BD Bioscience). Cells were stained with antibodies to cytokines (IFN-γ, IL-17) by incubating on ice for 30 min, followed by 3 washes with the Perm/Wash buffer (BD Bioscience). Data were acquired on a FACSCalibur (BD Bioscience) and analyzed with the CellQuest or FCS Express software.

Apoptosis *and In vivo* BrdU assays. T cell apoptosis was assessed by 7-AAD staining as described (*5*). *In vivo* BrdU assays were performed as described (*5*). Mice were injected intraperitoneally with a single dose of 50 mg BrdU (5-bromodeoxyuridine) per kg body weight. Cells incorporating BrdU were detected by intracellular staining 16 h later, using a BrdU Flow Kit following the instructions from the manufacturer (BD Pharmingen).

MOG_{35-55}-induced EAE. MOG_{35-55}-induced EAE was performed as described (*11*). Female 6-8 week-old *Pias1*$^{-/-}$ and WT mice were immunized with the MOG peptide (amino acids 35–55;

MEVGWYRSPFS ROVHLYRNGK) (150 ug/mouse) emulsified in CFA (Difco) supplemented with heat-inactivated *M. Tuberculosis* H37 RA (10 mg/ml; Difco) via subcutaneous injection. The following day, mice were i.p. injected with 0.5 ug of pertussis toxin (List Biological). The same procedure was repeated 7 days later. Signs of EAE were assigned scores on a scale of 1–5 as follows: 0, none; 1, limp tail or waddling gait with tail tonicity; 2, wobbly gait; 3, hindlimb paralysis; 4, hindlimb and forelimb paralysis; 5, death.

Restriction Enzyme Accessibility (REA) assay. REA assays were performed as described using the RsaI sites present in *Foxp3* promoter and CNS2, but not CNS1, regions (*9*). The primers used for PCR were: *Foxp3* promoter: forward-5'-CTCACTCAGAGACTCGCAGCA; reverse- 5'-GCAAGCATGCATATGATCACC. *Foxp3* CNS2: forward-5'-CAGAAAAATCTGGCCAAGT; reverse-5'-AGGACCTGAATTGGATATGGT. *Foxp3* CNS1: forward-5'-TTTTCTTGTGGGGCTTCTGT; reverse-5'-GACAGTCTGGCTCCCATACC.

References:

S1. B. Liu *et al.*, *Nat. Immunol.* **5**, 891-8 (2004).

S2. M. Kaneda *et al.*, *Nature* **429**, 900-3 (2004).

S3. J. E. Dodge *et al.*, *J Biol Chem* **280**, 17986-91 (2005).

S4. B. Liu *et al.*, *Cell* **129**, 903-14 (2007).

S5. Y. Liu *et al.*, *Nat Immunol* **9**, 632-40 (2008).

S6. M. A. Burchill, J. Yang, C. Vogtenhuber, B. R. Blazar, M. A. Farrar, *J Immunol* **178**, 280-90 (2007).

S7. Y. Tone *et al.*, *Nat Immunol* **9**, 194-202 (2008).

S8. M. Kondo, I. L. Weissman, K. Akashi, *Cell* **91**, 661-72 (1997).

S9. H. P. Kim, W. J. Leonard, *J Exp Med* **204**, 1543-51 (2007).

S10. S. J. Szabo *et al.*, *Science* **295**, 338-42 (2002).

S11. H. Park *et al.*, *Nat Immunol* **6**, 1133-41 (2005).

S12. F. J. Quintana *et al.*, *Nature* **453**, 65-71 (2008).

Supplemental Figures

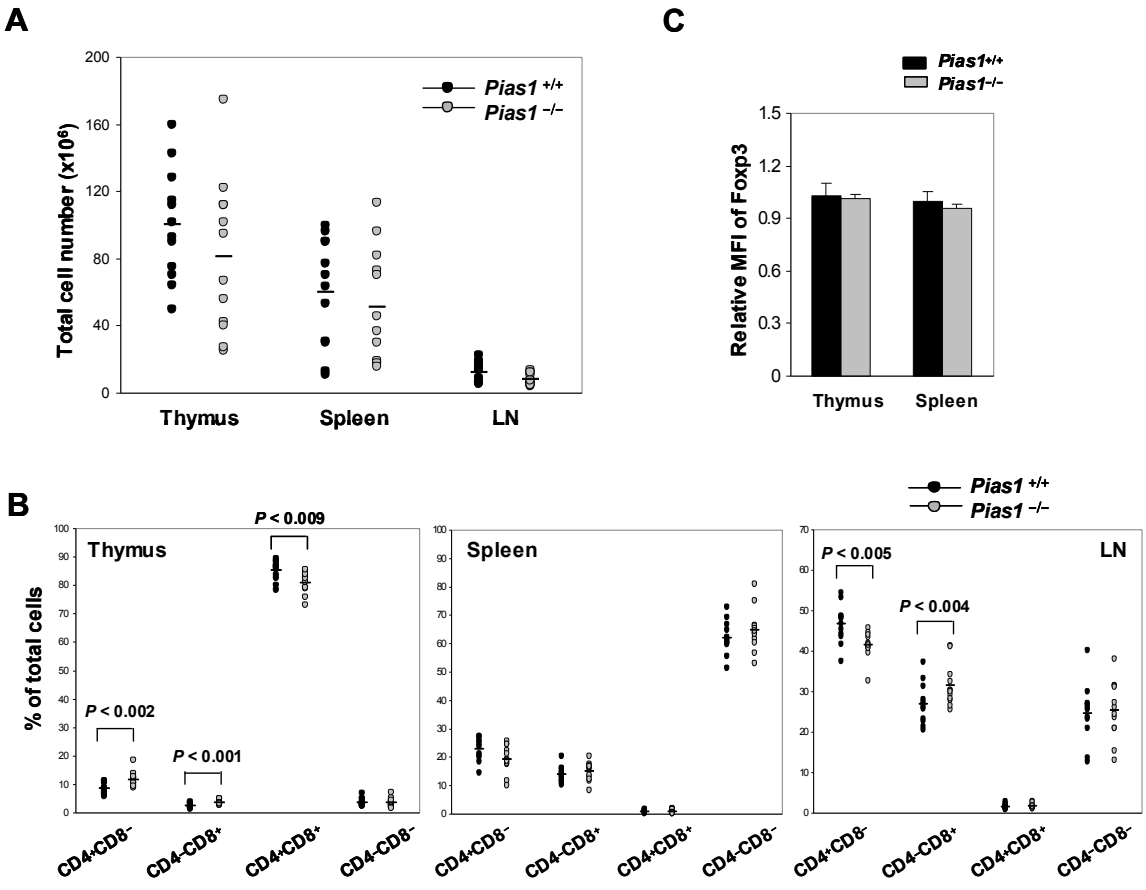

Fig. S2.1. **T cell cellularity and differentiation in wild type and *Pias1*$^{-/-}$ mice. (A)** No significant differences in total cell numbers from thymus, spleen and lymph nodes (LN) between *Pias*1$^{-/-}$ mice and WT littermates (*P*> 0.05 by non-paired *t*-test) (n=12). **(B)** The distribution of $CD4^+CD8^-$, $CD4^-CD8^+$, $CD4^+CD8^+$ and $CD4^-CD8^-$ cells in thymus, spleen and lymph nodes (LN) of *Pias1*$^{-/-}$ mice and their WT littermates (n=12). *P* value was determined by non-paired *t*-test. **(C)** Foxp3 Mean fluorescence intensity (MFI) of the $CD4^+Foxp3^+$ population determined by flow cytometry with cells from thymus or spleen of WT and *Pias1*$^{-/-}$ littermates (n=12). Error bars represent SEM.

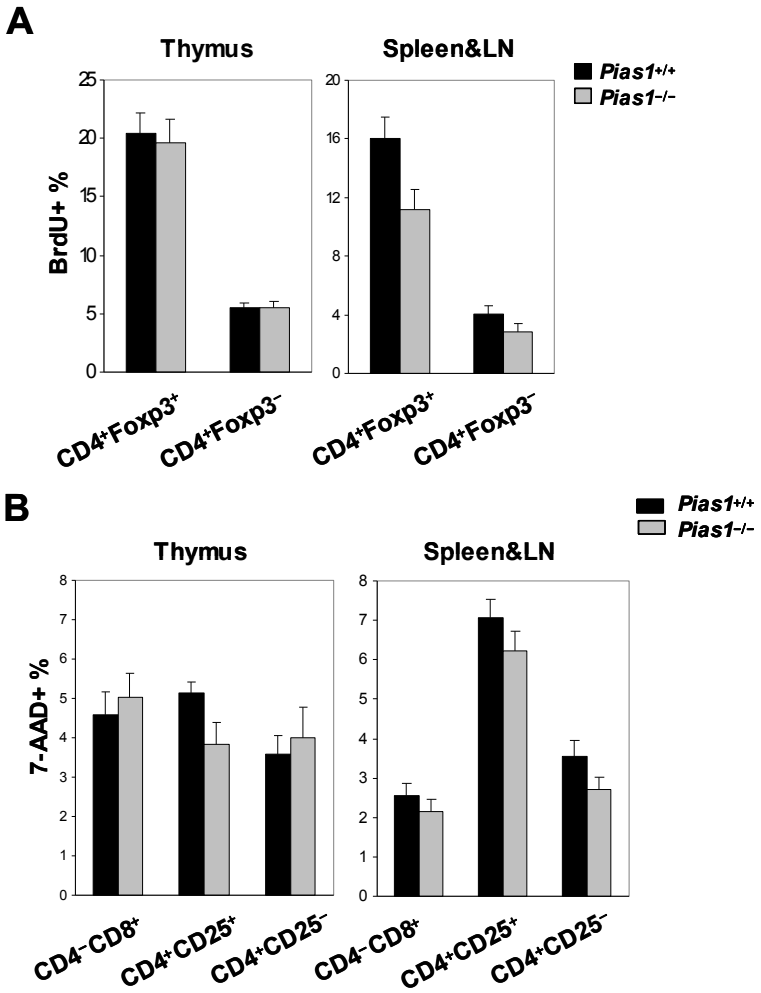

Fig. S2.2. **T cell proliferation and apoptosis are not altered in *Pias1*$^{-/-}$ mice.** (**A**) *In vivo* T cell proliferation in WT and *Pias1*$^{-/-}$ mice (n=5) was revealed by BrdU incorporation followed by flow cytometry analysis. (**B**) Apoptosis of freshly isolated T cells from *Pias1*$^{-/-}$ mice and their WT littermates (n=6) by 7-AAD staining followed by flow cytometry. Shown is a representative of 3 independent experiments (n=4-6 for each experiment). Error bars represent SEM. No significant differences were observed in all panels ($P > 0.05$).

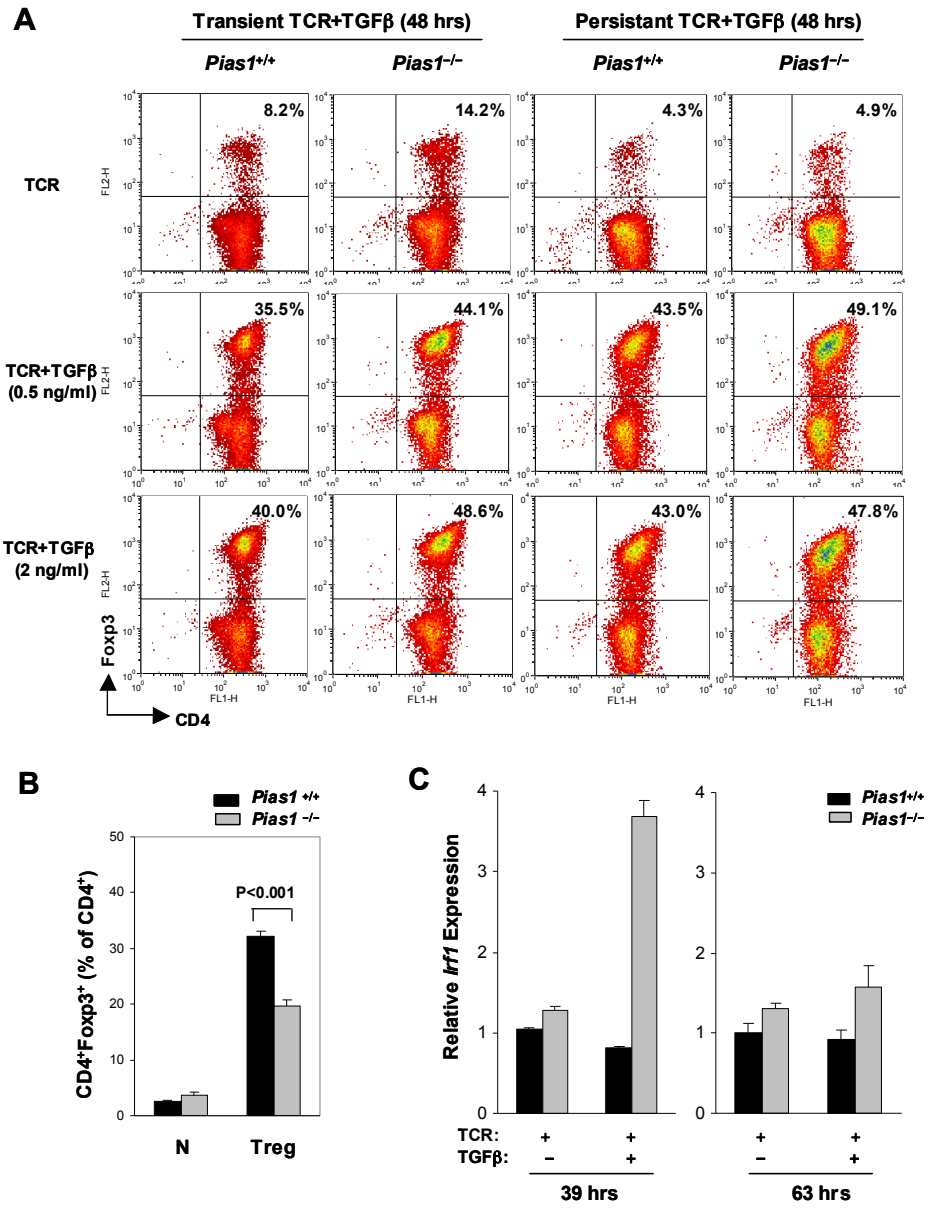

Fig. S2.3. ***In vitro*** **inducible Treg (iTreg) differentiation**. **(A)** FACS-sorted splenic $CD4^+CD25^-CD62L^+$ naïve T cells were cultured under modified iTreg conditions with transient or persistent TCR treatment as described in Material and Methods, and the percentage of $CD4^+Foxp3^+$ cells were determined by flow cytometry (indicated by the numbers in the upper right quadrants). Shown is a representative of 3 independent experiments (n=4-6 for each experiment). **(B)** Same as in A except that cells were cultured under persistent TCR activation and TGF-β for 3 days. N, neutral condition (no TGF-β). Shown is the average of 3 independent experiments (n=4-6 for each experiment). Error bars represent SEM. *P* value was determined by non-paired *t*-test. **(C)** FACS-sorted splenic $CD4^+CD25^-CD62L^+$ naïve T cells were cultured under TCR activation with or without TGFb (2 ng/ml) for indicated time periods. Total RNA was subjected to Q-PCR using specific primers for the *Irf1* gene and normalized by *Actin*.

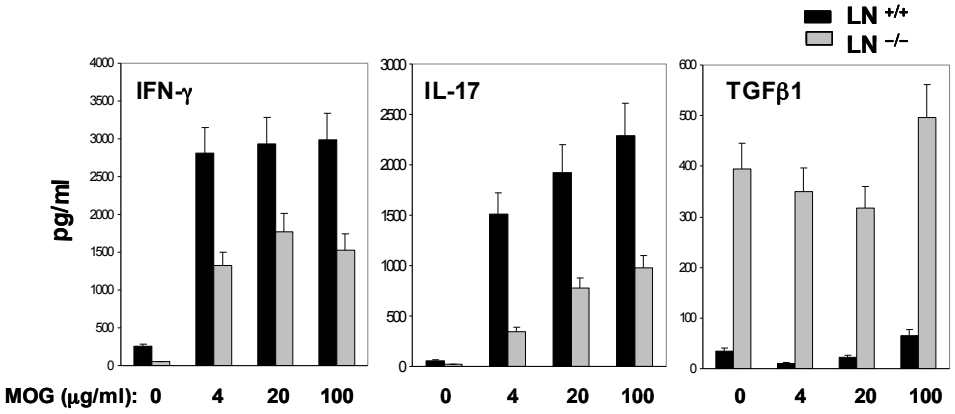

Fig. S2.4. **MOG-induced cytokine productions were altered in *Pias1*$^{-/-}$ lymphocytes.** Lymphocytes from *Pias1*$^{-/-}$ mice and WT littermates 10 days post a single MOG_{35-55} injection emulsified in CFA supplemented with H37 RA were either untreated or treated with MOG for 3 days, and IFN-γ, IL-17 and TGF-β1 in the cell supernatants were measured by ELISA. Shown is a representative of 3 independent experiments (n=4-6 for each experiment). Error bars represent SEM.

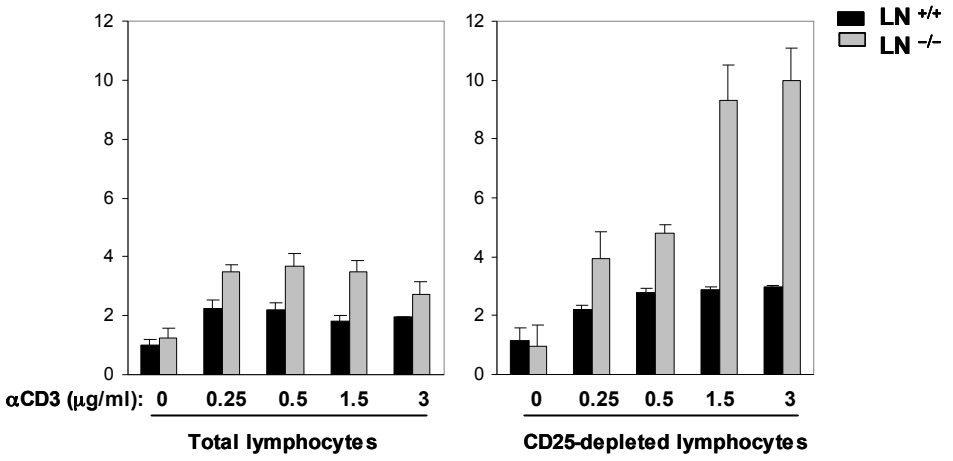

Fig. S2.5. **Enhanced cell proliferation of non-Treg lymphocytes from naïve *Pias1*$^{-/-}$ mice in response to anti-CD3**. Either total lymph node cells from the naïve WT and *Pias1*$^{-/-}$ mice, or lymph node cells depleted $CD25^+$ cells by MACS column were cultured *in vitro* with various doses of anti-CD3 for 3 days. Cell proliferation was determined by one-color cell proliferation kit.

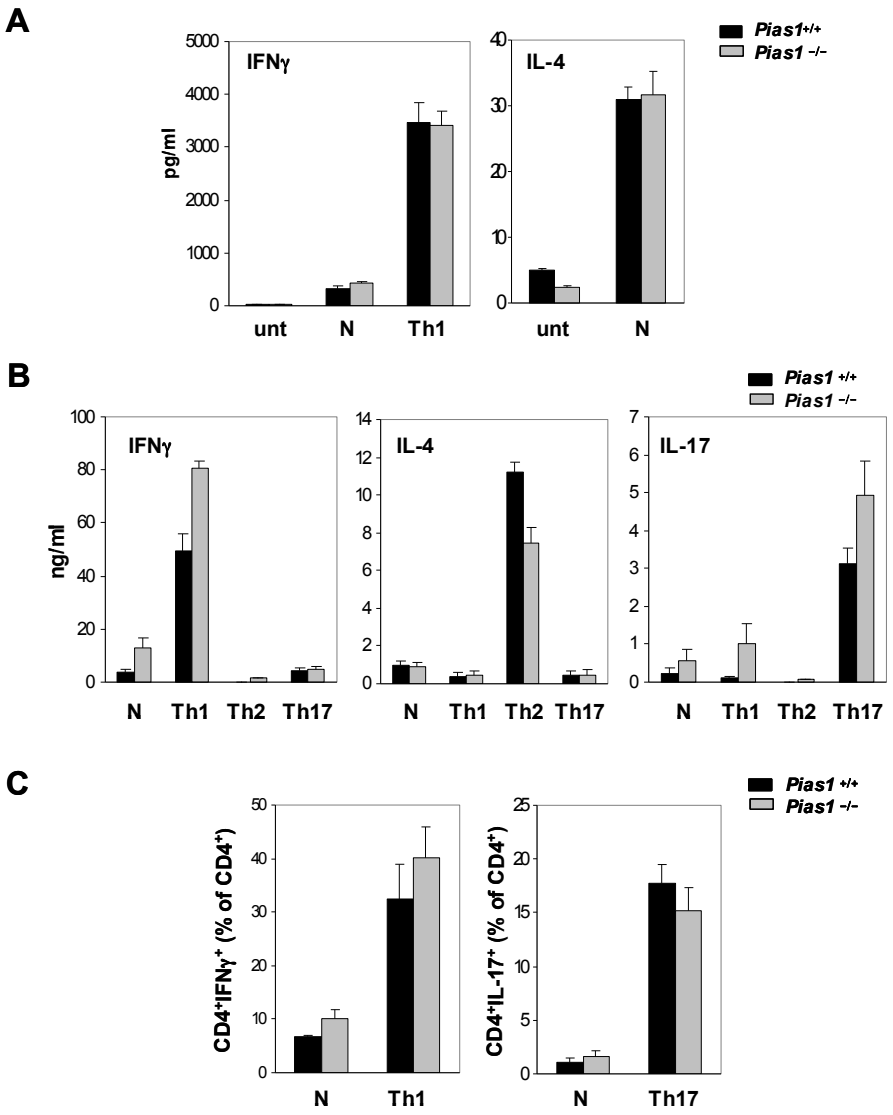

Fig. S2.6. The *in vitro* differentiation of Th1, Th2, and Th17 cells. (A) Primary response. Naïve $CD4^+$ $CD25^-CD62L^+$ T-cells were stimulated with anti-CD3 and anti-CD28 (N; neutral condition), or Th1 condition for 3 days. The production of IFN-γ and IL-4 was measured by ELISA. Unt, untreated. **(B)** Secondary response. The same as in **A** except that cells were stimulated under N, Th1, Th2 or Th17 conditions (as described in the Material and Methods) in the presence of human IL-2 for 5 days. Cells were restimulated with anti-CD3 and anti-CD28 for 16 h, and the cytokine productions of IFN-γ, IL-4 and IL-17 were measured by ELISA. **(C)** Same as in **B** except that cells were restimulated with PMA and ionomycin for 4h, and cytokine-producing $CD4^+$ cells were determined by intracellular staining followed by flow cytometry. Shown in **A-C** are the averages of 3 independent experiments (n=4 for each experiment). Error bars represent SEM. No significant differences were observed in all panels by non-paired *t*-test (*P*> 0.05).

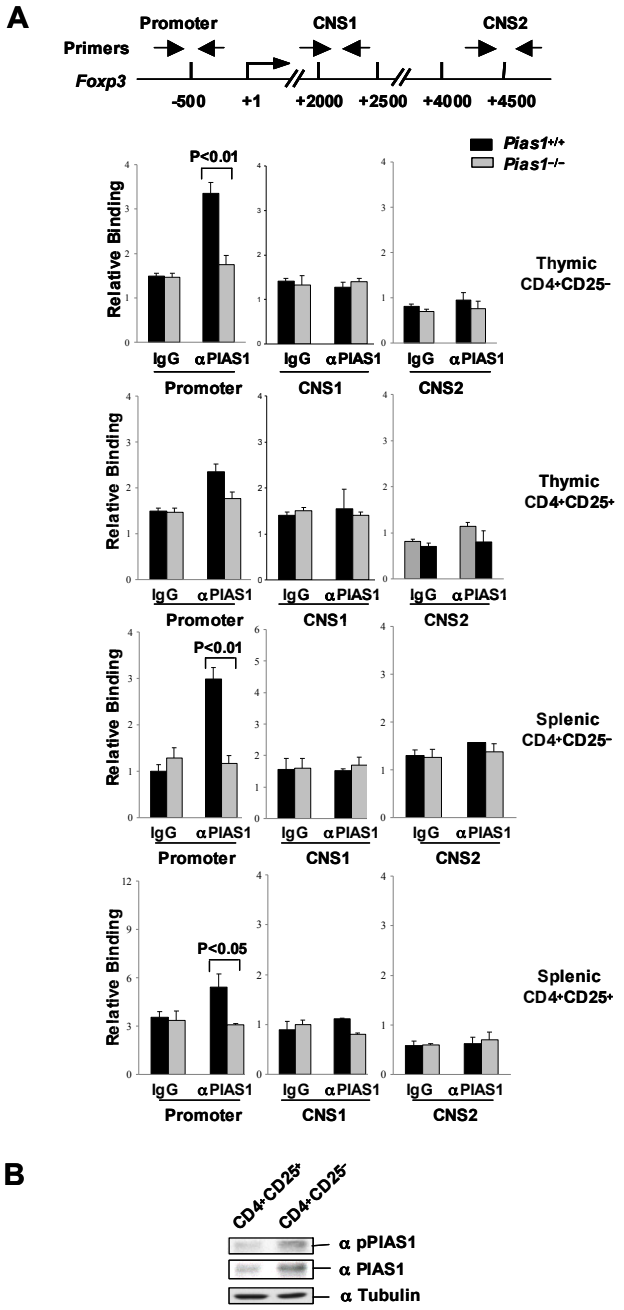

Fig. S2.7. PIAS1 preferentially binds to the *Foxp3* promoter in CD4$^+$CD25$^-$ T cells, but not CD4$^+$CD25$^+$ Treg cells. (A) ChIP assays were performed with various FACS-sorted T cells from male *Pias1*$^{+/+}$ or *Pias1*$^{-/-}$ mice (n=4-6), using anti-PIAS1 or IgG. Bound DNA was quantified by quantitative real-time PCR (Q-PCR) with the primers specific for the *Foxp3* locus and normalized with the input DNA. *P* value was determined by non-paired *t*-test.$^+$ **(B)** Western blot analysis of whole cell extracts from FACS-sorted CD4$^+$CD25$^+$ and CD4$^+$CD25$^-$ T cells from spleen of WT mice using an antibody specific for Ser90-phosphorylated PIAS1, total PIAS1, or Tubulin. The differential levels of PIAS1 expression may be regulated by posttranslational modifications such as phosphorylation

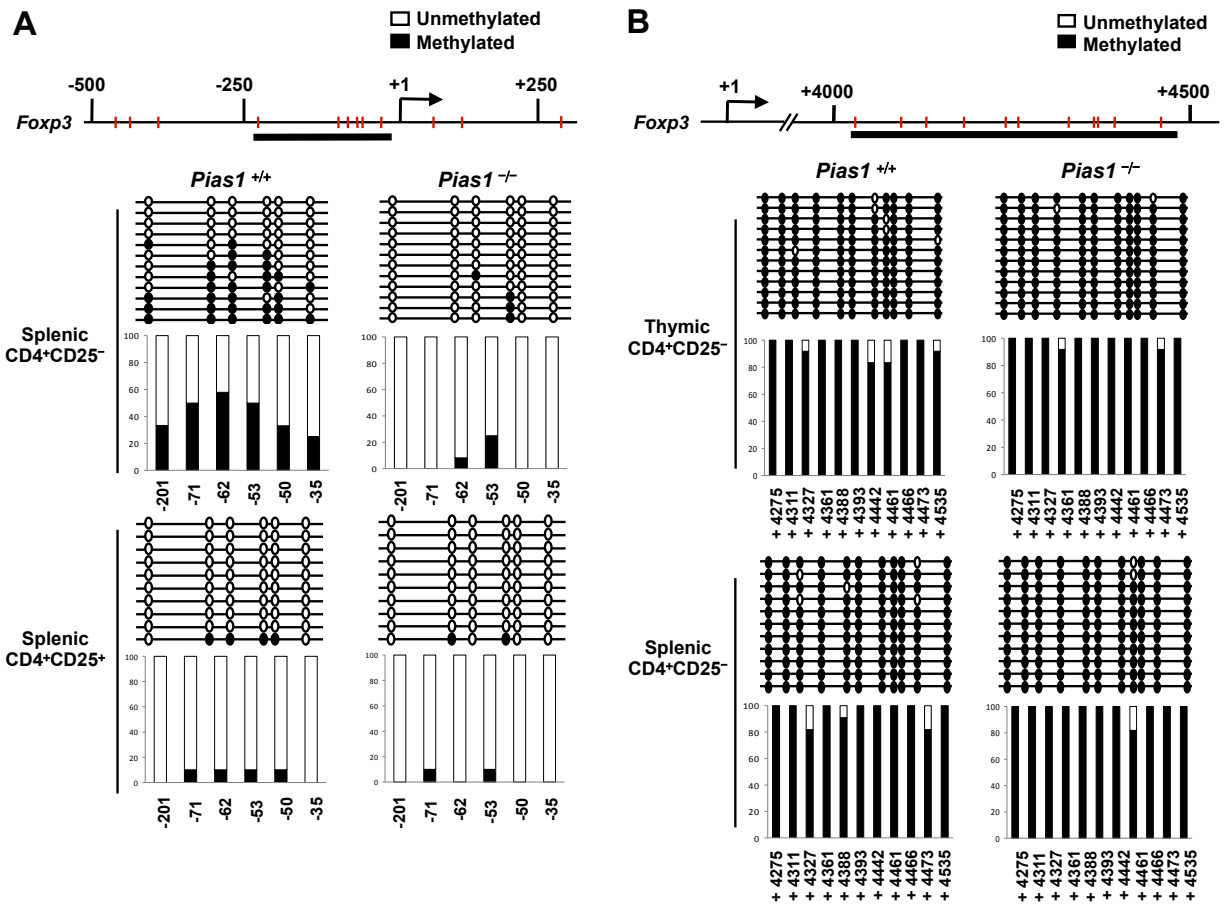

Fig. S2.8. Methylation of the *Foxp3* locus. (A) Methylation of the *Foxp3* promoter region. Methylation analysis was performed by bisulfite conversion of genomic DNA prepared from FACS-sorted T cells of WT and *Pias1* $^{-/-}$ male mice (n=4-6). The X-axis represents the positions of the CpG sites relative to the transcription start site (+1) in the *Foxp3* gene. The Y-axis represents the percentage. **(B)** same as in **A** except that the CNS2 region of the *Foxp3* locus was analyzed.

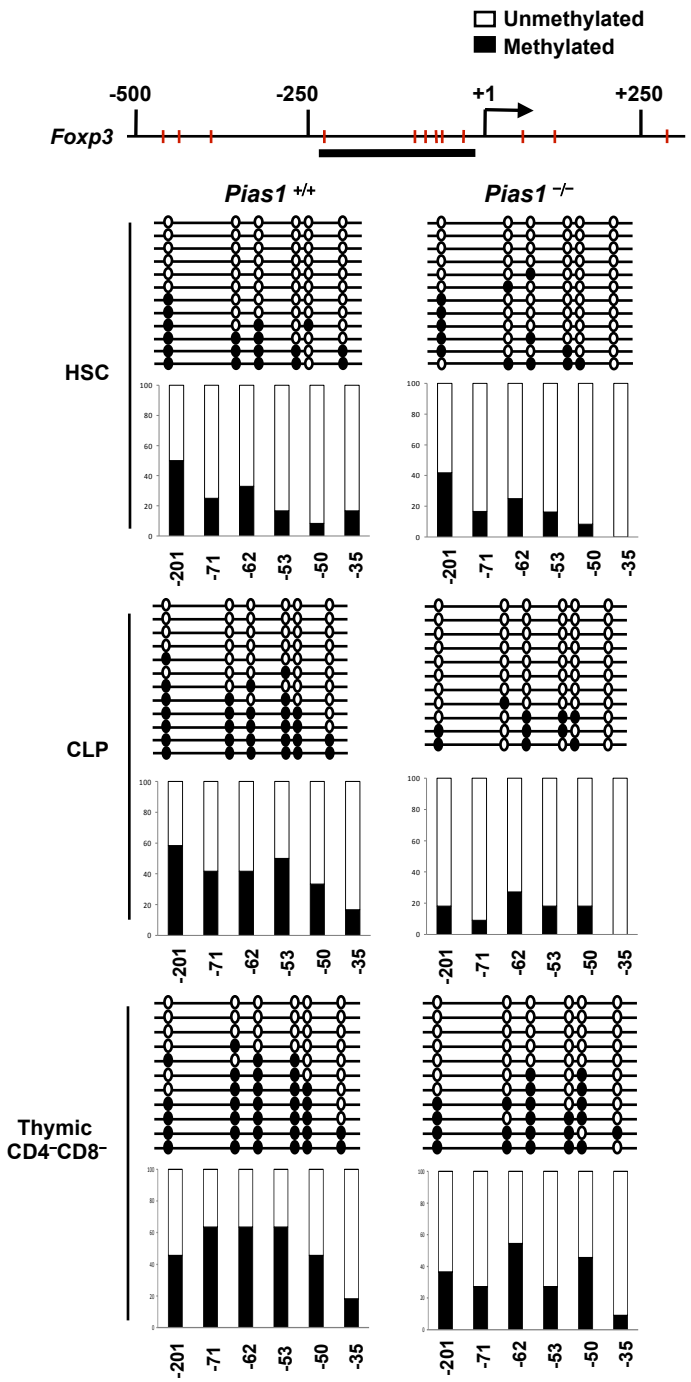

Fig. S2.9. Methylation of the *Foxp3* promoter in the precursor cells. Methylation analysis was performed by bisulfite conversion of genomic DNA prepared from FACS-sorted hematopoietic stem cells (HSC), common lymphoid progenitors (CLP) and thymic $CD4^{-}CD8^{-}$ T cells of WT and *Pias1* $^{-/-}$ male mice (n=4-6). The X-axis represents the positions of the CpG sites relative to the transcription start site (+1) in the *Foxp3* gene. The Y-axis represents the percentage.

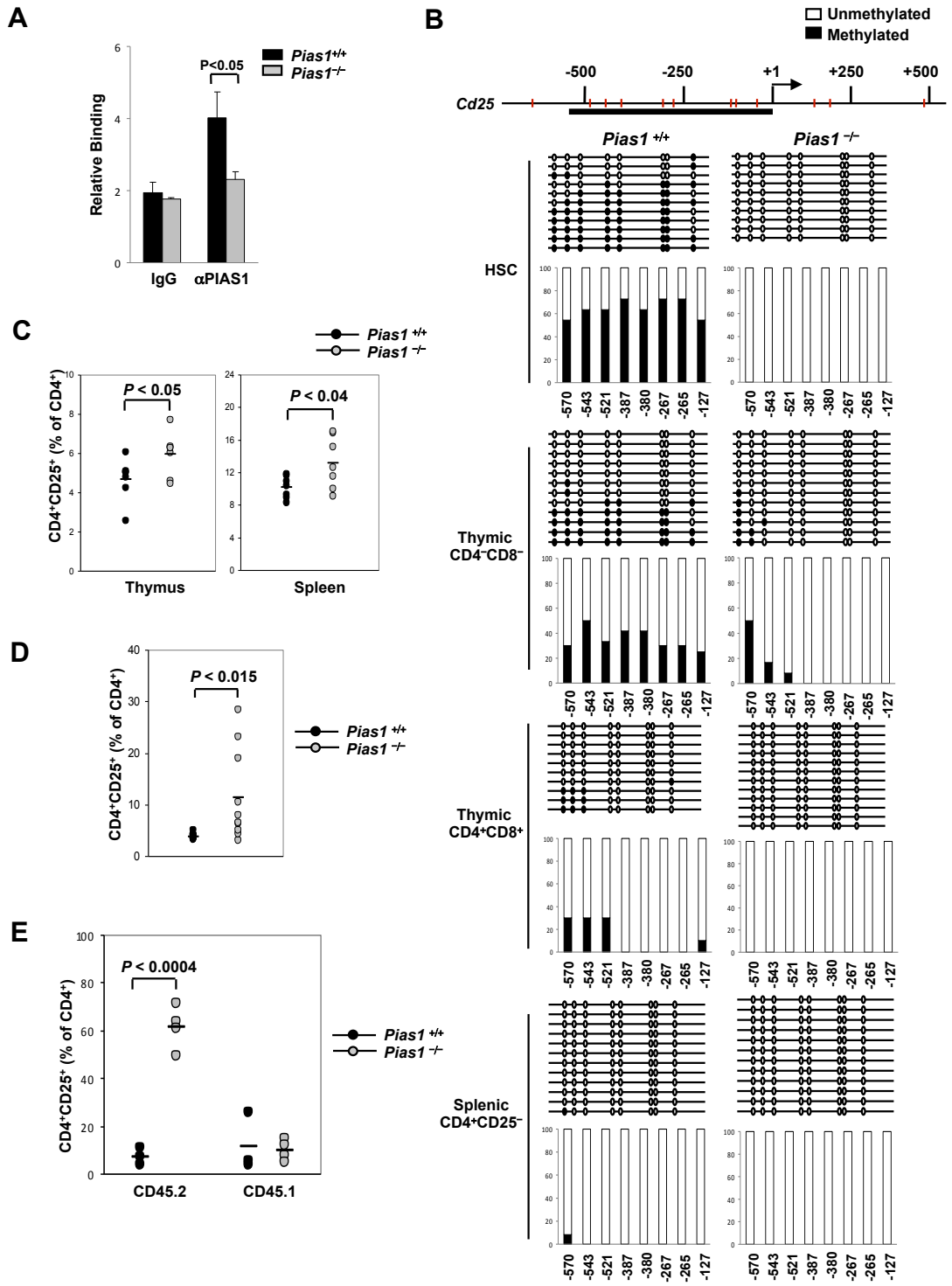

Fig. S2.10. PIAS1 mediates the epigenetic suppression of the *Cd25* promoter and inhibits *Cd25* induction. (A) ChIP assays were performed with freshly FACS-sorted $CD4^+CD8^+$ thymocytes from male *Pias1*$^{+/+}$or *Pias1*$^{-/-}$ mice (n=4), using anti-PIAS1 or IgG. Bound DNA was quantified by Q-PCR and normalized with the input DNA. **(B)** Methylation analysis was performed by bisulfite conversion of genomic DNA prepared from various FACS sorted cells of

WT and *Pias1* $^{-/-}$ male mice (n=4-6). The X-axis represents the positions of the CpG sites relative to the transcription start site (+1) in the *Cd25* gene. HSC: Lineage marker^{-}, Scal1^{+}, c-Kit^{+} (LSK) cells enriched in hematopoietic stem cells. **(C)** Cells freshly isolated from thymus and spleen of WT and *Pias1*$^{-/-}$ littermates (n=7) were analyzed for the percentage of CD4^{+}CD25^{+} cells by flow cytometry (gated on CD4^{+} population). **(D)** Bone marrow was isolated from WT and *Pias1*$^{-/-}$ littermates, and injected into the sublethally irradiated *Rag1*$^{-/-}$ recipient mice (n=10). The thymic CD4^{+}CD25^{+} population was analyzed 4 weeks post reconstitution by flow cytometry. **(E)** Same as in **D** except that *Pias1*$^{-/-}$ or WT bone marrow (CD45.2) was mixed with WT C57SJL bone marrow (CD45.1), and injected into the *Rag1*$^{-/-}$ mice (n=3 for WT and n=4 for *Pias1*$^{-/-}$). *P* values in **A, C-E** were determined by non-paired *t*-test.

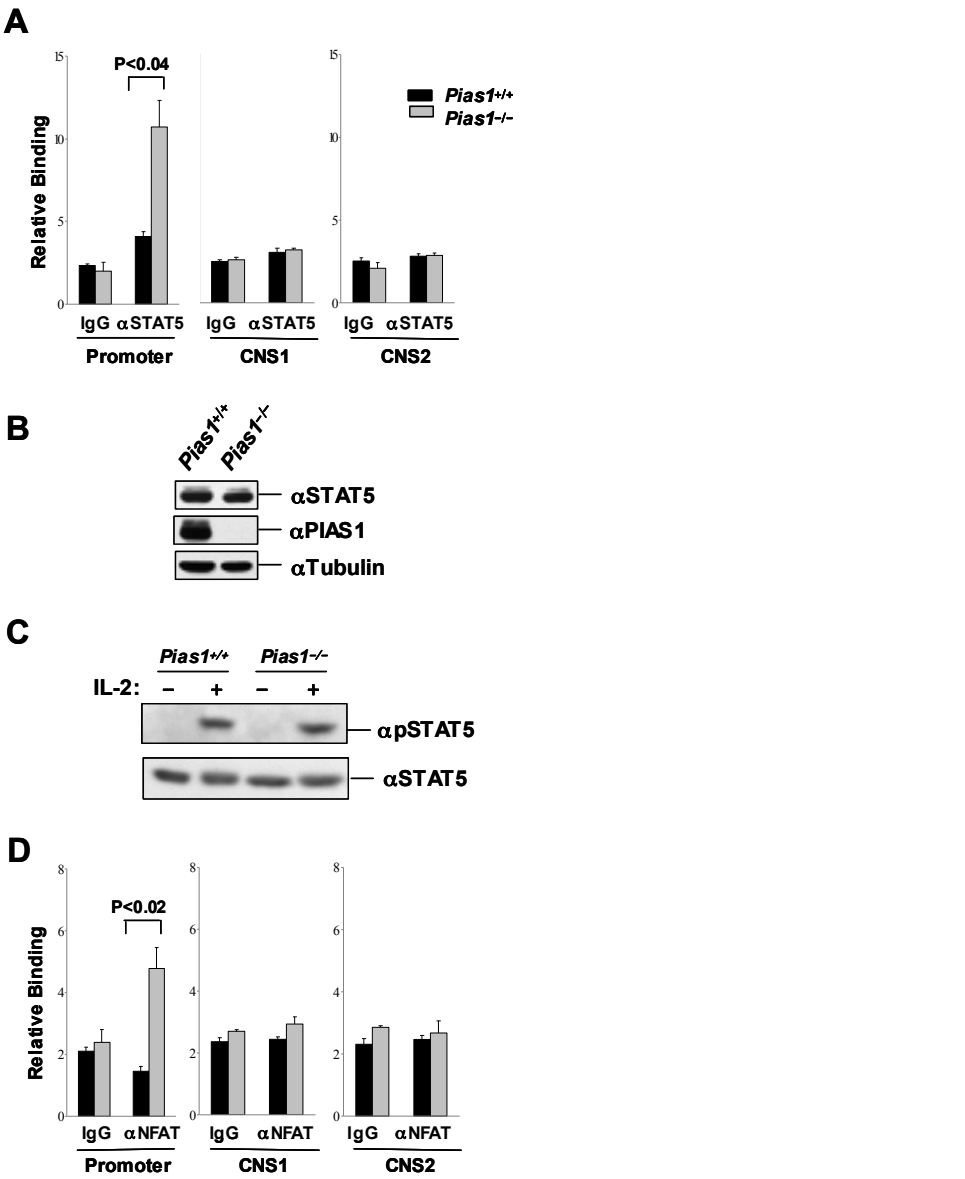

Fig. S2.11. Enhanced binding of STAT5 and NFAT to the *Foxp3* promoter in *Pias1*$^{-/-}$ thymic CD4^{+}CD8^{+} T cells. (A) ChIP assays were performed with freshly FACS-sorted CD4^{+}CD8^{+} thymocytes from male *Pias1*$^{+/+}$ or *Pias1*$^{-/-}$ mice (n=4), using anti-STAT5 or IgG. Bound DNA was quantified by Q-PCR using the specific primers against the *Foxp3* locus and normalized with the input DNA. *P* value was determined by non-paired *t*-test.$^{+}$ **(B)** Western blot was performed with whole cell extracts from thymocytes of WT and *Pias1*$^{-/-}$ mice, using antibodies against STAT5, PIAS1 or Tubulin. **(C)** same as in **B** except that extracts from splenocytes either untreated or treated with human IL-2 (10 ng/ml) for 15 min were used, and filters were probed with an antibody specific for phosphorylated STAT5 (pSTAT5) or total STAT5. **(D)** same as in **A** except that anti-NFAT was used.

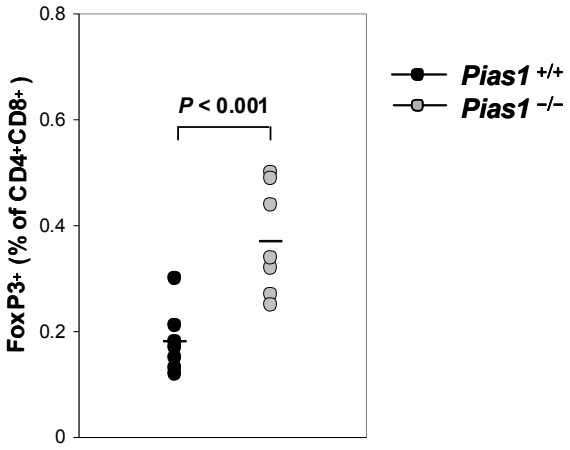

Fig. S2.12. Increased Foxp3$^+$ cells in thymic CD4$^+$CD8$^+$ DP T cells of *Pias1*$^{-/-}$ mice. Cells freshly isolated from thymus of male WT and *Pias1*$^{-/-}$ littermates (n=7) were analyzed for the percentage of Foxp3$^+$ cells by flow cytometry (gated on CD4$^+$CD8$^+$ population). *P* value was determined by non-paired *t*-test.$^+$

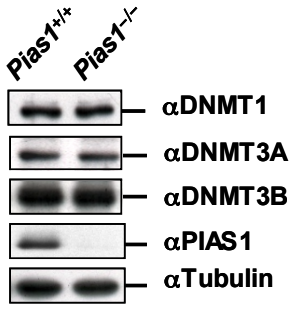

Fig. S2.13. The protein levels of DNMTs are not altered by *Pias1* disruption. Western blot was performed with whole cell extracts from thymocytes of WT and *Pias1*$^{-/-}$ mice, using antibodies against DNMT1, DNMT3A, DNMT3B, PIAS1 and Tubulin as indicated.

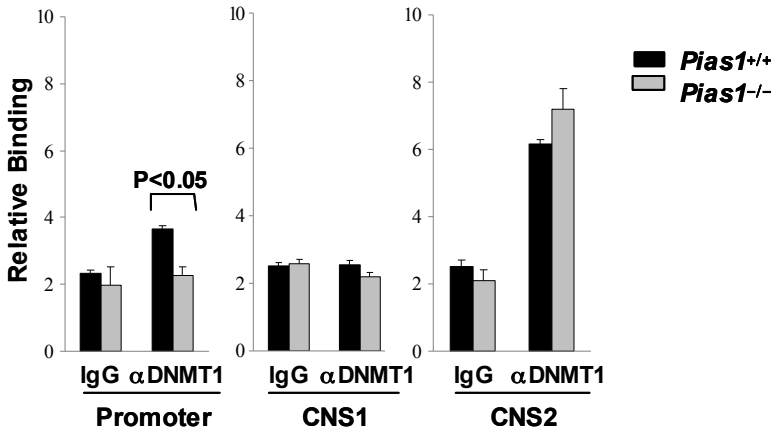

Fig. S2.14. Defective DNMT1 binding to the *Foxp3* promoter in *Pias1*$^{-/-}$ thymic CD4^{+}CD8^{+} T cells. ChIP assays were performed with freshly FACS-sorted CD4^{+}CD8^{+} thymocytes from male *Pias1*$^{+/+}$ or *Pias1*$^{-/-}$ mice (n=4), using anti-DNMT1 or IgG. Bound DNA was quantified by Q-PCR using the specific primers against the *Foxp3* locus and normalized with the input DNA. *P* value was determined by non-paired *t*-test.$^{+}$

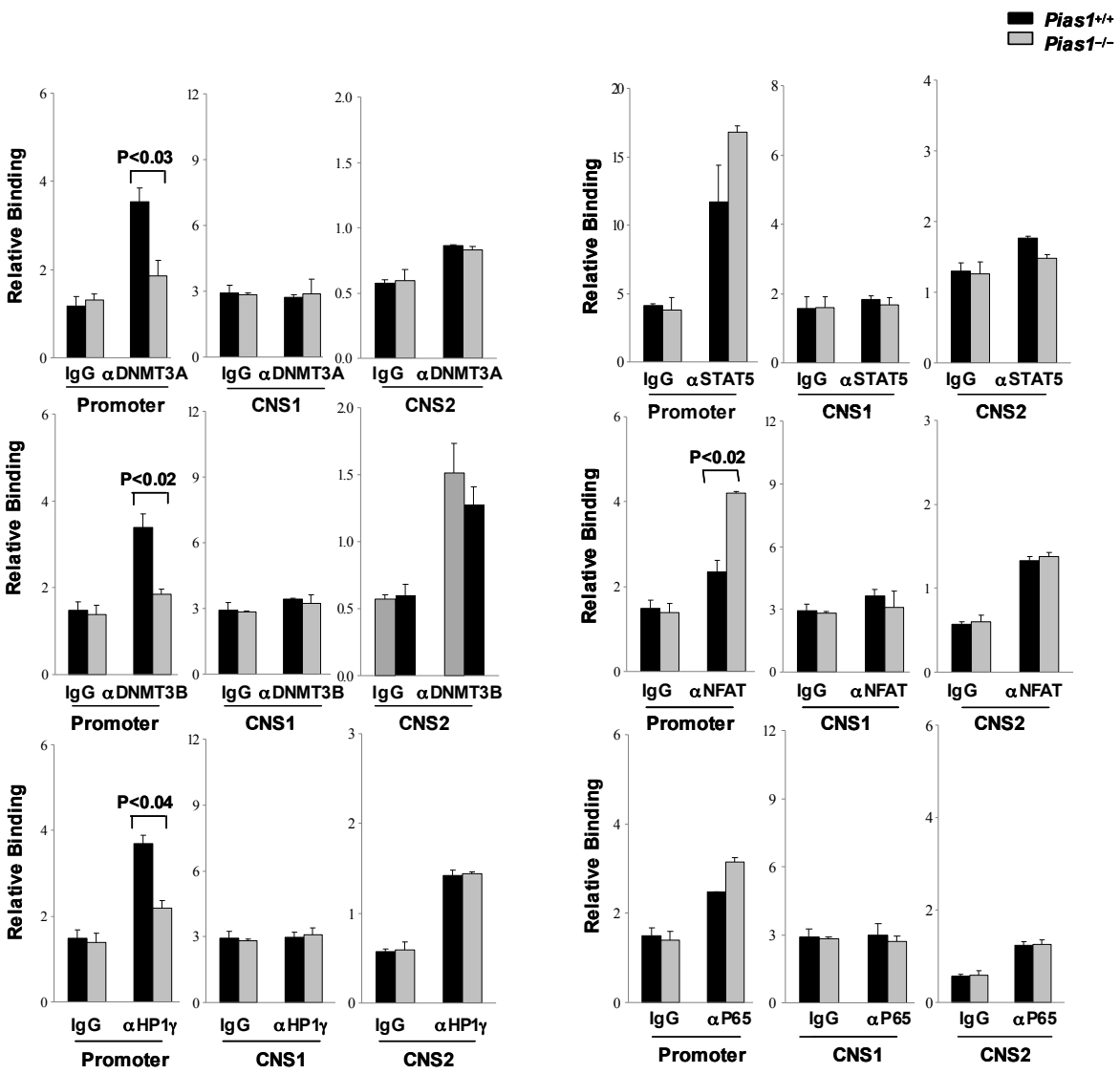

Fig. S2.15. PIAS1 affects the recruitment of DNMT3, HP1γ and transcription factors to the *Foxp3* promoter in splenic CD4$^+$CD25$^-$ T cells. ChIP assays were performed with FACS-sorted CD4$^+$CD25$^-$ splenic T cells from male *Pias1*$^{+/+}$ or *Pias1*$^{-/-}$ mice (n=4-6), using IgG or various antibodies as indicated. Bound DNA was quantified by Q-PCR using the specific primers against the *Foxp3* locus and normalized with the input DNA. *P* value was determined by non-paired *t*-test.$^+$

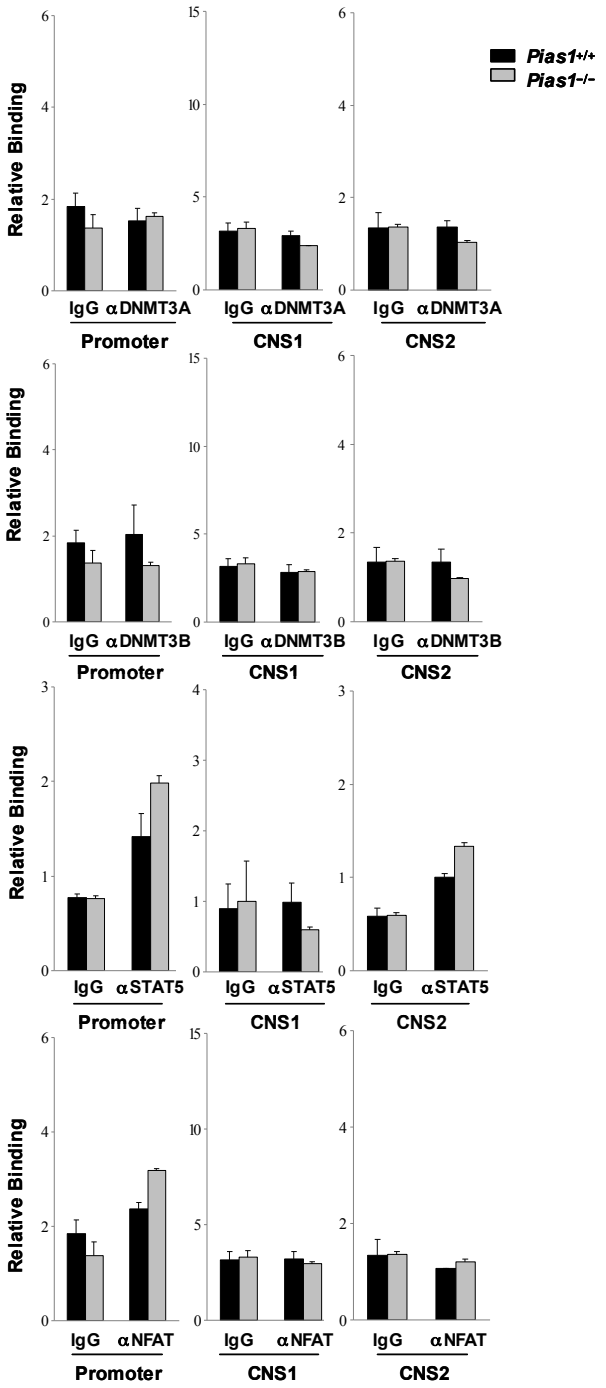

Fig. S2.16. The recruitment of DNMT3 and transcription factors to the *Foxp3* locus is not altered significantly in CD4$^+$CD25$^+$ Treg cells of *Pias1*$^{-/-}$ mice. ChIP assays were performed with FACS-sorted CD4$^+$CD25$^+$ splenic Treg cells from male *Pias1*$^{+/+}$ or *Pias1*$^{-/-}$ mice (n=4-6), using IgG or various antibodies as indicated. Bound DNA was quantified by Q-PCR and normalized with the input DNA. No significant differences were observed in all panels by non-paired *t*-test (*P*> 0.05).

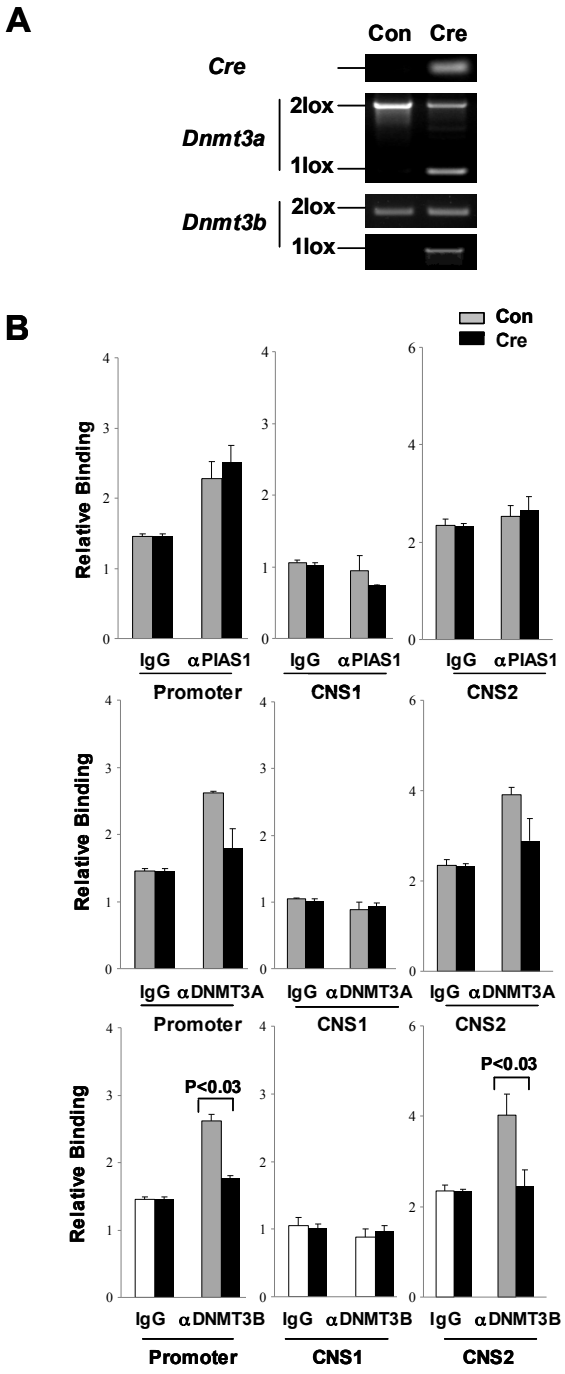

Fig. S2.17. DNMT3 does not affect the binding of PIAS1 to the *Foxp3* promoter. (A) Genotyping. Bone marrow cells from *Dnmt3a*$^{2lox/2lox}$/*Dnmt3b*$^{2lox/2lox}$ mice were infected with retrovirus encoding GFP (Con) or GFP-Cre (Cre). Genomic DNA was prepared from infected cells prior to FACS sorting for genotyping by PCR as described in Material and Methods. **(B)** ChIP assays were performed with FACS-sorted GFP^{+} splenic cells from *Dnmt3a*$^{2lox/2lox}$/*Dnmt3b*$^{2lox/2lox}$ mice 3 days post retroviral infection, using IgG or various antibodies as indicated. Bound DNA was quantified by Q-PCR with the primers specific for the *Foxp3* locus and normalized with the input DNA. *P* value was determined by non-paired *t*-test.$^{+}$

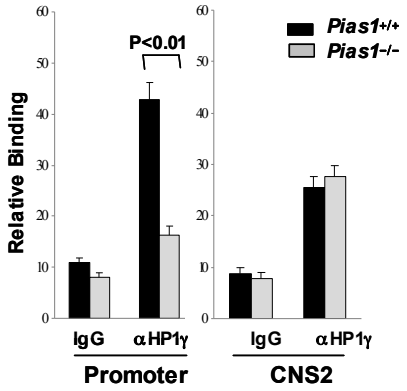

Fig. S2.18. Defective HP1γ binding to the *Foxp3* promoter in *Pias1*$^{-/-}$ thymic CD4^{+}CD8^{+} T cells. ChIP assays were performed with freshly FACS-sorted CD4^{+}CD8^{+} thymocytes from male *Pias1*$^{+/+}$ or *Pias1*$^{-/-}$ mice (n=4), using anti-HP1γ or IgG. Bound DNA was quantified by Q-PCR using the specific primers against the *Foxp3* locus and normalized with the input DNA. *P* value was determined by non-paired *t*-test.$^{+}$

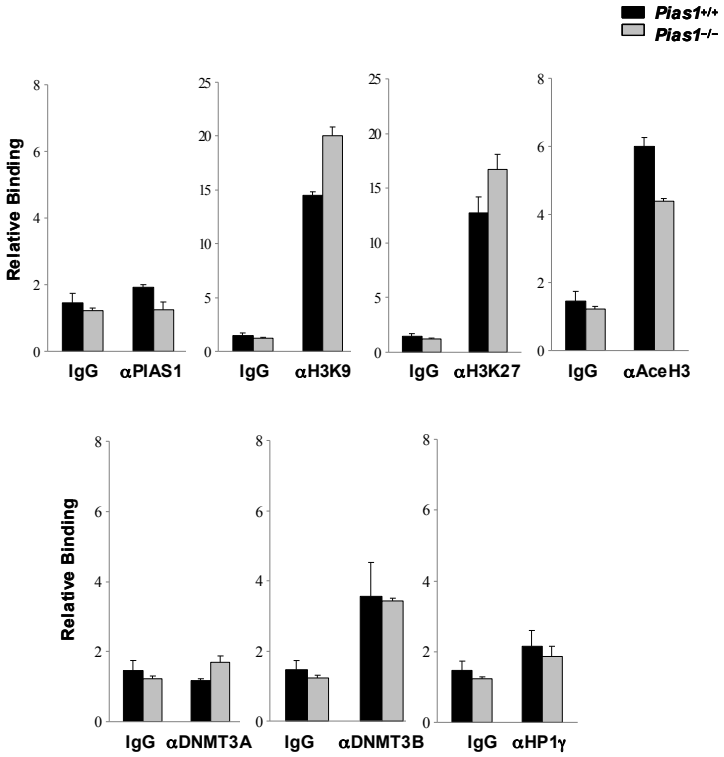

Fig. S2.19. PIAS1 does not affect the chromatin status of the *Ctla4* gene. ChIP assays were performed with FACS-sorted thymic CD4^{+}CD8^{+} T cells from male *Pias1*$^{+/+}$ or *Pias1*$^{-/-}$ mice (n=4-6), using IgG or various antibodies as indicated. Bound DNA was quantified by Q-PCR using primers specific for the *Ctla4* promoter and normalized with the input DNA. No significant differences were observed in all panels by non-paired *t*-test (*P*> 0.05).

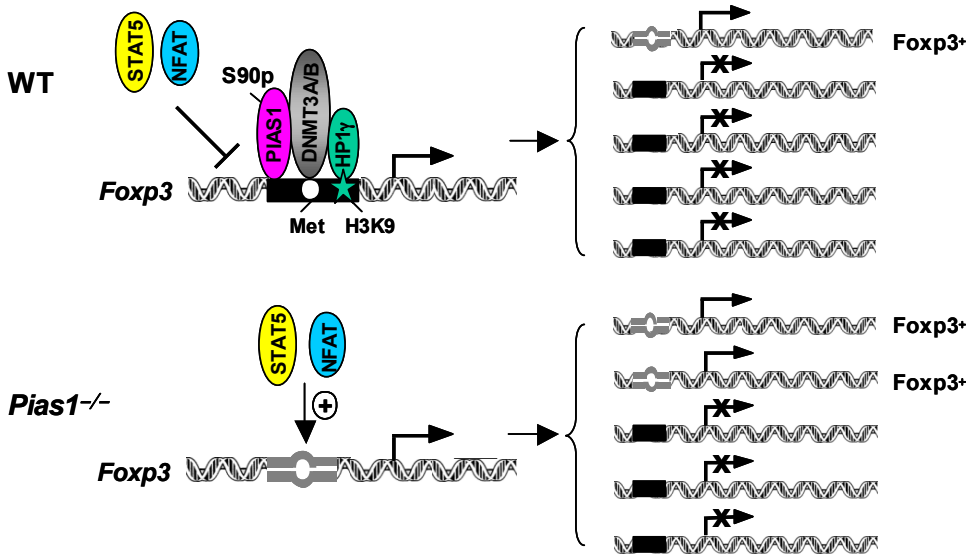

Fig. S2.20. A proposed model of PIAS1-mediated epigenetic regulation of Treg differentiation. PIAS1 binds to the *Foxp3* promoter to maintain a repressive chromatin state through the recruitment of DNMT3A, DNMT3B, and HP1γ. *Pias1* disruption leads to the formation of a permissive chromatin structure of the *Foxp3* promoter and the enhanced promoter accessibility toward transcription factors such as STAT5 and NFAT, resulting in the increased probability for precursor cells to differentiate into Foxp3^{+} Treg cells. S90p, phosphorylated Ser90; H3K9, Trimethyl-Histone H3 Lys9; Met, DNA methylation. Filled rectangle represents a repressive chromatin state, while open loop represents a permissive chromatin state.

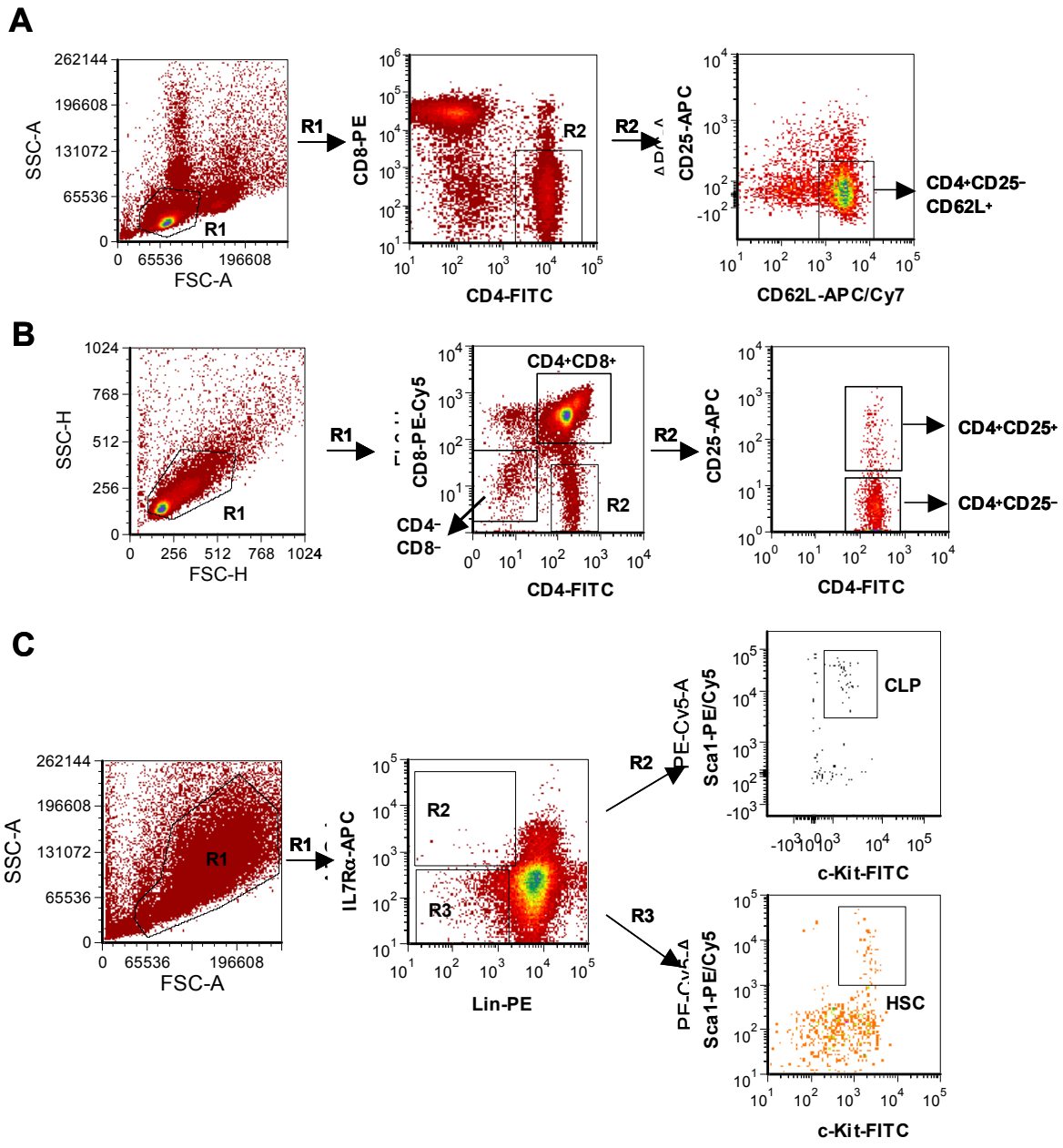

Fig. S2.21. FACS-sorting schemes. (A) Gating strategy for splenic naïve $CD4^+$ $CD25^-CD62L^+$ cells. **(B)** Gating strategy for thymic $CD4^-CD8^-$, $CD4^+$ $CD8^+$, $CD4^+$ $CD25^-$ and $CD4^+$ $CD25^+$ cells. **(C)** Gating strategy for hematopoietic stem cells (HSC) and common lymphoid progenitors (CLP) from bone marrow.

Chapter 3: PIAS1 SUMO Ligase Regulates the Self-Renewal and Differentiation of Hematopoietic Stem Cells

Note: included at the end of chapter 3 is Table 2, displaying unpublished work that was still ongoing when this article was published. Table 2 is an improvement in regards to statistical power over the published Table 1. Regardless, the original data in Table 1 is still valid, as both Table 1 and Table 2 display similar conclusions.

Article

TRANSPARENT PROCESS

THE EMBO JOURNAL

PIAS1 SUMO ligase regulates the self-renewal and differentiation of hematopoietic stem cells

Bin Liu[1,*,†], Kathleen M Yee[2,†], Samuel Tahk[1], Ryan Mackie[1], Cary Hsu[3] & Ke Shuai[1,2,**]

Abstract

The selective and temporal DNA methylation plays an important role in the self-renewal and differentiation of hematopoietic stem cells (HSCs), but the molecular mechanism that controls the dynamics of DNA methylation is not understood. Here, we report that the PIAS1 epigenetic pathway plays an important role in regulating HSC self-renewal and differentiation. PIAS1 is required for maintaining the quiescence of dormant HSCs and the long-term repopulating capacity of HSC. *Pias1* disruption caused the abnormal expression of lineage-associated genes. Bisulfite sequencing analysis revealed the premature promoter demethylation of *Gata1*, a key myeloerythroid transcription factor and a PIAS1-target gene, in *Pias1*$^{-/-}$ HSCs. As a result, *Pias1* disruption caused the inappropriate induction of *Gata1* in HSCs and common lymphoid progenitors (CLPs). The expression of other myeloerythroid genes was also enhanced in CLPs and lineage-negative progenitors, with a concurrent repression of B cell-specific genes. Consistently, *Pias1* disruption caused enhanced myeloerythroid, but reduced B lymphoid lineage differentiation. These results identify a novel role of PIAS1 in maintaining the quiescence of dormant HSCs and in the epigenetic repression of the myeloerythroid program.

Keywords epigenetic repression; hematopoietic stem cell; lineage differentiation; protein inhibitor of activated STAT1; self-renewal
Subject Categories Stem Cells; Development & Differentiation
DOI 10.1002/embj.201283326 | Received 18 September 2012 | Revised 15 October 2013 | Accepted 16 October 2013 | Published online 15 December 2013
EMBO Journal (2014) 33, 101–113

Introduction

Mouse hematopoiesis is a well characterized system to understand the regulation of hematopoietic stem cells (HSCs). HSCs are a small population of pluripotent cells in bone marrow (BM) capable of differentiating into all blood cells of the myeloerythroid and lymphoid lineages at a single cell level (Chao *et al*, 2008). HSCs can be identified by a combination of surface markers. Lin$^-$Sca1$^+$c-Kit$^+$ (LSK) cells are enriched in HSCs. Recent studies showed that dormant HSCs (d-HSCs) within the Lin$^-$Sca1$^+$c-Kit$^+$CD150$^+$CD48$^-$CD34$^-$ population harbor the vast majority of multipotent long-term self-renewal activity (Wilson *et al*, 2008). HSCs maintain the blood system through self-renewal and multi-lineage differentiation. The differentiation program of HSCs is thought to follow the hierarchy model and is governed by the coordinated expression of lineage-affiliated transcription factors (Copley *et al*, 2012).

Epigenetic mechanisms play essential roles in the regulation of the self-renewal and differentiation of HSCs (Attema *et al*, 2007; Cedar & Bergman, 2011). DNA methylation is mediated mainly by three DNA methyltransferases (DNMTs), including the de novo methyltransferases DNMT3A and DNMT3B, and the maintenance methyltransferase DNMT1 (Jaenisch & Bird, 2003). Recent studies have shown that DNMTs are critical for regulating the self-renewal and differentiation of HSCs (Tadokoro *et al*, 2007; Broske *et al*, 2009; Trowbridge *et al*, 2009; Challen *et al*, 2011). Although DNMTs do not possess sequence-specific DNA binding properties, gene-specific and temporal epigenetic changes are associated with the proper differentiation of self-renewing HSCs. The molecular mechanism that controls the methylation dynamics during HSC differentiation has not been understood.

PIAS1 (protein inhibitor of activated STAT1) is a SUMO E3 ligase that binds to chromatin to repress transcription (Shuai & Liu, 2005). Recent studies have uncovered a novel role of PIAS1 in mediating an epigenetic mechanism to restrict natural regulatory T cell (nTreg) differentiation. PIAS1 acts by recruiting DNMTs and histone modification factors such as HP1γ to promote epigenetic silencing of the *Foxp3* promoter, a transcription factor crucial for nTreg differentiation (Liu *et al*, 2010). These findings raise an interesting question on whether the PIAS1 epigenetic gene silencing pathway plays a role in stem cell biology. Here, we demonstrated that PIAS1 is important for maintaining the quiescence of dormant HSCs, and *Pias1*$^{-/-}$ LSK cells showed profound defects in long-term competitive reconstitution assays. Furthermore, PIAS1 is essential for preventing the premature and inappropriate activation of the myeloerythroid transcription factor *Gata1* through epigenetic repression. These studies identified PIAS1 as a novel epigenetic regulator of HSC self-renewal and differentiation.

1 Division of Hematology-Oncology, Department of Medicine, University of California Los Angeles, Los Angeles, CA, USA
2 Department of Biological Chemistry, University of California Los Angeles, Los Angeles, CA, USA
3 Department of General Surgery, University of California Los Angeles, Los Angeles, CA, USA
*Corresponding author. Tel: +310 206 9168; Fax: +310 825 2493; E-mail: bliu@ucla.edu
**Corresponding author. Tel: +310 206 9168; Fax: +310 825 2493; E-mail: kshuai@mednet.ucla.edu
†These authors contributed equally to this work.

Results

Altered HSCs and lineage-restricted progenitors in *Pias1*$^{-/-}$ mice

Previous studies showed that PIAS1 restricts the differentiation of $CD4^+Foxp3^+$ natural regulatory T cells (nTreg) (Liu *et al*, 2010). To address whether PIAS1 affects the differentiation of other lymphoid/myeloid lineages, flow cytometry analyses were performed with splenocytes and peripheral blood lymphocytes (PBL) from wild-type (WT) and *Pias1*$^{-/-}$ mice using lineage-specific markers (Fig S1). Minor increases in the percentages of myeloid cells were observed in periphery, with no differences in the cellularity of B cells, T cells, dendritic cells or erythroids. These data indicate that PIAS1 does not dramatically affect peripheral lineage differentiation in homeostasis.

Similar flow cytometry analyses were performed with bone marrow (BM) cells, where a reduction in the cell numbers as well as the percentage of $B220^+$ B cells was observed in *Pias1*$^{-/-}$ BM (Fig 1A and Fig S2A). When the lineage-negative (Lin^-) population was examined, a minor increase in the percentage of Lin^- cells was observed in *Pias1*$^{-/-}$ BM, although the cell number of Lin^- cells was not altered (Fig 1B and Fig S2B). Interestingly, while no significant differences were observed in common myeloid progenitor (CMP) and granulocyte monocyte progenitor (GMP) populations, a 50% decrease in common lymphoid progenitor (CLP) population was observed in *Pias1*$^{-/-}$ BM with a concurrent increase in megakaryocyte erythrocyte progenitor (MEP) as well as the myeloid-restricted $Lin^-Sca1^-c\text{-}Kit^+$ ($L^-S^-K^+$) cells (Fig 1C and Fig S2C). In addition, reduced Pre-B populations were observed in *Pias1*$^{-/-}$ BM (Fig 1C and Fig S2C).

Next, the effect of *Pias1* disruption on HSCs was examined. An approximately 2-fold increase in HSC-enriched LSK cells was observed in *Pias1*$^{-/-}$ BM (Fig 1D and Fig S2D). LSK can be further divided into long-term hematopoietic stem cells (LT-HSC; $Lin^-Sca1^+c\text{-}Kit^+CD34^-$) and short-term multi-potent progenitors (ST/MPP; $Lin^-Sca1^+c\text{-}Kit^+CD34^+$). Similar increases were observed in LT-HSC, but not ST/MPP, population (Fig 1D and Fig S2D). Dormant mouse HSCs (d-HSCs) within the $Lin^-Sca1^+c\text{-}Kit^+CD150^+CD48^-CD34^-$ population harbor the vast majority of multi-potent long-term self-renewal activity (Wilson *et al*, 2008). No significant difference was observed in the percentage or the cell number of d-HSC cells between WT and *Pias1*$^{-/-}$ BM (Fig 1E and Fig S2E).

Increased cell death of *Pias1*$^{-/-}$ lymphoid progenitors and enhanced cell proliferation of *Pias1*$^{-/-}$ dormant HSCs

To determine whether the changes in *Pias1*$^{-/-}$ progenitor populations were due to cell proliferation and/or cell death, flow cytometry analyses were performed with freshly isolated BM from WT and *Pias1*$^{-/-}$ mice using 7-AAD to reveal cell death, or Ki67 and Hoechst DNA staining to reveal cell cycle profiles. Increased cell death was observed in *Pias1*$^{-/-}$ CLP as well as Pro-B and Pre-B populations (Fig 2A), while minor difference was observed in their cell cycle properties (Fig S3). These data are consistent with the reduced B cells observed in *Pias1*$^{-/-}$ BM, and indicate that PIAS1 is important for the survival of CLP and B cell progenitors under homeostatic condition.

Interestingly, although no difference was observed in the cell cycle profiles of Lin^-, myeloid-restricted $L^-S^-K^+$, CMP, GMP, MEP and ST/MPP subpopulations, the percentage of cells in G0 phase was significantly reduced in *Pias1*$^{-/-}$ LSK cell, with a concurrent increase of the cells in G1 phase of the cell cycle (Fig 2B and Fig S3). More importantly, similar alteration in cell cycle profiles was observed in *Pias1*$^{-/-}$ LT-HSC and d-HSC, but not ST/MPP, populations as compared to that of WT controls (Fig 2B and C). These results suggest that PIAS1 is important for maintaining the quiescence of d-HSCs.

Defective long-term reconstitution capability of *Pias1*$^{-/-}$ HSCs

To directly test the functional role of PIAS1 in the regulation of HSC *in vivo*, competitive reconstitution assays were performed using WT or *Pias1*$^{-/-}$ BM cells ($CD45.2^+$) as donors and the congenic WT C57SJL BM ($CD45.1^+$) as competitors. *Pias1*$^{-/-}$ cells showed dramatic defects in reconstituting hematopoietic system of WT C57SJL recipient mice in multiple lineages, including B cells ($B220^+$), T cells ($CD3^+$) and myeloid cells ($Mac1^+$) (Fig 3A and B). The defects were significant at 5 weeks, and became more profound at later time points, with *Pias1*$^{-/-}$ donor cells exhibiting over 20-fold reduction in the ability to reconstitute blood system as compared to WT cells, indicating that PIAS1 affects the functions of progenitor cells as well as long-term HSCs. Similar results were obtained with *in vivo* competitive reconstitution assays using FACS-sorted WT or *Pias1*$^{-/-}$ LSK cells (Fig 3C and D), confirming that the reconstitution defects of *Pias1*$^{-/-}$ BM cells lie within the LSK population. These data indicate that PIAS1 is crucial for the *in vivo* reconstitution activities of HSCs and their progeny.

To further quantify the effect of PIAS1 on the long-term repopulation capability of HSCs, competitive limiting dilution assays were performed to determine the frequencies of functional HSCs in WT and *Pias1*$^{-/-}$ BM. No significant difference was observed in the percentage of donor-derived $CD45.2^+$ populations in the peripheral blood 21 weeks post the primary reconstitution (WT: 57.8 ± 11%; *Pias1*$^{-/-}$: 42.9 ± 11.5%). In contrast, by 10 weeks post secondary reconstitution, recipients of *Pias1*$^{-/-}$ BM revealed a 5-fold decrease in the competitive repopulating unit (CRU) as compared to that of WT controls (Table 1). Similar defects were observed 16 weeks post the secondary transplantation, indicating that PIAS1 is crucial for maintaining the long-term repopulation capacity of HSCs. These data strongly support for an important role of PIAS1 in the regulation of the self-renewal of HSCs *in vivo*.

The effect of PIAS1 on multi-lineage differentiation

To access the role of PIAS1 in lineage differentiation *in vivo*, the distribution of B cells, T cells and myeloid cells within the $CD45.2^+$ donor population at various time points was analyzed in competitive reconstitution assays. *Pias1*$^{-/-}$ BM cells showed defective B lymphocytes differentiation at both early and late time points, indicating that PIAS1 affects B cell progenitors as well as stem cells (Fig 3E). *Pias1*$^{-/-}$ BM also showed defective T cell differentiation at 10 and 16 weeks, while myeloid cells were not affected (Fig 3E). These data are consistent with the previous results that PIAS1 is important for the survival of CLP, while restricting the myeloid progenitor population. When reconstitution assays were performed for WT or *Pias1*$^{-/-}$ LSK cells, no difference was observed at 4 or

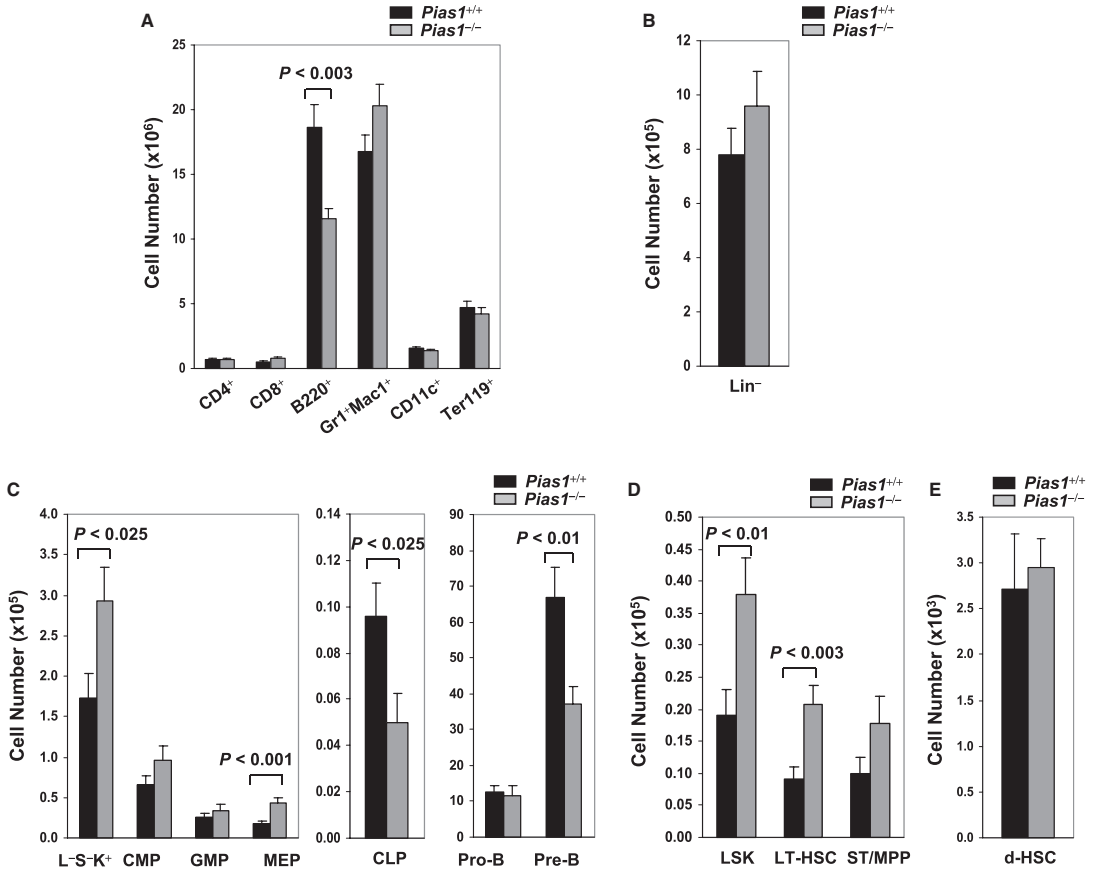

Figure 1. Altered lineage-restricted progenitors and LSK populations in *Pias1*$^{-/-}$ mice.

A Cell numbers of T cells ($CD4^+$ or $CD8^+$), B cells ($B220^+$), granulocytes/monocytes ($Gr1^+Mac1^+$), dendritic cells ($CD11c^+$) and erythroids ($Ter119^+$) in freshly isolated bone marrow (BM) from 8 to 12 weeks old WT (*Pias1*$^{+/+}$) and *Pias1*$^{-/-}$ littermates were assayed by flow cytometry.

B Same as in (A) except that cell numbers of Lin^- cells were assayed.

C Same as in (A) except that cell numbers of myeloid-restricted $Lin^-Sca1^-c\text{-}Kit^+$ ($L^-S^-K^+$) populations, common myeloid progenitors (CMP), granulocyte monocyte progenitors (GMP), megakaryocyte erythrocyte progenitors (MEP), common lymphoid progenitors (CLP), Pro-B and Pre-B cells as defined in supplementary Materials and Methods were assayed.

D Same as in (A) except that cell numbers of LSK, long-term hematopoietic stem cells (LT-HSC) and short-term multi-potent progenitors (ST/MPP) as defined in supplementary Materials and Methods in total BM were assayed.

E Same as in (A) except that cell numbers of dormant hematopoietic stem cells (d-HSCs; $Lin^-Sca1^+c\text{-}Kit^+CD150^+CD48^-CD34^-$) were assayed.

Data information: Shown in each panel is a pool of 3 independent experiments (n = 9–13). Error bars represent SEM. P-values were determined by non-paired t-test.
See also Fig S1 and S2.

10 weeks except for the reduced B cells from *Pias1*$^{-/-}$ LSK donors at 10 weeks, further suggesting that PIAS1 is important for B cell differentiation at multiple stages (Fig 3F). In contrast, both B and T cell lineages were defective, while myeloid cell differentiation was increased from *Pias1*$^{-/-}$ LSK donors at 17 weeks. These data indicate that PIAS1 is important for balancing the long-term multi-lineage differentiation of HSC between CLP and CMP.

Increased myeloid-restricted $Lin^-Sca1^-c\text{-}Kit^+$ ($L^-S^-K^+$) population was observed in *Pias1*$^{-/-}$ BM (Fig 1C and Fig S2C). To address whether PIAS1 affects the differentiation of $L^-S^-K^+$ cells into their progeny *in vivo*, short-term competitive reconstitution assays were performed with FACS-sorted $L^-S^-K^+$ cells from WT or *Pias1*$^{-/-}$ littermates (Fig S4). Surprisingly, *Pias1*$^{-/-}$ $L^-S^-K^+$ cells showed defects in differentiating into $Mac1^+$ cells as compared to WT controls, indicating that PIAS1 is important for the proper differentiation of $L^-S^-K^+$ cells into their progeny.

No defects in *Pias1*$^{-/-}$ BM homing and niche retention

The observed defects in the long-term reconstitution capacity of *Pias1*$^{-/-}$ HSC can be explained by several mechanisms, including the intrinsic properties of *Pias1*$^{-/-}$ cells such as self-renewal, as well

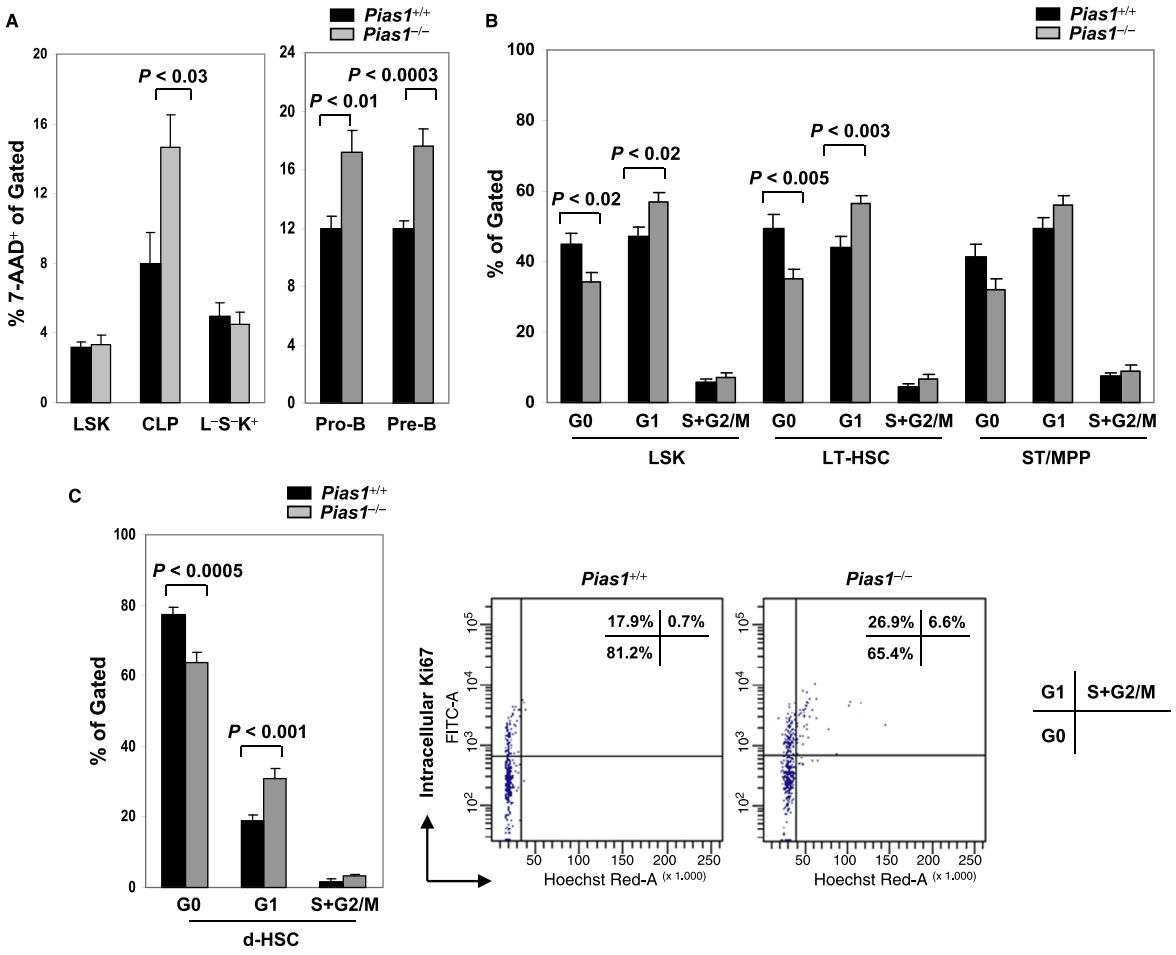

Figure 2. Increased cell death of *Pias1*$^{-/-}$ lymphoid progenitors and enhanced cell proliferation of *Pias1*$^{-/-}$ dormant HSCs (d-HSCs).

A Cell death of indicated BM subsets from *Pias1*$^{-/-}$ mice and their WT littermates (*Pias1*$^{+/+}$) were assayed by 7-AAD staining followed by flow cytometry.

B Cell proliferation of indicated BM subsets from WT and *Pias1*$^{-/-}$ mice was revealed by intracellular Ki67 (icKi67) and Hoechst DNA staining followed by flow cytometry. G0, icKi67^{-}, 2N DNA content; G1, icKi67^{+}, 2N DNA content; S+G2/M, icKi67^{+}, > 2N DNA content.

C Same as in (B) except that d-HSCs were assayed (left). A representative cell cycle profile of WT and *Pias1*$^{-/-}$ d-HSCs was also shown (right). Numbers in top right are the percentage of cells in each cell cycle.

Data information: Shown in each panel is a pool of 3 independent experiments (n = 10–13). Error bars represent SEM. *P*-values were determined by non-paired *t*-test. See also Fig S3.

Figure 3. Impaired long-term reconstitution capability and altered lineage differentiation of *Pias1*$^{-/-}$ HSCs.

A *In vivo* competitive reconstitution assays. Total bone marrow cells (2 × 10^5) from WT or *Pias1*$^{-/-}$ littermates (CD45.2$^+$) were mixed with 2 × 10^5 of WT C57SJL bone marrow cells (CD45.1$^+$) and injected into lethally irradiated WT C57SJL mice. The percentage of T cells (CD3$^+$), B cells (B220$^+$) and myeloid cells (Mac1$^+$) from donor mice in peripheral blood (PBL) were assayed by flow cytometry at 5, 10 and 16 weeks post reconstitution.

B Same as in (A) except that bone marrow (BM) cells from the recipient mice were assayed at 20 weeks post reconstitution.

C Same as in (A) except that FACS-sorted LSK cells (1000) from WT or *Pias1*$^{-/-}$ littermates were used.

D Same as in (B) except that FACS-sorted LSK cells (1000) from WT or *Pias1*$^{-/-}$ littermates were used.

E Same as in (A) except that the percentage of T cells (CD3$^+$), B cells (B220$^+$) and myeloid cells (Mac1$^+$) within the donor cells (CD45.2$^+$) in peripheral blood (PBL) were presented.

F Same as in (E) except that FACS-sorted LSK cells (1000) from WT or *Pias1*$^{-/-}$ littermates were used.

Data information: Shown is a pool of 3 independent experiments in all panels (n = 10). Error bars represent SEM. *P*-values were determined by non-paired *t*-test. See also Fig S4.

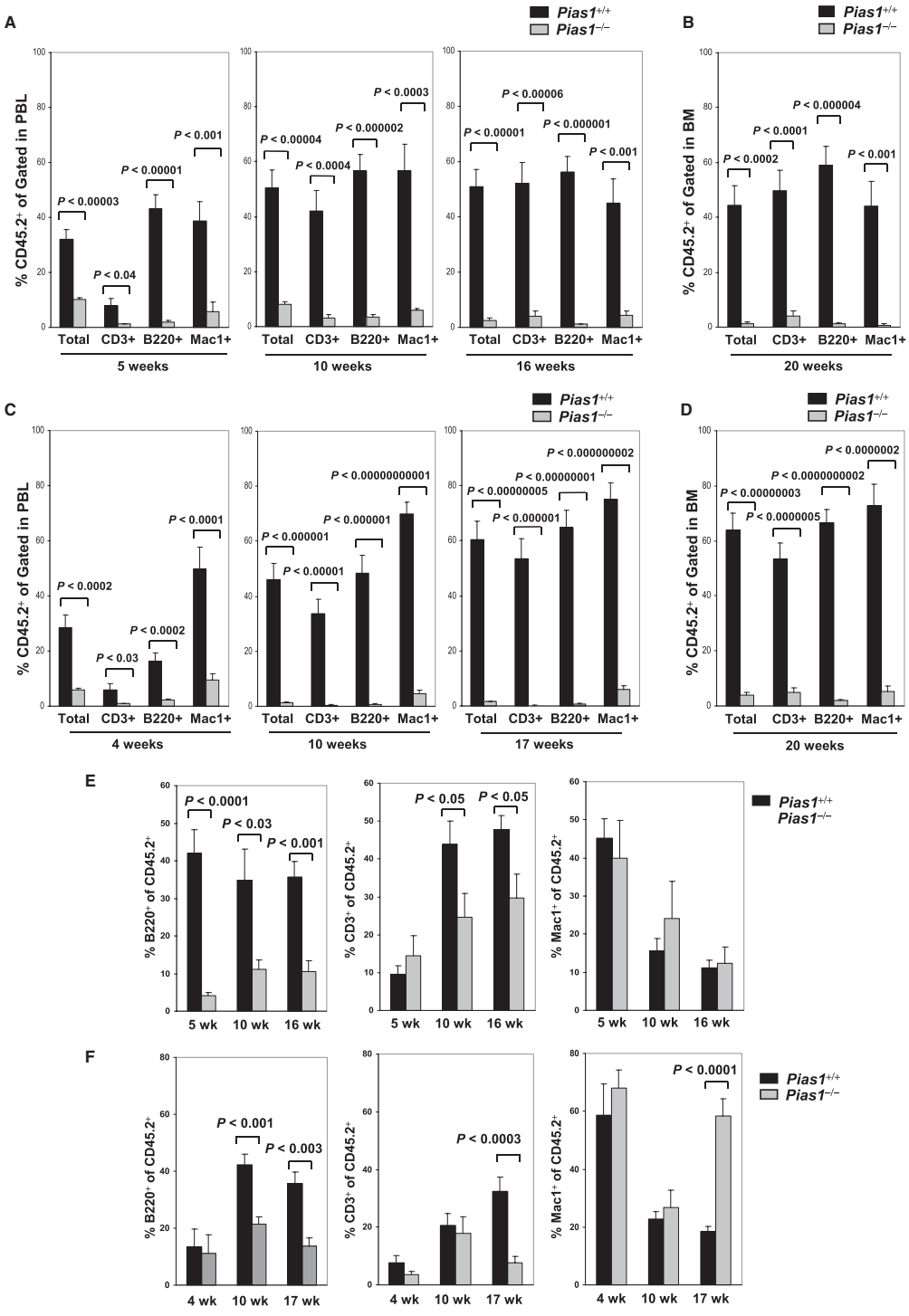
A
Pias1+/+
Pias1−/−
% CD45.2+ of Gated in PBL
P < 0.00003
P < 0.04
P < 0.00001
P < 0.001
P < 0.00004
P < 0.0004
P < 0.000002
P < 0.0003
P < 0.00001
P < 0.00006
P < 0.000001
P < 0.001
Total CD3+ B220+ Mac1+
5 weeks
10 weeks
16 weeks
B
% CD45.2+ of Gated in BM
P < 0.0002
P < 0.0001
P < 0.000004
P < 0.001
20 weeks
C
% CD45.2+ of Gated in PBL
P < 0.0002
P < 0.03
P < 0.0002
P < 0.0001
P < 0.000001
P < 0.00001
P < 0.000001
P < 0.00000000001
P < 0.00000005
P < 0.000001
P < 0.00000001
P < 0.000000002
4 weeks
10 weeks
17 weeks
D
% CD45.2+ of Gated in BM
P < 0.00000003
P < 0.0000005
P < 0.00000002
P < 0.0000002
20 weeks
E
% B220+ of CD45.2+
P < 0.0001
P < 0.03
P < 0.001
% CD3+ of CD45.2+
P < 0.05
P < 0.05
% Mac1+ of CD45.2+
5 wk 10 wk 16 wk
F
% B220+ of CD45.2+
P < 0.001
P < 0.003
% CD3+ of CD45.2+
P < 0.0003
% Mac1+ of CD45.2+
P < 0.0001
4 wk 10 wk 17 wk

Table 1. Evaluation by limiting dilution analysis of competitive long-term repopulating cells (CRU) in mice transplanted with WT (*Pias1*$^{+/+}$) or *Pias1*-null (*Pias1*$^{-/-}$) bone marrow cells

	CRU evaluation of primary recipients[a]			
	10 weeks post transplantation		16 weeks post transplantation	
Number of cells injected into secondary recipients	*Pias1*$^{+/+}$	*Pias1*$^{-/-}$	*Pias1*$^{+/+}$	*Pias1*$^{-/-}$
2,000,000	3/3 (24.5 ± 9.7)	4/4 (4.7 ± 2.7)	3/3 (32.5 ± 11.2)	3/4 (3.9 ± 2.5)
1,000,000	2/2 (29.5 ± 0.1)	1/2 (1.2 ± 1.1)	2/2 (29.4 ± 21.2)	1/2 (1.0 ± 0.8)
300,000	3/3 (8.9 ± 5.3)	0/3 (0.5 ± 0.1)	3/3 (16.5 ± 9.9)	0/3 (0.2 ± 0.1)
100,000	1/5 (0.5 ± 0.7)	0/5 (0.3 ± 0.2)	0/5 (0.2 ± 0.3)	0/5 (0.3 ± 0.2)
CRU frequency per 10^5 cells (range)[b]	0.52 (0.20–1.34)	0.09 (0.04–0.21)	0.37 (0.14–0.97)	0.06 (0.02–0.15)

[a]Results are expressed as number of mice repopulated with donor-derived cells (CD45.2$^+$; >1%) over total. Numbers in parentheses represent the mean % ± s.d. of peripheral blood CD45.2$^+$ cells found in the transplanted recipients.
[b]CRU frequency was calculated using Extreme Limiting Dilution Analysis (ELDA) software available at http://bioinf.wehi.edu.au/software/elda/.

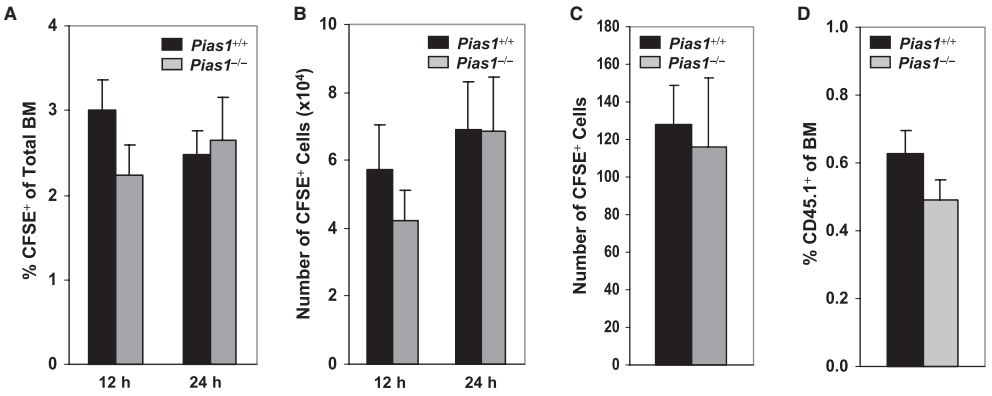

Figure 4. No defects in BM homing or niche retention in *Pias1*$^{-/-}$ mice.

A Homing of bone marrow (BM) cells. CFDA-SE (CFSE)-labeled total BM cells (2×10^7) from WT and *Pias1*$^{-/-}$ littermates were injected into lethally irradiated WT C57SJL mice. The percentage of CFSE$^+$ cells in BM of the recipient mice was determined by flow cytometry 12 and 24 h post injection.

B Same as in (A) except that the number of CFSE$^+$ cells was presented.

C Same as in (A) except that CFSE-labeled long-term hematopoietic stem cells (LT-HSC; Lin$^-$Sca1$^+$c-Kit$^+$CD34$^-$) cells (2000 cells/mouse) from WT and *Pias1*$^{-/-}$ littermates were used, and the number of CFSE$^+$ cells in BM of the recipient mice was determined 24 *h post injection.*

D Niche retention assays. Total BM cells (4×10^7) from WT C57SJL mice (CD45.1$^+$; n = 12) were injected into non-irradiated WT or *Pias1*$^{-/-}$ recipient mice (CD45.2$^+$). The percentage of CD45.1$^+$ cells in BM of the recipient mice were assayed by flow cytometry 12 weeks post injection.

Data information: Shown in each panel is a pool of 2 independent experiments (n = 9–10). Error bars represent SEM.

as *Pias1*$^{-/-}$ cells homing to BM and niche retention. To examine whether *Pias1*$^{-/-}$ BM cells are defective in homing to BM, CFDA-SE (CFSE)-labeled WT or *Pias1*$^{-/-}$ BM cells were injected into lethally irradiated WT C57SJL recipient mice, and cells migrated to BM were determined by measuring CFSE$^+$ cells in BM. No difference was observed in the ability of *Pias1*$^{-/-}$ cells to home to BM compared to that of WT controls (Fig 4A and B). Similar results were obtained with LT-HSC cells, suggesting that *Pias1*$^{-/-}$ LT-HSC cells are not defective in homing to BM (Fig 4C).

HSCs are thought to reside in niches, which are cellular and molecular microenvironments that regulate stem cell quiescence, self-renewal and differentiation (Jones & Wagers, 2008; Kiel & Morrison, 2008). The ability of *Pias1*$^{-/-}$ BM cells to be retained in the niche was examined by nonablative transplant assays, where BM from WT C57SJL mice (CD45.1$^+$) were injected into non-irradiated WT or *Pias1*$^{-/-}$ mice (Fig 4D). No difference was observed in the engraftment of WT C57SJL cells into WT or *Pias1*$^{-/-}$ mice, indicating that the HSC niche in both WT and *Pias1*$^{-/-}$ mice are stably occupied by host cells. Taken together, these results indicate that the observed defects in the long-term reconstitution capacity of *Pias1*$^{-/-}$ HSC are not due to defects in BM homing or niche retention, implying that PIAS1 is crucial for the intrinsic properties of HSCs.

No defects in the BM microenvironment of *Pias1*$^{-/-}$ mice

It is well established that BM microenvironment is important for HSC function and maintenance (Jones & Wagers, 2008; Kiel & Morrison, 2008; Ehninger & Trumpp, 2011). To test whether the impaired function of *Pias1*$^{-/-}$ HSC is due to altered BM microenvironments

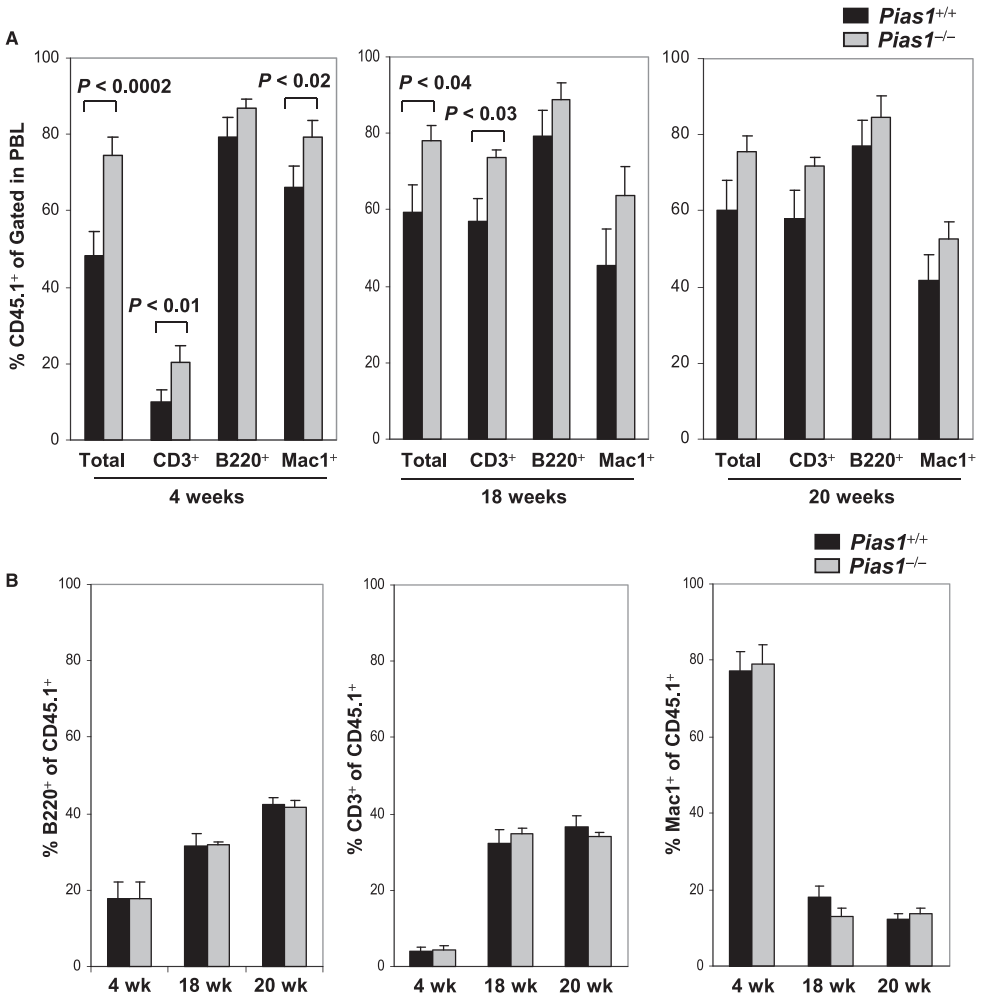

Figure 5. No defects in BM microenvironment in *Pias1*$^{-/-}$ mice.

A *In vivo* reconstitution assays. Total BM cells (4×10^5) from WT C57SJL mice (CD45.1$^+$) were injected into lethally irradiated WT or *Pias1*$^{-/-}$ recipient mice (CD45.2$^+$). The percentage of T cells (CD3$^+$), B cells (B220$^+$) and myeloid cells (Mac1$^+$) from donor mice in peripheral blood (PBL) were assayed by flow cytometry at 4, 18 and 20 weeks post reconstitution.

B Same as in (A) except that the percentage of T cells (CD3$^+$), B cells (B220$^+$) and myeloid cells (Mac1$^+$) within the donor cells (CD45.1$^+$) in PBL were assayed.

Data information: In (A) and (B) is shown a pool of 2 independent experiments (n = 9–10). Error bars represent SEM. *P*-values were determined by non-paired *t*-test.

in *Pias1*$^{-/-}$ mice, *in vivo* reconstitution assays were performed by transplanting WT C57SJL BM cells into lethally irradiated WT or *Pias1*$^{-/-}$ recipient mice. Interestingly, enhanced engraftment of WT C57SJL cells into *Pias1*$^{-/-}$ mice was observed at 4 weeks and 18 weeks, while the difference was diminished at 20 weeks (Fig 5A). In addition, no differences in the distribution of mature T cells, B cells and myeloid cells within WT donor cells were observed at all time points examined (Fig 5B). These results indicate that the BM microenvironment in *Pias1*$^{-/-}$ mice is not responsible for the impaired *Pias1*$^{-/-}$ HSC functions, further suggesting that PIAS1 regulates the intrinsic properties of HSCs.

Abnormal expression of lineage-specific genes in *Pias1*$^{-/-}$ cells

To test if *Pias1* disruption affects the transcription of lineage-specific genes, Q-PCR assays were performed with Lin$^-$ progenitors from WT and *Pias1*$^{-/-}$ BM. While no change or slight increase was observed in the expression of myeloerythroid-specific genes, including *Gata1* (GATA-binding factor 1), *Gata2* (GATA-binding factor 2), *Csf1r* (Macrophage colony-stimulating factor 1 receptor), *Mpo* (Myeloperoxidase) and *Cebpa* (CCAAT/enhancer-binding protein alpha) (Akashi *et al*, 2000), transcription of genes essential for B cell differentiation, including *Il7r* (Interleukin-7 receptor subunit

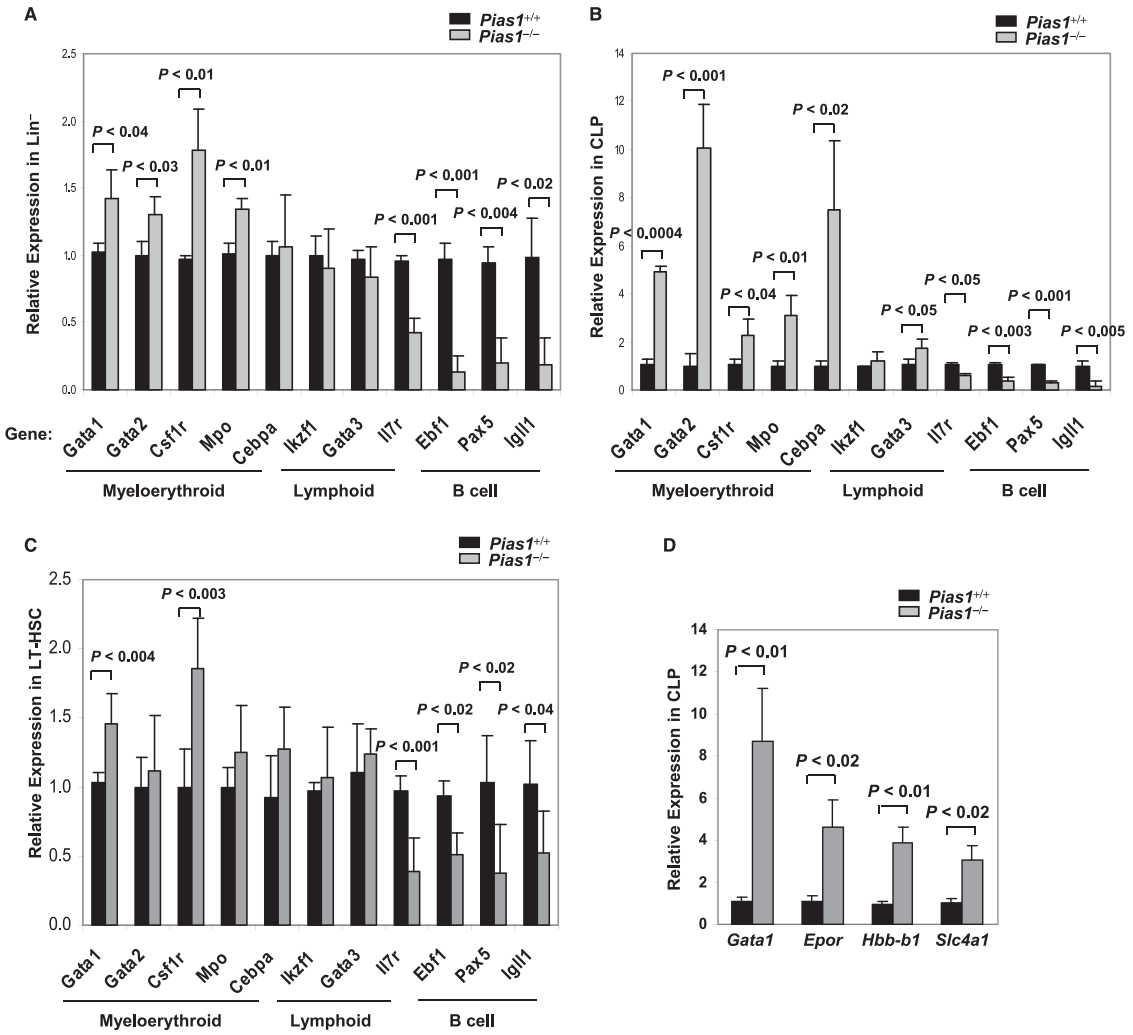

Figure 6. Transcription of the lineage-affiliated genes is regulated by PIAS1.

A Quantitative real time polymerase chain reaction (Q-PCR) analyses were performed with total RNA from WT or *Pias1*$^{-/-}$ Lin$^-$ population. The expression of each gene in WT cells was relatively set as 1, and the results were adjusted by *Hprt1*.

B Same as in (A) except that common lymphoid progenitors (CLP) cells were used.

C Same as in (A) except that long-term hematopoietic stem cells (LT-HSC; Lin$^-$Sca1$^+$c-Kit$^+$CD34$^-$) cells were used.

D Same as in (A) except that CLP cells were used, and the expression of GATA1-downstream genes was quantified.

Data information: Shown in each panel is the average of 3–5 independent experiments. Error bars represent SEM. *P*-values were determined by non-paired *t*-test. See also Fig S5.

alpha), *Ebf1* (Early B-cell factor 1), *Pax5* (Paired box protein Pax-5) and *Igll1* (Immunoglobulin lambda-like polypeptide 1) was significantly reduced (Fig 6A). In contrast, transcription of other lymphoid-associated genes, such as *Ikzf1* (Ikaros family zinc finger protein 1) and T cell-specific factor *Gata3* (GATA-binding factor 3), was not altered. These data are consistent with the defective B lymphoid differentiation phenotype observed in *Pias1*$^{-/-}$ BM cells, further supporting the notion that PIAS1 is important for maintaining the expression of B cell-specific genes while restricting the expression of myeloerythroid genes.

GATA1, a key transcription factor for erythropoiesis, can directly repress the transcription of *Ebf1* (Iwasaki *et al*, 2003; Xie *et al*, 2004). To further investigate the role of PIAS1 in the transcriptional regulation of lineage-associated genes, Q-PCR analyses were

performed with various FACS-sorted BM subpopulations from WT and *Pias1*$^{-/-}$ mice (Fig S5). Interestingly, transcription of myeloerythroid-associated genes, including *Gata1, Gata2, Csf1r, Mpo* and *Cebpa,* was dramatically increased in CLP cells, with a concurrent decrease in genes important for B cell differentiation, such as *Il7r, Ebf1, Pax5* and *Igll1* (Fig 6B). When HSC-enriched LT-HSC cells were examined, increased transcription of *Gata1, Csf1r* and *Csf1r* and decreases in B cell differentiation-related genes, including *Il7r, Ebf1, Pax5* and *Igll1*, were observed (Fig 6C). In addition, transcription of these genes was not affected in CMP (Fig S5). These data indicate that PIAS1 is an important transcriptional regulator for the proper expression of lineage-affiliated genes in LT-HSC and CLP.

To test whether PIAS1 affects the transcription of GATA1-downstream genes, Q-PCR analyses were performed with FACS-sorted CLP cells from WT and *Pias1*$^{-/-}$ BM to assess the transcription of several GATA1-regulated genes, including *Epor* (Erythropoietin receptor), *Hbb-b1* (Hemoglobin subunit beta-1) and *Slc4a1* (Solute carrier family 4 member 1; an erythroid specific factor) (Fig 6D). The transcription of all 3 genes were increased in *Pias1*$^{-/-}$ CLP cells as compared to that of WT controls, suggesting that enhanced *Gata1* transcription in *Pias1*$^{-/-}$ cells leads to the functional increase in GATA1-mediated gene activation.

PIAS1 suppresses *Gata1* through direct epigenetic silencing

To test whether *Gata1* is a direct PIAS1-target gene, chromatin immunoprecipitation (ChIP) assays were performed with WT and *Pias1*$^{-/-}$ BM cells using 2 independent PIAS1 antibodies (Fig 7A). Binding of PIAS1 to the promoter region of *Gata1* was observed in WT, but not *Pias1*$^{-/-}$ BM, indicating that *Gata1* is a direct target of PIAS1. ChIP assays were also performed with FACS-sorted LSK or myeloerythroid-restricted $L^-S^-K^+$ cells (Fig 7B). PIAS1 also binds to the promoter region of *Gata1* in these cells.

PIAS1 has been shown to regulate the promoter methylation of the *Foxp3* gene (Liu *et al*, 2010). To understand the mechanism of PIAS1-mediated transcriptional repression of *Gata1*, the methylation status of the *Gata1* promoter was analyzed by bisulfite-sequencing of WT and *Pias1*$^{-/-}$ BM subpopulations. Several CpG sites in the *Gata1* promoter were hypermethylated in WT LT-HSC and ST/MPP cells (Fig 7C). *Pias1* disruption caused a significant reduction of DNA methylation in the *Gata1* promoter, consistent with the enhanced transcription of *Gata1* observed in *Pias1*$^{-/-}$ LT-HSC cells (Fig 6C).

It has been demonstrated that PIAS1 is important for the recruitment of DNMT3A/3B to the *Foxp3* promoter (Liu *et al*, 2010). To test whether PIAS1 interacts with DNMT3A in BM cells *in vivo*, co-immunoprecipitation (Co-IP) assays were performed with cell extracts from BM using anti-PIAS1 antibody, followed by immunoblotting with anti-DNMT3A. PIAS1 can interact with DNMT3A in BM cells (Fig 7D). Furthermore, ChIP assays revealed that while DNMT3A binds to the *Gata1* promoter in WT BM cells, the binding of DNMT3A to the *Gata1* promoter was abolished in *Pias1*$^{-/-}$ BM (Fig 7E). These results indicate that PIAS1 is required for the recruitment of DNMT3A to the *Gata1* promoter in BM, and further suggest that PIAS1 represses *Gata1* transcription by maintaining DNA methylation of the *Gata1* promoter in HSCs.

Discussion

PIAS1 is a SUMO E3 ligase involved in the regulation of multiple transcriptional programs (Shuai & Liu, 2005; Liu *et al*, 2007; Liu & Shuai, 2008). Recent studies have uncovered an important role of PIAS1 in mediating a novel epigenetic mechanism to restrict the expression of *Foxp3* in natural regulatory T cells (Liu *et al*, 2010). In this manuscript, we explored the role of the newly identified PIAS1 epigenetic pathway in the regulation of HSCs. Our results have identified an essential role of PIAS1 in regulating the self-renewal and differentiation of HSCs (Fig 8).

We demonstrated that *Pias1*$^{-/-}$ BM cells as well as HSC-enriched LSK population failed to reconstitute blood system in the presence of WT competitors. No defects were observed in *Pias1*$^{-/-}$ BM microenvironment, niche retention, or homing, suggesting an intrinsic role of PIAS1 in regulating the self-renewal of HSCs. It has been documented that the $Lin^-Sca1^+c\text{-}Kit^+CD150^+CD48^-CD34^-$ population is enriched in dormant HSCs (d-HSCs), and the ability of d-HSCs to remain quiescent is crucial for maintaining the capacity for lifelong replenishment of all blood cells. *Pias1*$^{-/-}$ d-HSCs showed reduced G0 population with an increase in G1 phase (non-quiescent cells). These results suggest an important role of PIAS1 in maintaining the quiescence of d-HSCs. It is likely that the increased cell proliferation of *Pias1*$^{-/-}$ d-HSCs resulted in their exhaustion and reduced long-term reconstitution capacity. The effect of *Pias1* disruption on cell proliferation was only observed in HSC-enriched populations, including d-HSCs, LT-HSCs and LSK cells, but not differentiated BM progenitor subsets, such as CMP, GMP, MEP, CLP and myeloid-restricted $Lin^-Sca1^-c\text{-}Kit^+$. The precise molecular mechanism responsible for PIAS1-mediated regulation on the quiescence of d-HSCs is not known. It will be very interesting to test whether the PIAS1-mediated epigenetic control mechanism is involved in this process, although this is technically challenging due to the rareness of dormant HSCs.

It has been documented that DNA methylation plays an important role in the regulation of HSC self-renewal and differentiation (Tadokoro *et al*, 2007; Broske *et al*, 2009; Trowbridge *et al*, 2009; Challen *et al*, 2011), but how DNMTs are regulated to control methylation dynamics in hematopoiesis is not known. PIAS1 interacts with DNMTs *in vivo* (Liu *et al*, 2010) (Fig 7D). Our recent studies in regulatory T cells suggest that PIAS1 can recruit DNMTs to specific gene promoters to promote DNA methylation (Liu *et al*, 2010), suggesting that PIAS1 may function as a cofactor of DNMTs. In this report, we showed that *Gata1* is a direct target of PIAS1, and *Pias1* disruption resulted in the premature demethylation of the *Gata1* promoter in HSCs. Consistently, an inappropriate induction of *Gata1* in HSCs and CLPs was observed. *Gata1* is a key myeloerythroid transcription factor and its elevated expression can suppress the induction of crucial lymphoid genes such as *Ebf1* (Iwasaki *et al*, 2003). Indeed, the expression of a number of B lymphoid genes was significantly repressed in *Pias1*-null Lin^- progenitor cells (Fig 6A). As a result, defective B cell differentiation was observed in the absence of PIAS1 (Fig 1A). These results suggest that the PIAS1 epigenetic pathway plays an important role in preventing the inappropriate expression of the myeloerythroid gene program, which is essential for the balanced myeloerythroid vs lymphoid lineage differentiation.

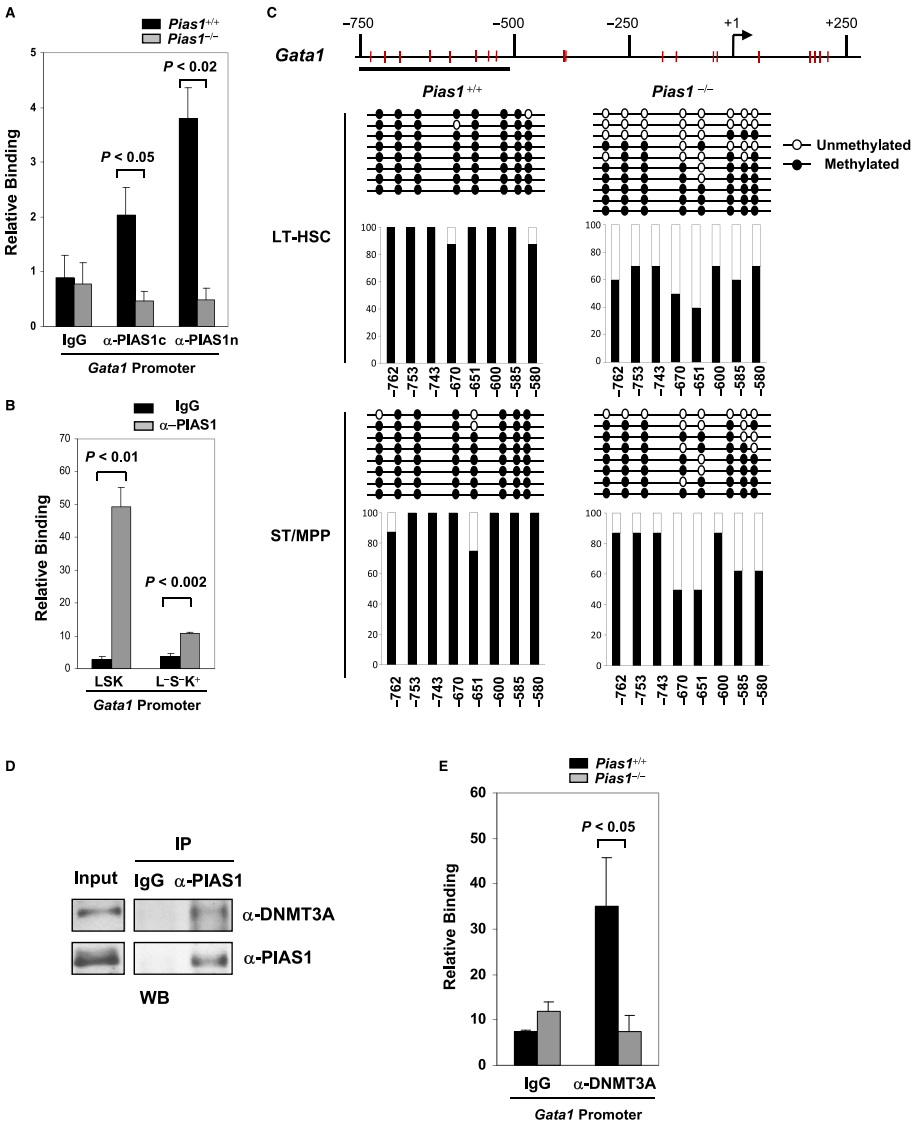

Figure 7. PIAS1 suppresses *Gata1* through direct epigenetic silencing.

A Chromatin immunoprecipitation (ChIP) assays were performed with cell extracts from WT or *Pias1*$^{-/-}$ BM, using 2 independent antibodies against either the C-terminal (α-PIAS1c) or the N-terminal (α-PIAS1n) PIAS1, or IgG as a negative control. Bound DNA was quantified by Q-PCR with specific primers against *Gata1* promoter, and normalized with the input DNA.

B Same as in (A) except that FACS-sorted LSK or Lin^{-}Sca1^{-}c-Kit^{+} (L^{-}S^{-}K^{+}) cells from WT BM were used.

C Methylation analysis of the *Gata1* promoter was performed by bisulfite conversion of genomic DNA from FACS sorted long-term hematopoietic stem cells (LT-HSC) and short-term multi-potent progenitors (ST/MPP) as defined in Materials and Methods from WT and *Pias1*$^{-/-}$ male mice (n = 5). The x axis represents the positions of the CpG sites relative to the transcription start site ($^{+}$1); the y axis represents the percentage.

D PIAS1 interacts with DNMT3A in BM cells. Co-immunoprecipitation (Co-IP) assays were performed with cell extracts from WT BM, using anti-PIAS1 or IgG, followed by immunoblotting with anti-DNMT3A or a monoclonal anti-PIAS1.

E PIAS1 is required for the recruitment of DNMT3A to the *Gata1* promoter. Same as in (A) except that anti-DNMT3A was used for ChIP assays.

Data information: Shown in each panel is a representative of 3 independent experiments (n = 4–6 for each experiment). Error bars represent SEM. P-values were determined by non-paired t-test.

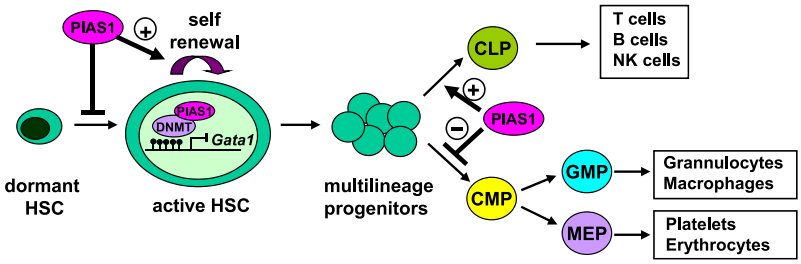

Figure 8. A proposed model of the essential function of PIAS1 in the regulation of self-renewal and lineage differentiation of HSCs.
PIAS1 restricts dormant cells to enter the active cell cycle, while supports the self-renewal of active HSC. PIAS1 also supports the proper differentiation of lymphoid cells, while restricting the myeloerythroid lineage.

Studies from several groups have shown that DNMTs play important roles in regulating the self-renewal and differentiation of HSCs (Tadokoro *et al*, 2007; Broske *et al*, 2009; Trowbridge *et al*, 2009; Challen *et al*, 2011). The conditional knockout of *Dnmt3a* impaired HSC differentiation, and *Dnmt3a*-null HSCs upregulated HSC multipotency genes and downregulated differentiation factors (Challen *et al*, 2011). The phenotype of *Pias1*$^{-/-}$ mice in regulating HSC lineage differentiation resembles that of *Dnmt1* knockout mice (Broske *et al*, 2009). Both *Pias1* disruption and DNMT1 reduction caused the premature demethylation of *Gata1* promoter in HSCs, the derepression of myeloerythroid genes in Lin^{-} progenitor cells, the reduction of CLPs, and the impaired B cell differentiation (Broske *et al*, 2009). These findings provide genetic evidence to support our hypothesis that PIAS1 is a key cofactor of DNMTs in promoting DNA methylation. Our results have uncovered a novel functional role of the PIAS1 epigenetic pathway in regulating the methylation dynamics in the HSC differentiation program.

Materials and Methods

Flow cytometry analysis and sorting of HSC and progenitors

Single cell suspensions were prepared from spleen, bone marrow (BM) or peripheral blood (PBL). Cells were stained with various combinations of surface markers followed by flow cytometry analysis using a FACSCalibur or FACScanX (Becton Dickinson, BD, San Jose, CA, USA). Data were analyzed using the FCS Express software (De Novo). FACS cell sorting was performed as described (Zeng *et al*, 2004; Wilson *et al*, 2008; Broske *et al*, 2009; Trowbridge *et al*, 2009; Ji *et al*, 2010; Mayle *et al*, 2012). Briefly, single cell suspensions were prepared from BM and subjected to surface staining with various markers. FACS sorting of HSC and progenitors was performed using a FACSAria (Becton Dickinson, BD). See supplementary Materials and Methods for definitions of each population.

Cell proliferation and cell death

Cell death was assessed by 7-AAD staining as described (Liu *et al*, 2004, 2010). Cell proliferation was assayed by intracellular anti-Ki67 and Hoechst DNA staining as described (Wilson *et al*, 2008). Briefly, single cell suspensions of BM were first stained with various surface markers, followed by fixation/permeabilization of the cells. Cells were then stained with anti-Ki67 and 1 μg/ml bisbenzimide (Hoechst no. 33342; Sigma, St. Louis, MO, USA), and analyzed on a LSR flow cytometer (Becton Dickinson, BD). Approximately 1 × 10^{6} cells were collected for each sample when the cell cycle profiles of dormant HSCs (d-HSCs) were analyzed to ensure that sufficient numbers of d-HSCs were collected.

In vivo competitive reconstitution assays

In vivo competitive reconstitution experiments were performed as described (Liu *et al*, 2008). Briefly, bone marrow was isolated from 4 to 8 week-old *Pias1*$^{-/-}$ mice and their WT littermates (CD45.2^{+}), or C57SJL wild-type mice (CD45.1^{+}). Total bone marrow (2 × 10^{5} cells) or FACS-sorted LSK cells (1000 cells) from *Pias1*$^{-/-}$ or WT mice was mixed with competitor bone marrow from C57SJL mice (2 × 10^{5} cells), and injected intravenously via retro-orbital eye injection into 6–8-week-old C57SJL recipient mice that were lethally irradiated 24 h previously (10 Gy at a split dose). The reverse was performed in some experiments, where BM from WT SJL mice (CD45.1^{+}; 4 × 10^{5}) were injected into lethally irradiated WT or *Pias1*$^{-/-}$ recipient mice (CD45.2^{+}). Reconstitution of donor T cells (CD3^{+}), B cells (B220^{+}) and Granulocytes/monocytes (Mac1^{+}) in peripheral blood (PBL) were assayed by flow cytometry 4–20 weeks post reconstitution.

Competitive limiting dilution assay

Competitive limiting dilution assays were performed as described (Sauvageau *et al*, 1995). Briefly, total bone marrow (BM) cells (3 × 10^{5} cells) from *Pias1*$^{-/-}$ or WT mice (CD45.2^{+}) were injected intravenously into 6–8-week-old lethally irradiated congenic WT C57SJL recipient mice (CD45.1^{+}). Reconstitution of donor cells in peripheral blood (PBL) was assayed by flow cytometry at various time points post reconstitution. For secondary transplantation, BM cells pooled from 3 to 4 mice transplanted 21 weeks earlier with either WT or *Pias1*$^{-/-}$ cells were injected at different doses into lethally irradiated WT C57SJL recipient mice, together with a life-sparing dose of 1 × 10^{5} competitor BM cells from C57SJL mice. The level of lymphomyeloid repopulation with donor-derived cells (CD45.2^{+}) in these secondary recipients was evaluated by flow cytometry at 10 and 16 weeks post transplantation. Recipients with ≥1%

donor-derived cells were considered to be repopulated by at least one competitive repopulating unit (CRU). CRU frequencies were calculated using Extreme Limiting Dilution Analysis (ELDA) software (http://bioinf.wehi.edu.au/software/elda/) (Hu & Smyth, 2009).

Bone marrow *in vivo* homing assay

In vivo homing assays were performed as described (Adams *et al*, 2006; Janzen *et al*, 2006). Briefly, freshly isolated total bone marrow cells were labeled with 2.5 μM carboxyfluorescein diacetate succinimidyl ester (CFDA-SE; Molecular Probes, Grand Island, NY, USA) as instructed by the manufacturer. Cells were then injected intravenously via retro-orbital eye injection into 6–8 weeks old lethally irradiated WT C57SJL mice. Mice were euthanized 12 or 24 h post injection and homed cells in the BM were assayed by measuring CFDA-SE$^+$ cells using flow cytometry. *In vivo* homing assays were also performed with CFSE-labeled long-term hematopoietic stem cells (LT-HSC; Lin$^-$Sca1$^+$c-Kit$^+$CD34$^-$) cells (2000 cells/mouse) FACS-sorted from WT and *Pias1*$^{-/-}$ littermates.

Niche retention assay

Niche retention assays were performed as described (Trowbridge *et al*, 2009). Total bone marrow cells (4×10^7) from WT C57/SJL mice (CD45.1$^+$) were injected into non-irradiated WT or *Pias1*$^{-/-}$ recipient mice (CD45.2$^+$). The percentage of CD45.1$^+$ cells in bone marrow of the recipient mice were assayed by flow cytometry 12 weeks post injection.

Quantitative real time polymerase chain reaction (Q-PCR) analysis

Quantitative real-time polymerase chain reaction (Q-PCR) analyses were performed as described (Liu *et al*, 2004) with the following modification. A conventional PCR reaction was carried out with a mixture of primers using the following program: 1. 95°C for 3 min; 2. 95°C for 15 s, 60°C for 15 s, 72°C for 30 s for 12 cycles; 3. 72°C for 5 min. PCR products were purified by QIAquickPCR purification kit (Qiagen, Valencia, CA, USA) and used as templates for subsequent Q-PCR analyses using individual primers and SYBR Green performed on CFX96 (BioRad, Hercules, CA, USA). Results were corrected by *Hprt1* (Hypoxanthine-guanine phosphoribosyltransferase 1). See supplementary Materials and Methods for primer sequences.

DNA methylation by bisulfite sequencing

Genomic DNA was purified with the ZR genomic DNA II kit (Zymo Research, Irvine, CA, USA). Methylation analysis was performed by bisulfite conversion of genomic DNA using the EZ DNA methylation-Gold kit (Zymo Research). The PCR product was cloned using the TOPO TA cloning kit (Invitrogen, Grand Island, NY, USA).

Coimmuprecipitation (Co-IP) assays

Co-IP assays were performed as described (Liu *et al*, 2010). Briefly, whole-cell extracts from bone marrow cells were prepared by using lysis buffer containing 1% Brij, 50 mM Tris (pH 8), 420 mM NaCl, 1 mM DTT, 0.5 mM phenylmethylsulfonyl fluoride, 0.5 μg/ml leupeptin, 3 μg/ml aprotinin, 1 μg/ml pepstatin and 0.1 mM sodium vanadate. The mixture was incubated on ice for 20 min and centrifuged at 15 000 *g* for 5 min. The supernatant was adjusted to 150 mM NaCl and used for immunoprecipitation with polyclonal anti-PIAS1 antibodies (Liu *et al*, 1998, 2005) at 1:100 dilution or IgG, followed by immunoblotting with anti-DNMT3A (Abiocode, Agoura Hills, CA, USA) or a monoclonal anti-PIAS1 (Abiocode).

Chromatin immunoprecipitation (ChIP) and MiniChIP assays

Chromatin immunoprecipitation (ChIP) assays were performed with bone marrow (BM) cells using the ChIP Assay Kit (Upstate Biotech) as described (Liu *et al*, 2010). Briefly, cell extracts from WT or *Pias1*$^{-/-}$ BMs (2×10^6 per sample) were prepared and chromatin was sheared by sonication (10 s at 30% of the maximum strength for a total of six times). ChIP assays were performed using anti-PIAS1, anti-DNMT3A (Abiocode), or rabbit IgG as a negative control. Bound DNA was quantified by Q-PCR and was normalized with the input DNA. MiniChIP assays were performed essentially as described (Attema *et al*, 2007), using LSK and L$^-$S$^-$K$^+$ cells purified by FACS sorting to a purity > 99%. For FACS sorting, a fast sort for Lin$^-$ cells was performed first to enrich Lin$^-$ cell, followed by a regular sort for LSK and L$^-$S$^-$K$^+$ cells. Approximately 50 000 LSK cells were obtained from 20 WT mice and subjected to MiniChIP assays. Of 25 000 LSK cells or 50 000 L$^-$S$^-$K$^+$ cells were used per sample for MiniChIP assays.

Supplementary information for this article is available online: http://emboj.embopress.org

Acknowledgements

We thank Irving Garcia for technical assistance, Min Zhou for assistance with FACS data analyses and UCLA flow cytometry core facility. Supported by grants from the NIH (R01AI063286, 3R01AI063286-05S1, and R01GM085797) and the UCLA Jonsson Comprehensive Cancer Center (K.S.). B.L. was supported by a Research Scientist Development Award from the NIH (K01 AR52717). S.T. was supported by a UCLA Tumor Immunology Training Fellowship.

Author contributions

BL and KS directed the project and wrote the manuscript. BL designed and executed most of the experiments. KMY performed experiments in Figs 2–5 and 7, Fig S4 and Table 1. ST performed experiments in Fig 7. RM provided supports for animal experiments and also performed experiments in Fig 6 and Fig S5. CH performed experiments in Fig 6.

Conflict of interest

K.S. and B.L. are board directors of Abiocode, Inc.

References

Adams GB, Chabner KT, Alley IR, Olson DP, Szczepiorkowski ZM, Poznansky MC, Kos CH, Pollak MR, Brown EM, Scadden DT (2006) Stem cell engraftment at the endosteal niche is specified by the calcium-sensing receptor. *Nature* 439: 599–603

Akashi K, Traver D, Miyamoto T, Weissman IL (2000) A clonogenic common myeloid progenitor that gives rise to all myeloid lineages. *Nature* 404: 193–197

Attema JL, Papathanasiou P, Forsberg EC, Xu J, Smale ST, Weissman IL (2007) Epigenetic characterization of hematopoietic stem cell differentiation using miniChIP and bisulfite sequencing analysis. *Proc Natl Acad Sci USA* 104: 12371–12376

Broske AM, Vockentanz L, Kharazi S, Huska MR, Mancini E, Scheller M, Kuhl C, Enns A, Prinz M, Jaenisch R, Nerlov C, Leutz A, Andrade-Navarro MA, Jacobsen SE, Rosenbauer F (2009) DNA methylation protects hematopoietic stem cell multipotency from myeloerythroid restriction. *Nat Genet* 41: 1207–1215

Cedar H, Bergman Y (2011) Epigenetics of haematopoietic cell development. *Nat Rev Immunol* 11: 478–488

Challen GA, Sun D, Jeong M, Luo M, Jelinek J, Berg JS, Bock C, Vasanthakumar A, Gu H, Xi Y, Liang S, Lu Y, Darlington GJ, Meissner A, Issa JP, Godley LA, Li W, Goodell MA (2011) Dnmt3a is essential for hematopoietic stem cell differentiation. *Nat Genet* 44: 23–31

Chao MP, Seita J, Weissman IL (2008) Establishment of a normal hematopoietic and leukemia stem cell hierarchy. *Cold Spring Harb Symp Quant Biol* 73: 439–449

Copley MR, Beer PA, Eaves CJ (2012) Hematopoietic stem cell heterogeneity takes center stage. *Cell Stem Cell* 10: 690–697

Ehninger A, Trumpp A (2011) The bone marrow stem cell niche grows up: mesenchymal stem cells and macrophages move in. *J Exp Med* 208: 421–428

Hu Y, Smyth GK (2009) ELDA: extreme limiting dilution analysis for comparing depleted and enriched populations in stem cell and other assays. *J Immunol Methods* 347: 70–78

wasaki H, Mizuno S, Wells RA, Cantor AB, Watanabe S, Akashi K (2003) GATA-1 converts lymphoid and myelomonocytic progenitors into the megakaryocyte/erythrocyte lineages. *Immunity* 19: 451–462

Jaenisch R, Bird A (2003) Epigenetic regulation of gene expression: how the genome integrates intrinsic and environmental signals. *Nat Genet* 33 (Suppl.): 245–254

Janzen V, Forkert R, Fleming HE, Saito Y, Waring MT, Dombkowski DM, Cheng T, DePinho RA, Sharpless NE, Scadden DT (2006) Stem-cell ageing modified by the cyclin-dependent kinase inhibitor p16INK4a. *Nature* 443: 421–426

Ji H, Ehrlich LI, Seita J, Murakami P, Doi A, Lindau P, Lee H, Aryee MJ, Irizarry RA, Kim K, Rossi DJ, Inlay MA, Serwold T, Karsunky H, Ho L, Daley GQ, Weissman IL, Feinberg AP (2010) Comprehensive methylome map of lineage commitment from haematopoietic progenitors. *Nature* 467: 338–342

Jones DL, Wagers AJ (2008) No place like home: anatomy and function of the stem cell niche. *Nat Rev Mol Cell Biol* 9: 11–21

Kiel MJ, Morrison SJ (2008) Uncertainty in the niches that maintain haematopoietic stem cells. *Nat Rev Immunol* 8: 290–301

Liu B, Liao J, Rao X, Kushner SA, Chung CD, Chang DD, Shuai K (1998) Inhibition of Stat1-mediated gene activation by PIAS1. *Proc Natl Acad Sci USA* 95: 10626–10631

Liu B, Mink S, Wong KA, Stein N, Getman C, Dempsey PW, Wu H, Shuai K (2004) PIAS1 selectively inhibits interferon-inducible genes and is important in innate immunity. *Nat Immunol* 5: 891–898

Liu B, Shuai K (2008) Targeting the PIAS1 SUMO ligase pathway to control inflammation. *Trends Pharmacol Sci* 29: 505–509

Liu B, Tahk S, Yee KM, Fan G, Shuai K (2010) The ligase PIAS1 restricts natural regulatory T cell differentiation by epigenetic repression. *Science* 330: 521–525

Liu B, Yang R, Wong KA, Getman C, Stein N, Teitell MA, Cheng G, Wu H, Shuai K (2005) Negative regulation of NF-kappaB signaling by PIAS1. *Mol Cell Biol* 25: 1113–1123

Liu B, Yang Y, Chernishof V, Loo RR, Jang H, Tahk S, Yang R, Mink S, Shultz D, Bellone CJ, Loo JA, Shuai K (2007) Proinflammatory stimuli induce IKKalpha-mediated phosphorylation of PIAS1 to restrict inflammation and immunity. *Cell* 129: 903–914

Liu Y, Zhang P, Li J, Kulkarni AB, Perruche S, Chen W (2008) A critical function for TGF-beta signaling in the development of natural CD4 + CD25 + Foxp3 + regulatory T cells. *Nat Immunol* 9: 632–640

Mayle A, Luo M, Jeong M, Goodell MA (2012) Flow cytometry analysis of murine hematopoietic stem cells. *Cytometry A* 83: 27–37

Sauvageau G, Thorsteinsdottir U, Eaves CJ, Lawrence HJ, Largman C, Lansdorp PM, Humphries RK (1995) Overexpression of HOXB4 in hematopoietic cells causes the selective expansion of more primitive populations *in vitro* and *in vivo*. *Genes Dev* 9: 1753–1765

Shuai K, Liu B (2005) Regulation of gene-activation pathways by PIAS proteins in the immune system. *Nat Rev Immunol* 5: 593–605

Tadokoro Y, Ema H, Okano M, Li E, Nakauchi H (2007) De novo DNA methyltransferase is essential for self-renewal, but not for differentiation, in hematopoietic stem cells. *J Exp Med* 204: 715–722

Trowbridge JJ, Snow JW, Kim J, Orkin SH (2009) DNA methyltransferase 1 is essential for and uniquely regulates hematopoietic stem and progenitor cells. *Cell Stem Cell* 5: 442–449

Wilson A, Laurenti E, Oser G, van der Wath RC, Blanco-Bose W, Jaworski M, Offner S, Dunant CF, Eshkind L, Bockamp E, Lio P, Macdonald HR, Trumpp A (2008) Hematopoietic stem cells reversibly switch from dormancy to self-renewal during homeostasis and repair. *Cell* 135: 1118–1129

Xie H, Ye M, Feng R, Graf T (2004) Stepwise reprogramming of B cells into macrophages. *Cell* 117: 663–676

Zeng H, Yucel R, Kosan C, Klein-Hitpass L, Moroy T (2004) Transcription factor Gfi1 regulates self-renewal and engraftment of hematopoietic stem cells. *EMBO J* 23: 4116–4125

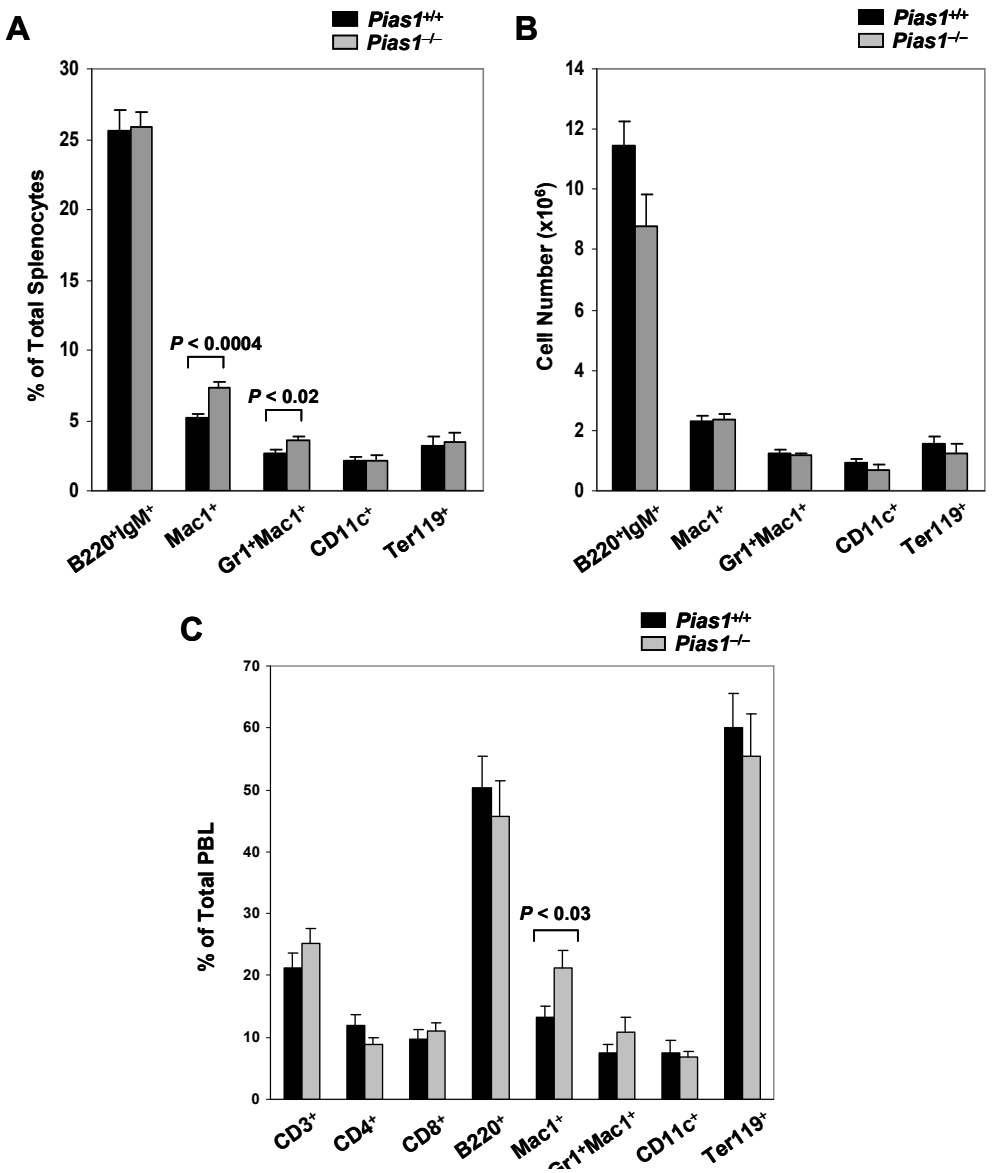

Figure S1. Normal peripheral lineage differentiation in *Pias1*$^{-/-}$ mice. (**A**) Frequencies of mature B cells (B220^{+}IgM^{+}), myeloid cells (Mac1^{+}), granulocyte/monocyte linage (Gr1^{+}Mac1^{+}), dendritic cells (CD11c^{+}) and erythroid cells (Ter119^{+}) in freshly isolated splenocytes from 8-12 weeks old WT and *Pias1*$^{-/-}$ littermates were assayed by flow cytometry. (**B**) Same as in **A** except that cell numbers of each population were presented. (**C**) Same as in **A** except that peripheral blood lymphocytes (PBL) were analyzed. Shown in each panel is a pool of 3 independent experiments (n=9-13). Error bars represent SEM. *P* values were determined by non-paired *t*-test.

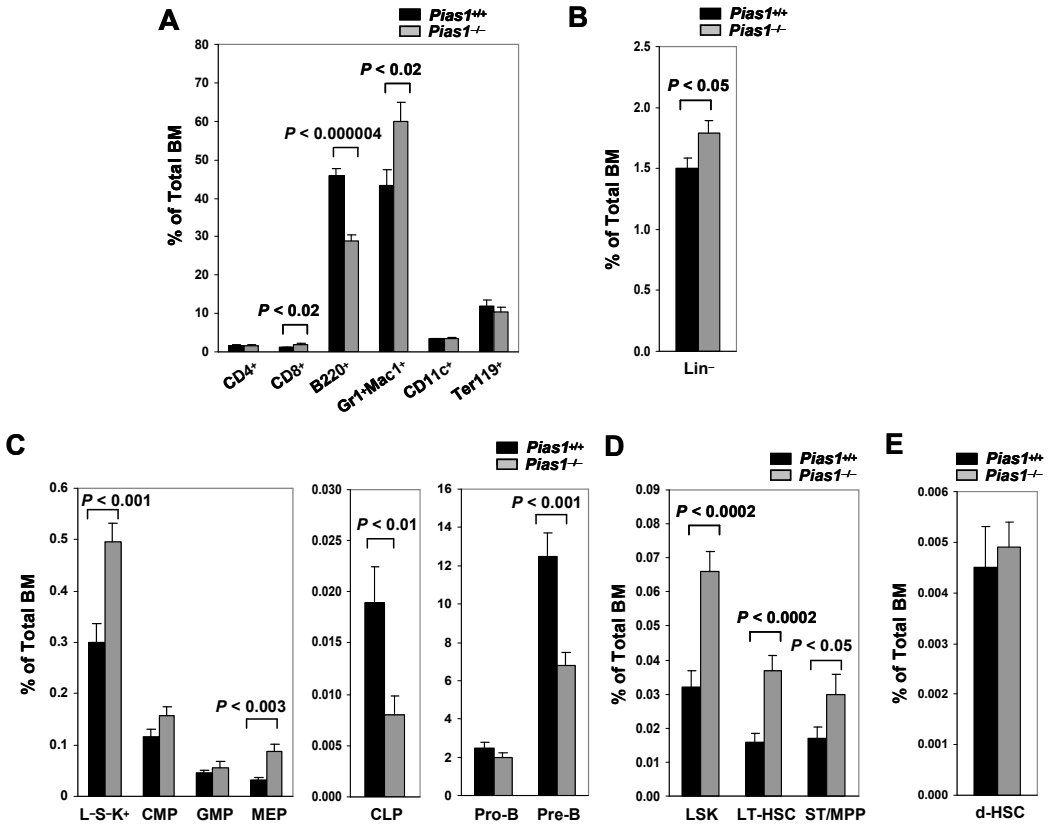

Figure S2. Altered lineage-restricted progenitors and LSK populations in *Pias1*$^{-/-}$ mice. (**A**) Percentage of T cells (CD4$^+$ or CD8$^+$), B cells (B220$^+$), granulocytes/monocytes (Gr1$^+$Mac1$^+$), dendritic cells (CD11c$^+$) and erythroids (Ter119$^+$) in freshly isolated bone marrow (BM) from 8-12 weeks old WT (*Pias1*$^{+/+}$) and *Pias1*$^{-/-}$ littermates were assayed by flow cytometry. (**B**) Same as in **A** except that frequencies of myeloid-restricted Lin$^-$Sca1$^-$c-Kit$^+$ (L$^-$S$^-$K$^+$) populations, common myeloid progenitors (CMP), granulocyte monocyte progenitors (GMP), megakaryocyte erythrocyte progenitors (MEP), common lymphoid progenitors (CLP), Pro-B and Pre-B cells as defined in Supplementary Materials and Methods were assayed. (**C**) Same as in **A** except that cell numbers of LSK, long-term hematopoietic stem cells (LT-HSC) and short-term multi-potent progenitors (ST/MPP) in total BM as defined in Supplementary Materials and Methods were assayed. (**D**) Same as in **A** except that the percentage of Lin$^-$ population was assayed. (**E**) Same as in **A** except that the percentage of dormant hematopoietic stem cells (d-HSCs; Lin$^-$Sca1$^+$c-Kit$^+$CD150$^+$CD48$^-$CD34$^-$) was assayed. Shown in each panel is a pool of 3 independent experiments (n=9-13). Error bars represent SEM. *P* values were determined by non-paired *t*-test.

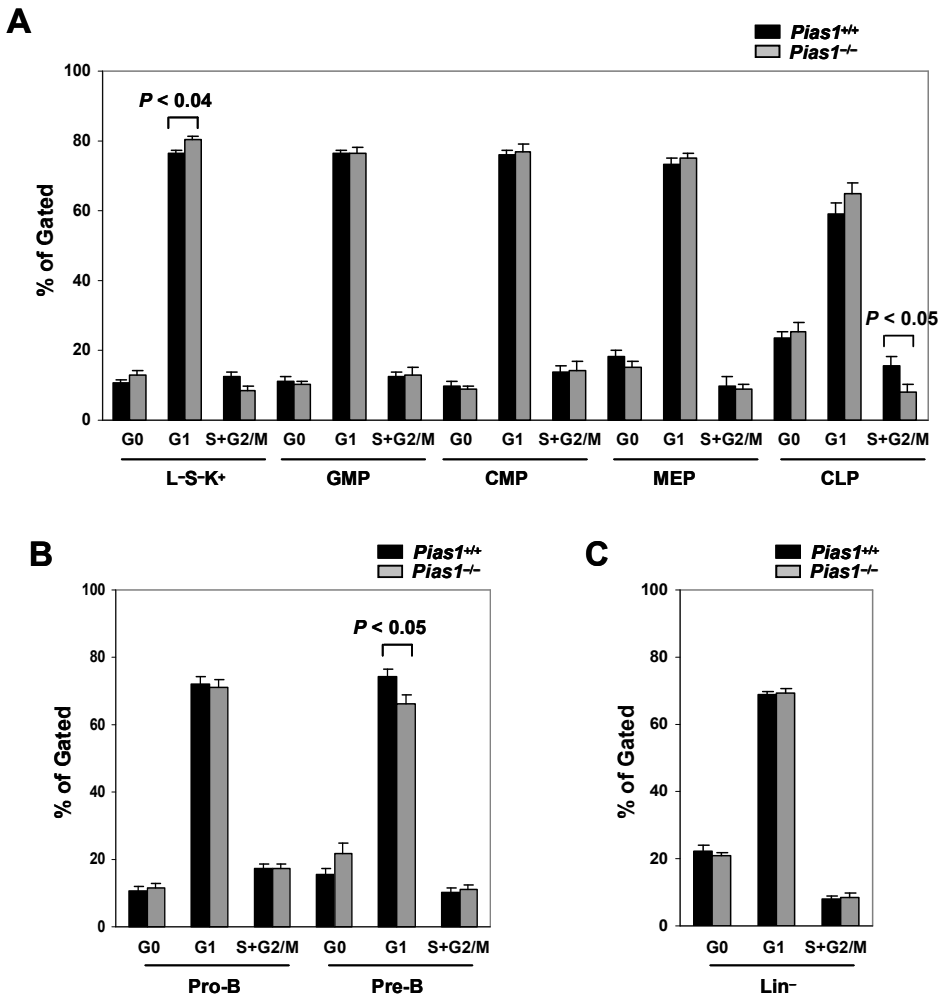

Figure S3. Normal cell proliferation of various progenitor populations. (**A**) Cell proliferation of indicated BM subsets from WT and *Pias1*$^{-/-}$ mice as defined in Supplementary Materials and Methods was revealed by intracellular Ki67 (icKi67) and Hoechst DNA staining followed by flow cytometry. G0, icKi67^{-}, 2N DNA content; G1, icKi67^{+}, 2N DNA content; S+G2/M, icKi67^{+}, > 2N DNA content. (**B**) Same as in **A** except that Pro-B and Pre-B cells were assayed. (**C**) Same as in **A** except that Lin^{-} cells were assayed. Shown in each panel is a pool of 3 independent experiments (n=10-13). Error bars represent SEM. *P* values were determined by non-paired *t*-test.

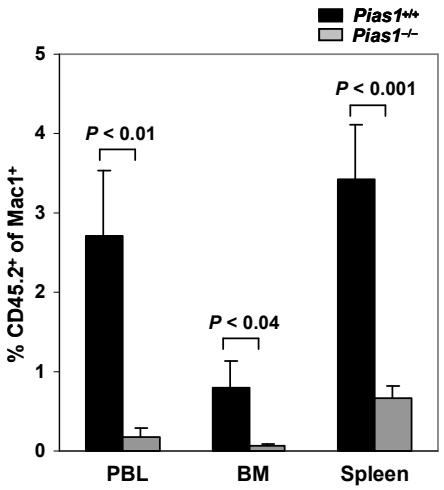

Figure S4. Defective short-term reconstitution capability of *Pias1*$^{-/-}$ myeloid-restricted Lin^{-}Sca1^{-}c-Kit^{+} (L^{-}S^{-}K^{+}) cells revealed by i*n vivo* short-term competitive reconstitution assays. FACS-sorted L^{-}S^{-}K^{+} cells (10,000) from WT or *Pias1*$^{-/-}$ littermates (CD45.2^{+}) were mixed with 2x10^{5} of WT C57SJL bone marrow (BM) cells (CD45.1^{+}) and injected into lethally irradiated WT C57SJL mice. The percentage of myeloid cells (Mac1^{+}) from donor mice in peripheral blood (PBL), BM and spleen were assayed by flow cytometry 13 days post reconstitution. Shown is a pool of 3 independent experiments in all panels (n=10). Error bars represent SEM. *P* values were determined by non-paired *t*-test.

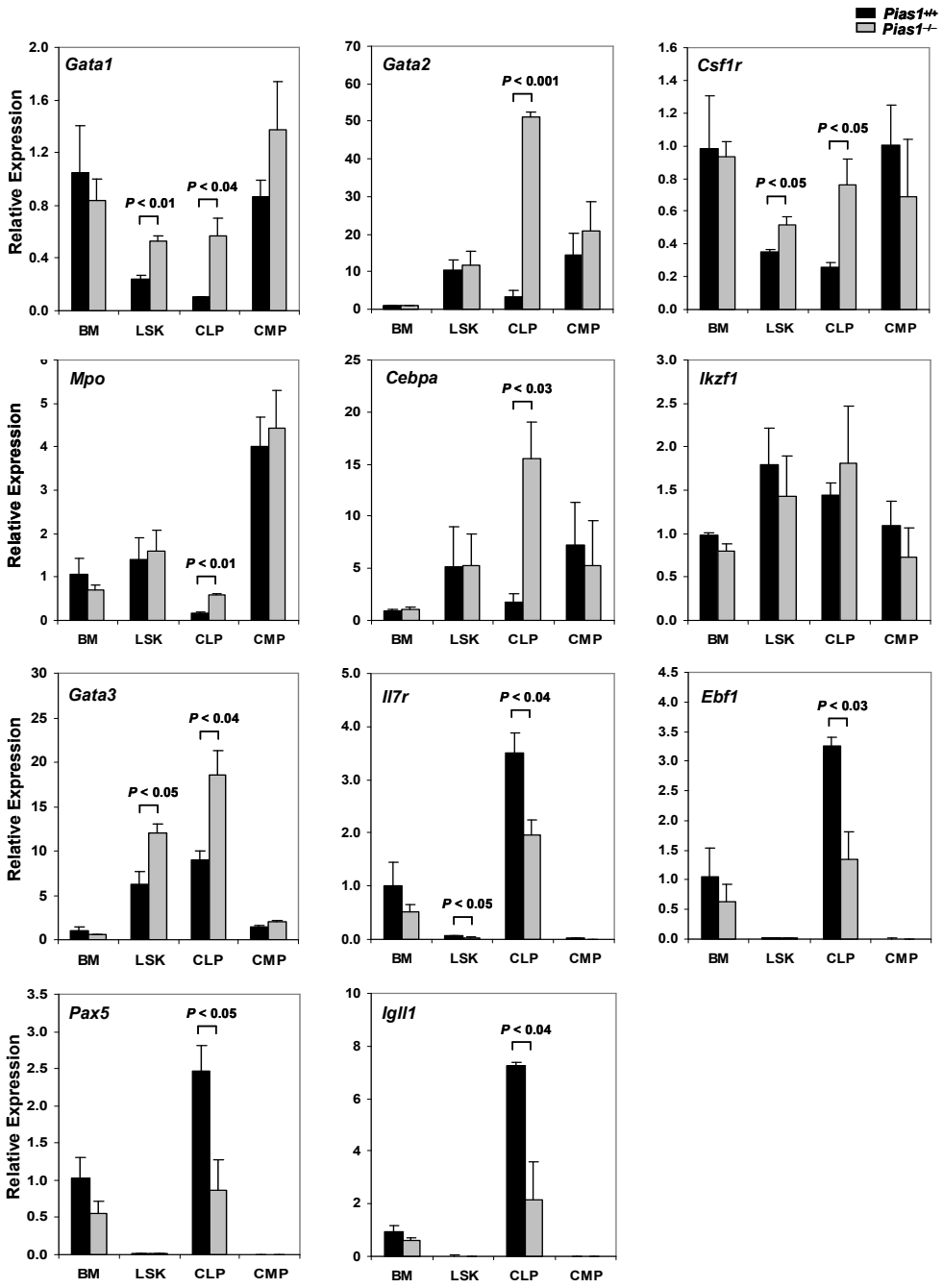

Figure S5. Transcription of the lineage-affiliated genes is regulated by PIAS1. Quantitative real time polymerase chain reaction (Q-PCR) analyses were performed with total RNA from WT or *Pias1*$^{-/-}$ bone marrow (BM), or FACS-sorted HSC-enriched Lin^{-}Sca1^{+}c-Kit^{+} (LSK), common lymphoid progenitors (CLP) and common myeloid progenitors (CMP) as defined in Supplementary Materials and Methods, using gene-specific primers. Each gene is indicated at the top left of each panel, and the results were adjusted by *Hprt1*. Shown is the average of 2 independent experiments (n=5 for each experiment). Error bars represent SD. *P* values were determined by non-paired *t*-test.

Supplementary Materials and Methods

Mice and Reagents

The generation of *Pias1*$^{-/-}$ mice has been described (Liu et al., 2004). C57SJL (CD45.1) mice were purchased from the Jackson Labs.

The following antibodies were purchased from BioLegend: fluorescein isothiocyanate (FITC)-conjugated anti-IgM (RMM-1), anti-Mac1 (CD11b; M1/70), anti-CD3 (145-2C11), anti-CD4 (RM4-5), anti-Sca1 (D7); phycoerythrin (PE)-conjugated anti-B220 (CD45R; RA3-6B2), anti-GR1 (Ly-6G/Ly-6C; RB6-8C5), anti-Mac1 (M1/70), anti-CD11c (N418), anti-Ter119 (TER119), anti-NK-1.1 (PE136), anti-CD5 (53-7.3), anti-CD8a (53-6.7), anti-IL7Ra (CD127; SB/199); Alexa Fluor 647-conjugated anti-IL7Ra (CD127; SB/199); Pacific Blue-conjugated anti-CD48 (HM48-1); allophycocyanin (APC)-conjugated anti-FCgRII/III (CD16/32; 93), anti-CD45.2 (104); PE/Cy7-conjugated anti-FCgRII/III (CD16/32; 93); PerCP-conjugated anti-CD45.1 (A20); PE/Cy5-conjugated anti-Sca1 (D7), anti-CD34 (MEC14.7); APC/Cy7-conjugated anti-c-Kit (2B8); and isotype controls. PE-conjugated anti-CD4 (GK1.5) and Alexa Fluor 488-conjugated anti-Ki67 (B56) are from BD Pharmingen. APC-conjugated anti-CD150 (mShad150) is from eBioscience.

Flow cytometry analysis and sorting of HSC and progenitors

Various cell populations are defined as the following: common lymphoid progenitors (CLP): Lin^- $Sca1^{low}$ c-Kit^{low} $IL7Ra^+$; common myeloid progenitors (CMP): Lin^- $Sca1^-$c-Kit^+ $CD34^+FcgRII/III^{low}$; granulocyte monocyte progenitors (GMP): Lin^- $Sca1^-$c-Kit^+ $CD34^+FcgRII/III^+$; megakaryocyte erythrocyte progenitors (MEP): Lin^- $Sca1^-$c-Kit^+ $CD34^-FcgRII/III^-$; Pro-B, $Lin^-IgM^-B220^+CD43^+$; Pre-B, $Lin^-IgM^-B220^+CD43^-$; LSK: Lin^-Sca1^+c-Kit^+; long-term hematopoietic stem cells (LT-HSC): Lin^-Sca1^+c-Kit^+CD34^- and short-term multi-potent progenitors (ST/MPP): Lin^-Sca1^+c-Kit^+CD34). Dormant hematopoietic stem cells (d-HSC) are defined as Lin^-Sca1^+c-$Kit^+CD48^-CD34^-CD150^+$. Lineage markers include CD3, CD4, CD5, CD8a, B220, GR1, Mac1 and Ter119, except that only CD3, CD4, CD8a and GR1 were used for Pro-B and Pre-B populations.

Short term competitive reconstitution assays

Short term competitive reconstitution assays were performed as described with slight modifications (Yang et al., 2005). Briefly, FACS-sorted myeloid-restricted $Lin^-Sca1^-cKit^+$ ($L^-S^-K^+$) cells (10,000) from WT or *Pias1*$^{-/-}$ littermates ($CD45.2^+$) were mixed with $2x10^5$ of WT C57SJL bone marrow (BM) cells ($CD45.1^+$) and injected into lethally irradiated WT C57SJL mice. The percentage of myeloid cells ($Mac1^+$) from donor mice in peripheral blood (PBL), BM and spleen were assayed by flow cytometry 13 days post reconstitution.

Primer sequences

The following primers for murine genes are used for Q-PCR:

Hprt1-f: 5'- CAGTACAGCCCCAAAATGGT
Hprt1-r: 3'- CAAGGGCATATCCAACAACA

Gata1-f: 5'- AGCAACGGCTACTCCACTGT
Gata1-r: 5'- TGCTGACAATCATTCGCTTC

Gata2-f: 5'- GATACCCACCTATCCCTCCTATGTG
Gata2-r: 3'- GTGGCACCACAGTTGACACACTC

Csf1r-f: 5'- CTTTGGTCTGGGCAAAGAAGAT
Csf1r-r: 5'- CAGGGCCTCCTTCTCATCAG

Mpo-f: 5'- GTTCCGCCTGAACAATCAGT
Mpo-r: 5'- ATTCAGTTTGGCTGGAGTGG

Cebpa-f: 5'- CAAGAACAGCAACGAGTACCG
Cebpa-r: 3'- GTCACTGGTCAACTCCAGCAC

Ikzf1-f: 5'- CACAACGAGATGGCAGAAGA
Ikzf1-r: 3'- CTGACAGGCACTTGTCTCCA

Gata3-f: 5'- CTACCGGGTTCGGATGTAAGTC
Gata3-r: 5'- GTTCACACACTCCCTGCCTTCT

Il7r-f: 5'- TGGCTCTGGGTAGAGCTTTC
Il7r-r: 5'- GTGGCACCAGAAGGAGTGAT

Ebf1-f: 5'- CGGAAATCCAACTTCTTCCA
Ebf1-r: 5'- GTCTTTTCGCTGTTGGCTTC

Pax5-f: 5'- AACTTGCCCATCAAGGTGTC
Pax5-r: 5'- GGCTTGATGCTTCCTGTCTC

Igll1-f: 5'- GAGCTTCAGTGGGAAGCAAC
Igll1-r: 5'- CCCACCACCAAAGACATACC

Epor-f: 5'- TGTCTCCTACTTGCTGGGGC
Epor-r: 5'- CAAGCGTTGGGTGAAGCACA

Hbb-b1-f: 5'- AACGATGGCCTGAATCACTT
Hbb-b1-r: 5'- ACGATCATATTGCCCAGGAG

Slc4a1-f: 5'- CCTCATCCTCACAGTGCCTC
Slc4a1-r: 5'- CAGGCCATTCTCCTCGTCAA

Pias1-f: 5'- CATCAACACCTCCCTCATCC
Pias1-r: 5'- CCTCCTGCACTTAGCTGGTC

The following primers are used for bisulfite sequencing:

Gata1-f: 5'- TTTATTTTAATTTTTTGGGATTTTTAGG
Gata1-r: 5'- AACTACAAACCACCTCTATAAAACAATCTA

The following primers are used for Chromatin immunoprecipitation (ChIP):

Gata1 promoter-f: 5'- ACCTGCAAAATGGGTACAGC
Gata1 promoter-r: 5'- TTCAGTGAGGAAAGCCCCTA

Number of cells injected into secondary recipients	CRU evaluation of primary recipients			
	10 weeks post-transplantation		16 weeks post-transplantation	
	***Pias1* +/+**	***Pias1* -/-**	***Pias1* +/+**	***Pias1* -/-**
2,000,000	6/6 (41.70 +/- 3.98)	5/6 (2.85 +/- 1.63)	6/6 (46.19 +/- 7.09)	4/6 (1.99 +/- 1.43)
1,000,000	9/9 (32.72 +/- 12.59)	5/8 (2.37 +/- 2.41)	9/9 (35.19 +/- 17.95)	4/8 (2.23 +/- 2.26)
300,000	8/8 (14.08 +/- 4.63)	4/9 (0.92 +/- 0.53)	8/8 (19.23 +/- 9.28)	3/9 (0.89 +/- 0.51)
100,000	5/6 (16.28 +/- 15.13)	0/5 (0.08 +/- 0.10)	5/6 (23.07 +/- 23.09)	0/5 (0.08 +/- 0.13)
CRU frequency per 10^5 cells (range)	1.869 (0.761-4.595)	0.108 (0.061-0.193)	1.869 (0.761-4.595)	0.071 (0.038-0.132)

Table 2. Evaluation by limiting dilution analysis of competitive long-term repopulating cells (CRU) in mice transplanted with *Pias1+/+* or *Pias1-/-* bone marrow cells (UPDATED).

Results are expressed as number of mice repopulated with donor-derived cells (CD45.2+; >1%) over total. Numbers in parentheses represent the mean % +/- standard deviation of peripheral blood CD45.2+ cells found in the transplanted recipients. CRU frequency was calculated using Extreme Limiting Dilution Analysis (ELDA) software available at http://bioinf.wehi.edu.au/software/elda/. Note: The difference between Table 1 (published) and Table 2 (unpublished) is that Table 2 has a greater n value, thus the reconstitution values are more accurate. Due to time constraints, the experiment represented here in Table 2 was still ongoing when the manuscript was accepted for publication, and data here was not published.

Chapter 4: PIAS1 Regulates Breast Tumorigenesis Through Selective Epigenetic Gene Silencing

OPEN ACCESS Freely available online

PLOS ONE

PIAS1 Regulates Breast Tumorigenesis through Selective Epigenetic Gene Silencing

Bin Liu[1]*, Samuel Tahk[1], Kathleen M. Yee[2], Randy Yang[2], Yonghui Yang[1], Ryan Mackie[1], Cary Hsu[3], Vasili Chernishof[1], Neil O'Brien[1], Yusheng Jin[4], Guoping Fan[5], Timothy F. Lane[6], Jianyu Rao[4], Dennis Slamon[1], Ke Shuai[1,2]*

1 Division of Hematology-Oncology, Department of Medicine, University of California Los Angeles, Los Angeles, California, United States of America, **2** Department of Biological Chemistry, University of California Los Angeles, Los Angeles, California, United States of America, **3** Department of General Surgery, University of California Los Angeles, Los Angeles, California, United States of America, **4** Department of Pathology and Laboratory Medicine, University of California Los Angeles, Los Angeles, California, United States of America, **5** Department of Human Genetics, University of California Los Angeles, Los Angeles, California, United States of America, **6** Department of Obstetrics and Gynecology, University of California Los Angeles, Los Angeles, California, United States of America

Abstract

Epigenetic gene silencing by histone modifications and DNA methylation is essential for cancer development. The molecular mechanism that promotes selective epigenetic changes during tumorigenesis is not understood. We report here that the PIAS1 SUMO ligase is involved in the progression of breast tumorigenesis. Elevated PIAS1 expression was observed in breast tumor samples. PIAS1 knockdown in breast cancer cells reduced the subpopulation of tumor-initiating cells, and inhibited breast tumor growth *in vivo*. PIAS1 acts by delineating histone modifications and DNA methylation to silence the expression of a subset of clinically relevant genes, including breast cancer DNA methylation signature genes such as cyclin D2 and estrogen receptor, and breast tumor suppressor WNT5A. Our studies identify a novel epigenetic mechanism that regulates breast tumorigenesis through selective gene silencing.

Citation: Liu B, Tahk S, Yee KM, Yang R, Yang Y, et al. (2014) PIAS1 Regulates Breast Tumorigenesis through Selective Epigenetic Gene Silencing. PLoS ONE 9(2): e89464. doi:10.1371/journal.pone.0089464

Editor: Rolf Müller, Philipps University, Germany

Received November 7, 2013; **Accepted** January 20, 2014; **Published** February 24, 2014

Funding: This research was supported by grants from the NIH (R01AI063286 and R01GM085797), Margaret E. Early Medical Research Trust, and the UCLA Jonsson Comprehensive Cancer Center (K.S.). B.L. was supported by a Research Scientist Development Award from the NIH (K01 AR52717-01). S.T. was supported by a UCLA Tumor Immunology Training Fellowship. The funders had no role in study design, data collection and analysis, decision to publish, or preparation of the manuscript.

Competing Interests: K.S. and B.L. are board directors of Abiocode, Inc. This does not alter the authors' adherence to PLOS ONE policies on sharing data and materials.

* E-mail: bliu@ucla.edu (BL); kshuai@mednet.ucla.edu (KS)

Introduction

Both genetic and epigenetic alterations contribute to cancer development [1–3]. Tumor suppressors and epigenetic gatekeeper genes are frequently silenced by epigenetic mechanisms during tumor initiation and progression [3–5]. Extensive studies have been performed in the identification and characterization of altered DNA methylation in breast cancer development and progression. More than 100 genes have been reported to be aberrantly hypermethylated in breast tumors or breast cancer cell lines [1,6]. Many of these genes play important roles in the regulation of cell cycle, apoptosis, angiogenesis, metastasis and tumor initiation. It has been proposed that breast cancer-specific DNA methylation signatures can extend our ability to classify breast cancer and predict outcome beyond what is currently possible [6]. Epigenetic therapy holds a promising potential for the successful treatment of cancer since epigenetic changes are reversible as opposed to mutations [7]. The approval of DNA methylation and histone deacetylase (HDAC) inhibitors for cancer treatment offers new promise for epigenetic therapy. However, these drugs are rather nonspecific, and the development of more effective strategies for epigenetic therapy requires a thorough understanding of the molecular specificity involved in epigenetic gene silencing.

Most tumors are composed of a mixture of cancer cells, and the heterogeneity of tumors is the major obstacle to effective cancer therapy. It has been demonstrated that a sub-population of cancer cells, referred to as tumor-initiating cells (TICs) or cancer stem cells, is tumorigenic when transplanted into immunosuppressed nonobese diabetic/severe combined immunodeficiency (NOD/SCID) mice [8]. TICs display some key properties of stem cells including self-renewal and multilineage differentiation [9]. In addition, TICs are found to be resistant to radiation and conventional chemotherapies [10–13]. Therefore, TICs may largely contribute to tumor cellular heterogeneity, tumor progression and tumor recurrence [14–17].

PIAS1 is a member of the PIAS (protein inhibitor of activated STAT) transcriptional regulator family that possesses SUMO (small ubiquitin-like modifier) E3 ligase activity [18]. Biochemical and genetic studies indicate that PIAS1 is a physiologically important transcriptional repressor of STAT1 and NF-kappaB [19–21]. PIAS1 is rapidly activated by phosphorylation on Ser90 residue in response to a variety of stimuli, including pro-inflammatory signals, TCR activation and growth factors. Activated PIAS1 is then recruited to gene promoters to repress transcription [22,23]. Recent studies indicate that PIAS1 mediates a novel epigenetic regulatory mechanism to control natural

regulatory T cell (Treg) differentiation. PIAS1 binds to the *Foxp3* promoter to maintain a repressive chromatin state through the recruitment of DNA methyltransferases (DNMTs) and HP1-gamma [24]. These findings indicate that this newly identified PIAS1 epigenetic mechanism plays an important role in T cell differentiation.

In this paper, we report that PIAS1 is important for breast tumorigenesis. Elevated PIAS1 expression was observed in breast cancer patient samples. PIAS1 knockdown in breast cancer cells inhibited tumor growth *in vivo*. Most interestingly, mechanistic studies indicate that PIAS1 suppresses a number of- genes clinically relevant to breast tumorigenesis through epigenetic mechanisms. These studies suggest that targeting the PIAS1 epigenetic signaling pathway may represent a novel therapeutic strategy for cancer treatment.

Results

Elevated PIAS1 expression in primary human breast cancer tissues

To test whether PIAS1 is involved in breast cancer progression, immunohistochemistry (IHC) tissue arrays were performed to examine the expression of PIAS1 protein in a panel of primary human breast tumor samples. PIAS1 is a nuclear protein, but it diffused to the cytoplasm under formalin fixation conditions (Figure S1 in File S1), a phenomenon observed with other nuclear proteins [25]. IHC analyses indicate that PIAS1 is significantly upregulated in primary breast cancer samples at early stages of breast ductal carcinoma *in situ* (DCIS) as well as invasive ductal carcinoma (IDC) (Fig. 1a).

PIAS1 is important for breast tumorigenesis

To directly test whether PIAS1 plays a functional role in breast tumorigenesis, RNA interference approach was used to knock-down the expression of PIAS1 protein in MDA-MB231 cells. Stable cell lines expressing a scramble short hairpin RNA (control shRNA) or two independent PIAS1 shRNAs (shRNA1 and shRNA2) were obtained. Western blot analysis showed that PIAS1 expression was significantly suppressed by both PIAS1 shRNAs, although a more efficient inhibition by PIAS1 shRNA2 was observed (Fig. 1b). PIAS1 knockdown did not affect the growth of MDA-MB231 cells under the conventional serum-containing conditions (DMEM) (Fig. 1c, left panel). In contrast, when these cells were cultured under serum-free growth factor-enriched conditions (Stem Cell Media; SCM), which favor normal stem cells and more closely resemble primary tumors than the DMEM condition [26], PIAS1 knockdown significantly inhibited the survival of MDA-MB231 cells (Fig. 1c, right panel). To directly test the effect of PIAS1 knockdown on tumor growth in vivo, xenograft experiments were performed in SCID mice. PIAS1 knockdown significantly inhibited the tumor formation of MDA-MB231 cells in both the subcutaneous and the fat pad models (Fig. 1d), suggesting an important role of PIAS1 in the regulation of breast tumorigenesis.

PIAS1 regulates the self-renewal of breast tumor initiating cells (TICs)

The finding that PIAS1 knockdown affects breast cancer cell survival specifically under the conditions that favor stem cell growth suggests a possibility that PIAS1 may play a role in the regulation of breast cancer stem cells/tumor-initiating cells (TICs). Previous studies suggest that the $ALDH^+$ subpopulation of breast cancer cells is highly enriched in breast TICs [27]. ALDEFLUOR assays revealed that PIAS1 knockdown almost completely eliminated the $ALDH^+$ population (Fig. 2a), supporting the hypothesis that PIAS1 knockdown inhibits breast TICs. To further test whether PIAS1 regulates breast TICs, the control and PIAS1 knockdown MDA-MB231 cells were subjected to mammosphere assays [14,28,29]. PIAS1 knockdown significantly inhibited the formation of mammospheres (Fig. 2b), suggesting that PIAS1 regulates the self-renewal of breast TICs.

PIAS1 Ser90 phosphorylation and SUMO ligase activity are required for PIAS1-mediated regulation of breast TICs

Previous studies indicate that PIAS1 is activated by Ser90 phosphorylation to bind to chromatin and repress transcription of target genes in response to pro-inflammatory stimuli [22], a process that is dependent on the SUMO ligase activity of PIAS1. We explored whether PIAS1 can also be activated by growth factor signals. Western blot analysis revealed that PIAS1 became phosphorylated on Ser90 in response to EGF or Heregulin in various breast cancer cell lines, including MDA-MB231, BT-20, BT-474 and HCC-1954 (Fig. 2c). To test the importance of PIAS1 Ser90 phosphorylation and PIAS1 SUMO ligase activity in the regulation of breast TICs, PIAS1 shRNA1 knockdown MDA-MB231 cells were rescued with either an empty vector (Vec), wild type PIAS1 (WT), PIAS1 Ser90 mutant (S90A), or PIAS1 SUMO ligase defective mutant (W372A) through an shRNA escape approach, in which silent mutations were introduced into PIAS1 expression constructs to escape the inhibitory effect of PIAS1 shRNA. Western blot analysis indicated that the expression of WT or mutant PIAS1 proteins in the rescued cell lines was comparable to that of the MDA-MB231 control cells (Fig. 2d).

Consistent with the previous results (Fig. 1c), the introduction of either WT or S90A and W372A PIAS1 mutants did not affect cell growth under the conventional DMEM conditions (Fig. 2e, left panel). In contrast, when these cells were cultured under SCM conditions, only WT, but not the vector (Vec) or W372A mutant PIAS1 reconstituted cells, rescued cells from cell death (Fig. 2e, right panel). PIAS1 S90A mutant showed minor increase in cell survival, although the increase is not statistically significant (Fig. 2e, right panel). In addition, mammosphere assays were performed to examine the ability of WT or PIAS1 mutants to support the self-renewal of TICs. The introduction of PIAS1 WT into PIAS1 knockdown cells promoted the formation of mammospheres (Fig. 2f). The introduction of PIAS1 S90 or W372 mutant resulted in minor increases in mammospheres, although the increases are not statistically significant (Fig. 2f). Consistently, ALDEFLUOR assays indicated that PIAS1 WT, but not S90 or W372 mutant, restored the population of $ALDH^+$ TICs (Fig. 2g). Taken together, these studies suggest that the observed inhibition of TICs in PIAS1 knockdown cells is due to the reduction of PIAS1 expression, and that both PIAS1 Ser90 phosphorylation and SUMO ligase activity are required for the maintenance of the breast TICs.

PIAS1 selectively represses a subset of genes clinically relevant to breast cancer

We explored the molecular mechanism of PIAS1-mediated regulation of breast TICs. Gene profiling studies were performed to identify PIAS1 downstream genes involved in tumorigenesis. Total RNAs from the control and PIAS1 knockdown MDA-MB231 cells cultured under DMEM or SCM conditions were subjected to microarray analysis. Since PIAS1 is a transcriptional repressor and PIAS1 knockdown inhibited self-renewal of breast TICs under SCM conditions, we focused on the genes that were preferentially upregulated in PIAS1 knockdown cells under SCM conditions (Table S1 in File S1). Interestingly, among the group of

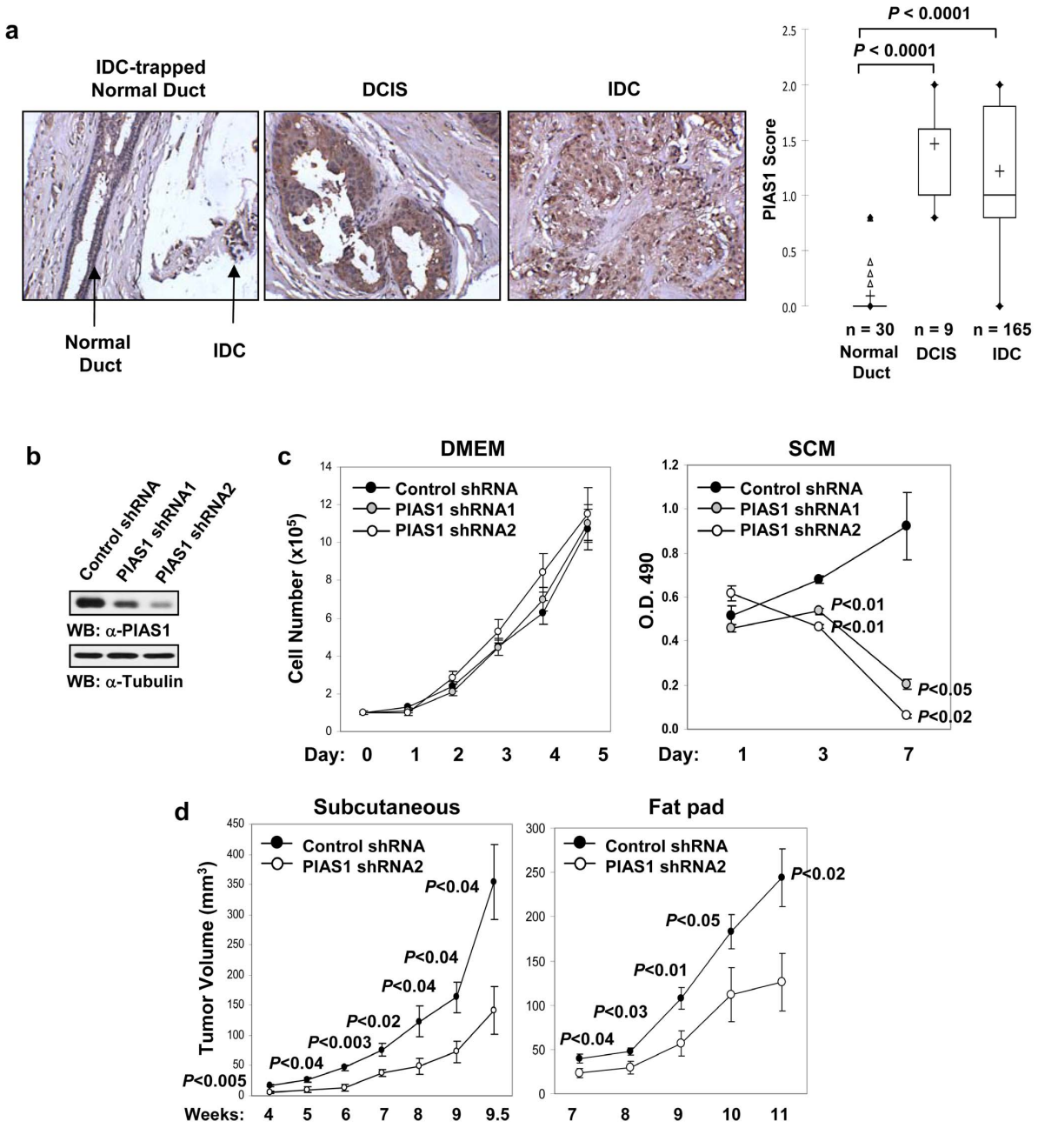

Figure 1. PIAS1 is important for tumorigenesis of breast cancer. (**a**) PIAS1 protein levels are increased in breast tumor samples as revealed by tissue microarray analysis. Left panel: Representative tissue microarray spot from morphologically normal duct, ductal carcinoma in situ (DCIS) and invasive ductal carcinoma (IDC). Right panel: a box and whisker plot of PIAS1 levels in various tissue samples. Total sample numbers (n) were indicated. *P* values are determined by non-parametric two-tailed Kruskal Wallis test with alpha level equals 0.05. ''+'', the mean of each population; ''Δ'', outliers. (**b**) Western blot analyses were performed with whole cell extracts from MDA-MB231 cells containing a control shRNA or two independent PIAS1 shRNAs (PIAS1 shRNA1 and 2). (**c**) The growth of MDA-MB231 control shRNA, PIAS1 shRNA1 and shRNA2 cells in DMEM supplemented with 10% FBS (left), or Stem Cell Media (SCM) (right) (mean ± SEM). Shown is a representative of 3 independent experiments. *P* values were determined by paired *t*-test. (**d**) *In vivo* tumorigenesis studies. MDA-MB231 cells containing a control shRNA or PIAS1 shRNA2 were injected into the female SCID-beige mice subcutaneously (left: 1×10^6 cells/mouse; n = 4), or in fat pad (right: 2×10^5 cells/mouse; n = 5). Shown is a representative of 3 independent experiments. Each data point represents mean ± SEM. *P* values were determined by non-paired *t*-test.
doi:10.1371/journal.pone.0089464.g001

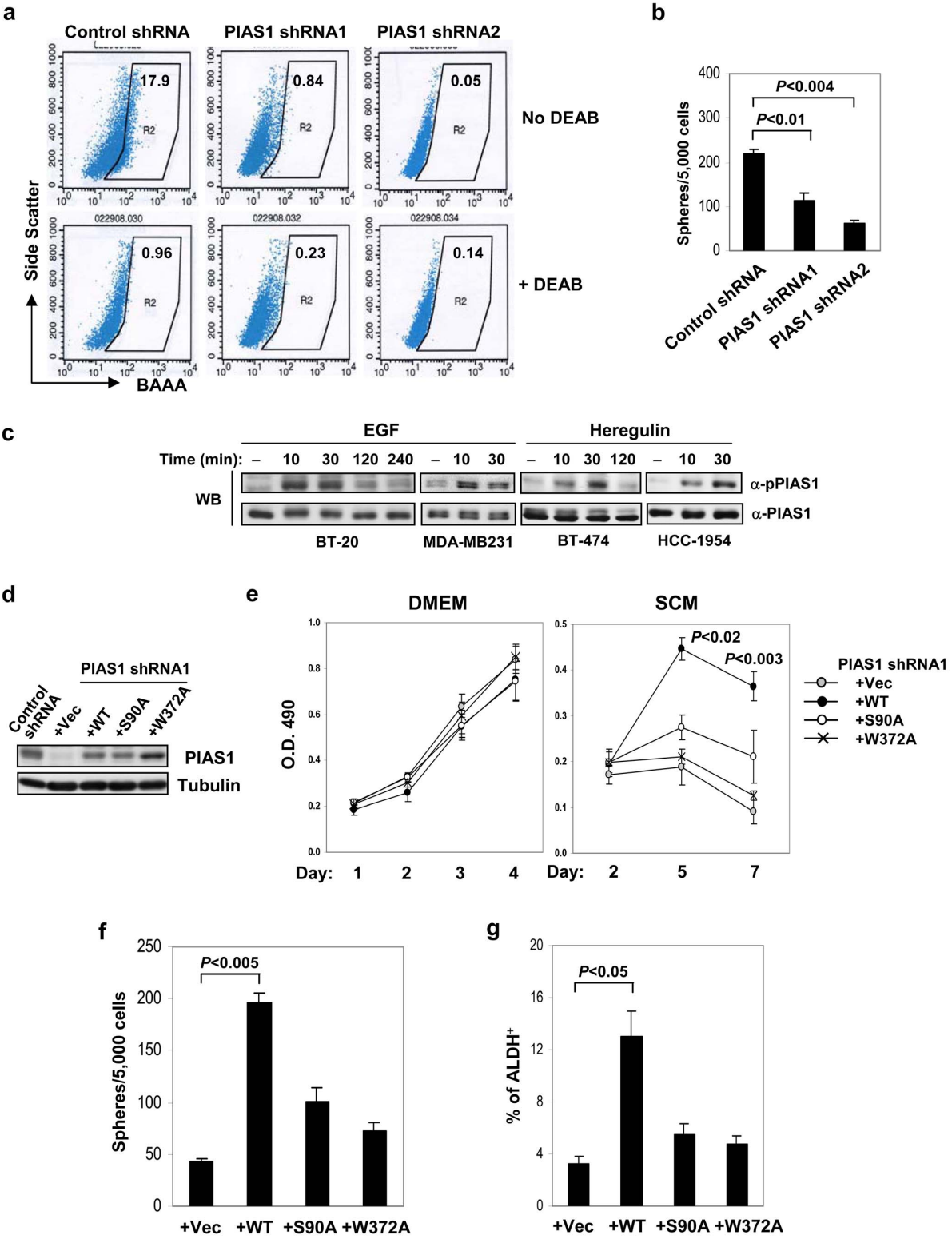
a
Control shRNA
PIAS1 shRNA1
PIAS1 shRNA2
17.9
0.84
0.05
No DEAB
0.96
0.23
0.14
+ DEAB
Side Scatter
BAAA
b
Spheres/5,000 cells
P<0.004
P<0.01
Control shRNA
PIAS1 shRNA1
PIAS1 shRNA2
c
EGF
Heregulin
Time (min): – 10 30 120 240 – 10 30 – 10 30 120 – 10 30
WB
α-pPIAS1
α-PIAS1
BT-20
MDA-MB231
BT-474
HCC-1954
d
PIAS1 shRNA1
Control shRNA
+Vec
+WT
+S90A
+W372A
PIAS1
Tubulin
e
DMEM
SCM
O.D. 490
Day: 1 2 3 4
Day: 2 5 7
P<0.02
P<0.003
PIAS1 shRNA1
+Vec
+WT
+S90A
+W372A
f
Spheres/5,000 cells
P<0.005
+Vec +WT +S90A +W372A
g
% of ALDH+
P<0.05
+Vec +WT +S90A +W372A

Figure 2. PIAS1 is important for the maintenance of the Tumor Initiating Cells (TICs) in MDA-MB231 cells. (**a**) Reduced ALDH$^+$ population in PIAS1 knockdown cells using the ALDEFLUOR assay. Cells cultured in Stem Cell Media (SCM) for 25 days were incubated with ALDEFLUOR substrate (BAAA) with or without the specific inhibitor of ALDH, DEAB, to define the ALDH$^+$ population (R2). The number indicates the percentage of the ALDH$^+$ population. (**b**) Mammosphere assays. MDA-MB231 control shRNA and PIAS1 shRNA1 and shRNA2 cells were seeded in SCM on 35 mm petri dishes (5,000 cells/dish) and spheres were counted 7 days later. (**c**) PIAS1 is phosphorylated on Ser90 in response to EGF and Heregulin in breast cancer cells. Various breast cancer cells were starved for 16 h, then either untreated or treated with EGF (100 ng/ml) or Heregulin (15 ng/ml) for indicated time points. Western blot analyses were performed with whole cell extracts, using an antibody specific for Ser90-phosphorylated PIAS1 (anti-pPIAS1) or total PIAS1 (anti-PIAS1). (**d**) Reconstitution of MDA-MB231 PIAS1 shRNA1 cells with the lenti-viruses encoding the empty vector (Vec), wild type PIAS1 (WT), PIAS1 S90A mutant (S90A), or PIAS1 W372A mutant (W372A). Western blot was performed with whole cell extracts from these cells using anti-PIAS1 or anti-Tubulin. (**e**) The effect of WT or S90A and W372A PIAS1 mutants on cell proliferation and survival. MDA-MB231 cells as in **d** were seeded in DMEM supplemented with 10% FBS (left), or Stem Cell Media (SCM) (right) (mean ± SEM). Shown is a representative of 3 independent experiments. *P* values were determined by paired *t*-test. (**f**) Mammosphere assay. MDA-MB231 cells as in **d** were seeded in SCM at 5,000 cells/dish. Spheres were counted 7 days after plating. (**g**) ALDEFLUOR assay. MDA-MB231 cells as in **d** were cultured in SCM for 5 days, and the ALDH$^+$ population was determined by the ALDEFLUOR assays. Shown in each panel is a representative of 3 independent experiments. Error bars represent SEM. *P* values were determined by paired *t*-test.
doi:10.1371/journal.pone.0089464.g002

genes strongly induced by PIAS1 knockdown, several genes are known to be clinically relevant to breast cancer, including breast cancer DNA methylation signature genes Cyclin D2 (*CCND2*) and Estrogen receptor (*ESR1*), candidate tumor suppressor *WNT5A*, progestagen-associated endometrial protein (*PAEP*), as well as leucine zipper, downregulated in cancer 1 (*LDOC1*). WNT5A, which signals through a non-canonical WNT pathway, is a candidate tumor suppressor in breast cancers [30]. The loss of WNT5A is associated with early relapse in invasive ductal breast carcinomas (IDC) and short recurrence-free survival. *PAEP* (also known as *GDA/PP14*) is an epithelial differentiation-related gene. *PAEP* expression is associated with a more favorable prognosis in breast and ovarian cancers, and PAEP inhibits breast tumor growth in SCID mice [31,32]. *CCND2* is frequently silenced in a variety of human cancers, including breast and ovarian cancers, through promoter hypermethylation [33,34]. *LDOC1* has been reported to be downregulated in pancreatic and gastric cancer cells [35].

The induction of these genes identified by microarray was validated by quantitative real time PCR (Q-PCR) analysis in two independent PIAS1 knockdown MDA-MB231 cell lines (Fig. 3a and Table S2 in File S1). As a control, PIAS1 knockdown did not show significant effect on the expression of *WNT1* and *CCND1*, which show sequence homologies, but are functionally distinct in tumorigenesis, from *WNT5A* and *CCND2*, respectively. These results suggest that PIAS1 shows specificity in gene repression. Consistently, the transcription of *WNT5A* and *CCND2*, but not *CCND1*, was also elevated in PIAS1 knockdown xenograft tumor samples (Fig. 3b).

PIAS1 promotes self-renewal of breast TICs through WNT5A suppression

The WNT pathway is known to play a role in the regulation of self-renewal of stem cells [36-38]. Consistent with the gene expression results, higher levels of WNT5A protein were detected in PIAS1 knockdown MDA-MB231 cells (Fig. 4a). WNT5A shRNA was introduced into PIAS1 shRNA2 knockdown MDA-MB231 cells to inhibit *WNT5A* expression. While WNT5A shRNA1 efficiently inhibited the expression of *WNT5A*, WNT5A shRNA2 showed only a minor inhibition of *WNT5A* expression (Fig. 4b). Mammosphere assays showed that the suppression of *WNT5A* expression by WNT5A shRNA1 significantly enhanced the formation of mammospheres (Fig. 4c). Furthermore, the exogenous administration of recombinant WNT5A protein efficiently inhibited the mammosphere formation of parental MDA-MB231 cells (Fig. 4d). Consistently, the knockdown of WNT5A by shRNA1 significantly enhanced the tumor growth of PIAS1 knockdown MDA-MB231 cells *in vivo* (Fig. 4e). These studies support a role of WNT5A in PIAS1 knockdown-mediated inhibition of the self-renewal of breast TICs and breast tumorigenesis.

PIAS1 promotes epigenetic gene silencing in breast cancer cells

Our recent studies showed that PIAS1 restricts nTreg differentiation by recruiting DNMTs to the *Foxp3* promoter to promote DNA methylation and epigenetic silencing [24]. We explored whether the PIAS1 epigenetic pathway also operates in breast cancer cells. Our previous results showed that PIAS1 inhibits the expression of *CCND2, ESR1* and *WNT5A*; but not *CCND1* (Fig. 3). Hypermethylation of the *CCND2, ESR1* and *WNT5A* loci has been reported in various cancer types [39–42]. Therefore, chromatin immunoprecipitation (ChIP) assays were performed to test whether PIAS1 was associated with the genomic loci with close proximity to the reported methylation regions of the *CCND2, ESR1* and *WNT5A* genes in MDA-MB231 cells. As shown in Fig. 5a, PIAS1 bound to the *CCND2, ESR1* and *WNT5A* loci in the control shRNA cells, while the binding was reduced in PIAS1 shRNA2 cells. Furthermore, PIAS1 was not associated with the *CCND1* promoter (Fig. 5a), consistent with the finding that PIAS1 does not affect the expression of *CCND1* (Fig. 3). Interestingly, PIAS1 knockdown resulted in a substantial increase of the active histone mark histone H3 acetylation (AcH3) on the *WNT5A* gene (Fig. 5b). In contrast, the repressive modifications, such as histone H3 K27 trimethylation (H3K27me3) and histone H3 K9 trimethylation (H3K9me3), were considerably reduced in PIAS1 knockdown cells (Fig. 5b). Similar changes in AcH3 and H3K9me3 were observed in the *CCND2* promoter (Fig. 5c). As a control, H3K9me3 was readily detectable in the centromeric satellite repeat, *Satellite 2*, a heterochromatin region [43] in MDA-MB231 cells (Fig. 5d). More importantly, the H3K9me3 level was not affected in PIAS1 knockdown cells, suggesting that PIAS1 does not affect global heterochromatin structure (Fig. 5d). In addition, while H3K9me3 and H3K27me3 were not detectable in the *CCND1* promoter, the AcH3 level was not affected by PIAS1 knockdown (Fig. 5e), consistent with the finding that PIAS1 does not affect the *CCND1* expression (Fig. 3). Taken together, these results suggest that PIAS1 regulates histone modifications of its target genes.

CCND2 and *ESR1* are signature genes that are frequently methylated in breast cancer [1]. Bisulfite sequencing analysis indicated that the promoter of *CCND2* was methylated in MDA-MB231 control cells, which was significantly reduced in PIAS1 knockdown cells (Fig. 6a). Similar reductions in DNA methylation were observed in *ESR1* and *WNT5A* genes (Fig. 6a). Consistently, ChIP assays indicated that both DNMT1 and DNMT3A bind to

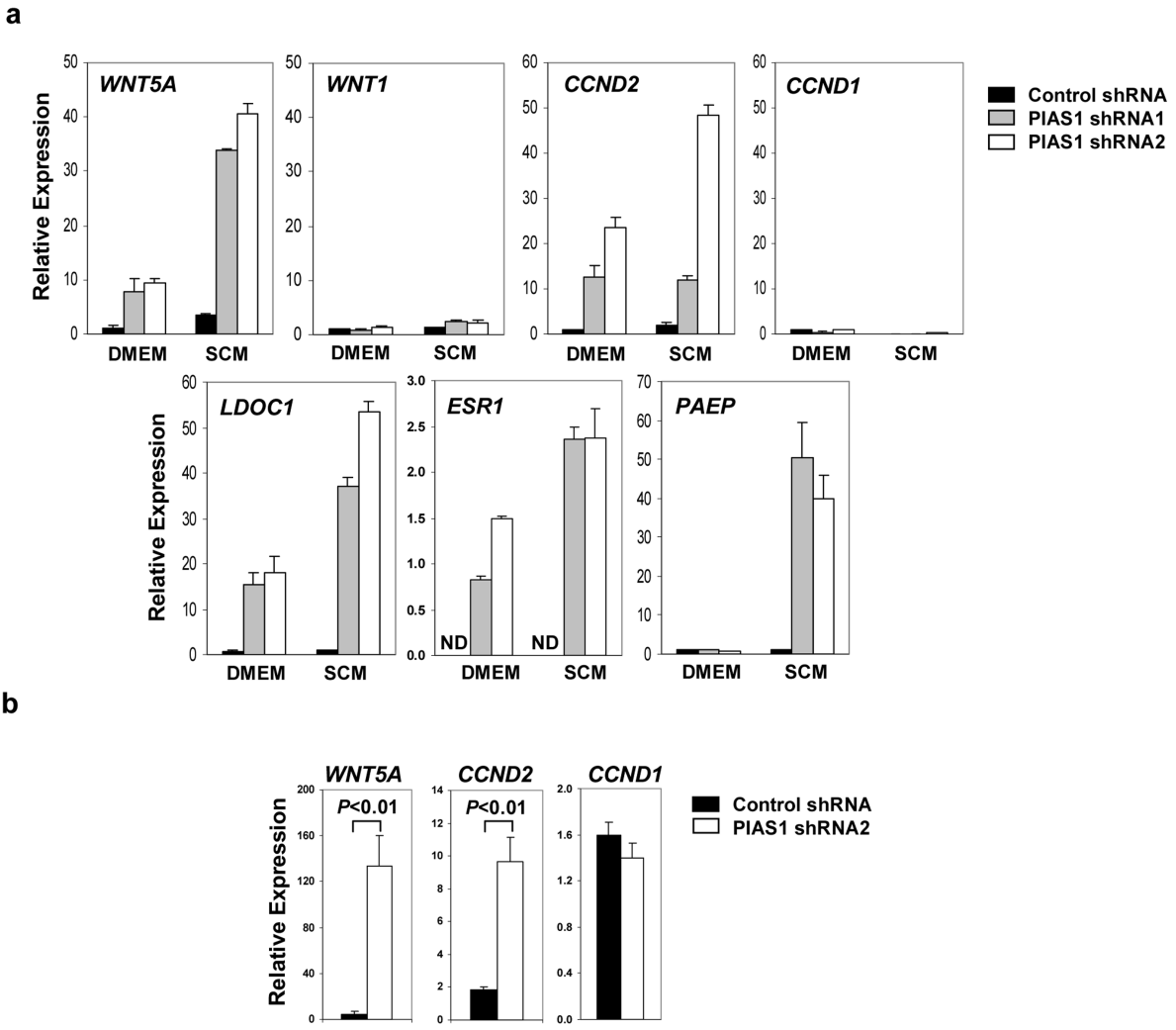

Figure 3. PIAS1 regulates the expression of a panel of tumor suppressor genes. (**a**) Real-time quantitative PCR (Q-PCR) assay. MDA-MB231 cells containing control shRNA, PIAS1 shRNA1 or shRNA2 were cultured in DMEM plus 10% FBS (DMEM) or Stem Cell Media (SCM) for 30 h, and total RNA was used for Q-PCR assays with gene-specific primers. The gene names are labeled at the top left of each panel. The data were normalized by beta-Actin (*ACTB*) and presented as "Relative Expression" as compared to that in control shRNA cells under DMEM condition, which was set as "1" except for the *ESR1* gene (the expression was not detectable in control shRNA cells). Shown is a representative of 3 independent experiments. Error bars represent SD. ND, not detected. See also Table S1 and Table S2 in File S1. (**b**) Same as in **a** except that total RNA from fat pad tumor xenograft samples were used (n = 5). Error bars represent SEM. *P* values were determined by non-paired *t*-test.
doi:10.1371/journal.pone.0089464.g003

the *CCND2* promoter in the control MDA-MB231 cells, while the binding was compromised by PIAS1 knockdown (Fig. 6b). These studies suggest that PIAS1 recruits DNMTs to promote DNA methylation in breast cancer cells.

Discussion

Although extensive studies have been performed in the identification and characterization of altered DNA methylation and epigenetic modifications in breast cancer development and progression [1,4–6], the molecular mechanism involved in this process has not been understood. Studies described in this manuscript have identified a novel epigenetic control mechanism in promoting selective epigenetic silencing in breast cancer. Our results suggest that the PIAS1 epigenetic pathway, which has been previously shown to function in regulatory T cell differentiation [24], is up-regulated in breast cancer and is involved in promoting DNA methylation and epigenetic silencing of breast cancer signature genes such as *ESR1* and *CCND2*, as well as the breast tumor suppressor *WNT5A*.

Microarray analysis of PIAS1 knockdown breast cancer cells has uncovered an essential role of PIAS1 in the suppression of a group of genes previously known to be clinically relevant to breast cancer, such as *WNT5A* (Fig. 3). The WNT family of proteins can signal through the canonical beta-catenin-dependent or the non-canonical beta-catenin-independent pathway [36–38]. WNT5A belongs to the nontransforming class of the WNT gene family that

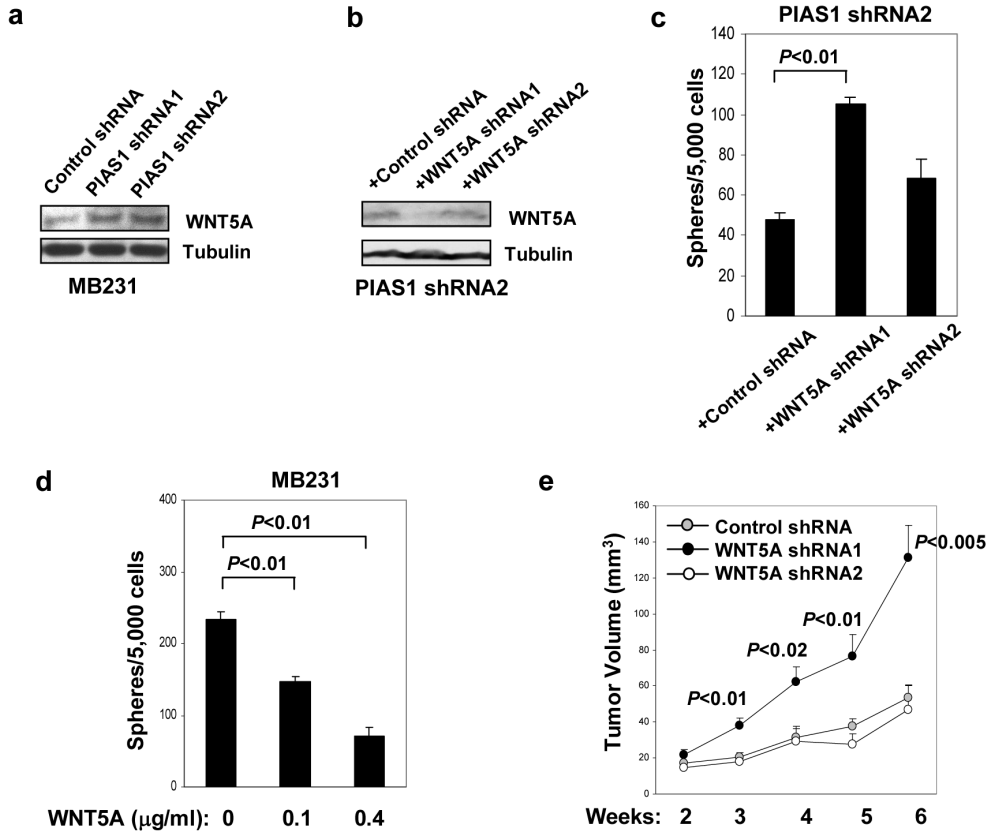

Figure 4. PIAS1-mediated *WNT5A* suppression is important for the maintenance of breast Tumor Initiating Cells (TICs). (**a**) Western blot analyses with whole cell extracts from MDA-MB231 cells containing control shRNA, PIAS1 shRNA1 or shRNA2 cultured in DMEM plus 10% FBS. (**b**) Western blot analyses with whole cell extracts from MDA-MB231 PIAS1 shRNA2 cells containing either a control shRNA, a WNT5A-specific shRNA (WNT5A shRNA1), or a non-working WNT5A shRNA (WNT5A shRNA2). (**c**) Mammosphere assay. Cells were seeded in Stem Cell Media (SCM) at 5,000 cells/dish, and spheres were counted 7 days later. Shown is a representative of 3 independent experiments. Error bars represent SEM. *P* values were determined by paired *t*-test. (**d**) Same as in **c** except that the parental MDA-MB231 cells were used with or without recombinant WNT5A treatment as indicated. (**e**) Tumorigenesis *in vivo*. Cells as in **b** were injected subcutaneously into SCID-beige mice (5×10^6 cells/mice; n = 6). Shown is a representative of 3 independent experiments. Each data point represents mean ± SEM. *P* values were determined by non-paired *t*-test.
doi:10.1371/journal.pone.0089464.g004

activates non-canonical signaling pathways. The biology of WNT5A is cell-type dependent, and it has been reported that WNT5A may signal through different WNT receptors to cause different cellular responses [44]. Gene targeting studies indicate that WNT5A is required for normal mammary gland development, and *Wnt5a*-null ammary tissue shows an accelerated developmental capacity [45]. In addition, WNT5A overexpression inhibits tumorigenesis of uroepithelial cell carcinoma and suppresses mammary cell migration [46,47]. The loss of WNT5A is associated with early relapse in invasive ductal breast carcinomas and short recurrence-free survival, supporting WNT5A as a candidate breast tumor suppressor [30]. The tumor suppressor function of WNT5A has also been suggested in other human cancers [48,49]. In this report, we showed that PIAS1-mediated regulation of the self-renewal of breast TICs is largely achieved through the transcriptional repression of WNT5A. The exogenous administration of recombinant WNT5A protein to MDA-MB231 breast cancer cells suppressed mammosphere. Consistently, WNT5A inhibition by shRNA rescued PIAS1 knockdown-mediated suppression of mammosphere and tumor growth *in vivo* (Fig. 4). Our results suggest that the PIAS1-WNT5A pathway regulates the self-renewal of breast TICs.

PIAS1 is a nuclear SUMO E3 ligase that functions as a transcriptional repressor. PIAS1 is activated by Ser90 phosphorylation in response to proinflammatory stimuli. Activated PIAS1 is then recruited to gene promoters to repress transcription [22,50]. In this report, we showed that PIAS1 is also phosphorylated/activated in response to growth stimuli, and the ability of PIAS1 to regulate the self-renewal of breast TICs requires PIAS1 Ser90 phosphorylation as well as PIAS1 SUMO E3 ligase activity (Fig. 2). Our studies suggest that PIAS1 may act as a sensor protein in the nucleus that responds to growth and inflammatory stimuli in the tumor microenvironment to regulate the self-renewal of TICs through epigenetic gene regulation.

In conclusion, studies described in this paper suggest that PIAS1 plays an important role in promoting selective epigenetic silencing during breast tumorigenesis. It is possible that the PIAS1 epigenetic pathway may provide a link between inflammation and the development of breast cancer (Fig. 7). Targeting the PIAS1 epigenetic pathway may represent a novel therapeutic strategy for the treatment of breast cancer.

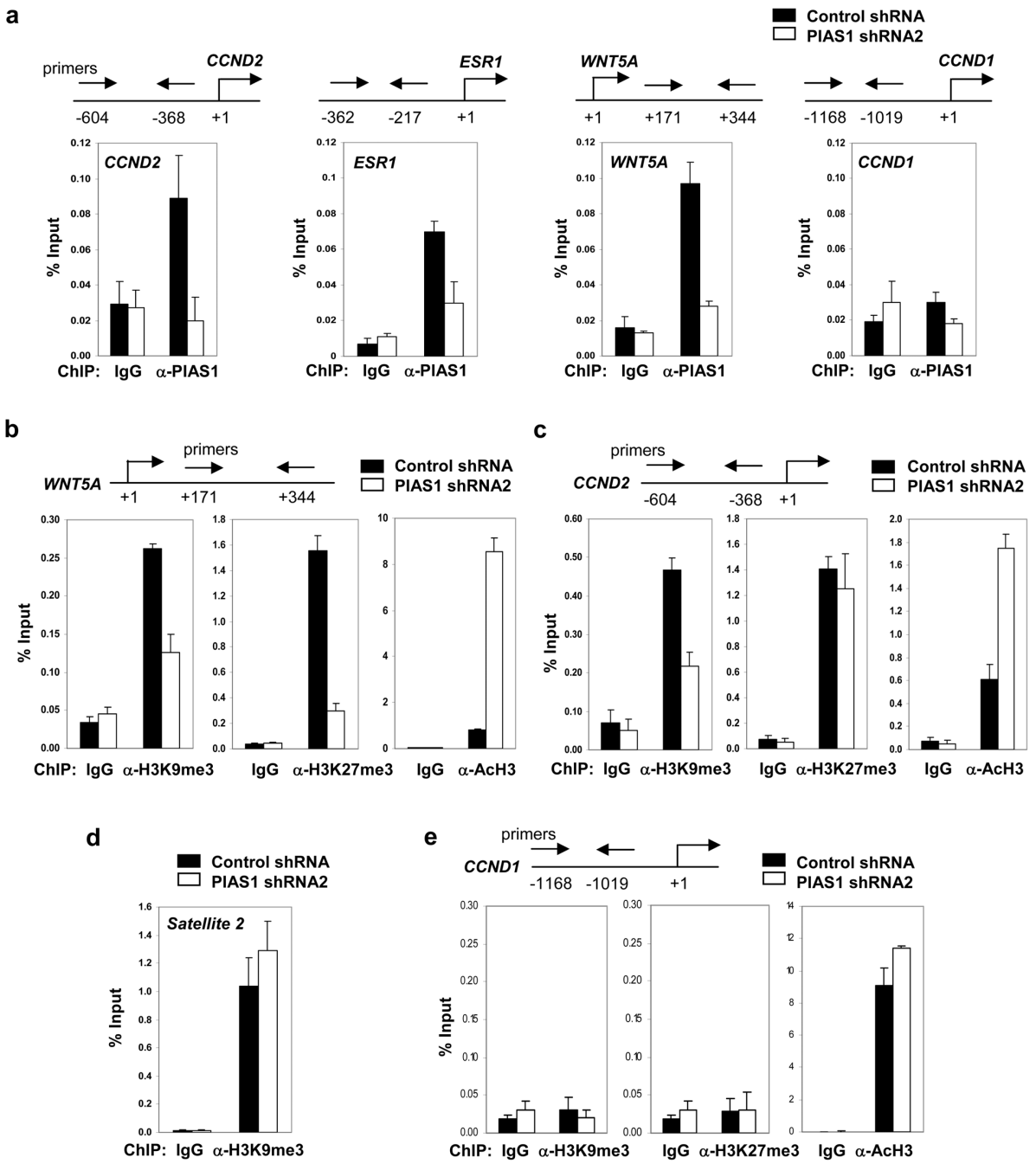

Figure 5. PIAS regulates the histone marks of the target genes. (**a**) Chromatin immunoprecipitation (ChIP) assay. Extracts from MDA-MB231 cells containing control shRNA, or PIAS1 shRNA2 were immunoprecipitated with anti-PIAS1 or IgG. The bound DNA was quantified by Q-PCR with gene-specific primers and presented as ''percent of input'' (% input). (**b**) Same as in **a** except that antibodies specific for acetylated histone H3 (AcH3), histone H3 trimethylated at Lys9 (H3K9me3), or histone H3 trimethylated at Lys27 (H3K27me3) were used, and the levels of these histone marks at the *WNT5A* loci were quantified. (**c**) Same as in **b** except that histone marks at the *CCND2* promoter were quantified. (**d**) Same as in **b** except that the level of H3K9me3 at the heterochromatin region *Satellite 2* was quantified. (**e**) Same as in **b** except that histone marks at the *CCND1* promoter were quantified. Shown in each panel is a representative of 3 independent experiments. Error bars represent SD.
doi:10.1371/journal.pone.0089464.g005

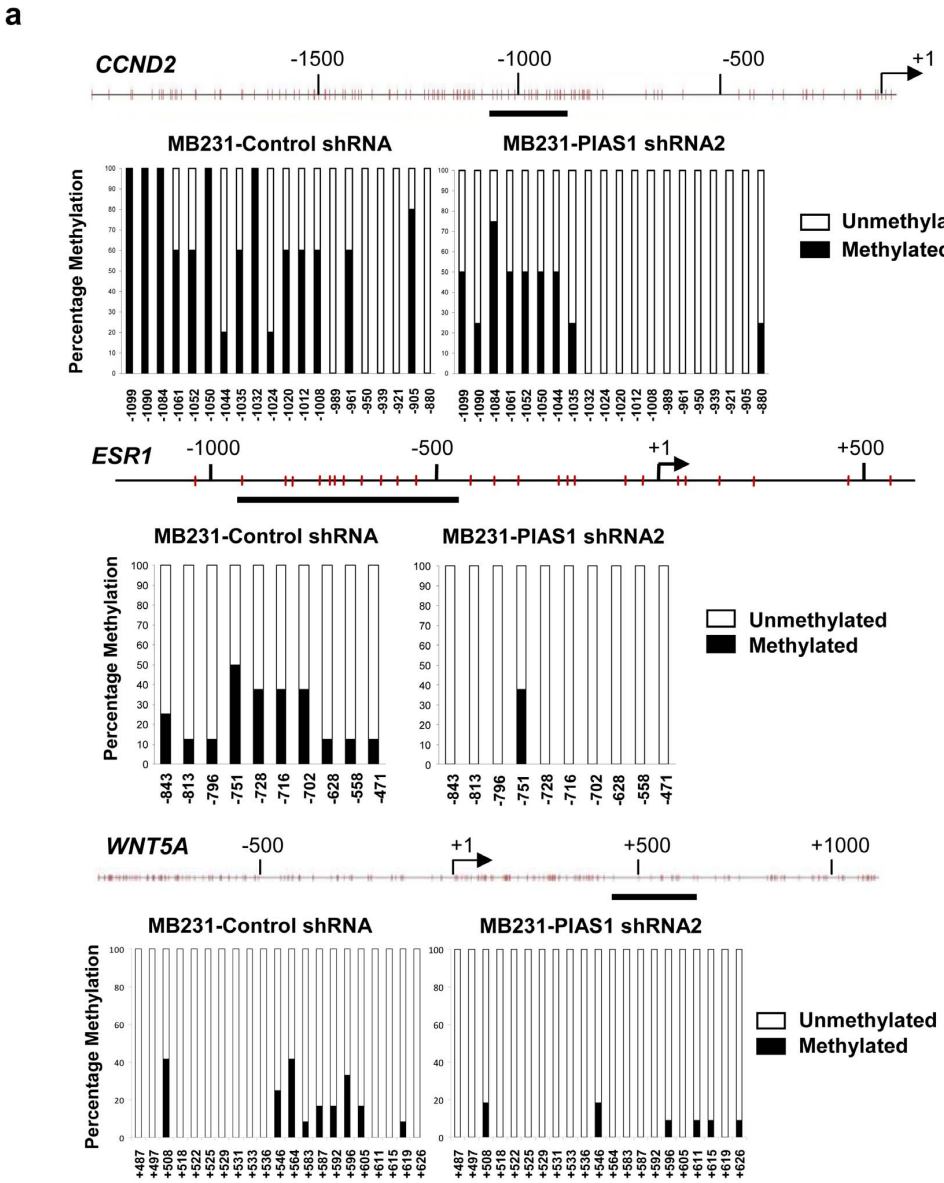
a
CCND2
-1500
-1000
-500
+1
MB231-Control shRNA
MB231-PIAS1 shRNA2
Percentage Methylation
Unmethylated
Methylated
ESR1
-1000
-500
+1
+500
MB231-Control shRNA
MB231-PIAS1 shRNA2
Percentage Methylation
Unmethylated
Methylated
WNT5A
-500
+1
+500
+1000
MB231-Control shRNA
MB231-PIAS1 shRNA2
Percentage Methylation
Unmethylated
Methylated

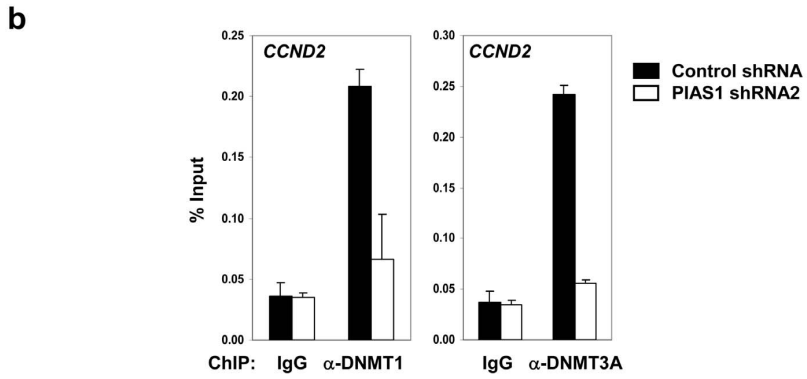
b
CCND2
CCND2
% Input
Control shRNA
PIAS1 shRNA2
ChIP: IgG α-DNMT1
IgG α-DNMT3A

Figure 6. PIAS1 regulates DNA methylation status of the target genes. (**a**) DNA Methylation analyses of the indicated loci were performed by bisulfite conversion of genomic DNA from MDA-MB231 cells containing control shRNA or PIAS1 shRNA2. The ***x*** axis represents the positions of the CpG sites relative to the transcription start site (+1); the ***y*** axis represents the percentage. (**b**) Chromatin immunoprecipitation (ChIP) assay. Extracts from MDA-MB231 cells containing control shRNA, or PIAS1 shRNA2 were immunoprecipitated with anti-DNMT1, anti-DNMT3A or IgG. The bound DNA was quantified by Q-PCR with *CCND2* promoter-specific primers and presented as "percent of input" (% input). Shown in each panel is a representative of 3 independent experiments. Error bars represent SD.
doi:10.1371/journal.pone.0089464.g006

Materials and Methods

Mice, cell Lines and reagents

Tissue samples from breast cancer patients used for IHC analysis were purchased from commercial companies (Imgenex and Full Moon Biosystems). The work is exempt from Human Research since the data were analyzed anonymously. Human breast cancer cell lines MDA-MB231, BT-20, BT-474 and HCC-1954 were obtained from ATCC. MDA-MB231 cells were maintained in DMEM supplemented with 10% fetal bovine serum (FBS) and 1% Penicillin/Streptomycin. All other cells were maintained in RPMI supplemented with 10% FBS and 1% Penicillin/Streptomycin. Stem Cell Media (SCM) is composed of DMEM/F-12 (Cellgro) supplemented with 0.4% BSA, 1% Penicillin/Streptomycin, 2 mM Glutamine, 25 ng/ml human EGF (R&D), 25 ng/ml human basic FGF (R&D) and 5 ug/ml human insulin (Sigma). The following agents have also been used: Heregulin (Upstate), anti-pPIAS1 (Ser90-phosphorylated PIAS1) [22], polyclonal anti-PIAS1 [20], [51]; anti-Tubulin (Sigma), anti-WNT5A/B (Cell Signaling) and recombinant murine WNT5A protein (R&D). This study was carried out in strict accordance with the recommendations in the Guide for the Care and Use of Laboratory Animals of the National Institutes of Health. The protocol was approved by The UCLA Institutional Animal Care and Use Committee (Protocol Number: 1999-015-43A).

shRNA knockdown and reconstitution

Oligonucleotides encoding a control small hairpin RNA (shRNA) or various shRNAs targeting PIAS1 or WNT5A were cloned under the control of the U6 promoter in the Lentiviral vector CS-CP for PIAS1 (containing a puromycin-resistant marker) or CS-CH for WNT5A (containing a hygromycin-resistant marker), which was modified from the CS-CG Lentiviral vector [52]. Lentiviruses were generated by co-transfecting 293T cells with shRNA constructs together with helper plasmids pCMV-VSV-G and pHR'8.9ΔVPR using the calcium phosphate method. The viral supernatant was collected 72 h post transfection, and used to infect various cancer cells. Cells were subjected to drug selection (puromycin: 2.5 ug/ml; hygromycin: 250 ug/ml) 48 h post infection. The target sequences of the shRNAs are: Control shRNA: GCACTACTGTCGATGACGA; PIAS1 shRNA1: GTTTCTGATAAACAAAACC; PIAS1 shRNA2: GAAAC-TATTCCATGGCAGT; WNT5A shRNA1: AGTG-CAATGTCTTCCAAGT; WNT5A shRNA2: TATTAAGCC-CAGGAGTTGC.

The wild type (WT), S90A and W372A mutant PIAS1 escape expression constructs were generated by insertion of WT or mutant PIAS1 cDNA fragments into the Lentiviral expression vector bearing a Hygromycin-resistant marker. These PIAS1 cDNAs carried 4 silent mutations that can escape the inhibition by shRNA without changing the codons of the protein (only the third nucleotide of each codon was altered). Lentiviruses were obtained as described above and target cells were infected with viral supernatant followed by Hygromycin selection.

***In vitro* mammosphere formation.** *In vitro* mammosphere assays with MDA-MB231 cells were performed as described [12,27]. Briefly, cells were seeded under SCM conditions at indicated densities on 35 mm petri dish. Fresh human EGF (25 ng/ml), basic FGF (25 ng/ml) and Insulin (5 ug/ml) were supplemented every 2 days. Spheres were counted under a microscope after 5–7 days of culture.

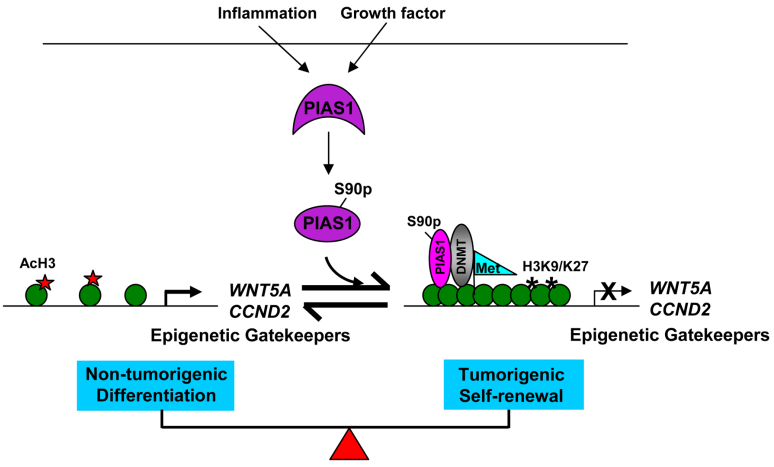

Figure 7. A proposed model of the function of PIAS1 in breast cancer. In response to growth factor and inflammatory signals, PIAS1 is activated via Ser90 phosphorylation (S90p), and recruited to the target gene promoters. PIAS1 represses the expression of epigenetic gatekeeper genes, such as *ESR1*, *WNT5A* and *CCND2*, by promoting inhibitory histone H3 lysine 9 and lysine 27 trimethylation (H3K9/K27) and DNA methylation (Met), while inhibiting acetylated histone H3 (AcH3). Therefore, PIAS1 promotes tumorigenesis by selective epigenetic gene silencing.
doi:10.1371/journal.pone.0089464.g007

Cell proliferation assay

For MDA-MB231 cell proliferation under DMEM conditions, cells were seeded in DMEM plus 10% FBS and 1% Penicillin/Streptomycin at a density of 1×10^5 cells per well in 6 well plate, and stained with trypan blue and counted for viable cells everyday for 5 days. Alternatively, cells were seeded at a density of 3,000 cells per well in 96 well tissue culture plate (08-772-3; Fisher), and cell growth was determined everyday for 4–5 days by CellTiter96 AQueous One Solution Cell Proliferation Assay as instructed by the manufacturer (Promega). For cell growth under SCM conditions, cells were seeded in SCM at a density of 3,000 cells per well in 96 well non-treated microplate (12-565-226; Fisher), and supplemented with fresh human EGF (25 ng/ml), basic FGF (25 ng/ml) and Insulin (5 ug/ml) every 2 days. Cell growth was determined at indicated time points by CellTiter96 AQueous One Solution Cell Proliferation Assay as instructed by the manufacturer (Promega). Triplicates were performed for each time point of the growth curve.

ALDEFLUOR assay

The $ALDH^+$ cell population was determined using an ALDEFLUOR assay kit as instructed (StemCell Technologies). Briefly, cells grown under SCM condition were incubated with the ALDH substrate BAAA in ALDEFLUOR assay buffer in the presence or absence of the specific ALDH inhibitor diethylaminobenzaldehyde (DEAB) at 37°C for 45 min, followed by flow cytometry. The $ALDH^+$ population of each sample was determined using its own negative control (DEAB containing sample) as a reference.

In vivo tumorigenesis

Exponentially growing cells were trypsinized and resuspended in serum free-DMEM or RPMI, mixed with equal volume of Matrigel (BD Biosciences), and injected into the fat pad, or subcutaneously into the flank of 6–10 week old SCID beige mice (UCLA Department of Radiation Oncology) in a volume of 150 ul per site. Tumors were measured weekly with a caliper and tumor volume was calculated as width x length x height x 0.526.

Tissue microarray analysis

Tissue microarray slides were obtained from Imgenex and Full Moon Biosystems, and immunohistochemistry (IHC) staining was performed using polyclonal anti-PIAS1 [20] as instructed by the manufacturers. "Normal duct" was defined as normal breast tissues from healthy individuals as well as histologically normal tissues adjacent to tumors. Semiquantitative assessment of PIAS1 staining was performed using a 0–2 scale (0 = negative; 1 = weak staining; 2 = strong staining) based on the average intensity per epithelial cell, and PIAS1 score was defined as the product of PIAS1 staining scale and the percentage of PIAS1 positive staining. A total of 3 independent tissue arrays containing 30–100 samples each were performed and the data were pooled. Statistic analysis was performed using non-parametric two-tailed Kruskal Wallis test with alpha level equals 0.05 for all tests, since both "Normal duct" and "IDC" populations are not normally distributed.

Microarray analysis

MDA-MB231 cells containing a control shRNA or PIAS1 shRNA2 were cultured in DMEM plus 10% FBS (DMEM) or SCM for 30 h. Total RNA was prepared and subjected to microarray analyses using the human genome U133A 2.0 array chip (Affymetrix) as described [19]. The microarray data is presented in Table S1 in File S1 and has been deposited to Gene Expression Omnibus (GEO) database (GSE44024).

Quantitative real time PCR (Q-PCR)

Quantitative real time PCR (Q-PCR) analyses were performed with breast cancer cells or tumor xenograft samples as described previously [19]. Briefly, total RNA was prepared using RNA STAT60 (Tel-Test). First strand complementary DNA was produced by reverse transcription (RT) of 1 ug total RNA using iScript cDNA synthesis kit (Bio-Rad). Q-PCR was carried out using the CFX96 real-time PCR detection system (Bio-Rad) in a final volume of 25 ul containing Taq polymerase, 1xTaq buffer, 125 uM dNTP, SYBR Green I (Molecular Probes) and gene-specific primers. Amplification conditions were: 95°C (3 min), 40 cycles of 95°C (10 s) and 61°C (30 s). Q-PCR data were analyzed by CFX Manager 2.0 software (Bio-Rad), and normalized by beta-Actin (*ACTB*). The results were presented as "Relative Expression" as compared to that in the control shRNA cells, which was set as "1". Primers are listed in Table S2 in File S1.

Chromatin immunoprecipitation (ChIP) assay

ChIP assays were performed using the ChIP analysis kit as instructed (Upstate). Briefly, cells grown in DMEM plus 10% FBS were cross-linked and lysed. Chromatin was sheared by sonication (10 s at 30% of the maximum strength for a total of six times). Cell extracts were immunoprecipitated with indicated antibodies, or IgG as a negative control. The binding of these factors to various DNA regions was quantified by quantitative real time PCR (Q-PCR) using the immunoprecipitates as templates and specific primers (Table S2 in File S1). The results were presented as "percent of input". The following antibodies were used in the ChIP assay: normal rabbit IgG (sc-2027; Santa Cruz), anti-PIAS1 [51], anti-histone H3 trimethylated at Lys9 (H3K9me3) (17-625; Millipore); anti-histone H3 trimethylated at Lys27 (H3K27me3) (17-622; Millipore); anti-Acetylated histone H3 (AcH3) (17-615; Millipore); anti-DNMT1 (Ab13537; Abcam) and anti-DNMT3A (R0015-2; Abiocode).

Bisulfite treatment and methylation analysis

Bisulfite modification of DNA was performed using EZ Methylation-Gold kit (Zymo Research). Bisulfite genomic sequencing (BGS) was conducted using cells grown in DMEM plus 10% FBS as described [39–42]. Taq DNA polymerase (Zymo Research) was used for PCR amplification using specific primers (Table S2 in File S1). The PCR conditions were as follows: 1 cycle of 95°C for 10 min, then 40 cycles of 95°C for 45 s, 56°C for 1 min, and 72°C for 1 min; and 1 cycle of 72°C for 10 min. Amplified products were cloned into pCR4-Topo (Invitrogen), with 8 to 12 colonies randomly chosen and sequenced.

Supporting Information

File S1 Contains the following files: Figure S1, Table S1 and Table S2. **Figure S1.** Validation of the polyclonal anti-PIAS1 antibody by immunofluorescence. MDA-MB231 cells containing control shRNA or PIAS1 shRNA2 were fixed by 3 different methods as indicated, followed by staining with polyclonal anti-PIAS1. FMA, formaldehyde. **Table S1.** Microarray analysis. Fold induction is defined as the ratio of the expression levels of a given gene in PIAS1 shRNA2 vs. control shRNA cells. Genes with greater than 10-fold induction under Stem Cell Media (SCM) condition are shown. **Table S2.** Primers used for Q-PCR, ChIP and methylation.
(DOC)

Acknowledgments

We thank Irving Garcia for technical assistance, and UCLA flow cytometry core facility.

Author Contributions

Conceived and designed the experiments: BL KS. Performed the experiments: BL ST KMY RY YY RM CH VC YJ. Analyzed the data: BL GF JR TFL KS. Contributed reagents/materials/analysis tools: NO DS. Wrote the paper: BL KS.

References

1. Jovanovic J, Ronneberg JA, Tost J, Kristensen V (2010) The epigenetics of breast cancer. *Mol Oncol* 4: 242–254.
2. Ting AH, McGarvey KM, Baylin SB (2006) The cancer epigenome–components and functional correlates. *Genes Dev* 20: 3215–3231.
3. Jones PA, Baylin SB (2007) The epigenomics of cancer. *Cell* 128: 683–692.
4. Dedeurwaerder S, Fumagalli D, Fuks F (2011) Unravelling the epigenomic dimension of breast cancers. *Curr Opin Oncol* 23: 559–565.
5. Huang Y, Nayak S, Jankowitz R, Davidson NE, Oesterreich S (2011) Epigenetics in breast cancer: what's new? *Breast Cancer Res* 13: 225.
6. Szyf M (2012) DNA methylation signatures for breast cancer classification and prognosis. *Genome Med* 4: 26.
7. Connolly R, Stearns V (2012) Epigenetics as a Therapeutic Target in Breast Cancer. *J Mammary Gland Biol Neoplasia*.
8. Bonnet D, Dick JE (1997) Human acute myeloid leukemia is organized as a hierarchy that originates from a primitive hematopoietic cell. *Nat Med* 3: 730–737
9. Molofsky AV, Pardal R, Morrison SJ (2004) Diverse mechanisms regulate stem cell self-renewal. *Curr Opin Cell Biol* 16: 700–707
10. Phillips TM, McBride WH, Pajonk F (2006) The response of CD24(-/low)/CD44+ breast cancer-initiating cells to radiation. *J Natl Cancer Inst* 98: 1777–1785.
11. Li X, Lewis MT, Huang J, Gutierrez C, Osborne CK, et al. (2008) Intrinsic resistance of tumorigenic breast cancer cells to chemotherapy. *J Natl Cancer Inst* 100: 672–679.
12. Yu F, Yao H, Zhu P, Zhang X, Pan Q, et al. (2007) let-7 regulates self renewal and tumorigenicity of breast cancer cells. *Cell* 131: 1109–1123.
13. Woodward WA, Chen MS, Behbod F, Alfaro MP, Buchholz TA, et al. (2007) WNT/beta-catenin mediates radiation resistance of mouse mammary progenitor cells. *Proc Natl Acad Sci U S A* 104: 618–623.
14. Dalerba P, Cho RW, Clarke MF (2007) Cancer stem cells: models and concepts. *Annu Rev Med* 58: 267–284
15. Ailles LE, Weissman IL (2007) Cancer stem cells in solid tumors. *Curr Opin Biotechnol* 18: 460–466.
16. Kakarala M, Wicha MS (2008) Implications of the cancer stem-cell hypothesis for breast cancer prevention and therapy. *J Clin Oncol* 26: 2813–2820.
17. Mimeault M, Hauke R, Mehta PP, Batra SK (2007) Recent advances in cancer stem/progenitor cell research: therapeutic implications for overcoming resistance to the most aggressive cancers. *J Cell Mol Med* 11: 981–1011.
18. Shuai K, Liu B (2005) Regulation of gene-activation pathways by PIAS proteins in the immune system. *Nat Rev Immunol* 5: 593–605.
19. Liu B, Mink S, Wong KA, Stein N, Getman C, et al. (2004) PIAS1 selectively inhibits interferon-inducible genes and is important in innate immunity. *Nat. Immunol.* 5: 891–898.
20. Liu B, Yang R, Wong KA, Getman C, Stein N, et al. (2005) Negative regulation of NF-kappaB signaling by PIAS1. *Mol. Cell. Biol.* 25: 1113–1123.
21. Tahk S, Liu B, Chernishof V, Wong KA, Wu H, et al. (2007) Control of specificity and magnitude of NF-kB and STAT1-mediated gene activation through PIASy and PIAS1 cooperation. *Proc. Natl Acad. Sci. USA* 104: 11643–11648.
22. Liu B, Yang Y, Chernishof V, Loo RR, Jang H, et al. (2007) Proinflammatory stimuli induce IKKalpha-mediated phosphorylation of PIAS1 to restrict inflammation and immunity. *Cell* 129: 903–914.
23. Liu B, Shuai K (2008) Targeting the PIAS1 SUMO ligase pathway to control inflammation. *Trends Pharmacol Sci* 29: 505–509
24. Liu B, Tahk S, Yee KM, Fan G, Shuai K (2010) The ligase PIAS1 restricts natural regulatory T cell differentiation by epigenetic repression. *Science* 330: 521–525.
25. Loke SL, Neckers LM, Schwab G, Jaffe ES (1988) c-myc protein in normal tissue. Effects of fixation on its apparent subcellular distribution. *Am J Pathol* 131: 29–37
26. Lee J, Kotliarova S, Kotliarov Y, Li A, Su Q, et al. (2006) Tumor stem cells derived from glioblastomas cultured in bFGF and EGF more closely mirror the phenotype and genotype of primary tumors than do serum-cultured cell lines. *Cancer Cell* 9: 391–403.
27. Ginestier C, Hur MH, Charafe-Jauffret E, Monville F, Dutcher J, et al. (2007) ALDH1 Is a Marker of Normal and Malignant Human Mammary Stem Cells and a Predictor of Poor Clinical Outcome. *Cell Stem Cell* 1: 555–567.
28. Dontu G, Abdallah WM, Foley JM, Jackson KW, Clarke MF, et al. (2003) In vitro propagation and transcriptional profiling of human mammary stem/progenitor cells. *Genes Dev* 17: 1253–1270.
29. Dontu G, Liu S, Wicha MS (2005) Stem cells in mammary development and carcinogenesis: implications for prevention and treatment. *Stem Cell Rev* 1: 207–213
30. Jonsson M, Dejmek J, Bendahl PO, Andersson T (2002) Loss of Wnt-5a protein is associated with early relapse in invasive ductal breast carcinomas. *Cancer Res* 62: 409–416.
31. Mandelin E, Lassus H, Seppala M, Leminen A, Gustafsson JA, et al. (2003) Glycodelin in ovarian serous carcinoma: association with differentiation and survival. *Cancer Res* 63: 6258–6264.
32. Hautala LC, Koistinen R, Seppala M, Butzow R, Stenman UH, et al. (2008) Glycodelin reduces breast cancer xenograft growth in vivo. *Int J Cancer* 123: 2279–2284.
33. Sakuma M, Akahira J, Ito K, Niikura H, Moriya T, et al. (2007) Promoter methylation status of the Cyclin D2 gene is associated with poor prognosis in human epithelial ovarian cancer. *Cancer Sci* 98: 380–386.
34. Evron E, Umbricht CB, Korz D, Raman V, Loeb DM, et al. (2001) Loss of cyclin D2 expression in the majority of breast cancers is associated with promoter hypermethylation. *Cancer Res* 61: 2782–2787.
35. Inoue M, Takahashi K, Niide O, Shibata M, Fukuzawa M, et al. (2005) LDOC1, a novel MZF-1-interacting protein, induces apoptosis. *FEBS Lett* 579: 604–608
36. Reya T, Clevers H (2005) Wnt signalling in stem cells and cancer. *Nature* 434: 843–850
37. Huang H, He X (2008) Wnt/beta-catenin signaling: new (and old) players and new insights. *Curr Opin Cell Biol* 20: 119–125.
38. Malanchi I, Peinado H, Kassen D, Hussenet T, Metzger D, et al. (2008) Cutaneous cancer stem cell maintenance is dependent on beta-catenin signalling. *Nature* 452: 650–653.
39. Ying J, Li H, Chen YW, Srivastava G, Gao Z, et al. (2007) WNT5A is epigenetically silenced in hematologic malignancies and inhibits leukemia cell growth as a tumor suppressor. *Blood* 110: 4130–4132.
40. Ying J, Li H, Yu J, Ng KM, Poon FF, et al. (2008) WNT5A exhibits tumor-suppressive activity through antagonizing the Wnt/beta-catenin signaling, and is frequently methylated in colorectal cancer. *Clin Cancer Res* 14: 55–61.
41. Yu J, Leung WK, Ebert MP, Leong RW, Tse PC, et al. (2003) Absence of cyclin D2 expression is associated with promoter hypermethylation in gastric cancer. *Br J Cancer* 88: 1560–1565.
42. Li LC, Chui R, Nakajima K, Oh BR, Au HC, et al. (2000) Frequent methylation of estrogen receptor in prostate cancer: correlation with tumor progression. *Cancer Res* 60: 702–706.
43. Wang D, Zhou J, Liu X, Lu D, Shen C, et al. (2013) Methylation of SUV39H1 by SET7/9 results in heterochromatin relaxation and genome instability. *Proc Natl Acad Sci U S A* 110: 5516–5521.
44. Mikels AJ, Nusse R (2006) Purified Wnt5a protein activates or inhibits beta-catenin-TCF signaling depending on receptor context. *PLoS Biol* 4: e115.
45. Roarty K, Serra R (2007) Wnt5a is required for proper mammary gland development and TGF-beta-mediated inhibition of ductal growth. *Development* 134: 3929–3939.
46. Olson DJ, Gibo DM, Saggers G, Debinski W, Kumar R (1997) Reversion of uroepithelial cell tumorigenesis by the ectopic expression of human wnt-5a. *Cell Growth Differ* 8: 417–423.
47. Jonsson M, Andersson T (2001) Repression of Wnt-5a impairs DDR1 phosphorylation and modifies adhesion and migration of mammary cells. *J Cell Sci* 114: 2043–2053.
48. Liang H, Chen Q, Coles AH, Anderson SJ, Pihan G, et al. (2003) Wnt5a inhibits B cell proliferation and functions as a tumor suppressor in hematopoietic tissue. *Cancer Cell* 4: 349–360.
49. Blanc E, Goldschneider D, Douc-Rasy S, Benard J, Raguenez G (2005) Wnt-5a gene expression in malignant human neuroblasts. *Cancer Lett* 228: 117–123.
50. Liu B, Shuai K (2008) Regulation of the sumoylation system in gene expression. *Curr Opin Cell Biol* 20: 288–293.
51. Liu B, Liao J, Rao X, Kushner SA, Chung CD, et al. (1998) Inhibition of Stat1-mediated gene activation by PIAS1. *Proc. Natl Acad. Sci. USA* 95: 10626–10631.
52. Miyoshi H, Blomer U, Takahashi M, Gage FH, Verma IM (1998) Development of a self-inactivating lentivirus vector. *J Virol* 72: 8150–8157.

Supporting Information

PIAS1 regulates breast tumorigenesis through selective epigenetic gene silencing

Bin Liu, Samuel Tahk, Kathleen M. Yee, Randy Yang, Yonghui Yang, Ryan Mackie, Cary Hsu, Vasili Chernishof, Neil O'Brien, Yusheng Jin, Guoping Fan, Timothy F. Lane, Jianyu Rao, Dennis Slamon, Ke Shuai

Inventory of Supplementary Information:

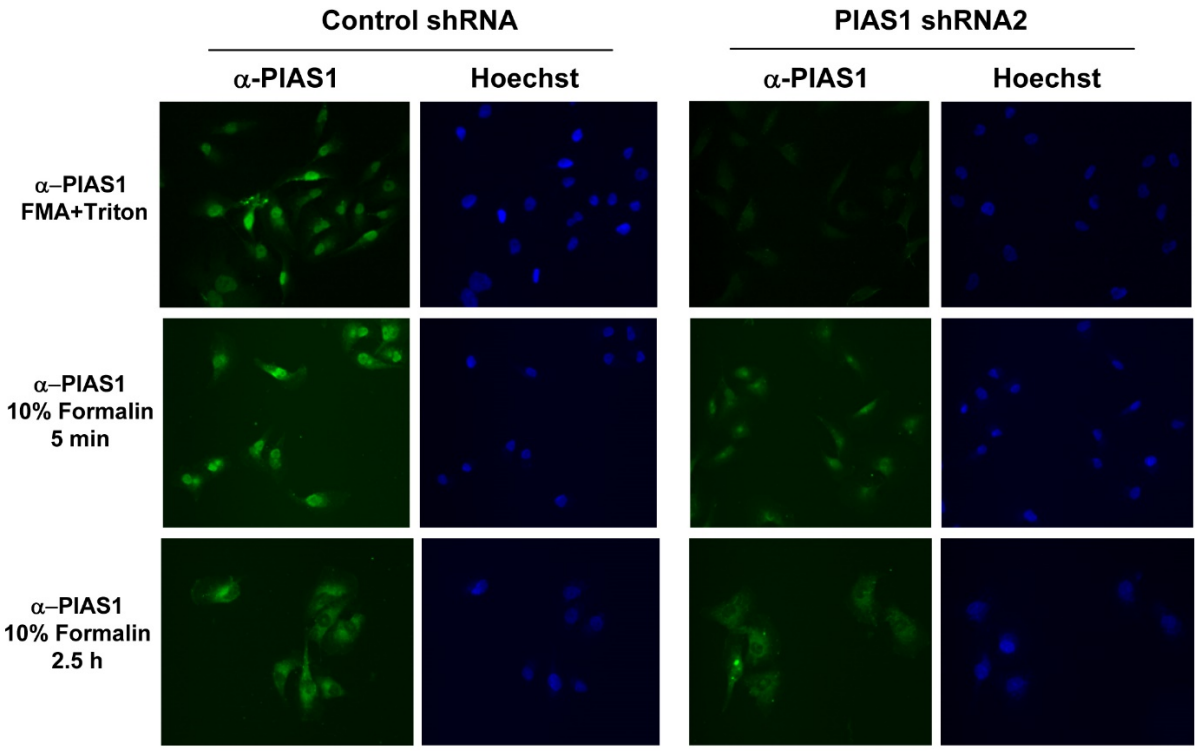

Figure S1. Validation of the polyclonal anti-PIAS1 antibody by immunofluorescence.

MDA-MB231 cells containing control shRNA or PIAS1 shRNA2 were fixed by 3 different methods as indicated, followed by staining with polyclonal anti-PIAS1. FMA, formaldehyde.

Table S1. Microarray analysis

Fold induction is defined as the ratio of the expression levels of a given gene in PIAS1 shRNA2 vs. control shRNA cells. Genes with greater than 10-fold induction under Stem Cell Media (SCM) condition are shown.

		Fold induction	
Gene	**Acession numbe**	**SCM**	**DMEM**
SPANXA1	gb:NM_013453.1	78.6	18.86
LDOC1	gb:NM_012317.1	58.1	9.04
MMP1	gb:NM_002421.2	36.38	36.18
SPANXA1	gb:NM_013453.1	35.49	28.63
WNT5A	gb:NM_003392.1	34.55	6.73
PAEP	gb:NM_002571.1	30.65	2.77
GJA7	gb:NM_005497.1	24.01	0.34
WNT5A	gb:AI968085	22.7	4.17
SELL	gb:NM_000655.2	21.03	3.67
ORM1	gb:NM_000607.1	20.67	2.14
MGC2463	gb:NM_024070.1	19.93	3.29
CD84	gb:AF054816.1	19.92	0.16
HEY1	gb:NM_012258.1	19.19	2.45
MUC5B	gb:AI697108	18.21	2.2
FLJ21369	gb:NM_024802.1	17.97	0.04
FZD8	gb:AL121749	17.6	4.18
SCYA8	gb:AI984980	17.17	0.18
MC4R	gb:NM_005912.1	16.65	2.28
FLJ22494	gb:NM_024815.1	15.98	0.5
RPL5	gb:U66589.1	15.58	2.19
H4F2	gb:NM_003548.1	15.34	2.52
PSCDBP	gb:L06633.1	15.29	0.22
FLJ12130 fis	gb:AK022192.1	14.92	5.28
SLC5A7	gb:NM_021815.1	14.86	5.71
APBA2	gb:AW571582	14.32	4.38
NF2	gb:AF122827.1	13.9	22.25
HSD17B2	gb:NM_002153.1	13.89	0.34
SPANXC	gb:NM_022661.1	13.81	11.48
FCGR1A	gb:X14355.1	13.43	0.41
FLJ10178	gb:AK001040.1	13.3	6.68

Table S1. Microarray analysis (continued)

		Fold induction	
Gene	**Acession numbe**	**SCM**	**DMEM**
LCN1	gb:NM_002297.1	13.27	3.34
FLJ21610	gb:NM_022751.1	13.2	10.83
SLC15A2	gb:BF223679	12.73	16.23
PAI2/SERPINB2	gb:NM_002575.1	12.57	20.35
BHBGT IIB	gb:S83374.1	12.55	2.74
FLJ11507 fis	gb:AK021569.1	12.54	2.49
LECT2	gb:NM_002302.1	12.44	3.67
EPB41L4	gb:NM_022140.1	12.41	2.41
CGI-96	gb:AL450314.1	12.29	6.59
NME5	gb:NM_003551.1	12.03	0.35
SYT1	gb:AV723167	12	9.02
KIAA1060	gb:AB028983.1	11.95	0.13
TRPC6	gb:NM_004621.2	11.88	0.28
VAMP5	gb:AI814466	11.77	10.37
CCND2	gb:AW026491	11.69	4.22
pseudogene	gb:AL163533	11.55	0.49
SH3D5	gb:NM_015385.1	11.36	2.17
DCT	gb:AL139318	11.05	3.53
HRMT1L1	gb:U79286.1	10.91	5.21
ELL2	gb:NM_012081.1	10.88	12.08
GADD45G	gb:NM_006705.2	10.84	5.63
C11ORF25	gb:AJ300461.1	10.72	0.26
SLC19A3	gb:NM_025243.1	10.71	10.62
GAS2	gb:NM_005256.1	10.55	0.22
DACH	gb:NM_004392.1	10.55	0.1
RLBP1	gb:NM_000326.1	10.51	3.11
ADCY1	gb:L05500.1	10.48	0.38
SYT5	gb:NM_003180.1	10.36	0.34
PAD	gb:NM_012387.1	10.2	11.25
unknown	gb:AL049786.1	10.11	0.18
CTNND2	gb:AF035302.1	10.1	0.2
KIAA0983	gb:AB023200.1	10.07	6.51
OAZ4	gb:AF293339.1	10.04	4.82

Table S2. Primers used for Q-PCR, ChIP and methylation.

Species	Gene	5' or 3'	DNA sequence
Q-PCR primers:			
human	*WNT5A*	5'	CAAGGGCTCCTACGAGAGTG
		3'	GCCAGCATGTCTTCAGGCTA
	WNT1	5'	CTCCTCCACGAACCTGCTTA
		3'	CGGATTTTGGCGTATCAGAC
	CCND2	5'	TCACCAACACAGACGTGGAT
		3'	ACGGTACTGCTGCAGGCTAT
	CCND1	5'	GCCATGAACTACCTGGACCG
		3'	TGATCTGTTTGTTCTCCTCCGC
	LDOC1	5'	GCTGCCAGGCTTACATCTTC
		3'	CCAGGTTGGTCCTGATCTC
	PAEP	5'	ACTATACGGTGGCGAACGAG
		3'	CAGGTACTGGCACATCATGC
	ESR1	5'	CGGCTCCGTAAATGCTACGA
		3'	AACATTCTCCCTCCTCTTCGG
	ACTB	5'	AGGCACCAGGGCGTGATGG
		3'	CATGGCTGGGGTGTTGAAGG
ChIP primers:			
human	*WNT5A*	5'	GGCCACAGTTGAGTAGTGGT
		3'	CAACTGTTCCACGGAGAGG
	CCND2	5'	TGTTCTGGTCCCTTTAATCG
		3'	AACGGATCCTAATCCTCCTG
	ESR1	5'	AAACCACCCATGTCCTATTTTG
		3'	AGGCTGGAAAGTACCCTATGCT
	CCND1	5'	TGGGGACCCTCTCATGTAAC
		3'	TAGAATTTGCCCTGGGACTG
	Satellite 2	5'	CATCGAATGGAAATGAAAGGAGTC
		3'	ACCATTGGATGATTGCAGTCAA
Methylation primers:			
human	*WNT5A*	5'	TGGGGTTGGAAAGTTTTAATTAT
		3'	ACTAAACACCTACCTTCATAAC
	CCND2	5'	TTTTGGAGTGAAATATATTAAAGGG
		3'	CCCCTACATCTAACAAACC
	ESR1	5'	TAATGTTTGGTAATAAAGTTTTTATTGG
		3'	AAAACCTTCTAAAATACATATAAATCAAAT

Chapter 5: TET2 is a Regulator of the Innate Immune Response in Murine Macrophages

Abstract

The ten-eleven translocation (TET) proteins are important epigenetic modifiers. TET proteins possess enzymatic activity to create the DNA modification 5-hydroxymethylcytosine (5hmC) which can affect gene regulation. Deficiencies in TET2 have been reported in numerous human hematopoietic disorders and in addition animal studies indicate an enhanced myeloid proliferation in mice lacking TET2. Despite this, little is known about the role of TET2 in the innate immune response. Using TET2 deficient mice, we show that TET2 is a negative inhibitor of a subset of the microbial responsive genes associated with M1 polarized macrophages. Simultaneously, TET2 is required for the expression of a subset of M2 associated genes. *Tet2-/-* mice exhibit protection against *Listeria monocytogenes* infection, likely due to the overexpression of proinflammatory genes.

Introduction

Macrophages are phagocytic cells that survey their microenvironment and play a key role in the initiation of the immune response. Possessing a multitude of specialized receptors such as the interferon receptors and toll-like receptors (TLR), macrophages can respond to a myriad of external cues such as cytokines, growth factors, microbes, microbial products, and glucocorticoids (Murray et al., 2014). Through the combination and intensity of the stimuli, macrophages can mount appropriate immune responses, ranging from “classical”/M1 responses associated with bacteria, virus, and protozoa infections, to the “alternative”/M2 responses associated with other macrophage functions that are not part of the anti-microbial response, such as the resolution of inflammation, parasite clearance, wound healing and fibrosis, and allergic responses (Ishii et al., 2009; Murray et al., 2011). *In vitro*, IFN-γ and/or LPS can polarize macrophages to the inflammatory associated M1 phenotype, whereas IL-4 polarizes macrophage to the alternative, M2 phenotype (Martinez and Gordon, 2014).

As the M2 phenotype encompasses a variety of potential macrophage functions, widely used markers of IL-4 induced M2 polarization include Chitinase-like 3 (*Chil3*, also known as *Chi3l3* and *Ym1*), Chitinase-like 4 (*Chil4*, also known as *Chi3l4* and *Ym2*), Arginase 1 (*Arg1*), Mannose Receptor 1 (*Mrc1*, also known as *CD206*), and the chemokines C-C motif ligand 17 (*Ccl17*) and C-C motif ligand 22 (*Ccl22*) (Murray et al., 2014). *Chil3* and *Chil4* have roles in the allergic response and also are important for nematode killing (Webb, McKenzie, and Foster, 2011; Welch et al., 2002; Sutherland et al., 2014). *Arg1* is involved in immunosuppression, as it down-regulates nitric oxide synthesis (Munder, 2009). *Mrc1* is upregulated in helminth infections (Anthony et al., 2006), and *Ccl17* and *Ccl22* are Th2 chemokines and have been implicated in fibrosis (Belperio et al., 2004).

Over 2000 proteins are produced upon stimulation with IFN-γ, of which roughly 20% are Guanylate binding proteins (GBP) (Kim et al., 2012). The GBP family is highly conserved in vertebrates and includes seven members in humans and eleven members in mice. GBPs are a family of large guanosine triphosphatases (GTPases) and, while described as part of the dynamin superfamily, GBPs share little homology with other dynamin proteins (Praefcke and McMahon, 2004). Multiple studies have uncovered important anti-viral and anti-pathogenic roles for GBPs, including host defense to intracellular pathogens such as influenza virus, *Salmonella typhimurium, Chlamydia muridarum, Francisella novidica, Listeria monocytogenes,* and *Toxoplasma gondii*, among others (Pilla-Moffett et al., 2016). GBPs have been observed to deliver lysosome to *L. monocytogenes* and *Mycobacterium bovis BCG* for pathogen killing. In fact, mice lacking GBP1 are more susceptible to listeriosis than their wildtype control due to impaired macrophage activity (Kim et al., 2011).

The ten-eleven translocation (TET) methylcytosine dioxygenase family of proteins can epigenetically regulate gene expression by altering the expression of genes controlled by DNA methylation. TET proteins catalyze the conversion of 5-methylcytosine (5mC) into 5-hydroxymethylcytosine (5hmC), the first step towards active DNA demethylation (Tahiliani et al.,

2009). Numerous studies have been performed on embryonic stem cells and neuronal cells to characterize the role of TET proteins. So far, both enzymatic and non-enzymatic role of TET proteins in gene regulation have been uncovered (Pastor et al., 2013). However, there are few studies characterizing the role of TET proteins in innate immunity. Three groups have independently created *Tet2* deficient mice, and in all cases found dysregulated hematopoietic stem cells (HSC) with an increase in myeloid cells (Moran-Crusio et al., 2011; Ko et al., 2011; Li et al., 2011). Additionally, TET2 is commonly mutated in several human myeloid malignancies, such as acute myeloid leukemia (AML), in which 22% of cases have TET2 mutations (Delhommeau et al., 2009; Ficz and Gribben, 2014). This demonstrates that TET2 plays an important role in myeloid cell differentiation. As the hematopoietic system is the source of mature blood cells that includes myeloid-derived macrophages and dendritic cells (Seita and Weissman, 2010), we determined if TET proteins play a role in the gene regulation of immune responses.

Here we characterized the role of TET2 in macrophages in the context of the innate immune system. We show that TET2 levels are induced upon pro-inflammatory stimuli, suggesting a role for TET2 in the gene regulation of inflammatory genes. Gene analysis of stimulated macrophages reveal that TET2 represses several genes important for bacterial and viral clearance, such as *Ifn-β, Il-6, Gbp1,* and *Isg15.* In the absence of TET2, macrophage cells are more polarized towards the M1 phenotype and exhibit corresponding deficiencies in several M2 genes. Finally*, in vivo* results with *Listeria monocytogenes* show that TET2 has a negative impact with pathogen clearance.

Results

TET proteins are induced by proinflammatory stimuli.

To determine if TET proteins have a role in the inflammatory response, wild-type and littermate matched *Tet1-/-* or *Tet2-/-* bone marrow-derived macrophages (BMDM) were treated

with various immune stimulatory factors and cytokines in a time course dependent manner. Gene expression was analyzed by qPCR. Lipopolysaccharide (LPS) is a component of the outer membrane of Gram-negative bacteria that strongly induces TLR4. Zymosan is found on the surface of *Saccharomyces cerevisiae* and is composed of protein-carbohydrate complexes and can activate TLR2. Polyinosinic:polycytidylic acid (poly I:C) is a synthetic analog of double-stranded RNA typically associated with viral RNA and signals through TLR3 (Kawai and Akira, 2010). Interferon beta (IFN-β), interferon gamma (IFN-γ) and interleukin 4 (IL-4) are cytokines with strong immunoregulatory roles (Hu and Ivashkiv, 2009; Gordon and Martinez, 2010).

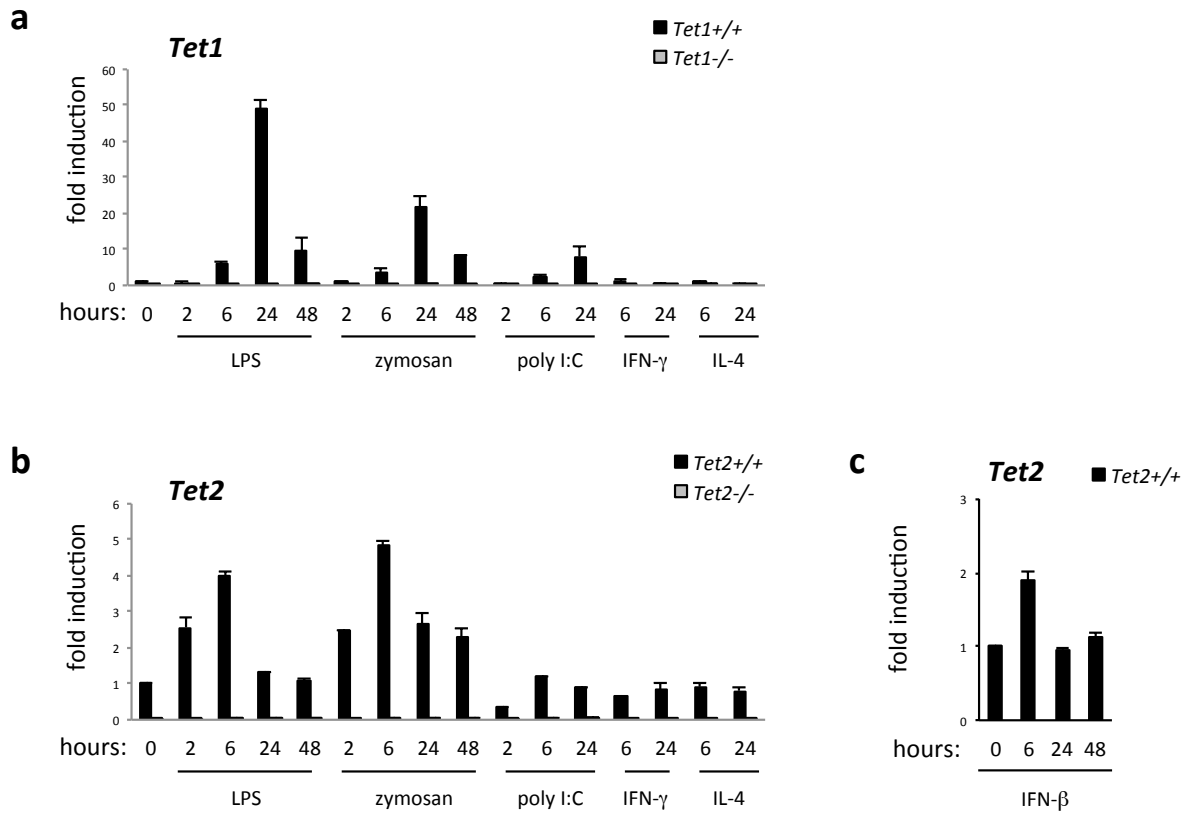

Figure 5.1. Proinflammatory signals stimulate TET expression in BMDM.
(a) BMDM from *Tet1+/+* and *Tet1-/-* littermate matched mice were treated with either LPS (20 ng/ml), zymosan (100 ug/ml), high molecular weight (HMW) poly I:C (20 ug/ml), IFN-γ (100 ng/ml), or IL-4 (10 ng/ml) for indicated time points. Gene expression levels were determined by qPCR using total RNA. **(b)**. Same as in (a) but using *Tet2+/+* and *Tet2-/-* littermate mice. **(c)** Same as in (a) except only *Tet2+/+* cells were treated with IFN-β (500 units/ml). Experiments were repeated at least three times. Shown are representative data. Values are normalized to *Hprt*. Error bars indicate standard deviation among duplicates in qPCR.

As shown in Figure 5.1a, *Tet1* expression is induced within 6 hours of stimulation with LPS, zymosan and poly I:C, reaching a peak for LPS and zymosan by 24 hours. In contrast, IFN-γ or IL-4 alone did not induce *Tet1* expression. Likewise, *Tet2* expression is also induced by LPS and zymosan but with an earlier induction profile that is apparent at 2 hours of stimulation and peaks around 6 hours (Figure 5.1b). IFN-β can also induce *Tet2*, although modestly (Figure 5.1c). In contrast, there was no *Tet3* induction when cells were stimulated with LPS, IFN-β, and IFN-γ (data not shown). We determined if either *Tet1* or *Tet2* can compensate for the lack of the other, and found that generally there is no compensation as analyzed by qPCR (data not shown). This is in agreement with other published reports (Ko et al., 2011; Dawlaty et al., 2011). These results show that both *Tet1* and *Tet2* are induced by inflammatory stimuli.

Next, protein immunoblots were performed to validate the gene expression data for TET2. As shown in Figure 5.2a, BMDM treated with LPS, zymosan, and IFN-β, resulted in the detection of a stimulus and time dependent increase in TET2 protein levels that corresponds with the qPCR data. Unfortunately, our TET1 antibody is not sensitive enough to detect TET1 protein in these cells (data not shown). The activation of TLR4 by LPS can produce IFN-β, and IFN-β can signal through the Type I interferon-α/β receptor (IFNAR), which is composed of two chains, IFNAR1 and IFNAR2. Both chains are required for signaling (Noppert, Fitzgerald, and Hertzog, 2007). To asked if the IFNAR pathway is involved in LPS-induced TET2 expression, *Ifnar1-/-* BMDM was stimulated with LPS. Treatment of *Ifnar1-/-* BMDM with LPS still resulted in the induction of TET2, indicating that TET2 expression is not dependent on the Type I interferon receptor pathway. As a control, *Ifnar1-/-* BMDM did not respond to IFN-β stimulation, as expected due to the lack of the receptor chain (Figure 5.2b).

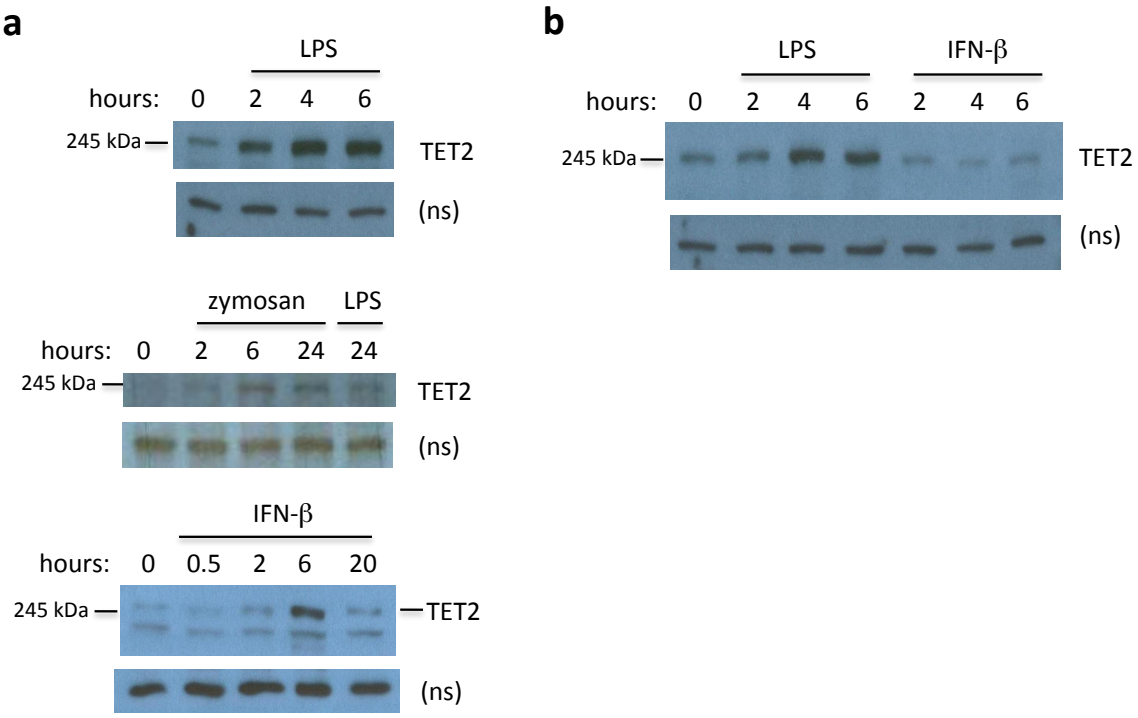

Figure 5.2. Induction of TET2 protein is independent of the IFNα receptor.
(a) Wild-type BMDM were treated with LPS (20 ng/ml), zymosan (100 ug/ml), or IFN-β (500 units/ml) for indicated time points. Protein lysates were harvested and an immunoblot was performed. (**b)** *Ifnar1-/-* BMDM were treated with LPS or IFN-β similarly as in (a) and protein lysates were subjected to immunoblotting. Protein loading was normalized to non-specific bands (ns). Note: all TET2 antibodies used here were from Abiocode (Aguora Hills, USA), but various antibody clones are used here. Both 5.2a and 5.2b "LPS" were probed with clone #E6-197, 5.2a "zymosan" probed with clone #E10-47, and 5.2a "IFN-β" probed with clone #713.

TET2 represses a subset of immune regulatory genes.

Next, the role of TET2 in response to proinflammatory stimuli was determined. As mentioned in chapter 1, TET proteins can stimulate or repress gene expression through various mechanisms. To ask if TET2 and PIAS1 play potentially opposite roles in the inflammatory response, our initial focus was on proinflammatory genes previously found to be negatively regulated by PIAS1 (Liu et al., 2004; Liu et al., 2005). Analysis of TET2 deficient BMDM treated with LPS or IFN-γ by qPCR show enhanced expression of the cytokines *Ifn-β* and interleukin-6 (*Il-6*), along with *Gbp1* and interferon-stimulated gene 15 (*Isg15*) (Figure 5.3). ISG15 is a di-ubiquitin-like molecule that can conjugate to cellular proteins and also function as a cytokine to

induce IFN-γ production (D'Cunha et al., 1996; Giannakopoulos et al., 2005). However, the induction of other classical proinflammatory genes such as CXC chemokine ligand 2 (*Cxcl2*, also known as *MIP2*), CXC chemokine ligand 9 (*Cxcl9*, also known as *MIG*), CXC chemokine ligand 10 (*Cxcl10*, also known as *IP10*), and nitric oxide synthase 2 (*Nos2*) were not affected in *Tet2-/-* BMDM (Figure 5.3). This indicates that TET2 does not globally affect the expression of inflammatory genes, but rather TET2 regulates a subset of genes, similar to PIAS1. Whereas PIAS1 is a negative regulator of *Il-6, Gbp1, Cxcl9* and *Cxcl10*, of these four genes, TET2 only represses *Il-6* and *Gbp1*.

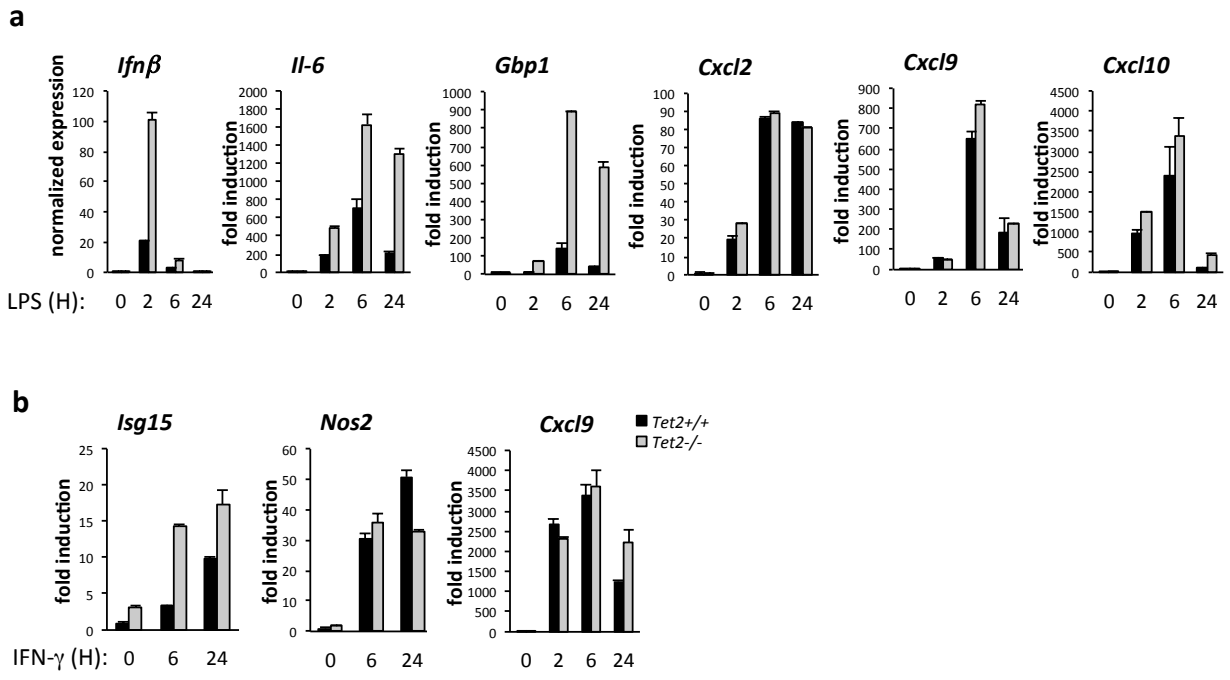

Figure 5.3. TET2 is a repressor of a subset of inflammatory genes.
(a) BMDM from *Tet2+/+* and *Tet2-/-* littermate matched mice were treated with LPS (20 ng/ml) for indicated time points. Gene expression levels were determined by qPCR analysis of total RNA. **(b)** Same as in (a) except that cells were treated with IFN-γ (100 ng/ml). Experiments were repeated at least three times. Shown are representative data. Values are normalized to *Hprt*. Error bars indicate standard deviation among duplicates in qPCR.

TET2 represses IFN-β promoter activity.

To study the effect of TET2 on IFN-β signaling, luciferase reporter assays were performed in human 293T cells. The IFN-β promoter region from -400 bp to +20 bp of the transcription start site (TSS) was cloned into a luciferase reporter construct (Figure 5.4a). To ask if TET2 can repress IFN-β signaling, this reporter construct was then transiently transfected with an increasing amount of mouse TET2 plasmid (either 6x or 30x the amount compared to the luciferase construct). To activate IFN-β signaling, cells were additionally transfected with TBK1 to induce IFN-β transcription. TANK-binding kinase 1 (TBK1) is a protein that activates the transcription factor IRF3 to signal IFN-β production (Perry et al., 2005). Twenty-four hours post transfection, cells were lysed and luciferase activity recorded. TET2 negatively affected the expression of IFN-β, confirming the qPCR results (Figure 5.4b). To determine if the 5-hydroxylmethylcytosine activity of TET2 is required for IFN-β repression, transient transfection assays were performed with a TET2 mutant carrying H1302Y and D1304A mutations in the catalytic domain, which severely abolishes TET2 enzymatic activity (Ko et al., 2010). Results show that the enzymatic mutant TET2 can still repress IFN-β promoter activity (Figure 5.4b). As a control, transfection with PIAS1 repressed IFN-β-luciferase activity, as previously seen (unpublished data). These results show that TET2 does not require catalytic activity to repress IFN-β expression *in vitro.*

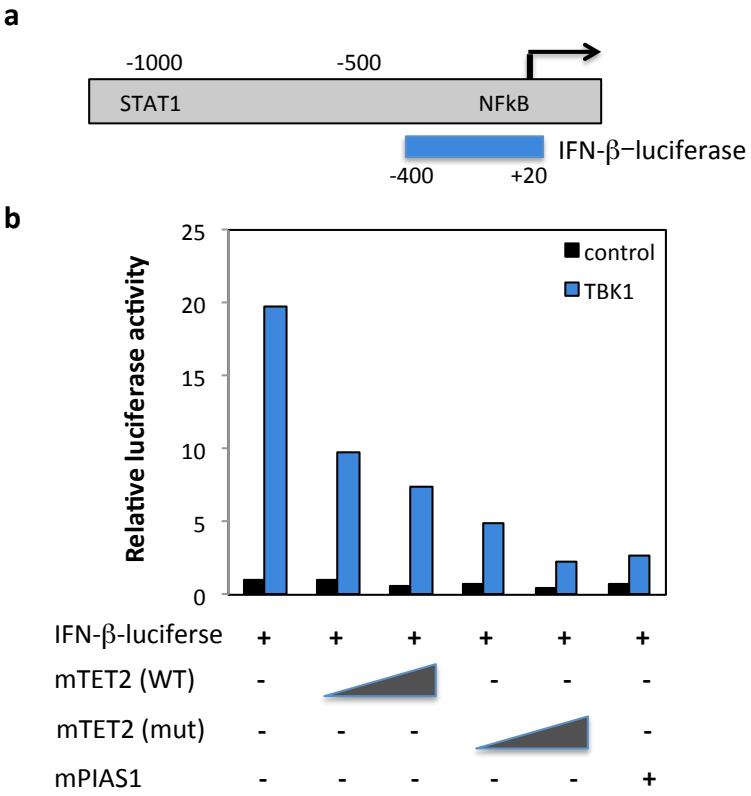

Figure 5.4. TET2 represses IFN-β promoter activity.
(a) Schematic drawing of the murine IFN-β promoter. Indicated in blue is the IFN-β promoter region cloned into pGL3-luciferase reporter construct. Arrow indicates transcription start site (TSS). Numbers indicate base pair from TSS. STAT1 and NF-κB transcription factor binding sites are approximate. (**b)** Luciferase activity in lysates of 293T cells transfected 24 hours prior with indicated plasmids. TBK1 was used to stimulate luciferase activity. Renilla was used for normalization. Abbreviations: WT (wild-type); mut (catalytic mutant).

TET2 highly suppresses *Gbp1* expression.

IFN-γ is classically used to induce the expression of *Gbp* family members. We analyzed if treatment with IFN-γ can recapitulate the gene expression results obtained with LPS stimulation (Figure 5.3a). Upon IFN-γ treatment, *Gbp1* is hyperactivated in *Tet2-/-* BMDM compared to the wild-type control as analyzed by qPCR. Surprisingly *Gbp2* induction is defective in *Tet2-/-* BMDM. *Gbp3* expression is generally not affected by the loss of TET2 (Figure 5.5a). The binding of IFN-γ to its receptor triggers activation of STAT1 (Darnell Jr., 1997), which then activates *Gbp* expression. Additionally IRF1 is required for *Gbp* activation in

response to IFN-γ (Briken et al., 1995). Gene analysis was performed to asked if potential differences in *Stat1* and/or *Irf1* gene expression can account for the hyperactivation of *Gbp1* in *Tet2-/-* BMDM. Generally there was no defect in the induction of these two genes in TET2 deficient cells (Figure 5.5a).

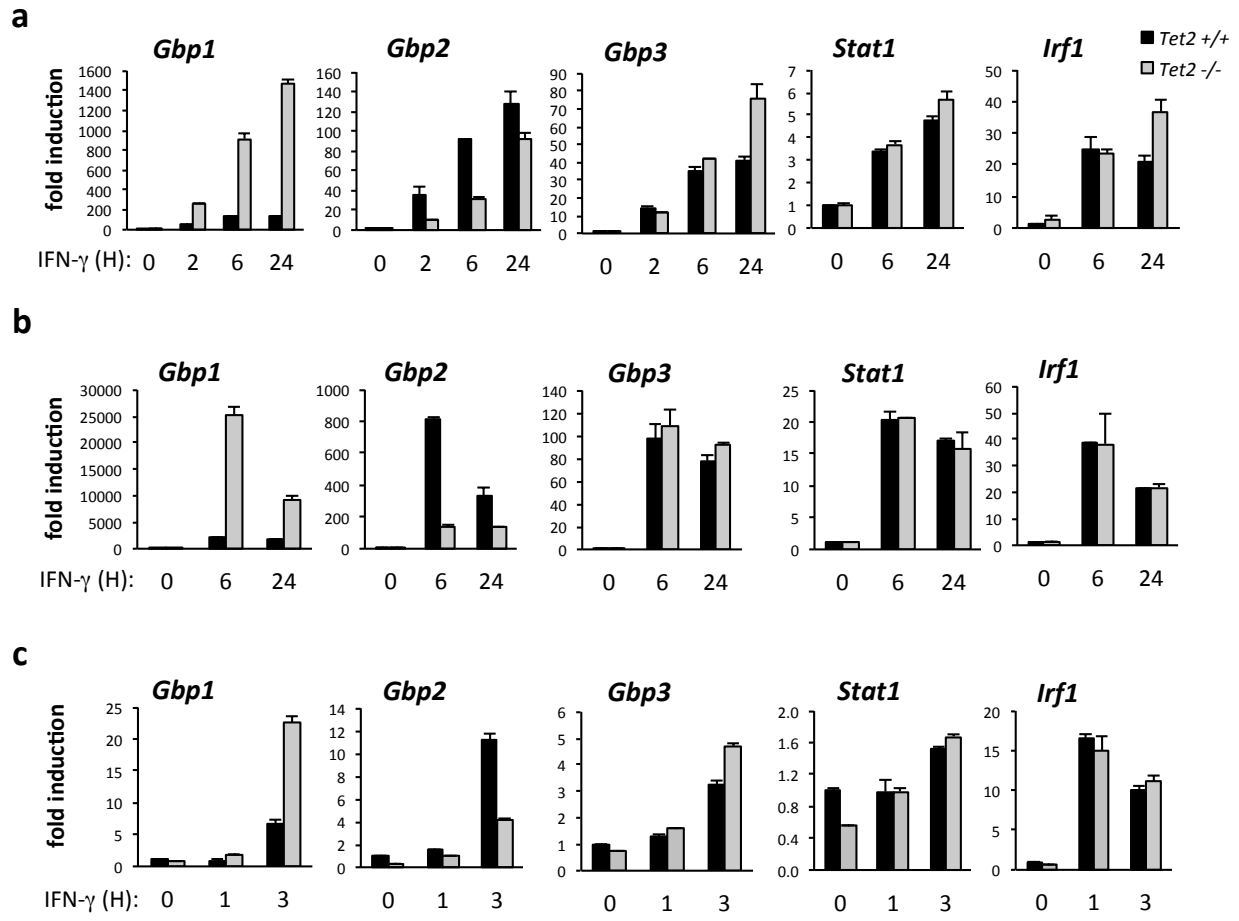

Figure 5.5. TET2 differentially regulates Gbp proteins.
(a) BMDM from *Tet2+/+* and *Tet2-/-* littermate matched mice were treated with IFN-γ (100 ng/ml) for indicated time points. Gene expression levels were determined by qPCR of total RNA. **(b)** Same as in (a) except that resident peritoneal macrophages were analyzed. **(c)** Same as in (a) except that littermate-matched primary MEF cells were treated with IFN-γ at a lower dose (20 ng/ml). Experiments were repeated at least four times for BMDM, and two times for peritoneal macrophages and primary MEF. Shown are representative data. Values in (a) and (c) are normalized to *Hprt*, and values in (b) are normalized to *Gapdh* because IFN-γ affects *Hprt* levels in peritoneal macrophages. Error bars indicate standard deviation among duplicates in qPCR.

As BMDM are derived *in vitro*, they may not be representative of other macrophage cell types found *in vivo*. Therefore the IFN-γ time course assay was repeated using primary resident peritoneal macrophages (Figure 5.5b). Additionally, these assays were repeated in primary mouse embryo fibroblast (MEF) cells to ask if the TET2 effect on *Gbp1* expression is macrophage specific (Figure 5.5c). Regardless of the source of the cell population, *Gbp1* is consistently upregulated, and *Gbp2* is consistently downregulated in *Tet2-/-* cells. *Stat1* and *Irf1* expression levels remain unaffected by the loss of TET2 and cannot account for the hyperactivation of *Gbp1* seen in these three cell types.

TET2 deficient macrophages are defective in several M2 genes

Gene analysis of *Tet2-/-* BMDM and peritoneal macrophages stimulated with LPS and IFN-γ revealed either no difference in gene expression, or an overexpression of several key immune responsive genes (Figure 5.3). In the spectrum of M1 vs. M2 macrophage polarization, it appears that *Tet2-/-* macrophages are polarized more towards the M1 phenotype. Therefore, gene analysis was performed by qPCR to address if there are corresponding defects in gene expression in key M2 genes. BMDM were treated with IL-4 in a time course dependent manner to induce M2 genes. Expression analysis show a significant defective response in *Chil3* and *Chil4* in *Tet2-/-* BMDM. While the defect in *Arg1* expression at 24 hours is less than two-fold, this small defect was consistently observed in six independent experiments (Figure 5.6a). However, not all key M2 genes are defective in *Tet2-/-* BMDM, as *Ccl17, Ccl22* and *Mrc1* expression is not affected by the loss of TET2. Next, to elucidate if the defect in M2 genes is consistent in other macrophage cell types, resident peritoneal macrophages were analyzed. A consistent defect in *Chil3* and *Chil4* induction was observed in TET2 deficient peritoneal macrophages, although this defect is not as dramatic as seen in BMDM (Figure 5.6b). The defect in *Arg1* expression is no longer observed, although a slight defect in *Ccl22* expression is still apparent in peritoneal macrophages. Similar to BMDM, there is no defect in *Ccl17* induction

in peritoneal macrophages. These results show that TET2 is required for the expression of a subset of M2 genes.

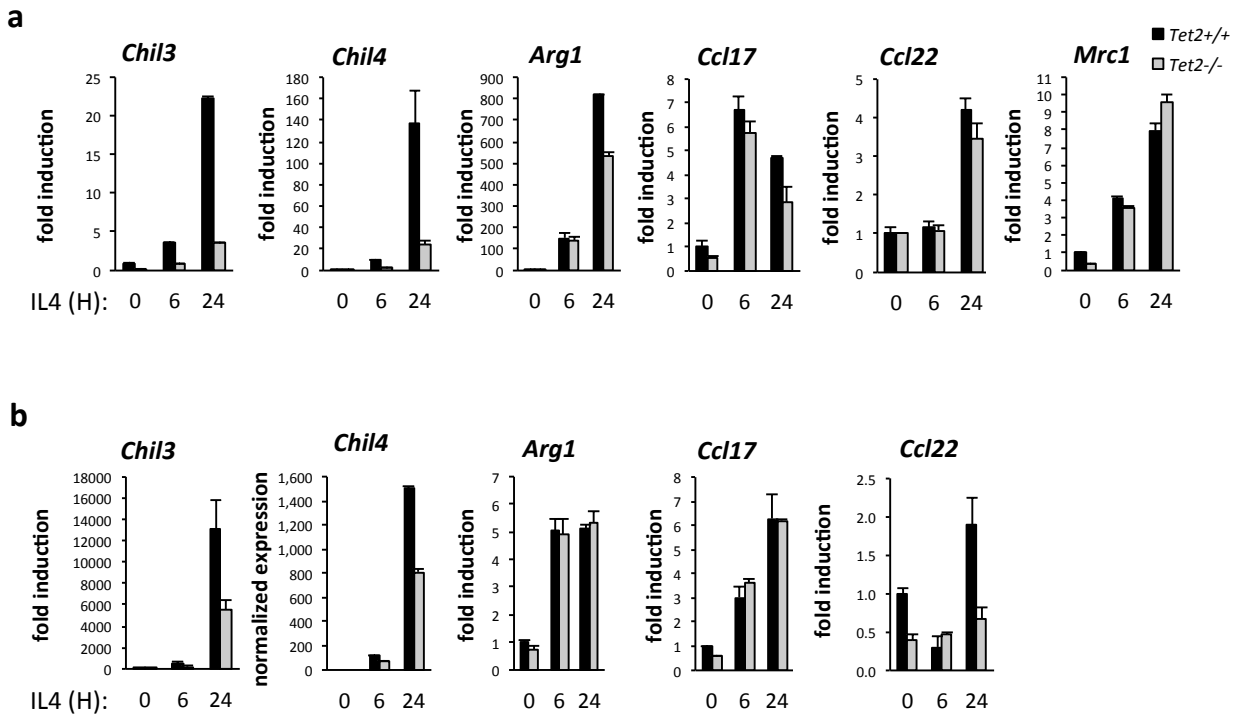

Figure 5.6. TET2 is essential for the expression of several key M2 genes.
(a) BMDM from *Tet2+/+* and *Tet2-/-* littermate matched mice were treated with IL-4 (10 ng/ml) for indicated time points. Gene expression levels were determined by qPCR of total RNA. **(b)** Same as in (a) except that resident peritoneal macrophages were analyzed. Experiments were repeated at least four times for BMDM, and two times for peritoneal macrophages. Shown are representative data. Values are normalized to *Hprt*. Error bars indicate standard deviation among duplicates in qPCR.

STAT1 and STAT6 are similarly activated in *Tet2-/-* BMDM

IFN-γ stimulation signals through the STAT1 pathway for M1 macrophage polarization, whereas IL-4 signals though STAT6 for M2 polarization (Murray et al., 2014). STAT proteins are a family of latent transcription factors found in the cytoplasm but become activated by phosphorylation and translocate to the nucleus upon stimulation of specific interferon receptor(s) (Darnell Jr., 1997). To explain the skew of our *Tet2-/-* macrophages towards the M1

activation spectrum and concurrent defects in several M2 genes, protein immunoblots were performed to detect potential defects in either STAT1 or STAT6 activation upon IFN-γ or IL-4 stimulation, respectively. As shown in Figure 5.7, wild-type and *Tet2-/-* BMDM have similar STAT1 and STAT6 induction profiles. Therefore, STAT1 and STAT6 activation cannot account for the differences seen in gene expression.

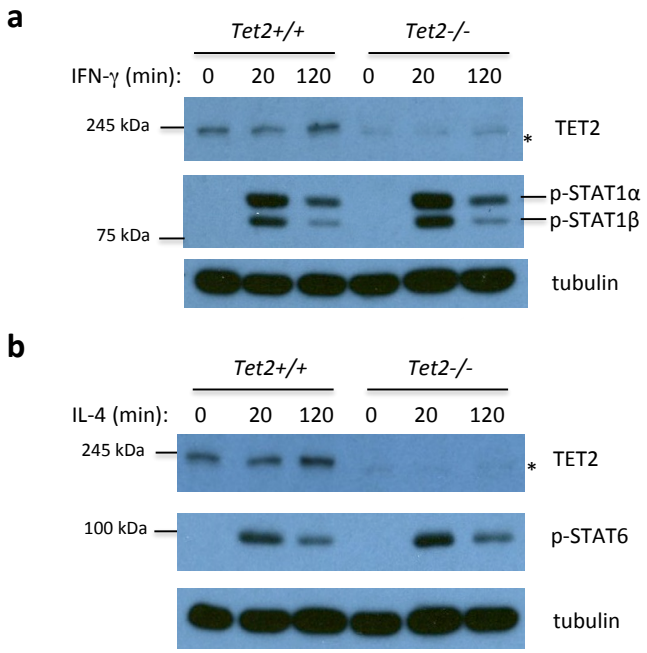

Figure 5.7. No defect in STAT1 and STAT6 activation in *Tet2-/-* BMDM.
BMDM from littermate matched *Tet2+/+* and *Tet2-/-* mice were treated with **(a)** IFN-γ (100 units/ml) or **(b)** IL-4 (10 ng/ml) for indicated time points. Protein lysates were harvested and an immunoblot was performed. Protein loading is normalized to tubulin. Both STAT1α (91 kDa) and STAT1β (84 kDa) isoforms are detectable with this phospho-STAT1 antibody. *Non-specific protein band located just below the TET2 protein. TET2 antibody used here is clone E6-198 (Abiocode).

Tet2-/- mice show protection against *Listeria monocytogenes* infection

Mounting an immune response to intracellular pathogens such as *Listeria monocytogenes* and influenza virus are key features of M1 polarized macrophages. Additionally, GBP proteins are important for the anti-bacterial response, as all 10 GBP family members are induced upon *L. monocytogenes* infection in ANA-1 murine macrophage cells (Degrandi et al.,

2007). Furthermore, *Isg15* expression stimulated by *L. monocytogenes* infection can restrict the growth of the bacteria *in vitro* and *in vivo* (Radoshevich et al., 2015). Based on the skew towards the M1 polarization, the hyperactivation of *Gbp1*, and the increased *Isg15* expression in TET2 deficient cells (Figures 5.5 and 5.3b, respectively), we next determined if TET2 deficiency protects mice against *L. monocytogenes* infection. Mice were intraperitoneally injected with a sublethal dose of 10^5 colony forming units (CFU) of *L. monocytogenes*. Three days later spleens were harvested to determine bacterial burden. Ten pairs of littermate matched female mice were used for the *L. monocytogenes* infection assay, four of which were heterozygous for *Tet2* vs. *Tet2-/-*. *Tet2* heterozygous mice generally behaved in a similar fashion as wildtype mice when infected with *L. monocytogenes*. Results from CFU titers found in the spleen reveal that *Tet2-/-* mice have a significantly lower bacteria burden than their wildtype and heterozygous controls (p-value 0.0327) (Figure 5.8). This shows that TET2 negatively affects the ability to control *L. monocytogenes* infections, *in vivo*.

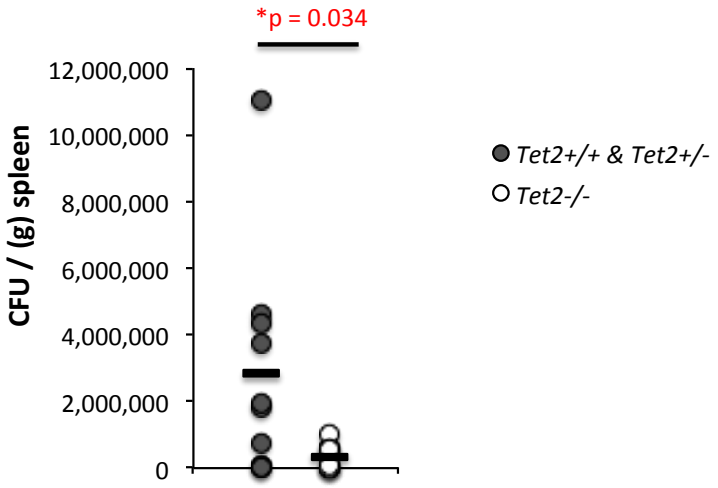

Figure 5.8. Loss of TET2 results in protection against *Listeria monocytogenes* infection. Female *Tet2-/-* mice with their matched *Tet2+/+* or *Tet2+/-* littermates were infected with $1x10^5$ CFU *Listeria monocytogenes* (strain 10403s) by intraperitoneal injection (n =10). Three days later, spleens were removed, weighed, and mechanically homogenized. Bacteria titer was determined by serial dilution and plating of spleen homogenates on LB agar plates. Statistics were performed using Students t-test. Each circle represents one mouse. Horizontal bars indicate mean value. Abbreviations: CFU (colony forming unit), LB (Luria broth).

Discussion

Among the TET family proteins, *Tet2* expression is highest in myeloid progenitors (Ko et al., 2010), suggesting that *Tet2* has an important function in myeloid differentiation. As macrophages and dendritic cells are derived from myeloid progenitors, we set out to uncover the potential role of TET2 in innate immunity. Here we show that proinflammatory stimuli induces both *Tet1* and *Tet2* expression, suggesting a role for these proteins in the immune response. Additionally, a subset of inflammatory genes *(Ifn-β, il-6, Gbp1*, and *Isg15*, Figure 5.3*),* are hyperactivated in *Tet2-/-* cells, suggesting that TET2 has a role in the negative regulation of these genes. As further evidence, luciferase assays show that TET2 is a repressor of *Ifn-β* expression. Furthermore, in the spectrum of M1 vs. M2 macrophage polarization, gene expression analysis reveal that TET2 deficient cells are more polarized to the M1 state, as they over express several key M1 proinflammatory genes and have defects in the expression of several M2 genes. Finally, as the M1 polarized state is associated with increased pathogen killing, we show that TET2 deficient mice indeed have protection against *L. monocytogenes* infection.

LPS-induced expression of *Tet2* is especially exciting because the induction profile is relatively rapid; starting at 2 hours, it reaches a peak at 6 hours, and by 24 hours expression levels drop to almost basal level, indicating that induction of *Tet2* is tightly controlled (Figure 5.1). Two different groups have made similar observations (Neves-Costa and Moita, 2013; Zhang et al., 2015). Interestingly, in response to LPS, the expression levels of *Tet1* peak as levels of *Tet2* drop down to basal level. One possibility is that TET1 may be part of a feedback mechanism to inhibit TET2. Another possibility is that as *Tet2* expression drops, *Tet1* becomes induced as compensation. Future studies will explore these two possibilities.

With the catalytic activity of TET proteins implicated in active demethylation, we initially hypothesized that genes would be repressed in the absence of TET2. Our data indicate that TET2 is both a repressor (for M1 genes) and an activator (of M2 genes). The repressive effect

of TET2 has been reported by Zhang et al. (2015), using dendritic cells as their model system. Similar to our finding, Zhang et al. noticed that *Il-6* was overexpressed in TET2 deficient cells. They show that TET2 is targeted to the *Il-6* promoter by the transcription factor IκBζ and in turn, TET2 recruits HDAC2 to specifically repress *Il-6*. Further studies can determine if TET2 inhibits gene expression in a similar fashion in macrophages.

Curiously, stimuli treated TET2 deficient cells show hyperactivation of *Gbp1* with a correspondingly defective *Gbp2* response. The inverse relationship between *Gbp1* and *Gbp2* expression is especially interesting because in mice the *Gbp1* gene is immediately upstream of *Gbp2* with only 1,466 base pairs separating the two genes. Previous reports indicate that *Gbp1* and *Gbp2* transcription are co-regulated, as the promoter region of both genes are very similar (Ramsauer et al., 2007). Indeed, we observe that wild-type cells induce *Gbp1* and *Gbp2* in a similar fashion. One possibility to account for the vast difference in *Gbp1* and *Gbp2* expression in *Tet2-/-* cells is that the hyperactivation of *Gbp1* induces tertiary changes in the DNA structure such as supercoiling, which negatively affects the expression of the immediately downstream *Gbp2* gene.

The differential induction of M1 and M2 genes in TET2 deficient macrophages led to a search for factors that may account for the differences in gene expression. We have determined that there is no defect in IFN-γ and IL-4 receptor signaling as it pertains to STAT1 and STAT6 activation (Figure 5.7). A likely scenario is that epigenetic modifiers at the promoters are affecting the expression of individual genes, as has been shown for the silencing of *Il-6* by HDAC2 as mentioned above. Conversely, it is possible that the M2 genes deficient in *Tet2-/-* mice are due to DNA hypermethylation, and that TET2 enzymatic activity is necessary for gene expression. Future studies will explore histone and DNA methylation status in our differentially expressed genes.

Here we show TET2 is a repressor of the inflammatory response. Likewise, TET2 is required for proper expression of several key M2 macrophage genes. To date, we are the first to

report the role of TET2 in macrophage polarization by analysis of M1 and M2 gene expression. Additionally, we are the first to show *Tet2-/-* mice have enhanced protection against intracellular pathogens such as *Listeria monocytogenes*, corresponding to their increased M1 macrophage polarized state. The hyper inflammatory state associated with M1 macrophages seen in *Tet2-/-* cells may provide an explanation why TET2 mutations are commonly found in human leukemia and myeloproliferative disorders – the constant inflammatory response causes unwanted transformation of cells that lead to disorders.

Materials and Methods

Mice

Mixed background *Tet2 fl/fl* mice (Moran-Crusio et al., 2011), mixed background *Tet1+/-* mice (Dawlaty et al., 2011), and *EIIA-Cre* mice were purchased from The Jackson Laboratory. *Ifnar1-/-* mice were kindly provided by Dr. Genhong Cheng (Univ. of California, Los Angeles). *Tet1+/-* mice were mated to produce littermate matched wild-type vs *Tet1-/-* mice. *EIIA-Cre* mice were crossed with *Tet2 fl/fl* mice to produced heterozygous *Tet2+/Δ* mice, who were then used as breeders to produce littermate matched *Tet2+/+* or *Tet2 Δ/Δ* (referred to as *Tet2-/-* here). For experiments, littermate and gender matched wild-type and knockout pairs were used, except for listeria-treated mice (Figure 5.8), where some pairs were of *Tet2* heterozygous and knockout littermates.

Mouse bone marrow-derived macrophages (BMDM)

Bone marrow was harvested from lower hind limbs of mice. Red blood cells were lysed with ACK buffer (0.15 M NH_4Cl, 10 mM $KHCO_3$, 0.1 mM EDTA). For BMDM, $2x10^6$ cells were seeded per 10 cm plate with DMEM containing 10% FBS, 1% penicillin-streptomycin and 30% L929 conditioned media. Media was changed at day 3. At day 7 cells were used for experiments. To prepare L929 conditioned media, L929 cells were split 1:3 and allowed to grow to confluency. Three days later, conditioned media was collected and frozen for storage.

Peritoneal macrophages

Peritoneal cell exudate (PEC) were harvested by careful insertion of 5 ml of cold RPMI into the peritoneal cavity of naïve mice via a 22G needle and 5ml syringe, and then the inserted RPMI was carefully collected to prevent accidental blood contamination. This was repeated, for a total of 10 ml collection volume. Samples with blood were discarded. PEC was washed once with

PBS, then resuspended in RPMI with 10% FBS and 1% penicillin-streptomycin and seeded onto 12-well plates. The next day, non-adherent cells were washed off with PBS. Fresh media was added to the adherent cells (i.e. peritoneal macrophages) and cells were immediately used for experiments.

Mouse embryonic fibroblast cells (MEF)

Mouse embryos were collected around embryonic day 14. Briefly, visible organs such as the brain, liver, and spleen were removed, and the leftover tissue was incubated in trypsin for 2 hours at 37°C. Cells were then washed with media and seeded in DMEM with 10% FBS, 1% penicillin/streptomycin and 0.055 mM β-mercaptoethanol. Every three days cells were passaged. At passage 2, cells were used for experiments.

Cloning and Luciferase assay

Interferon-β promoter region from -400 to +20 of the transcription start site (TSS) was amplified from BMDM genomic DNA using Platinum Taq High Fidelity DNA polymerase (Invitrogen) and cloned into pGL3-basic (Promega) through KpnI and BglII cloning sites. pcDNA-mTET2 was kindly provided by Dr. Hongjun Song (John Hopkins Univ.). Cloning primers used are mIFN-β -400 5'-TCGGTACCGGATGAGCAGCTACTCTGCCT-3' and mIFN-β +20 5'-TTGAGATCT GATGGAAGCCAGGCTGGTGTC-3'. Creation of pcDNA-PIAS1 has been described (Liu et al., 1998). TET2 enzymatic mutants were created at sites H1302Y and D1304A as described (Ko et al., 2010). Using pcDNA-TET2 was the template, TET2 enzymatic mutants were created by 2-step PCR with primers containing the mutation sites and the resulting full-length product re-ligated into pcDNA using EcoRI and SalI cloning sites. Briefly, for the first-step PCR, primers A+B created fragment 1, and primers C+D created fragment 2. In the second-step PCR,

fragments 1+2 were used as template with primers A+D to create full length, TET2 mutant cDNA.

Primer A: 5'-CAAGAATTCTATGGAACAGGACAGAACCACCCAT-3'.

Primer B: 5'-AATTGGCATGTTCTGCTGggctctgtaGGAATGAGCAGAGAAGTC-3'.

Primer C: 5'-TTCTCTGCTCATTCCtacagagccCAGCAGAACATGCCAAAT-3'.

Primer D: 5'-CGATGTCGACTCATACAAATGTGTTGTAAGGCCC-3'

Transfections were performed by calcium phosphate method into 293T cells. Twenty-four hours after transfection, luciferase activity was determined using the Dual-Luciferase Reporter Assay System (Promega) according to manufacturer's protocol.

RNA purification, reverse transcription and quantitative RT-PCR (qPCR)

Total RNA was prepared with STAT60 (Tel-Test, Inc.) according to manufacturer's protocol. 0.5 ug of total RNA was prepared using iScript cDNA Synthesis kit (Bio-Rad) according to manufacturer's protocol. Diluted cDNAs were analyzed by qPCR using the CFX-96 Real-Time Detection System (Bio-Rad). The program was set as 95°C for 3 min, 42 cycles of 95°C for 10 sec, 61°C for 30 sec, and a melt curve analysis. Data was analyzed using Bio-Rad CFX Manager software. Relative expression values were normalized to *Hprt* and *β-actin* and/or *Gapdh* (to verify *Hprt* values).

Protein lysates and immunoblotting

Cells were washed once with cold PBS, scrapped, collected, pelleted, and lysed on ice for 20 minutes in protein lysis buffer (50 mM Tris-HCl pH 8, 0.4 M NaCl, 0.5% NP-40, 10% glycerol, 1 mM EDTA) in the presence of freshly added inhibitors (1 mM PMSF, 0.1 mM $NaVO_4$, 10 mM N-ethylmaleimide and 1ug/ml leupeptin). Antibodies used were phospho-STAT1 (Tyr 701) and phospho-STAT6 (Tyr 641) both from Cell Signaling, tubulin (Sigma), and TET2 antibodies

clones E6-194, E10-47, 713, and E6-198 (Abiocode) See figure legends for more information regarding specific TET2 antibodies used.

Pathogen propagation and infections

Listeria monocytogenes (10403s) was kindly provided by Dr. Jeffrey F. Miller (Univ. of California, Los Angeles). Log phase bacteria grown in Luria Broth (LB) at 37°C was collected, OD 600 reading recorded, then adjusted to 15% glycerol in LB. Aliquots of 60 ul of bacteria were frozen at -80°C. The next day one aliquot was thawed and allowed to recover in 1 ml LB for 90 minutes at 37°C, then washed three times with cold PBS. The bacteria was finally resuspended in cold PBS and used immediately. To determine titer, *Listeria* was serially diluted in PBS and spread onto 6 cm LB agar plates performed in duplicates. Plates were placed in 37°C incubator for at least 20 hours, and colonies were counted. Only plates with at least 10 colonies were recorded. For animal infections, listeria aliquots were thawed and prepared as above to allow listeria to recover, and then 10^5 CFU in 100ul PBS was i.p. injected into mice. Three days later spleens were removed, weighed, and mechanically homogenized in 1ml cold PBS. This homogenate was used to determine titer by serial dilution and plating onto 6 cm LB agar plates performed in duplicates.

Table 5.1. Primers used for qPCR

β–actin	Forward 5'-TAGGCACCAGGGTGTGATGG Reverse 5'-CATGGCTGGGGTGTTGAAGG
Hprt	Forward 5'-CAGTACAGCCCCAAAATGGT Reverse 5'-CAAGGGCATATCCAACAACA
Gapdh	Forward 5'-AACTTTGGCATTGTGGAAGG Reverse 5'-GGATGCAGGGATGATGTTCT
Tet1	Forward 5'-CTGCACCCTGTGACTGTGAT Reverse 5'-GTCTCCATGAGCTCCCTGAC
Tet2	Forward 5'-TGATCCAGGAGGAGCAGTGA Reverse 5'-CGGGCTTCCATTCTGGAGTT
Ifn-β	Forward 5'-GCTCCTGGAGCAGCTGAATG Reverse 5'-CGTCATCTCCATAGGGATCTTGA
Il-6	Forward 5'-CACTTCACAAGTCGGAGGCT Reverse 5'-CTGCAAGTGCATCATCGTTGT
Irf1	Forward 5'-CCGAAGACCTTATGAAGCTCTTTG Reverse 5'-GCAAGTATCCCTTGCCATCG
Isg15	Forward 5'-AAGCAGCCAGAAGCAGACTC Reverse 5'-CAGTTCTGACACCGTCATGG
Nos2	Forward 5'-ACATCGACCCGTCCACAGTAT Reverse 5'-CAGAGGGGTAGGCTTGTCTC
Stat1	Forward 5'-GTGGTTCACCATTGTTGCAG Reverse 5'-GCTGGAAGAGGAGGAAGGTT
Cxcl2 (Mip-2)	Forward 5'-ATCCAGAGCTTGAGTGTGACGC Reverse 5'-AAGGCAAACTTTTTGACCGCC
Cxcl9 (Mig)	Forward 5'-CTTTTCCTTTTGGGCATCATCT Reverse 5'-GCAGGAGCATCGTGCATTC
Cxcl10 (IP-10)	Forward 5'-CCTGCCCACGTGTTGAGAT Reverse 5'-TGATGGTCTTAGATTCCGGATTC

Table 5.1 (continued)

Gbp1	Forward 5'-ATCATATCCCTTAAACTTCAGGAACAG Reverse 5'-GTGGAAACAGGGTAGAGAGCTTTAGT
Gbp2	Forward 5'-GTGAGGCCATTGAGGTCTTC Reverse 5'-CAGCAAGTCTGAGCAACGAG
Gbp3	Forward 5'-TTCCAGAAGAAGCTGGTGGT Reverse 5'-GAAAGCTCCACAGGAGATGC
Arg1	Forward 5'-CGCCTTTCTCAAAAGGACAG Reverse 5'-GACATCAACAAAGGCCAGGT
Ccl22	Forward 5'-ACCCTCTGCCATCACGTTTA Reverse 5'-AGCTTCTTCACCCAGACCTG
Ccl17	Forward 5'-TACCATGAGGTCACTTCAGATGC Reverse 5'-GCACTCTCGGCCTACATTGG
Chil3 (Chl3l3, Ym1)	Forward 5'-TCCAAGGCTGCTACTCACTT Reverse 5'-TCCAGTGTAGCCATCCTTAGG
Chil4 (Chi3l4, Ym2)	Forward 5'-TGGGTAATGAGTGGGTTGGT Reverse 5'-CACGGCACCTCCTAAATTGT
Mrc1 (CD206)	Forward 5'-TGGTTTCCATCGAGACTGCT Reverse 5'-GTCGTTCAACCAAAGCCACT

References

Anthony, R.M., J.F. Urban, F. Alem, H.A. Hamed, C.T. Rozo, J.-L. Boucher, N. Van Rooijen, and W.C. Gause. 2006. Memory TH2 cells induce alternatively activated macrophages to mediate protection against nematode parasites. *Nature Medicine*. 12:955–960. doi:10.1038/nm1451.

Belperio, J.A., M. Dy, L. Murray, M.D. Burdick, Y.Y. Xue, R.M. Strieter, and M.P. Keane. 2004. The role of the th2 CC Chemokine ligand CCL17 in pulmonary fibrosis. *The Journal of Immunology*. 173:4692–4698. doi:10.4049/jimmunol.173.7.4692.

Briken, V., H. Ruffner, U. Schultz, A. Schwarz, L.F. Reis, I. Strehlow, T. Decker, and P. Staeheli. 1995. Interferon regulatory factor 1 is required for mouse Gbp gene activation by gamma interferon. *Molecular and Cellular Biology*. 15:975–982. doi:10.1128/mcb.15.2.975.

Darnell Jr., J.E. 1997. STATs and gene regulation. *Science*. 277:1630–1635. doi:10.1126/science.277.5332.1630.

Dawlaty, M.M., K. Ganz, B.E. Powell, Y.-C. Hu, S. Markoulaki, A.W. Cheng, Q. Gao, J. Kim, S.-W. Choi, D.C. Page, and R. Jaenisch. 2011. Tet1 is dispensable for maintaining Pluripotency and its loss is compatible with embryonic and Postnatal development. *Cell Stem Cell*. 9:166–175. doi:10.1016/j.stem.2011.07.010.

D'Cunha, J., S. Ramanujam, R. Wagner, P. Witt, E. Knight Jr, and E. Borden. 1996. In vitro and in vivo secretion of human ISG15, an IFN-induced immunomodulatory cytokine. *Journal of Immunology*. 157:4100–4108.

Degrandi, D., C. Konermann, C. Beuter-Gunia, A. Kresse, J. Wurthner, S. Kurig, S. Beer, and K. Pfeffer. 2007. Extensive characterization of IFN-Induced GTPases mGBP1 to mGBP10 involved in host defense. *The Journal of Immunology*. 179:7729–7740. doi:10.4049/jimmunol.179.11.7729.

Delhommeau, F., S. Dupont, V.D. Valle, C. James, S. Trannoy, A. Massé, O. Kosmider, J.-P. Le Couedic, F. Robert, A. Alberdi, Y. Lécluse, I. Plo, F.J. Dreyfus, C. Marzac, N. Casadevall, C. Lacombe, S.P. Romana, P. Dessen, J. Soulier, F. Viguié, M. Fontenay, W. Vainchenker, and O.A. Bernard. 2009. Mutation in TET2 in myeloid cancers. *New England Journal of Medicine*. 360:2289–2301. doi:10.1056/nejmoa0810069.

Ficz, G., and J.G. Gribben. 2014. Loss of 5-hydroxymethylcytosine in cancer: Cause or consequence? *Genomics*. 104:352–357. doi:10.1016/j.ygeno.2014.08.017.

Giannakopoulos, N.V., J.-K. Luo, V. Papov, W. Zou, D.J. Lenschow, B.S. Jacobs, E.C. Borden, J. Li, H.W. Virgin, and D.-E. Zhang. 2005. Proteomic identification of proteins conjugated to ISG15 in mouse and human cells. *Biochemical and Biophysical Research Communications*. 336:496–506. doi:10.1016/j.bbrc.2005.08.132.

Gordon, S., and F.O. Martinez. 2010. Alternative activation of Macrophages: Mechanism and functions. *Immunity*. 32:593–604. doi:10.1016/j.immuni.2010.05.007.

Hu, X., and L.B. Ivashkiv. 2009. Cross-regulation of signaling pathways by Interferon-γ: Implications for immune responses and autoimmune diseases. *Immunity*. 31:539–550. doi:10.1016/j.immuni.2009.09.002.

Ishii, M., H. Wen, C.A.S. Corsa, T. Liu, A.L. Coelho, R.M. Allen, W.F. Carson, K.A. Cavassani, X. Li, N.W. Lukacs, C.M. Hogaboam, Y. Dou, and S.L. Kunkel. 2009. Epigenetic regulation of the alternatively activated macrophage phenotype. *Blood*. 114:3244–3254. doi:10.1182/blood-2009-04-217620.

Kawai, T., and S. Akira. 2010. The role of pattern-recognition receptors in innate immunity: Update on toll-like receptors. *Nature Immunology*. 11:373–384. doi:10.1038/ni.1863.

Kim, B.-H., A.R. Shenoy, P. Kumar, C.J. Bradfield, and J.D. MacMicking. 2012. IFN-Inducible GTPases in host cell defense. *Cell Host & Microbe*. 12:432–444. doi:10.1016/j.chom.2012.09.007.

Kim, B.-H., A.R. Shenoy, P. Kumar, R. Das, S. Tiwari, and J.D. MacMicking. 2011. A family of IFN- -Inducible 65-kD GTPases protects against bacterial infection. *Science*. 332:717–721. doi:10.1126/science.1201711.

Ko, M., H.S. Bandukwala, J. An, E.D. Lamperti, E.C. Thompson, R. Hastie, A. Tsangaratou, K. Rajewsky, S.B. Koralov, and A. Rao. 2011. Ten-Eleven-Translocation 2 (TET2) negatively regulates homeostasis and differentiation of hematopoietic stem cells in mice. *Proceedings of the National Academy of Sciences*. 108:14566–14571. doi:10.1073/pnas.1112317108.

Ko, M., Y. Huang, A.M. Jankowska, U.J. Pape, M. Tahiliani, H.S. Bandukwala, J. An, E.D. Lamperti, K.P. Koh, R. Ganetzky, X.S. Liu, L. Aravind, S. Agarwal, J.P. Maciejewski, and A. Rao. 2010. Impaired hydroxylation of 5-methylcytosine in myeloid cancers with mutant TET2. *Nature*. 468:839–843. doi:10.1038/nature09586.

Liu, B., S. Mink, K.A. Wong, N. Stein, C. Getman, P.W. Dempsey, H. Wu, and K. Shuai. 2004. PIAS1 selectively inhibits interferon-inducible genes and is important in innate immunity. *Nature Immunology*. 5:891–898. doi:10.1038/ni1104.

Liu, B., R. Yang, K.A. Wong, C. Getman, N. Stein, M.A. Teitell, G. Cheng, H. Wu, and K. Shuai. 2005. Negative regulation of NF- B signaling by PIAS1. *Molecular and Cellular Biology*. 25:1113–1123. doi:10.1128/mcb.25.3.1113-1123.2005.

Li, Z., X. Cai, C.-L. Cai, J. Wang, W. Zhang, B.E. Petersen, F.-C. Yang, and M. Xu. 2011. Deletion of Tet2 in mice leads to dysregulated hematopoietic stem cells and subsequent development of myeloid malignancies. *Blood*. 118:4509–4518. doi:10.1182/blood-2010-12-325241.

Martinez, F.O., and S. Gordon. 2014. The M1 and M2 paradigm of macrophage activation: Time for reassessment. *F1000Prime Reports*. 6. doi:10.12703/p6-13.

Moran-Crusio, K., L. Reavie, A. Shih, O. Abdel-Wahab, D. Ndiaye-Lobry, C. Lobry, M.E. Figueroa, A. Vasanthakumar, J. Patel, X. Zhao, F. Perna, S. Pandey, J. Madzo, C. Song, Q. Dai, C. He, S. Ibrahim, M. Beran, J. Zavadil, S.D. Nimer, A. Melnick, L.A. Godley, I. Aifantis, and R.L. Levine. 2011. Tet2 loss leads to increased Hematopoietic stem cell self-renewal and myeloid transformation. *Cancer Cell*. 20:11–24. doi:10.1016/j.ccr.2011.06.001.

Munder, M. 2009. Arginase: An emerging key player in the mammalian immune system. *British Journal of Pharmacology*. 158:638–651. doi:10.1111/j.1476-5381.2009.00291.x.

Murray, P.J., J.E. Allen, S.K. Biswas, E.A. Fisher, D.W. Gilroy, S. Goerdt, S. Gordon, J.A. Hamilton, L.B. Ivashkiv, T. Lawrence, M. Locati, A. Mantovani, F.O. Martinez, J.-L. Mege, D.M. Mosser, G. Natoli, J.P. Saeij, J.L. Schultze, K.A. Shirey, A. Sica, J. Suttles, I. Udalova, J.A. van Ginderachter, S.N. Vogel, and T.A. Wynn. 2014. Macrophage activation and polarization: Nomenclature and experimental guidelines. *Immunity*. 41:339–340. doi:10.1016/j.immuni.2014.07.009.

Murray, P.J., and T.A. Wynn. 2011. Protective and pathogenic functions of macrophage subsets. *Nature Reviews Immunology*. 11:723–737. doi:10.1038/nri3073.

Neves-Costa, A., and L.F. Moita. 2013. TET1 is a negative transcriptional regulator of IL-1β in the THP-1 cell line. *Molecular Immunology*. 54:264–270. doi:10.1016/j.molimm.2012.12.014.

Noppert, S.J., K.A. Fitzgerald, and P.J. Hertzog. 2007. The role of type I interferons in TLR responses. *Immunology and Cell Biology*. 85:446–457. doi:10.1038/sj.icb.7100099.

Pastor, W.A., L. Aravind, and A. Rao. 2013. TETonic shift: Biological roles of TET proteins in DNA demethylation and transcription. *Nature Reviews Molecular Cell Biology*. 14:341–356. doi:10.1038/nrm3589.

Perry, A.K., G. Chen, D. Zheng, H. Tang, and G. Cheng. 2005. The host type I interferon response to viral and bacterial infections. *Cell Research*. 15:407–422. doi:10.1038/sj.cr.7290309.

Pilla-Moffett, D., M.F. Barber, G.A. Taylor, and J. Coers. 2016. Interferon-Inducible GTPases in host resistance, inflammation and disease. *Journal of Molecular Biology*. doi:10.1016/j.jmb.2016.04.032.

Praefcke, G.J.K., and H.T. McMahon. 2004. The dynamin superfamily: Universal membrane tubulation and fission molecules? *Nature Reviews Molecular Cell Biology*. 5:133–147. doi:10.1038/nrm1313.

Radoshevich, L., F. Impens, D. Ribet, J.J. Quereda, T. Nam Tham, M.-A. Nahori, H. Bierne, O. Dussurget, J. Pizarro-Cerdá, K.-P. Knobeloch, and P. Cossart. 2015. ISG15 counteracts listeria monocytogenes infection. *eLife*. 4. doi:10.7554/elife.06848.

Ramsauer, K., M. Farlik, G. Zupkovitz, C. Seiser, A. Kroger, H. Hauser, and T. Decker. 2007. Distinct modes of action applied by transcription factors STAT1 and IRF1 to initiate transcription of the IFN- -inducible gbp2 gene. *Proceedings of the National Academy of Sciences*. 104:2849–2854. doi:10.1073/pnas.0610944104.

Seita, J., and I.L. Weissman. 2010. Hematopoietic stem cell: Self-renewal versus differentiation. *Wiley Interdisciplinary Reviews: Systems Biology and Medicine*. 2:640–653. doi:10.1002/wsbm.86.

Sutherland, T.E., N. Logan, D. Rückerl, A.A. Humbles, S.M. Allan, V. Papayannopoulos, B. Stockinger, R.M. Maizels, and J.E. Allen. 2014. Chitinase-like proteins promote IL-17-mediated

neutrophilia in a tradeoff between nematode killing and host damage. *Nature Immunology*. 15:1116–1125. doi:10.1038/ni.3023.

Tahiliani, M., K.P. Koh, Y. Shen, W.A. Pastor, H. Bandukwala, Y. Brudno, S. Agarwal, L.M. Iyer, D.R. Liu, L. Aravind, and A. Rao. 2009. Conversion of 5-Methylcytosine to 5-Hydroxymethylcytosine in mammalian DNA by MLL partner TET1. *Science*. 324:930–935. doi:10.1126/science.1170116.

Webb, D.C., A.N. McKenzie, and P.S. Foster. 2001. Expression of the ym2 Lectin-binding protein is dependent on Interleukin (IL)-4 and IL-13 signal transduction. IDENTIFICATION OF A NOVEL ALLERGY-ASSOCIATED PROTEIN. *Journal of Biological Chemistry*. 276:41969–41976. doi:10.1074/jbc.m106223200.

Welch, J.S., L. Escoubet-Lozach, D.B. Sykes, K. Liddiardǁ, D. Greaves, and C. Glass. 2002. TH2 Cytokines and allergic challenge induce ym1 expression in Macrophages by a STAT6-dependent mechanism. *Journal of Biological Chemistry*. 277:42821–42829. doi:10.1074/jbc.m205873200.

Zhang, Q., K. Zhao, Q. Shen, Y. Han, Y. Gu, X. Li, D. Zhao, Y. Liu, C. Wang, X. Zhang, X. Su, J. Liu, W. Ge, R.L. Levine, N. Li, and X. Cao. 2015. Tet2 is required to resolve inflammation by recruiting Hdac2 to specifically repress IL-6. *Nature*. 525:389–393. doi:10.1038/nature15252.

Chapter 6: Concluding Remarks

In this dissertation I show how DNA methylation modifiers such as PIAS1 can impact normal development, differentiation, and tumorigenesis. PIAS1 and DNMT3 are part of a complex that targets specific genes for silencing. Currently it is unknown if the other PIAS family members have similar roles in DNA methylation. One group performed yeast two-hybrid screens and found that overexpressed DNMT3A and PIASXa can interact, but whether this is true endogenously is unknown (Ling et al., 2004). While not as evident as seen in *Pias1-/-* mice, unpublished data show that *Piasy-/-* mice also have a small, but noticeable increase in Foxp3+ T cells compared to wild-type control. This suggests that PIASy might also have a role in silencing the *Foxp3* promoter. Future studies can address if PIASy, or any of the other PIAS family members, are also epigenetic modifiers.

Due to our recent exciting findings on the role of PIAS1 in epigenetic silencing of genes through DNA methylation as seen in Chapters 2, 3, and, 4 (Liu et al., 2010; Liu et al., 2013; Liu et al., 2014), we were naturally drawn to the ten-eleven translocation (TET) methylcytosine dioxygenase protein family due to their role in active DNA demethylation (Tahiliani et al., 2009). Results from our mRNA microarrays performed on PIAS1 BMDM over a decade ago show that upon stimulation with various cytokines, PIAS1 can repress a subset of proinflammatory genes, although the exact molecular mechanism(s) is unknown (Liu et al., 2004; Liu et al., 2005). With our newly discovered role of PIAS1 recruitment of DNMT3 for gene silencing, we hypothesized that several genes we saw repressed by PIAS1 in the microarray may be due to PIAS1-mediated DNA methylation on the promoter. Conversely, if these genes are repressed due to DNA methylation, we hypothesized that these genes may remain repressed when TET proteins

are absent, due to the inability to remove the repressive 5mC on the promoter by TET catalytic activity. While much work has been published regarding the role of TET proteins in stem cell development and cell differentiation, little is known about the role of TET proteins in the regulation of immunity and inflammation. By focusing on genes that are PIAS1 targets, we hope to uncover both a role for TET proteins in inflammation and also to further characterize the role of PIAS1 in the silencing of proinflammatory genes. The results presented in Chapter 5 show that the role of TET2 is more complicated than we initially hypothesized, as we discovered that TET2 can both repress and also activate a subset of specific genes.

An interesting question of both PIAS1 and TET2 is how do they target specific genes for DNA modification? Both proteins do not exhibit a consensus DNA binding sequence, such as that found on transcription factors, yet they both seem to have specificity in the genes they affect. One clue may be from a previously published work from our lab, in which PIAS1 preferentially affects the transcription of genes that have weak STAT1 binding (Liu et al., 2004). As evidence accumulates that TET2 can interact with transcription factors (Ichiyama et al., 2015; Zhang et al., 2015), it is possible that TET2 gene specificity is influenced by transcription factor binding to the promoter. Even then, further studies are necessary to elucidate the mechanisms that determine whether recruited TET2 will be an inducer or repressor of gene activation.

References

Ichiyama, K., T. Chen, X. Wang, X. Yan, B.-S. Kim, S. Tanaka, D. Ndiaye-Lobry, Y. Deng, Y. Zou, P. Zheng, Q. Tian, I. Aifantis, L. Wei, and C. Dong. 2015. The Methylcytosine Dioxygenase Tet2 promotes DNA Demethylation and activation of cytokine gene expression in T cells. *Immunity*. 42:613–626. doi:10.1016/j.immuni.2015.03.005.

Ling, Y., U. Sankpal, A. Robertson, J. McNally, T. Karpova, and K. Robertson. 2004. Modification of de novo DNA methyltransferase 3a (Dnmt3a) by SUMO-1 modulates its interaction with histone deacetylases (HDACs) and its capacity to repress transcription. *Nucleic Acids Research*. 32:598–610. doi:10.1093/nar/gkh195.

Liu, B., S. Mink, K.A. Wong, N. Stein, C. Getman, P.W. Dempsey, H. Wu, and K. Shuai. 2004. PIAS1 selectively inhibits interferon-inducible genes and is important in innate immunity. *Nature Immunology*. 5:891–898. doi:10.1038/ni1104.

Liu, B., R. Yang, K.A. Wong, C. Getman, N. Stein, M.A. Teitell, G. Cheng, H. Wu, and K. Shuai. 2005. Negative regulation of NF- B signaling by PIAS1. *Molecular and Cellular Biology*. 25:1113–1123. doi:10.1128/mcb.25.3.1113-1123.2005.

Liu, B., S. Tahk, K.M. Yee, G. Fan, and K. Shuai. 2010. The Ligase PIAS1 restricts natural regulatory T cell differentiation by epigenetic repression. *Science*. 330:521–525. doi:10.1126/science.1193787.

Liu, B., K.M. Yee, S. Tahk, R. Mackie, C. Hsu, and K. Shuai. 2013. PIAS1 SUMO ligase regulates the self-renewal and differentiation of hematopoietic stem cells. *The EMBO Journal*. 33:101–113. doi:10.1002/embj.201283326.

Liu, B., S. Tahk, K.M. Yee, R. Yang, Y. Yang, R. Mackie, C. Hsu, V. Chernishof, N. O'Brien, Y. Jin, G. Fan, T.F. Lane, J. Rao, D. Slamon, and K. Shuai. 2014. PIAS1 regulates breast Tumorigenesis through selective epigenetic gene silencing. *PLoS ONE*. 9:e89464. doi:10.1371/journal.pone.0089464.

Tahiliani, M., K.P. Koh, Y. Shen, W.A. Pastor, H. Bandukwala, Y. Brudno, S. Agarwal, L.M. Iyer, D.R. Liu, L. Aravind, and A. Rao. 2009. Conversion of 5-Methylcytosine to 5-Hydroxymethylcytosine in mammalian DNA by MLL partner TET1. *Science*. 324:930–935. doi:10.1126/science.1170116.

Zhang, Q., K. Zhao, Q. Shen, Y. Han, Y. Gu, X. Li, D. Zhao, Y. Liu, C. Wang, X. Zhang, X. Su, J. Liu, W. Ge, R.L. Levine, N. Li, and X. Cao. 2015. Tet2 is required to resolve inflammation by recruiting Hdac2 to specifically repress IL-6. *Nature*. 525:389–393. doi:10.1038/nature15252.